Int'l Conference Proceedings

CBEMS-18, DMCCIA-18, AGFES-18, BDMCTE-18,

EHSSM-18, BLEIS-18, ICLTET-18, ICBEL-18,

ICIET-18, ICHBES-18, ICLHE-18,

ICATE-18 & ICIME-18

March 21-23, 2018

Istanbul (Turkey)

Editors:

Prof. Dr. Bülent TOPCUOĞLU

Prof. BOUDEN Toufik

Prof. Tse-Ping Dong

ISBN 978-93-86878-11-3

Organized By:

Program Committee (ICLTET-2018)

Prof. Kazuaki Maeda, Chubu University, Matsumoto, Kasugai, Aichi, Japan

Prof. Dr. Bülent TOPCUOGLU, Akdeniz University, Antalya, Turkey

Dr. Y. Thaweesak, King Mongkut's University of Technology, Thonburi, Thailand

Dr. Michel PLAISENT, University of Quebec in Montreal, Canada

Prof. Kei Eguchi, Dept. of Information Electronics, Fukuoka Institute of Tech., Japan

Dr. Koorosh Gharehbaghi, MIEAust, MIIE, MCIAust, MATSE, RMIT University, Melbourne, Australia

Dr. Md. Aminur Rahman, Lab.of Marine Biotechnology, Institute of Bioscience, Univ. Putra Malaysia (UPM), Malaysia

Prof. Dr. Dimiter Velev, Dept. of Information Techn. & Communications, Univ. of National & World Economy, Bulgaria

Prof. Jemal Antidze, Georgian Technical University, Faculty of Informatics, Tbilisi, Georgia

Prof. Mihai Caramihai, Control Eng & Computer Sci Faculty, Univ. POLITEHNICA Bucharest, Romania

Dr Eng. Panagiotis Kyratsis, Asst. Prof., TEI of Western Macedonia, Dept. of Mech. Engg. & Ind. Design, Greece

Dr. Ahmed ARARA, Associate Professor, University of Tripoli, Computer Engg. Dept., Libya

Assoc. Prof. Dr. Florin Negoescu, Faculty of Machine Mfg. & Ind. Mgmt., Technical Univ. "Gheorghe Asachi" of Iasi / Romania

Dr. N.Ch.S. Sriman Narayana Iyengar, Professor, Department of Information Technology, Sreenidhi Institute of Science and Technology, Yamnapet,Ghatkesr,Hyderabad, Telengana

Asso. Prof. Walid Barhoumi, Intelligent Systems in Imaging & Artificial Vision, (SIIVA), RIADI Laboratory, Tunisia

Prof. Dr. S. Mohd. Abd-Allah, Beni-Suif University, Egypt

Prof. Dr. Huifang DENG, South China University of Technology, China

Dr. Iqbal Khaleel Khan, Assoc. Professor, Dept. of Civil Engg., Aligarh Muslim University, India

Prof. Dr. Subarna Shakya, Institute of Engg., Tribhuvan University, Nepal

Assist. Prof. Philip Ermita, College of Engg., Univ. of Perpetual Help, Phillipine Instt. of Ind. Engineers, Philippines

Prof. Aderemi A. Atayero, Dept. of Electrical & Information Engg., Covenant University, Nigeria

Assoc. Prof. Amir Nakib, Université Paris Est Créteil, Laboratoire LISSI (France)

Dr. Ali Said Al Nuaimi, Assoc. Professor, Dept. of Civil & Arch. Engg., Sultan Qaboos University, Oman

Assoc. Prof. Dr. Riktesh Srivastava, Information Systems, Skyline Univ. College, Sharjah, UAE

Asst. Prof. Dr. Kenichi Fujimoto, Univ. Consortium for e learning, Shikoku Center, Kagawa University, Japan

Dr. G. Anjan Babu, Sri Venkateswara University, Tirupati, Andhra Pradesh, India

Prof. Dr. Abu Talib Othman, Malaysian Spanish Institute, Dean Univ., Kuala Lumpur, Malaysia

Prof. Milad Alshebani Dept. of Civil Engineering, University of Tripoli – Libya

Prof. Dr. A.M. Bisen, Mech. Engg. Dept., INDUS University, Ahmadabad, Gujarat, India

Program Committee Cont’d (ICLTET-2018)

Prof. Dr. J. Sadhik Basha, Senior Faculty-Process Operations Technology, Int'l Maritime College Oman, Sohar, Sultanate of Oman

Prof. Osman Adiguzel, Firat University, Dept. of Physics, Elazig, Turkey

Prof. Samy Oraby, Faculty of Engg., Port Said Univ., Egypt, & Currently: Dept. of Mfg Engg. Tech., College of Tech. Studies, PAAET, Kuwait

Prof. Dr. Mohd. N M Jaafar, Dept. of Aeronautical Engg., Faculty of Mech. Engg., Univ. Teknologi Malaysia, Malaysia

Dr. M. Chithirai Pon Selvan Associate Professor, Amity University, Dubai

Prof. Valentina M Pomazan, Ph.D, Faculty of Mech. Engg., Ovidius Univ. from Constanta, Romania

Prof. Dr. Tech, Sc. Ryspek Usubamatov, University Malaysia Perlis, Malaysia

Assoc. Prof. Dr. Hasan AYDOGAN, Mech. Engg. Dept., Selcuk University, Konya, Turkey

Prof. Snezhana Georgieva Gocheva-Ilieva, Faculty of Mathematics & Informatics, Plovdiv Univ. Paisii Hilendarski, Bulgaria

Dr. Prof. S. N. Boranbayev, L.N.Gumilyov Eurasian National University, Kazakhstan

Assoc. Prof. Mohd. Mahmoud Emara, American University in Cairo, Egypt

Program Committee (ISAET)

IEEE Fellow Prof. Dr. Alan Chin-Chen Chang, Feng Chia University, Taiwan
Prof. Dr. Huifang DENG, South China University of Technology, Guangzhou, China
Dr. Karen Armstrong, University of British Columbia, Vancouver, Canada
Dr. Md. Aminur Rahman, University Putra Malaysia, UPM Serdang, Selangor Darul Ehsan, Malaysia
Dr. Arun N Nambiar, California State University - Fresno, CA, USA
Dr. Paiboon Kiattikomol, Department of Media Technology, King Mongkut's University of Technology Thonburi, BangKhuntian, Thailand
Prof. Dr. Jiri Strouhal, University of Economics Prague, Prague, Czech Republic
Prof. Monteiro Figueira, CEO CEIT–Consulting, Lisboa, Portugal
Prof. Dr. Bo Wun Huang, Cheng Shiu University, Taiwan
Dr. Saji Baby, Environmental Manager (Research and Consultation) & Principal Scientist, GEO Environmental Consultation, Kuwait
Dr. Natalya (Natasha) Delcoure, Academic Associate Dean and Director of Graduate Business Programs, Cameron School of Business, University of St. Thomas, USA
Dr. M. Hadi Bordbar, Lappeenranta University of Technology, FINLAND
Prof. Dr. M. Sadiq Sohail, King Fahd University of Petroleum & Minerals, Saudi Arabia
Assoc. Prof. Anatoli Torokhti, University of South Australia, Australia
Dr. Moulay Akhloufi, Director Research & Development, Québec, Canada
Dr. Amr Arisha, 3S Group Manager, College of Business, DIT, Dublin, Ireland
Prof. Kazuaki Maeda, Chubu University, Kasugai, JAPAN
Dr. A Aburas, AL Dalla Company, Tripoli - Libya
Prof. Dr. Abu Talib Othman, Malaysian Institute of Information Technology, Universiti Kuala Lumpur,Malaysia
Prof. Dr. Naeema. H. Jabur, College of Arts and Social Sciences, Muscat, Oman
Assoc.Prof. Radoslav Delina, Technical University of Kosice, Slovakia
Dr. Reza Eslami Farsani, K. N. Toosi University of Technology, Tehran, Iran
Dr. Raghu Prakash, Indian Institute of Technology Madras, Chennai, India
Dr. AbdarRahman Al-Mekhlafi, United Arab Emirates University , UAE
Dr. Waqar Shahid Qureshi, Air University, Islamabad, Pakistan
Aries Heru Prasetyo, PPM School of Management, Jakarta Pusat, Indonesia
Prof. Dr. Eugene LEVNER, Bar-Ilan University, Department of Management, ISRAEL
Dr. Speranta Sofia Milancovici, Vasile Goldis Western University, Arad, Romania
Dr. Wan Mohd Faizal Wan Ishak, Universiti Malaysia Pahang, Malaysia
Dr. Thaweesak Yingthawornsuk, Department of Media Technology, King Mongkut's University of Technology Thonburi, BangKhuntian, Thailand
Prof. Madya Hatim Mohamad Tahir, Iniversiti Utara malaysia, Malaysia
Prof. A. ZEROUAL, Cadi Ayyad University, Marrakesh, Morocco
Prof. Dr. Parvinder S. Sandhu, Rayat & Bahra University, India
Dr. Alfonds Andrew Maramis, S.Si., M.Si., State University of Manado (UNIMA),Tondano, Indonesia
Dr. Lotfy Azaz, College of Arts and Social Sciences, Sultan Qaboos University, Oman
Valentine Cawley, HELP University College, Kuala Lumpur, Malaysia
Prof. Dr. Emad a. Abu-Shanab, Yarmouk university, Jordon
Prof. Dr. Ashok Aima, University of Jammu, India

Program Committee Cont’d (ISAET)

R. S. Harika, British Gas, London, United Kingdom
Dr. Alfredo J. Anceno, Asian Institute of Technology, Klong Luang, Pathum Thani, THAILAND
Dr. Gajel Lhundup, royal University of Bhutan, Bhutan
Dr. Fawzi Irshaid, Al al-Bayt University, Jordan
Prof. Dr. Narasimhaiah Gorla, American University of Sharjah, Sharjah, UAE
Dr. Mwafaq M. Dandan, Aljouf University, Kingdom of Saudi Arabia
Dr. Zhihui Du, Tsinghua University, Beijing, P.R.China
Dr. Basim Alhadidi, Albalqa' Applied University, Jordan
Dr. Ashraf M. A. Ahmad, Princess Sumya University for Technology, Amman
Dr. Hemantkumar P. Bulsara, In charge - Management section, Applied Mathematics and Humanities Department, S. V. National Institute of Technology, Surat, India
Dr. Raymond Kosala, The Loseph Wibowo Center for Advanced Learning, Jakarta, Indonesia
Dr. Rusli Hj Abdullah, Universiti Putra, Malaysia
Dr. Mazdak Zamani, Advanced Informatics School, Universiti Teknologi Malaysia, Malaysia
Dr. Yuan Haiying, Beijing University of Technology, China.
Prof. Fang-Fang Wang, Ming Hsin University of Science & Technology, Hsinchu, Taiwan
Prof. Dr. R.Krishnamoorthy, Ana University of Technology, Tiruchirappalli, India
Prof. Michael Sega Gumelar, Universitas Multimedia Nusantara, Indonesia
Prof. Hong Guo, 3rd Research Institute of Ministry of Public Security, ChinaProf. Choe, Byung-Hak, Dept. of Advanced Metal and Materials Engineering, Korea
Hua Shijie, Norman, Senior Staff Mechanical Engineer, Penang Design Centre, Motorola Solutions, Malaysia
Prof. Yoongho Jung, School of Mechanical Engineering, Pusan National University, S. Korea
Assoc. Prof. Yuji SAKAI, Dept. of Environmental and Energy Chemistry Kogakuin University, Japan
Prof. Hitoshi TANAKA, Tokushima University, Japan

Program Committee (PSRC)

IEEE Fellow Prof. Dr. Alan Chin-Chen Chang, Feng Chia University, Taiwan
Prof. Sonia Swanepoel, North-West University, South Africa
Prof. Nicolene Barkhuizen, North-West University, South Africa
Prof. Dr. Abu Talib Othman, Malaysian Institute of Information Technology, Universiti Kuala Lumpur, Malaysia
Prof. Dr. Wen-Lin Yang, Dean, College of Science and Engineering, National University of Tainan, Taiwan
Prof. Parvinder Singh Sandhu, Rayat & Bahra Institute of Engineering & Bio-Technology, India
Prof. Dr. Rahim Ahmadi, Department of Biology, Islamic Azad University, Hamedan Branch, Hamedan, Iran
Prof. Dr. Huifang DENG, South China University of Technology, Guangzhou, China
Prof. Monteiro Figueira, CEO CEIT–Consulting, Lisboa, Portugal
Dr. Saji Baby, Environmental Manager (Research and Consultation) & Principal Scientist, GEO Environmental Consultation, Kuwait
Dr. Hamid Ali Abed AL-Asadi, Faculty of Education for Pure Science, Basra University, Basra, Iraq
Dr. Natalya (Natasha) Delcoure, Academic Associate Dean and Director of Graduate Business Programs, Cameron School of Business, University of St. Thomas, USA
Prof. Dr. Naeema. H. Jabur, College of Arts and Social Sciences, Muscat, Oman
Dr. AbdarRahman Al-Mekhlafi, United Arab Emirates University , UAE
Aries Heru Prasetyo, PPM School of Management, Jakarta Pusat, Indonesia
Dr. Speranta Sofia Milancovici, Vasile Goldis Western University, Arad, Romania
Prof. Madya Hatim Mohamad Tahir, Iniversiti Utara malaysia, Malaysia
Valentine Cawley, HELP University College, Kuala Lumpur, Malaysia
Prof. Dr. Emad a. Abu-Shanab, Yarmouk university, Jordon
Prof. Dr. Ashok Aima, University of Jammu, India
R. S. Harika, British Gas, London, United Kingdom
Dr. Gajel Lhundup, Royal University of Bhutan, Bhutan
Prof. Dr. Narasimhaiah Gorla, American University of Sharjah, Sharjah, UAE
Dr. Mwafaq M. Dandan, Aljouf University, Kingdom of Saudi Arabia
Dr. Zhihui Du, Tsinghua University, Beijing, P.R.China
Dr. Basim Alhadidi, Albalqa' Applied University, Jordan
Dr. Ashraf M. A. Ahmad, Princess Sumya University for Technology, Amman
Dr. Raymond Kosala, The Loseph Wibowo Center for Advanced Learning, Jakarta, Indonesia
Dr. Mazdak Zamani, Advanced Informatics School, Universiti Teknologi Malaysia, Malaysia
Dr. Yuan Haiying, Beijing University of Technology, China.
Prof. Fang-Fang Wang, Ming Hsin University of Science & Technology, Hsinchu, Taiwan
Prof. Dr. R.Krishnamoorthy, Ana University of Technology, Tiruchirappalli, India
Prof. Michael Sega Gumelar, Universitas Multimedia Nusantara, Indonesia
Prof. Hong Guo, 3rd Research Institute of Ministry of Public Security, China
Dr. Rusli Hj Abdullah, Universiti Putra, Malaysia
Prof. Choe, Byung-Hak, Dept. of Advanced Metal and Materials Engineering, Korea
Hua Shijie, Norman, Senior Staff Mechanical Engineer, Penang Design Centre, Motorola Solutions, Malaysia

Program Committee Cont'd (PSRC)

Prof. Yoongho Jung, School of Mechanical Engineering, Pusan National University, S. Korea
Assoc. Prof. Yuji SAKAI, Dept. of Environmental and Energy Chemistry Kogakuin University, Japan
Prof. Hitoshi TANAKA, Tokushima University, Japan

PREFACE

Dear Distinguished Delegates, Colleagues and Guests,

The DiRPUB, IICBE, IIE, ISAET and PSRC Organizing Committee warmly welcomes our distinguished delegates and guests at CBEMS-18, DMCCIA-18, AGFES-18, BDMCTE-18, EHSSM-18, BLEIS-18, ICLTET-18, ICBEL-18, ICIET-18, ICHBES-18, ICLHE-18, ICATE-18 & ICIME-18 scheduled on March 21-23, 2018 Istanbul (Turkey). The main themes and track are organized Conferences on Chemical, Biological, Environmental, Medical Sciences, Data Mining, Computers, Communication, Industrial Applications, Agricultural, Genetics, Food, Environmental Sciences, Building Design, Materials, Civil, Transportation Engineering, Education, Humanities, Social Sciences, Management, Business, Law, Education and Interdisciplinary Studies

These conferences are managed and sponsored by DiRPUB, IICBE, IIE, ISAET and PSRC are striving hard to compile the research efforts of scientists, researchers and academicians across the broad spectrum of Science, Engineering and Technology. These conferences are aimed at discussing the wide range of problems encountered in present and future high technologies among the research fraternity.

The conferences are organized to bring together the members of our international community at a common platform, so that, the researchers from around the world can present their leading-edge work. This will help in expansion of our community's knowledge and provide an insight into the significant challenges currently being addressed in that research. The conference Program Committee is itself quite diverse and truly international, with membership from the America, Australia, Europe, Asia and Africa.

The conference has solicited and gathered technical research submissions related to all aspects of major conference themes and tracks. This proceeding records the fully refereed papers presented at the conference.

All the submitted papers in the proceeding have been peer reviewed by the reviewers drawn from the scientific committee, external reviewers and editorial board depending on the subject matter of the paper. Reviewing and initial selection were undertaken electronically. After the rigorous peer-review process, the submitted papers were selected on the basis of originality, significance, and clarity for the purpose of the conference. The main goal of these events is to provide international scientific forums for exchange of new ideas in a number of fields that interact in-depth through discussions with their peers from around the world.

The program has been structured to favor interactions among attendees coming from many diverse horizons, scientifically, geographically, from academia and from industry. We would like to thank the program chairs, organization staff, and the members of the program committee for their work. We like to thank and show gratitude to Editors from DiRPUB, IICBE, IIE, ISAET and PSRC. We are grateful to all those who have contributed to the success of DiRPUB, IICBE,

IIE, ISAET and PSRC March 2018 Conference. We hope that all participants and other interested readers benefit scientifically from the proceedings and also find it stimulating in the process in their quest of achieving greater heights. Finally, we would like to wish you success in your technical presentations and social networking.

We hope you have a unique, rewarding and enjoyable week at DiRPUB, IICBE, IIE, ISAET and PSRC Conference at colorful Istanbul.

With our warmest regards,

Organizing Committee

March 21-23, 2018
Istanbul (Turkey)

INDEX

March 21-23, 2018 Istanbul (Turkey))

14th International Conference on Manufacturing and Automobile Engineering (ICMAE-2018)

14th International Conference on Chemical, Civil, Environmental and Medical Sciences (ICHBES-2018)

14th International Conference on Business, Economics and Law (ICBEL-2018)

14th International Conference on Innovations in Engineering & Technology (ICIET-2018)

Effect of Lubricants: Experimental Investigation in SPIF Process

Mariem. Dakhli[1,*], Atef. Boulila[2], Zoubeir. Tourki[1] and Pierre-Yves Manach[3]

***Abstract*—** Few studies have focused on the incremental forming of copper sheets. Moreover, the pyramid shape containing circular generatrix has not been investigated yet. Considering the friction produced during the incremental sheet forming process, between the sheet and the forming tool, a lubricant is used during the experiments in order to get a better surface finish quality. In this work, the influence of lubrication on surface roughness and forming forces in single point incremental forming (SPIF) of copper sheets is studied. This is considered keeping the same parameters such as the feed rate, the step increment and the sheet thickness.

***Keywords*—** SPIF, Lubricant, Surface Quality, Experiment, Forces.

I. Introduction

Single point incremental sheet forming (SPIF) is a fairly recent forming process. It is used to locally deform a thin sheet gradually. This process is performed using a hemispherical tool with small diameter compared to the stamping process. The used tool is controlled by a CNC machine. The interest of this method is to guarantee the sheet shape by managing the tool-path. Despite the complexity of the existing forms in the biomedical, aeronautical and mechanical fields [1], the SPIF process is able to produce shapes by dint of the development of CNC machine following the development of computer-aided and design manufacturing software (CAD/CAM).

Mariem Dakhli is currently a Ph.D. student at Department of Mechanical Engineering, University of Sousse, Tunisia

Atef Boulila is a teacher-researcher and Master-Assistant at the National Institute of Applied Sciences and Technology (INSAT)

Zoubeir TOURKI is Professor in Mechanical Engineering, graduated from the University of Metz (France)

Pierre Yves Manach is the director of the research laboratory named Institute de Recherche Dupuy de Lôme (IRDL), University of South Brittany in France.

This SPIF process has been investigated in several works [2, 3]. In the literature, the majority of authors have studied the influence of parameters such as step increment, feed rate, rotation speed, thickness of the sheet and material types on forming forces, t formability, surface roughness of produced parts quality and dimensional accuracy. However, little regard has been given to the influence of lubricant. Using lubrication at the contact area tool/sheet seems necessary to reduce the friction and consequently the wear. In addition, it improves the heat distribution over the entire part and excludes shavings [4, 5]. Ben messaoud et al [6] have shown that the use of lubricant during the forming process of Al-3003-H12 sheet helps to obtain an optimized surface roughness quality.

Azevedo et al [7] have evaluated the effect of the lubricant type used for the incremental forming of aluminium and steel sheets. They have shown that the use of lubricant improves the quality of surface roughness and reduces the forming forces values. Jawale et al [8] have found that the use of lubricant has no effect on formability and reduces the surface roughness of copper sheets. Else, the diversity in the lubrication has not influenced by the grain shapes of the formed parts. Few studies have evinced that the use of lubrication during the SPIF process improves the obtained surface part' quality.

In this paper, the effect of lubricant is evaluated on the forming forces and the surface quality roughness.

II. Experimental Procedure

A. The geometry of studied part and the process parameters

In this study, three tests were carried out using copper sheets with the thickness of 10/10 mm. Two experiments (N1, N2) are realized using parameters such as the feed rate (V=600mm/min) and the same step increment (Z= 0.25mm). The third experiment was accomplished with a smaller feed rate (V=300mm/min) and a larger increment (Z= 0.75mm). A truncated pyramid shape having a sides equal to 100mm and 20 mm of depth. This contain a circular generatix. To deform the truncated pyramid a continuous tool-path has been used as presented in Figure 1.

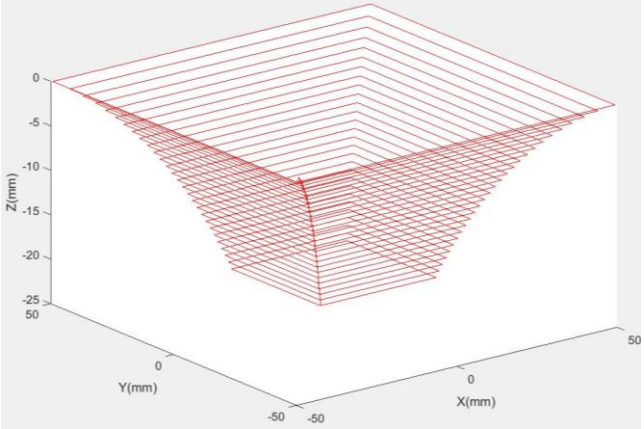

Fig. 1 Tool path

For the conducted experiments, three lubricants were used characterized by the properties summarized in Table I.

TABLE I
CHEMICAL PROPERTIES OF USED LUBRICANT

Test N °	Lubricant	Density (g/l)	Viscosity at 40°C (Cst)
1	Oil Jelt	0.93	136
2	Slide Oil	0.894	100
3	88% water +12% Oil	0.891	--

B. The SPIF machine and the roughness measurements tool

The experiments were performed on a Heidenhain CNC machine equipped with 802 D SIEMENS numerical command. The specifications of the used machine are 560 mm longitudinal travel X, 500 mm transversal travel Y and 400 mm vertical travel Z. The SPIF device is fixed on the CNC machine tray. The forming tool is set on the tool holder which is fixed in rotation into a mandrel. According to the defined path, the tool advances in depth in the blank sheet. Then, it performs the first contour of the forming path. After that, it makes a radial increment until the programmed depth is reached.

In order to study the influence of lubrication on the deformed parts roughness, an altimeter Roughness device is used as it is presented in Figure 2

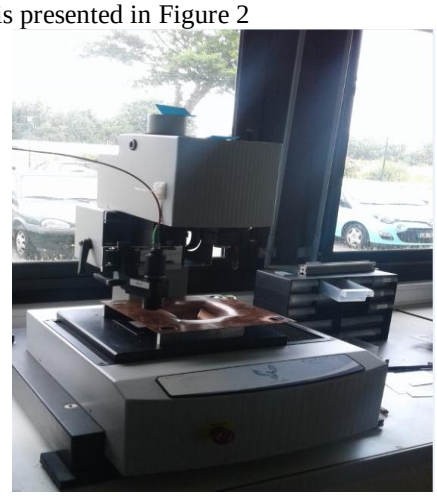

Fig. 2 Roughness measuring device

III. RESULTS AND DISCUSSIONS

A. Forming force

The forming forces were measured using a load sensor type FN7325-FGB (NI) able to measure the axial and radial forces in real time. The evolution of the axial forces for tests N1, N2 and N3 are shown in Figure 3. In Table II, the maximum for axial and radial forces for each test is summarized.

TABLE II
MAXIMUM FORMING FORCES AND COEFFICIENT OF SHAPE

Test N °	Maximum axial force (N)	Maximum radial force(N)
1	1797.39	2.84
2	1815.9	4.30
3	1704.38	20.10

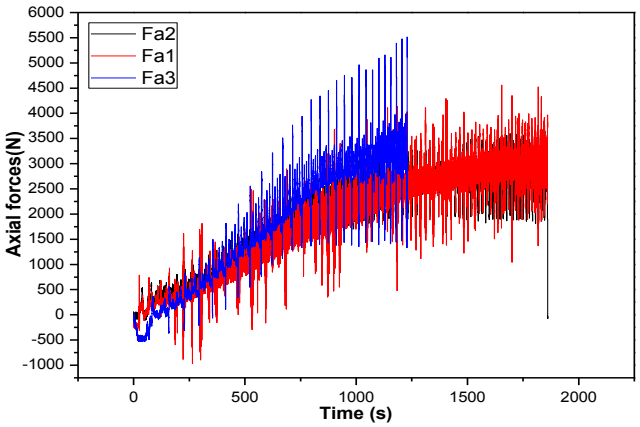

Fig. 3 Axial forces versus time

The examination of the data presented in Figure 3 and Table II show that it is no significant difference between the axial and radial force for experiment 1 and 2 since they present the same maximum for axial forces. The workpieces were formed in about 31 minutes with two different lubricant and two rotation speed. There is no difference between the lubricant 1 and the lubricant 2 despite the difference in the chemical properties of the lubricant. Both led to the same results for the forming forces in the same experimental conditions. By decreasing the feed rate and increasing the step increment of the experiment N3, a large deviation in the evolution of axial and radial forces is observed. This deviation seems due to the lubricant properties such as density and viscosity. Then, the used lubricant with low density seems reducing the axial forces and increases the radial one.as it was observed by Azevedo et al. in forming a AA1050 sheet.

B. Roughness Measurements

To predict the quality of the surface roughness, the arithmetic mean deviation Ra was determined. Fig. 4 presented a comparison between the initial roughness Ra of the sheet and the average roughness of the obtained parts for the three tests.

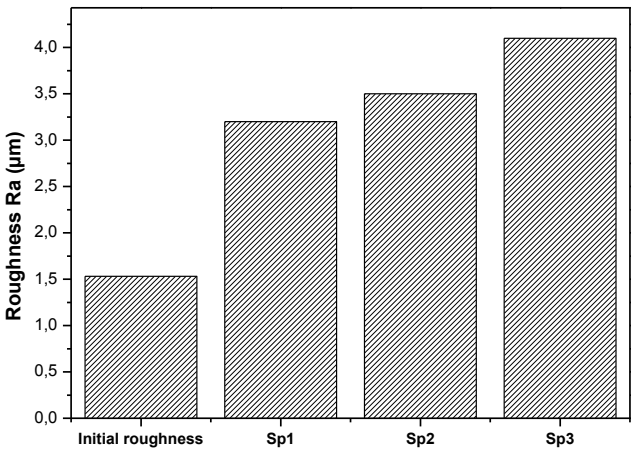

Fig. 4 Arithmetic roughness values

Regarding the formed copper sheets surfaces, it is observed that the surface sheet is smooth. There are no metal fragment at the deformed surfaces compared to the steel and the aluminum in some previous studies [1,2]. The initial roughness Ra for all specimens in the undeformed area is 1.53 µm. The percentage of the arithmetic mean profile deviations was determined with respect to the initial roughness of the workpiece before the forming process. The calculated percentage for the three specimens SP1, SP2 and SP3 are respectively 52.13%, 52.38% and 62.68%.

By analyzing the percentage gaps, it seems that the roughness of obtained copper sheets using a lubricant 3 which contains 88% of water and 12% of Oil leads to poor surface state. On the other hand, the lubricant that has the largest density had the better surface quality.

IV. CONCLUSION

At the contact area between the forming tool and the sheet metal, a friction will occur during the SPIF process which induces a local heating. To reduce the temperature level, it is necessary to use a lubricant. In our investigation, three lubricants are used to detect their influence on the forming forces and the surface roughness, for SPIF process of copper sheet. From this work, some conclusions are drawn:

- The type of lubricant does not affect the forming time despite the increasing in the step time increment.
- The use of lubrication prevents the appearance of metal fragments. Otherwise, the type of lubricant has a significantly impact in the maximum values of axial and radial forces. The lubricant with lower density reduces the axial force.
- The use of lubrication improves the quality of manufactured surfaces. Moreover, the lubricant with lower density has the highest value of surface roughness.

REFERENCES

[1] A. Boulila, "Contribution to biomedical component production by incremental sheet forming, "in The International Journal of Advanced Manufacturing Technology," 2017.

[2] M. Dakhli, "Effect of generatrix profile on single-point incremental forming parameters, "in The International Journal of Advanced Manufuring Technology, vol 93, Issue 5–8, pp. 2505–2516, 2017.

[3] B. Saidi, "Experimental force measurements in single point incremental sheet forming SPIF, "in Mechanics & Industry 16, 410 (2015), pp: 1-5.

[4] Fülöp and M. T. T, " A General Overview of Tribology of Sheet Metal Forming, "in Journal for Technology of Plasticity, vol 26, No. 2, pp. 11-25, 2001. 13.

[5] Lee .B. H, "Modeling of the Friction Caused by Lubrication and Surface Roughness in Sheet Metal Forming ",in Journal of Materials Processing Technology, vol. 130-131, pp. 60-63, 2002.

[6] R.BENMESSAOUD, "Tool, lubricant and process parameters investigation to form an AA 3003-H12 sheet by single point incremental sheet forming process," vol 7, Issue 11,pp.950-960, 2016.

[7] N. Gil Azevedo, "Lubrication Aspects during Single Point Incremental Forming for Steel and Aluminum Materials ",in INTERNATIONAL JOURNAL OF PRECISION ENGINEERING AND MANUFACTURING , vol. 16, No. 3, pp. 589-595, 2015.

[8] Kishore. Jawalea, "Microstructural investigation and lubrication study for single point incremental forming of copper ", in International Journal of Solids and Structures, pp.1–7,2017

Mariem Dakhli received her engineering degree in Mechatronics Engineering from National Engineering School of Sousse, Tunisia, in 2013. She is currently a Ph.D. student at Department of Mechanical Engineering, University of Sousse, Tunisia. She is currently a Ph.D. student at Department of Mechanical Engineering, University of Sousse, Tunisia.
Her research interest is Incremental sheet forming.

Atef Boulila is a teacher-researcher and Master-Assistant at the National Institute of Applied Sciences and Technology (INSAT). He received the Ph.D degree in mechanic from National Engineering School of Tunis and University of the Mediterranean (Aix-Marseille II, France). He teaches different courses for the specialties of industrial maintenance and industrial computer science. He participated in the preparation of national competitions input to engineering schools in industrial science and technology. He leads and supervises research work on the shaping of structures by plastic deformation and the Digital Plant & PLM.

Zoubeir TOURKI is currently the director General of University Renovation. Previously, he is director of the National School of Engineering of Sousse (ENISo) since 2011. He is Professor in Mechanical Engineering, graduated from the University of Metz (France). He received the M.S.T. Degree in Mechanical Engineering option CAD/CAM in 1990 from the University of Metz (France). In 1999, he got his Qualification as Associated Professor in France (Number: 9926084020). He obtained his Ph.D. in Engineering Science Mechanical in 1995 from the University of Metz.
He received his habilitation Universitaire in Mechanical Engineering in June 2004 from National Engineering School of Monastir (Tunisia).
He had a Post-Doctoral Federal Fluminense in the University of Brasil (Rio de Janeiro- Brasil) in 1995-1996. He participated in different European Projects like HiT4med / ACM Master pro in Applied Computational Mechanics ENISo-Ingolstadt (European Accreditation of Engineering Programmes EUR- ACE). His research activities are devoted to Shape memory alloys and manufacturing process.

Pierre Yves Manach is the director of the research laboratory named Institute de Recherche Dupuy de Lôme (IRDL), University of South Brittany in France. He obtained his PhD in 1993 in the National Polytechnic Institute of Grenoble in France and defended an Hability of Researchers Management at the University of South Brittany on the topic of "Constitutive laws and forming of metallic materials". He is now full Professor in Mechanical and Material Engineering. He has published more than 50 articles in international journals and supervised 12 PhD students. His research activities are devoted to plasticity and damage of metallic materials, with applications to various multi-step forming processes.

Mechanical Behavior of Clay Reinforced by Layers of Polymer

Rehab Bekkouche Souhila, Boukhatem Ghania and Mendjel Djenette

***Abstract*—** In this work, we suggest the use of polymers as additives to coherent soils in order to know their influence on the latters, an experimental study in the laboratory was carried out on a clayey soil reinforced by layers in polymers. Our findings clearly showed that the adding of a small percentage of polymer increases sensibly the inflated character of the latter. This conclusion is completely justified by the experimental planning of the essays realized by the laboratory.

***Keywords*—** Soil Stabilization, Polymer, Expansive clay, compressibility.

I. Introduction

In civil engineering the phenomena of shrinking inflation of certain clayey soils and some geological clayey formations induces differential tamps which are demonstrated by disorders affecting mainly constructed structures in surfaces and buried sets [1].

Although its drawbacks, the properties of its inflated clays make some materials very interesting in numerous applications, particularly, in geotechnic of the environment for the construction of working fences to stale parcels of nuclear wastes stored in depth, for the elaboration of the stone of the dams in the soil [2], [3]. The improvement of mechanical characteristics of the soils, the stand of all work in the land of civil engineering, is a worry to geotechnicians. A technical reinforcement of soils consists in improving the initial resistance and the mechanical characteristics of soil by resistant inclusion. Among the most useful methods for improving the behavior of soils, we can cite the reinforcement of soils by geosynthetic layers (geotextile and plastic). The use of plastic materials in the field of civil engineering and public works is not really a new event. A certain number of studies and experimentation was realized.

In civil engineering, polymers make a part of materials which allow to realize different geotechnical sets of retaining, of protection of the basins of tightness, under the causeways, in the tunnels… their use requires mastering their behavior to a long term (the duration of exacted life is generally of the order of 100 years). As a general rule, the lapses of its sets are of a mechanical order [4].

Now, the works of researches treat essentially the problem of determining the quantity of polymer adsorbed by the clay. The themes carry generally about the effect of structural nature of the additive or the clay, the nature of the existing cations in the system, and the load of polymer or also the effect of the ionic load (or the salinity) of the environment [5]-[10].

The advantages which can represent a reinforcement solution by geosynthetic are put in evidence by the different authors [11]-[14]. They insist on the economic interest of this solution according to other heavy solutions (for example: pillars of the soil treated with cement or pillars which are ballasted). [15] Evoke the environmental problems which are settled more and more in cases of total purge, for the putting in the depositing of excavation.

Polymers, which are organic salts, are attracted by the surface of the clay when they carry positive charges and, in certain pH conditions, by the ends of the sheets when the charges they carry are negative. The large size of these molecules allows a kind of encapsulation which limits the subsequent hydration of the clay. The interaction of the polymers with the clay depends on the type of the clay, the grain size and nature of the exchangeable cations [6]. It has been shown that the combination of a salt and a polymer could be more effective vis-à-vis the stabilization than the mere use of one or the other component [16].

Our study interests most on the influence of this addition on some mechanical characteristics of clay because it was proved by former studies the very positive effect of this addition on the improvement of properties of the inflation of clayey soils.

II. Localization and Identification of the Site

The ground subject of this study is reshuffled clay of Elhadeik region which is situated in the North of Skikda (a town in the North East of Algeria). The sampling was done by a hydraulic shovel to a depth of 40 cm.

Rehab Bekkouche Souhila and Mendjel Djenette are with the Department of Civil Engineering, Skikda University, Algeria (corresponding author to provide phone: 213669379959; e-mail: solrehab@yahoo.fr), other authors e-mails: rech_mendjel@yahoo.fr

Boukhatem Ghania is with the Department of Civil Engineering, Annaba University, Algeria (e-mail: gboukhatem3@yahoo.fr).

III. The Property of Polymer

The material of reinforcement used is composed of plastic layers (translucent polyethylene) commercially available of weak density, white in color and soluble in water. It is a natural biodegradable polymer of a high performance developed for providing the needs of technologies specialized in drilling. Table I regroups the characteristics of the reinforcement of the used material.

TABLE I
PROPERTIES OF POLYMER USED IN THE TRIALS

Property	Quantity
Appearance: Whitish, very fluid powder PH 1% soil: approximately 7 Dispersal: very good Toxicity: non-toxic	25 Kg multiplying the paper bags in internal polyethylene in block wrapped and fastened.

IV. The Experimental Program

The experimental program in this study consists of evaluating the effect of different percentage of polymer or some geotechnical parameters (pressure of inflation, coefficient of compressibility and coefficient of inflation).

The quantities of clay and polymer for the preparation of mixtures are determined according to a massive percentage: (the material in the natural state, the material reinforced by a percentage of 5% of polymer and the material reinforced by a percentage of 10% of polymer)

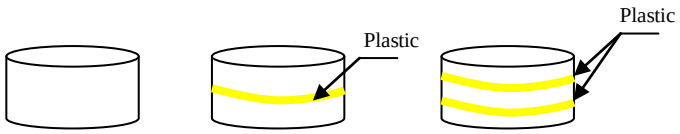

Fig. 1 Emplacement of layers of polymer in test pieces

V. Results and Discussions

In order to study the inflation of the clay mixed with different rates of polyethylene and to evaluate the effect of adding polyethylene on this parameter, a series of essays to the oedometer was realized on some specimen made by mixing to a water content of 22% and a dry density of 1.6 and compacted statistically in a ring of oedometer (H= 19 mm, d =70 mm) to a press aid.

The sample is subjected to the weight of the piston only, and contacted with a water reservoir at zero load. The variation in the height of the piston is measured as a function of time until it stabilizes. The swelling curve (Fig. 2) presents two parts that can be analyzed, by analogy with the consolidation process, such as primary and secondary phases of swelling.

The final value of the swelling, after stabilization, allows us to calculate the relative change of the volume of the sample which is expressed in percentage.

The same procedure is used to study the swelling of the samples in the presence of different polymers rate.

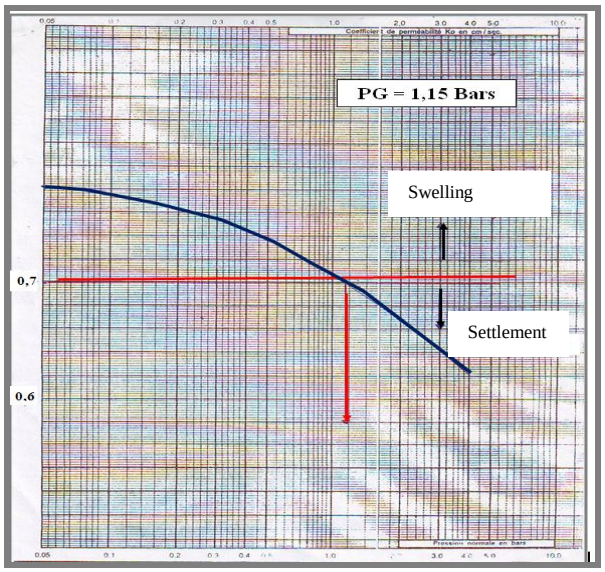

Fig. 2 Curve of free swelling of the untreated clay.

The obtained results are presented in Fig. 3, 4, 5 and 6. It is found that the paces of the obtained curves are too much similar to those obtained in literature [16].

The effect of adding polymer is visible. Its curves show that the potential of inflation increases in a substantial way by adding 5%. This proves that the inflation is related to plasticity and it affects the pure particles [17], [18].

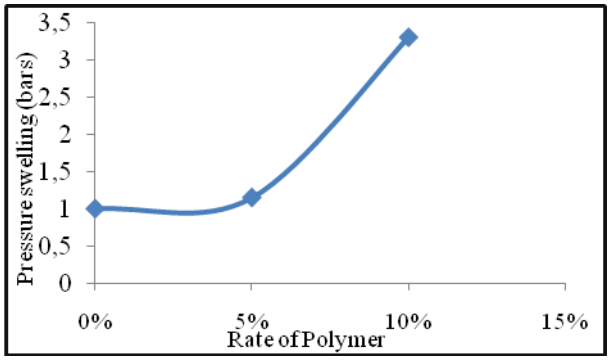

Fig. 3 Curve of inflation functioning of the percentage of polymer

Another parameter of an important compressibility, which is the constraint of pre-consolidation (Fig. 4). The latter corresponds to the effective constraint which is vertical and maximum supported by specimen in the course of its preparation by static compacting. It appears that the dosage in polymer from 5% has a negligible effect on the pressure of pre-consolidation [19], [20].

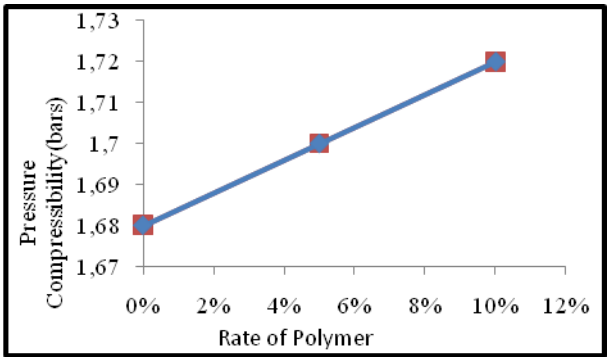

Fig. 4 Variation of Pressure Compressibility in function of the rate of the polymer

In order to visualize better the variation of the compressibility, Fig. 5 gives the evolution of indications of compressibility (Cc) and of inflation (Cg) in function of percentage of polymer.

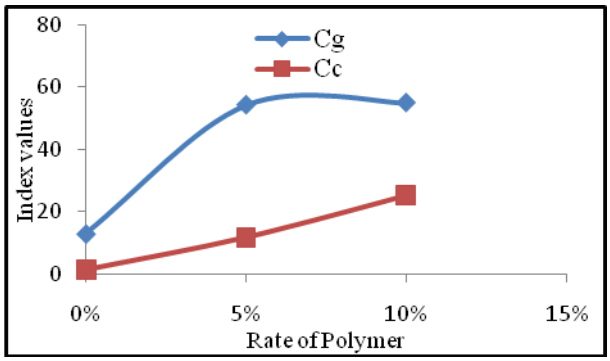

Fig. 5 Variation of index values Cc and Cg in function of the rate of the polymer

The two indications increase with the increase of the percentage of polymer added in a substantial way by adding 5%. One possible mechanism is the progressive coverage of the clay surface in contact with the polymer, which grows with the increasing of the polymer levels

Finally, the vertical shifts were measured with the help of a captor of shift related to a billsticker. The captor of the used shifts allows having a precision of the order of 0.01 mm. the vertical deformations were corrected with taking into account the deformations of the system “frame- cell- captor” which were evaluated using a wedge in steel being able to be considered as not being deforming.

It was noted that the variations of volume deformations is also influenced by the presence of the rate of the polymer. The graphs of evolution of volume deformations in function of weight represented in figure 5 interpret a known behavior: its graphs have the same aspect and indicate that there is an important increase of the volume of specimen from the addition of 5% of polymer.

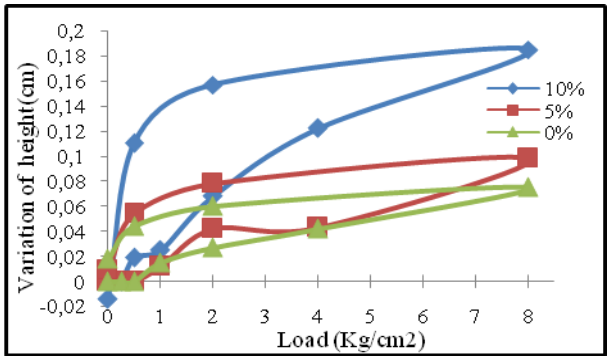

Fig. 6 Variation of the height in function of weight

Numerous works were consecrated to description of the behavior of inflated coherent soils. These works have put in evidence that adding polymer rigidify the soil, increases its pressure of preconsolidation and its resistance.

In our study, we discovered that the mechanical loads realized in a room temperature revealed the effect of adding polymer on the compressibility of clay: the inflation is due to hydration, the dependence of parameters of compression (Cc) and of inflation (Cs) and the increase of pressure of pre-consolidation due to hydration [21].

VI. Conclusions

The clays and the clayey rocks are incontestably very interesting in the frame of storage of wastes for a long time. At the same time like an elaborated barrier or like a natural geologic barrier. Like salt, they possess the capacity to realize around the works of stocking an auto-wrapping. They possess more many properties which interest the stocking. This study allowed us to study the behavior of clayey inflated soils used for the conception of elaborated barriers. The objective of this work is to answer a question which concerns the effect of treating the soil by adding polymer on the parameters of inflation. According to these results, we noticed that the increase of the percentage of polymer provokes an improvement of the capacity of inflation of clay.

The potential of inflation of the reconstituted soil increases from 5% of polymer. So, the trials of inflation on the clay studied showed well the increase of inflation with the growth of the rate of polymer.

References

[1] R.L. Anderson, I. Ratcliffe, H.C. Greenwell, P.A. Williams, S. Cliffe, P.V. Coveney, “Clay swelling, A challenge in the oilfield,” *Earth-Science Reviews*, 98, 201–216, 2010.

[2] Hossein Nowamooz, “Retrait/gonflement des sols argileux compactés et naturels,” Thèse de doctorat, Institut National Polytechnique de Lorraine, 2007.

[3] Marty. Nicolas, “Modélisation couplée (transport - réaction) des interactions fluides - argiles et de leurs effets en retour sur les propriétés physiques de barrières ouvragées en bentonite,” Thèses de doctorat, Université Louis Pasteur, 2006.

[4] Emmanuel Richaud, “Durabilité des Géotextiles en Polypropylène, Thèses de doctorat,” Ecole Nationale supérieure d'arts et métier, 2006.

[5] Luckham, P. F. and S. Rossi, “Colloidal and rheological properties of bentonite suspensions,” *Adv. Colloid Interface Sci*. 82, 43-92, 1999.

[6] Breen. C, "The characterization and use of polycation-exchanged bentonite," *Appl. Clay Sci.* 15, 187- 219, 1999.
[7] Ramos-Tejada, M.M., De Vicente, J., Ontiveros, A., Durán, J.D.G, "Effect of humic acid adsorption on the rheological properties of sodium montmorillonite suspensions," *J. Rheol.* 45, 1159-1172, 2001.
[8] Ramos-Tejada, M.M, Ontiveros, A, del Carmen Plaza, R, Delgado, A.V, Durán, J.D.G, "A rheological approach to the stability of humic acid/clay colloidal suspensions," *Rheol. Acta*. 42, 148-157, 2003.
[9] Simon, S., Le Cerf, D., Picton, L., Muller, G., "Adsorption of cellulose derivatives onto montmorillonite: a SEC-MALLS study of molar masses influence," *Colloids Surf.* 203, 77-86, 2002.
[10] Mpofu, P., Addai-Mensah, J. and Ralston, J., "Flocculation and dewatering behaviour of smectite dispersions: effect of polymer structure type," *Minerals Engineerin*. 17, 411-423, 2004.
[11] Rowe R.K, "Geosynthetic-reinforced embankments over soft foundations," 7th International Conference on Geotextiles, Nice, France, 1, 5-34, 2002.
[12] Imanishi H., Hirai T., Takaba Y., Adachi M, "Embankment technology with geogrid on very soft clay," 7th International Conference on Geotextiles, Nice, France, l. 1, 177-180, 2002.
[13] Bergado D.T., Horpibulsuk S., Ngouchaurieng P, "Innovative use of geosynthetics for repair of slope failures along irrigation/drainage canals on soft ground," 7th International Conference on Geotextiles, Nice, France, 1, 147-150, 2002.
[14] S.M. Lahalih, N. Ahmed, "Effect of new stabilizers on the compressive strength of dune sand," Constr. *Build. Mater*. 12, 321–328, 1998.
[15] De Mello L.G., Mondolfo M., Gomes J.C.M., Caran A, "Optimised design and construction of an urban highway embankment on soft soils," 7th International Conference on Geotextiles, Nice, France. 1, 159-164, 2002.
[16] Andry Rico Razakamanantsoa, "Etude du comportement hydromécanique, chimique et de la durabilité des géomatériaux d'étanchéité renforcés par ajout de polymères," Thèse de doctorat, Lyon, 2009.
[17] Brown, J.J., Brandon, T.L., Daniels, W.L., De Fazio, T.L., Filz, G.M., and Mitchell, J.K, "Rapid Stabilization/Polymerization of Wet Clay Soils: Phase I, Literature Review," Air Force Research Laboratory, Tyndall AFB FL, 2004.
[18] Fatemeh Mousavi, Ehsan Abdi, Hassan Rahimi, "Effect of polymer stabilizer on swelling potential and CBR of forest road material," *KSCE Journal of Civil Engineering* , 18, Issue 7, 2064-2071, 2014.
[19] Christopher M. Geiman, "Stabilization of soft clay subgrades in Virginia phase I laboratory study," Thesis Master of Science Faculty of the Virginia Polytechnic Institute, 2005.
[20] Inyang, H., Bae, S., Mbamalu, G., and Park, S, "Aqueous Polymer Effects on Volumetric Swelling of Na-Montmorillonite," J. Mater. Civ. Eng. 19, SPECIAL ISSUE: *Geochemical Aspects of Stabilized Materials*, 84–90, 2007.
[21] L. Hammadi , N. Boudjenane, M. Belhadri, "Effect of polyethylene oxide (PEO) and shear rate on rheological properties of bentonite clay," *Applied Clay Science*, 99, 306–311, 2014.

The Effect of Lime Rates on the Mechanical Behavior of Clay

Ghania. Boukhatem[1], Djennete. Mendjel[2] and Souhila. Rehab bekkouche[3]

***Abstract*—**With the reduction of resources in quality materials, more and more constructions of civil engineering structures are made on low resistance soil, which leads to think of the development of techniques of stabilization of this type of soil. Lime stabilization has been widely applied in civil engineering practice as foundations. With the addition of lime to soils, reactions are established with the soil grains that lead to improved geotechnical properties of the treated soil. An experimental methodology was developed to study the physical and mechanical behavior of mixtures treated by evaluating the influence of a variety of lime percentages on the Atterberg limits, the blue value, the compactibility. A continuous increase in lime of 2 to 10% implies an improvement of the physicomechanical parameters, which means the good behavior of the treated mixtures. The stabilization of the clay-lime matrix is due to chemical reactions between the clay minerals in the soil and the hydrated lime (flocculation and agglomeration, pozzolanic reaction).

***Keywords*—**Clay, Consistency, Lime, Plasticity, Resistance, Soil Stabilization, Treatment.

I. INTRODUCTION

The natural durability of the soil can be improved by the process of soil stabilization using different types of stabilizers (cement, lime, fly ash ... ..)[1],[7]. The goal is to increase resistance against destructive forces over time by increasing cohesion and decreasing the movement of moisture in the soil. The treatment of lime floors is a technique that is easy to implement[2],[3], economical and efficient. The objective of this work is to study the behavior of clay treated with quicklime, the work focuses on evaluating in the LNHC laboratory of EL-TAREF,Algeria, the influence of a variation of the percentage in lime on the physical and mechanical parameters of soil.

II. PURPOSE OF THE WORK

The purpose of this study is the observation of the behavior of clays and the influence of the addition of lime on the characteristics of this clay. Especially: methylene blue value, Atterberg limits, mechanical characteristics to compaction.

For the preparation of the mixture we put in a tray a quantity of sieved clay to 5 mm and then added amounts of lime in the desired percentage (2%, 6% and 10%) ; mixing is done dry using shovels until homogenization, this operation takes about 5 to 10 min to avoid the loss of reactivity lime.

III. STUDIED MATERIALS

A. Lime

Vive lime comes from the region of Elbouni in Annaba,Algeria, Microcrystalline Limestone 100% calcite these properties are provided in the technical sheet of the material.

B. Clay

The natural soil comes from the land of BENAMMAR, located in daïra EL CHATT the wilaya of EL TAREF, Algeria, at a depth of 1 m to 2m, it is prepared by drying in an oven at 105 ° C for 24 hours, grinding, then 1 mm screen sieving.

IV. TESTS ON CLAY

A. Methylene Blue Value Test

The methylene blue test was conducted according to the French standard NF-P94-069 [3] at the LNHC laboratory of E L-TAREF,Algeria. A methylene blue value of V B = 7.66 and allowed to obtain a specific surface area of 160.86 m2 / g.

B. Atterberg Limites

The results are in the tableI used (NF P 94-051) [4]

TABLE I
RESULTS OBTAINED FOR THE ATTERBERG LIMITS

Atterberg Limites			
Simple clay	WL %)	WP (%)	IP(%)
	57,56%	29,13%	28,32%

Ghania. Boukhatem[1] Department of Civil Engineering, Badji Mokhtar University, Laboratory LSH, Annaba, Algeria ; e-mail: gboukhatem3@yahoo.fr

Djennet. Mendjel[2], Laboratory LMGHU, Skikda, Algéria (e-mail: rech_mendjel@yahoo.fr).

Souhila. Rehab Bekkouche [3] Laboratory LMGHU, Skikda, Algéria (e-mail: solrehab@yahoo.fr).

C. The Compaction Test

The Proctor curve presented on (Figure 1), (NF P 94-093) [5] gives the values of the optimum water content of 26.67% and a maximum dry density of ɣd = 1.49 (t / m3). this pointed shape explains the sensitivity of the clay to the water content.

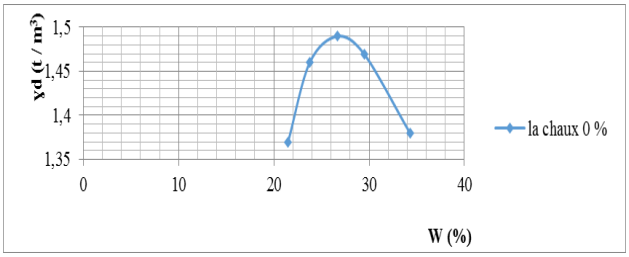

Fig 1. Compaction curves of untreated clay.

V. Soil Classification

The plasticity index of the soil shows that the soil is a very plastic clay.

Methylene blue value (VBS) indicates that the soil is clayey.

Which means that the soil is classified as a clay soil, very plastic.

VI. Results and Interpretation for the Clay Lime Mix

A. Influence of the percentage of lime on methylene blue VB

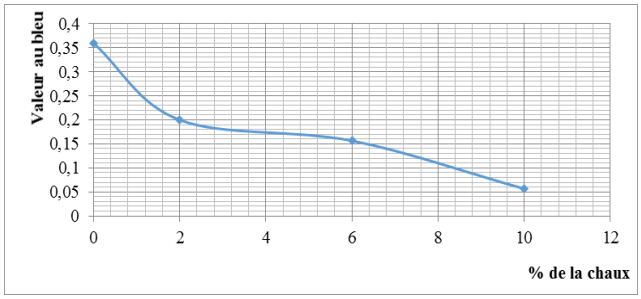

Fig 2. Variation of blue values for different percentages of lime.

The results show an irreversible revolution, an almost linear decrease of VB with the increase of the percentage of lime.

Then the addition of lime gives a very important decrease in the sensitivity of the clay.

B. Influence of lime on Atterberg limits

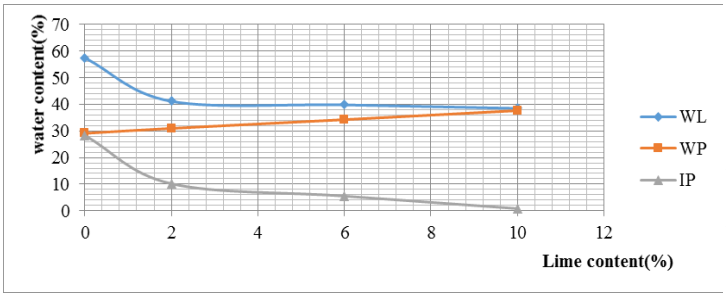

Fig. 3. Influence of Percentage of Lime on Atterberg Limits.

TABLE II
THE ATTERBERG LIMITS OF UNTREATED AND TREATED SOIL

Lime (%)	WL	WP	IP	Soil condition (according to IP)	Classification of the soil according to the abacus of casagrande
0	57,56	29,13	28,43	plastic clay	very plastic
2	41,16	30,97	10,19	Can plastic	Little plastic lemon
6	39,81	34,27	5,54	Can plastic	Little plastic lemon
10	38,50	37,66	0,84	Not plastic	Little plastic lemon

From the results found we can say that the addition of quicklime to our clay with the percentages 2%, 6% and 10% implies a reduction of plasticity, a decrease in the sensitivity to water.

The addition of lime can move a soil from the plastic state (deformable, sticky - so hard to compact) to dry (rigid, rubbing, friable - so much easier to work).

C. Influence of lime percentage on compaction

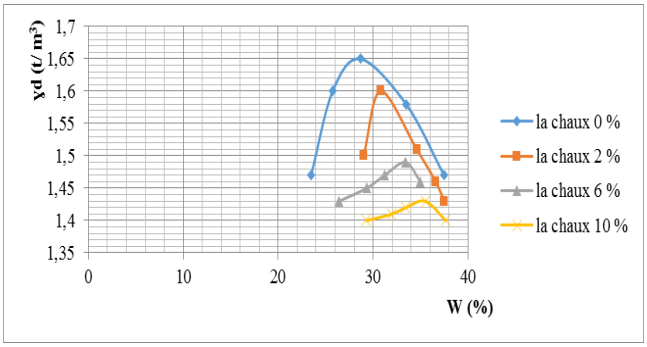

Fig. 4. Influence of Percentage of Lime on compaction of clay

The increase in the optimum water content is due to the hydration reaction of the lime, hence the decrease in the maximum dry density.

VII. Conclusion

The stabilization of the soil by limes allows the immediate improvement and over time performance of treated soil. These performances are sometimes obtained at very low lime levels. The performances translate remarkably on all the characteristics of the soil treated.

The reduction of the maximum dry density.

The increase in optimal water content and plasticity content.

Various test have been made in this work to determine the influence of the lime content on the geotechnical properties of the soil. According to these results, it is noted that the increase in the percentage of lime implies a significant reduction of the plasticity indices and the value to the blue which is explained by the change in the texture of the soil and its behavior with respect to water, the Ca2 + cations provided by the lime develop electric forces leading to the agglomeration of fine clay particles in rough and friable particles which reduces the sensitivity to water.

The addition of lime implies a significant decrease in the plasticity that makes the soil pass from a plastic state to a solid state.

The lime also attacks the parameters of the compactibility, one observes an increase of the optimal water content and a decrease of the maximum dry density which facilitates the implementation on site.

REFERENCES

[1] FATIMA MELLAL, BELKACEM LAMRI, Etude du comportement d'une marne argileuse traitée à la chaux pour son réemploi dans la construction d'un remblai routier Cas de l'autoroute Est-Ouest Tronçon Oued Fodda/Khemis Miliana (Algérie), Colloque International Sols Non Saturés et Environnement « UNSATlemcen09 » Tlemcen, 27 et 28 Octobre 2009

[2] FEDIEX section Chaux, (2011), " Traitement de sols et Recyclage de terres à la chaux".

[3] Gontran H., Didier L. et Daniel P., (2011), "Chaux aérienne applications en Génie Civil", Technique de l'ingénieur

[4] Norme AFNOR bleu de méthylène NF P 94-068 LTPS.

[5] Norme AFNOR limite d'Attrebarg NF P 94-051 LTPS.

[6] Norme AFNOR Reconnaissance et Essais – Détermination des références de compactage d'un matériau - Essai Proctor normal – Essai Proctor modifié NF P 94-093.

[7] Zalihe .NALBANTOGLU, Lime stabilization of expansive clay. Expansive soils-recent advances in characterization and treatment, Taylor & Francis group, London, 2006, p. 341-348.

Analysis of the Response of Piles under Lateral Stresses

Djenette. Mendjel, Souhila. Rehab Bekkouche, and Ghania. Boukhatem

***Abstract*—** The present study aims to understand the behavior of piles placed in uniform soil (monolayer) and subjected to a lateral static load. Depending on the loading conditions and the type of soil in which the pile is placed, the response of the piles is determined by a numerical finite element calculation describing the variation of displacements along the pile. The study made it possible to characterize the influence of the lateral loading on the displacements at the head of the pile. The comparison of numerical simulation results with those obtained from the analytical analysis was presented.

***Keywords*—** displacement, lateral load, numerical analysis, piles.

I. INTRODUCTION

PILES foundations are structural elements commonly used in civil engineering. They are dimensioned to take at the same time axial forces, lateral forces, and moments. Their mechanical behavior has been the subject of much research that led to the widely adopted design methods in the profession [1].

The response of a pile subjected to a lateral load is influenced by the mechanical characteristics of the pile, by nature and the linear and nonlinear behavior of the soil and the loading law. The parameters to consider when sizing are so varied and numerous, they concern the boundary conditions, geometry, nature of the pile and soil [2].

In most cases, the dimensioning criterion is not the ultimate lateral capacity of the pile but the displacements at the head and the maximum moment. On these bases, various methods have been established for the analysis of piles under lateral loads. In general, there are three types of methods: analytical, numerical and experimental.

An effective method for sizing thus requires: a relevant soil behavior law, a model to define the soil-pile interaction (P-y curves) and a technique for numerical resolution [3].

Djenette. Mendjel is a Associate Prof. in the Civil Engineering Department, Skikda University, Algeria (corresponding author; e-mail: rech_mendjel@yahoo.fr).

Souhila. Rehab Bekkouche is a Associate Prof. in the Civil Engineering Department, Skikda University, Algeria (e-mail: solrehab@yahoo.fr).

Ghania. Boukhatem is a Associate Prof. in the Civil Engineering Department, Annaba University, Algeria (e-mail: gboukhatem3@yahoo.fr).

The behavior of a single pile subjected to horizontal loading has been studied by several authors [4]–[9].

It remains difficult to grasp comprehensively the reactions of the soil to piles solicitations, for this purpose we try to identify some parameters that can influence the behavior of piles. This study presents the behavior of a single pile under lateral load in a single layer soil by considering two models of soil elastic and elastoplastic (Mohr-Coulomb). The mechanical characteristics of piles are higher compared with those of soils, for this reason, the materials constituting the piles are frequently considered as elastic for the usual solicitations.

II. ANALYSIS MODEL

Usually laterally loaded single piles are analyzed by methods derived directly from the classical "beam on elastic foundation" mode in which the soil support is approximated by a series of independent elastic spring. The finite element method is most widely used to perform the analysis of piles under lateral loads [7].

The present study will focus on investigating the behavior of steel pile subjected to pure lateral loads in dry sandy soil by finite element analysis using the software PLAXIS 2D version 8.2 and subgrade reaction approach that assumed that soil acts as a series of independent linear elastic springs in which it is necessary to predict the value of modulus of subgrade reaction. The influence of applied lateral load magnitude and pile length on the lateral response of single pile will assess in this paper.

For the analysis model, the soil is sand with the following properties: Young's modulus (E_s= 23000 kN/m^2), Poisson's modulus (ν=0.37), cohesion (c=0), friction angle (φ=35°), coefficient of dilatants (ψ=5°), unsaturated soil weight γ=19 kN /m^3, and modulus of subgrade reaction for dense sand is k_h=6300 kN/m^2. Pile is with a diameter of D=0.4 m, E_p=2.1x10^8 kN/m^2, and length of L=13 m.

Several numerical results are presented with an interesting soil-pile behavior summarized by figures.

III. RESULTS AND DISCUSSION

A. Lateral load magnitude impact

The magnitude of load started from the small loading (50 kN) and increased gradually in equal magnitude during the

load stages until maximum intensity of (500 kN). The comparative study is made on the lateral displacements at the head of the pile and the maximum moment for different types of analysis: analytical with an elastic model of the soil and numerical considering two models of soil elastic and elastoplastic (Mohr-Coulomb). The results are shown in Fig. 1 and 2.

We find that for the elastic model the variation of lateral displacements and moment is linear which, is not the case for elastoplastic model. The analytical values of displacements coincide with those of numerical elastic model, and they are less compared to the elastoplastic model.

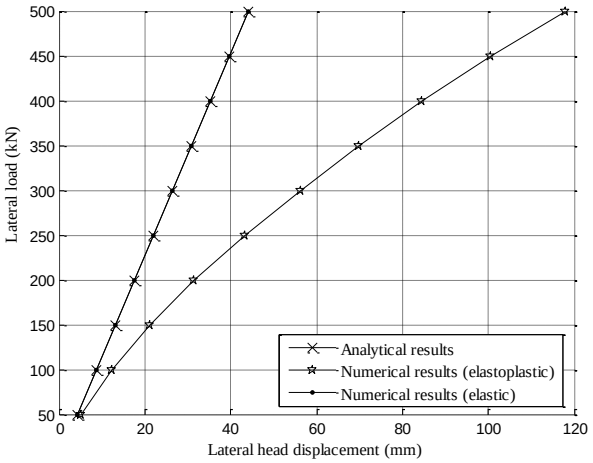

Fig. 1 Lateral load magnitude impact on head displacement

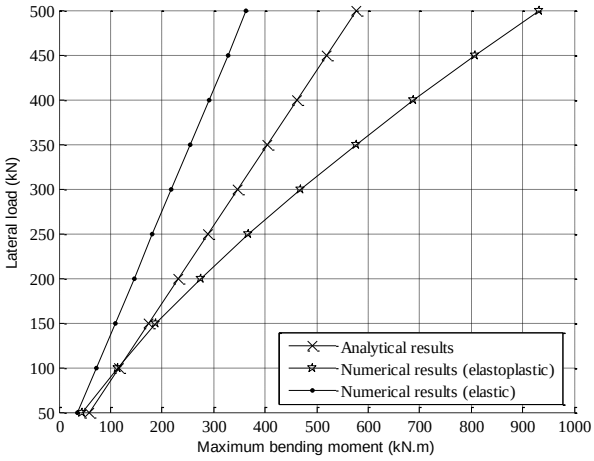

Fig. 2 Lateral load magnitude impact on maximum moment

B. Pile length impact

This section includes the effect of length variation on pile under lateral loads equal to 500 kN.

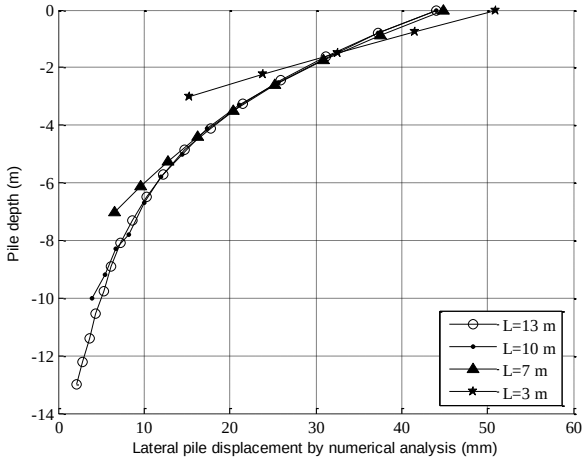

Fig. 3 Displacement variation along to pile depth for different pile length by numerical analysis.

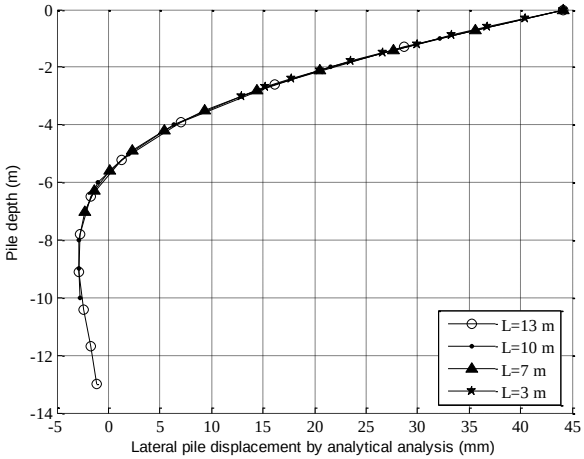

Fig. 4 Displacement variation along to pile depth for different pile length by analytical analysis.

The diameter is considered constant. The lengths taken in this study are 3 m, 7 m, 10 m, and 13 m.

Fig. 3 and 4 shows for both types of analysis that the pile which is free at the head and foot, moves linearly for L=3 m, and begins to flex beyond L=10 m.

Frank (1999) gives a transfer length (l_o) defined by the following equation [9]:

$$l_O = \sqrt[4]{\frac{4 E_p I_p}{E_S}} \quad (1)$$

Where: E_pI_p: bending rigidity of the pile

In this case, l_o=3.6 m, comparing to L we find:

L=3 m < l_o so the pile is stiff,

l_o < L=7 m and 10 m < 3.l_o so the pile is semi flexible.

L=13 m >3.l_o so the pile is flexible.

For different values of lateral load, lateral displacements tend to 0 for a depth equal to 22 m by the analytical method. Fig. 5 and 6 shows respectively displacements variation curve

for lateral loads equal to 500 kN and 50 kN.

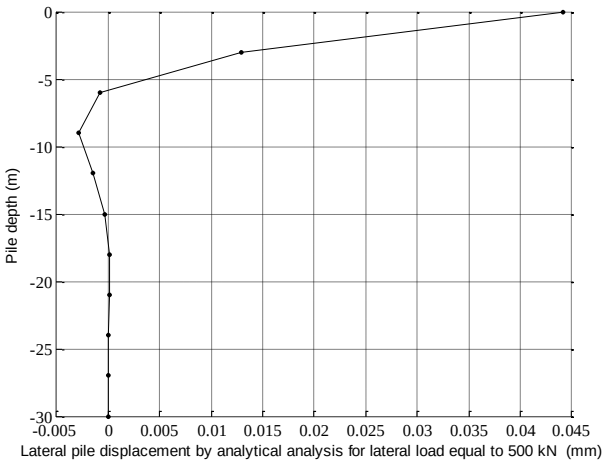

Fig. 5 Displacement variation along to pile depth by analytical analysis for lateral load equal to 500 kN.

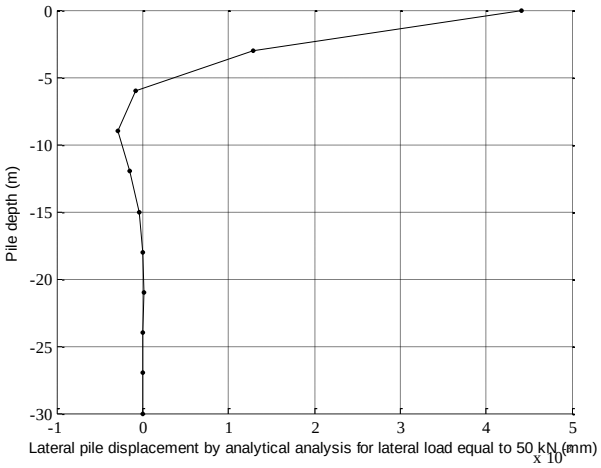

Fig. 6 Displacement variation along to pile depth by analytical analysis for lateral load equal to 50 kN.

And lateral displacements tend to 0 for a depth equal to 18 m by the numerical method.

Fig. 7 (a), 7 (b), and 8 (a), 8 (b) shows respectively displacements variation curve for lateral loads equal to 500 kN and 50 kN for elastic and elastoplastic behavior.

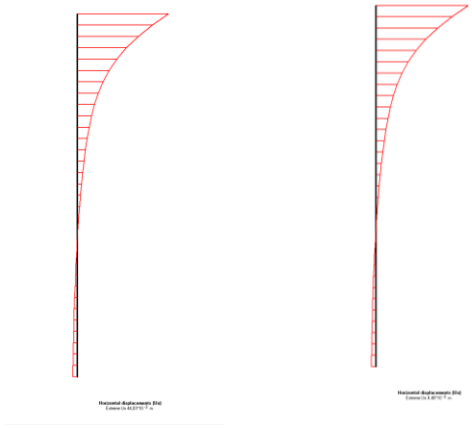

(a) (b)

Fig. 7 Displacements variation along to pile depth by numerical analysis for elastic behavior.

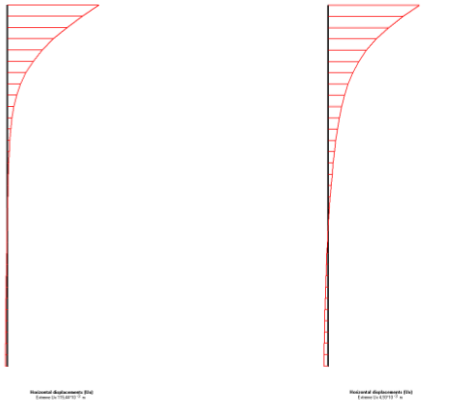

(a) (b)

Fig. 8 Displacements variation along to pile depth by numerical analysis for elastoplastic behavior.

IV. Conclusion

This study is carried out on a free single pile at the top and at the foot in sandy dry soil under the effect of a horizontal effort by two methods of analysis, finite element analysis using the software PLAXIS 2D version 8.2 and subgrade reaction approach. Lateral force and pile length variations were taken into consideration.

The results found concluded that:

Lateral displacements at the head of the pile and maximum moments increase with the increase of lateral load, the variation curves of analytical and numerical methods with an elastic behavior for lateral displacements are the same, which shows the reliability of the models chosen.

The variation in the lengths of the piles shows how the pile behaves rigidly to lengths less than the transfer length and flexible beyond three times the transfer length.

The pile appears recessed for a fixed length whatever the value of the applied load, which shows that the embedding length does not depend on the load value. Under the effect of

lateral loading, the response of a pile depends on its stiffness and soil.

REFERENCES

[1] L. Hazzar, *Analyse numérique de la réponse des pieux sous sollicitations latérales*, Thèse de doctorat, Sherbrooke (Québec), 2014.

[2] D. Remaud, *Pieux sous charges latérales : étude expérimentale de l'effet de groupe*, Thèse de doctorat, Nantes, 1999.

[3] O. Addaci, *Analyse numérique par la méthode des éléments finis d'un pieu isole sollicite par une charge latérale*, Thèse de magistère, Université El Hadj Lakhdar Batna, Algérie, 2012. .

[4] [4] Jasim M. Abbas, Qassun S. Mohammed Shafiqu, and Mohd R. Taha "Effect of shape and slenderness ratio on the behavior of laterally Loaded piles*" The 1st Regional Conference of Eng. Sci. NUCEJ Spatial ISSUE*, vol.11, no.1, 2008 pp 19-27.

[5] H. G. Poulos, and E. H. Davis, "Pile foundation analysis and design," University of Sydey, 1980, pp. 163–225.

[6] O. Taheri, R. Z. Moayed, and M. Nozari, "Lateral soil-pile stiffness subjected to vertical and lateral loading", *Journal of geotechnical and transportation engineering*, vol. 1, no. 2, pp. 30-37, 2015.

[7] W. Jerin Wiba, V. Jeyanthi Vineetha, "Behavior of laterally loaded piles in cohesionless soils", *IJRET*, vol. 3, no. 11, pp. 179-181, 2014.

[8] V.S. Phanikanth, D. Choudhury, and G.R. Reddy, "Response of single pile in cohesive soil under lateral load", *13th International Conference of the IACMAG*, pp. 889- 904, 2011.

[9] F. Rosquoet, *Pieux sous charge latérale cyclique : étude expérimentale de l'effet de groupe*, Thèse de doctorat, Nantes, 2004.

Factors Affecting the Talent Development of Early Career Academics

Nicolene Barkhuizen, Nico Schutte, Dorcas Lesenyeho

***Abstract*—** Continuous changes in higher education require academic staff to adapt, maintain, and advance their careers. The main objectives of this research were to explore the perceptions of early career academics of the available career development opportunities, and to investigate the extent to which they are taking responsibility for their own career development through dispositional employability. A mixed-method research approach was followed. The Talent Development Questionnaire and the Dispositional Measure of Employability were distributed among early career academics of selected merged South African higher education institutions (n = 117). Follow-up interviews were conducted with early career academics to validate the quantitative results (N = 23). The results showed that early the career academics experienced role clarity in terms of their development opportunities, that they were able to apply skills learned to their job, and that they could make joint decisions with their managers regarding their career development. These early career academics were able to take care of their own employability by displaying high levels of optimism, career proactivity, openness to change, career resilience, and career motivation.

***Keywords*—** Career development, Dispositional employability, Early career academics, Talent Management

I. Introduction

Massification and globalisation have brought about a changed workplace for South African academics, one in which they have to adapt to new expectations and identities of students [1]. Accordingly, academics need to broaden their portfolio of expertise to adapt, maintain, and advance in their careers, in order to remain relevant and meet broader society's needs [2]. At the same time, higher education institutions (HEIs) are required to institute formal career development opportunities and career-orientated strategic plans to equip academics with the teaching skills to meet the needs of a new generation of students [3]

The career development of academic staff is not without challenges. Garraway [4] found confusion between the purpose of academic staff development and the methods to achieve it. This study further showed that structures, institutions' cultures, and marginalisation may hamper the career development of academic staff. According to Styger, van Vuuren, and Heymans [5], insufficient government funding hampers academic staff's development initiatives significantly. The insufficiency of career- and development opportunities for academic staff has implications for the motivation, commitment, success, and employability of academics, and could ultimately lead to the devaluation of a professoriate [6].

As a result, academics are, in many cases, forced to take control of their own career development in order to remain attractive hires [7]. A study by Hopkins [8] showed that academic staff continuously choose to migrate to HEIs in different countries as part of their career development. Career advancement and the development of the 'new' academic career are thus individually determined, and academics may adopt certain 'dispositions' to enhance their employability.

Dispositional employability refers to psycho-social characteristics (i.e. openness to change, career motivation, career resilience, career proactivity, career optimism, and work identity) that make people employable [9]. An investigation of dispositional employability is imperative where talented individuals are challenged to obtain and retain a desired job [10].

The main objective of the present study was twofold. First, the research aimed to explore the perceptions of early career academics in terms of the available career development opportunities. Second, the study investigated the extent to which early career academics are taking responsibility for their own career development through dispositional employability. The present research was motivated by the fact that little research currently exists on the career development of academics in general [11].

In what follows, the literature review for this research is presented.

II. Literature Review

A. Academic career development in Higher Education

The importance of institutional support in the career development of academics is well documented. A study by Bashir and Long [12] showed that supervisor support for

Nicolene Barkhuizen, is the Director of the Global Innovative Forefront Talent (GIFT) Research Niche Area, North-West University, South Africa, 2745, nicolene.barkhuizen@nwu.ac.za

Nico Schutte is a Full Professor of GIFT Research Niche Area, North-West University, South Africa, 2745

Dorcas Lesenyeho is a Director at the Office of the Public Service Commission, Mmabatho, South Africa, 2745

training enhanced the sense of belonging and loyalty of academic staff to HEIs. This research further highlighted the importance of communicating the availability of training and in-house training and developing activities to enhance the teaching and research skills of academic staff. A study by Barkhuizen [13] among academics in South African HEIs showed that academics valued opportunities to participate in training courses and joint decision-making in work activities. The study further pointed out the importance of role clarity and expectations for career advancement and development.

Studies have also pointed out the importance of acquiring job-specific skills through career development and the application thereof in the work context. Svetlik and Braček Lalić [14] found that academics from Slovenian public universities valued their involvement in international activities, and that the experience contributed significantly to their professional development and promotion. A study by Frantz, Leach, Pharaoh, Basset, and Roman et al. [15] found that international collaboration not only enhanced the research capacity of academic staff, but also fostered intra- and inter-disciplinary relationships. Ansmann et al. [16] noted the importance of providing effective networking opportunities for early career academics to promote their career development.

Although early career teaching experience is an expectation, great emphasis is placed on developing teaching expertise of academic staff through mandatory continuous professional development [2]. According to Centra (in Stes & van Petegem [17], the focus of instructional development is "to develop faculty members in their role as teachers," while professional development is concerned with career development of the faculty member, and is not limited to teaching, but includes research and social services.

Weimer and Lenze [18] stated that there are two reasons why early career academics are often targeted for instructional development, these being: 1) they have little or no teaching experience, which results in a low teaching quality, and 2) they have not yet been given tenure, which makes it easier to encourage them to engage in instructional development. According to Brew [19] academic development may focus too much on enhancing research, neglecting teaching and learning. Likewise, Essack and Naidoo [20] argued that teaching quality and its indicators are not adequately debated within the higher education sector, despite the importance thereof in producing quality students. This could be the result of a misalignment between the focus of academic staff development and institutional imperatives (Greyling, in Botha & Potgieter, [21]. According to Singh [22], the need for increased postgraduate outputs forces HEIs to focus on research capacity-building in the areas of supervision, publication, and staff qualifications. Research, as a measure of competitiveness and attraction of government funding, is therefore high on the agenda of HEIs [5].

B. Dispositional Employability

Fugate and Kinicki [23] developed the concept of dispositional employability, which denotes a "constellation of individual differences that predispose employees to proactively adapt to their work and career environments." Dispositional employability has been related to several positive work-related outcomes, such as career success, job satisfaction, perceived employability, and reduced turnover intentions [8]; [24]; [25]; [26]; [27]. Dispositional employability consists of six dimensions: openness to change, work- and career proactivity, work- and career resilience, career motivation, optimism, and work identity [23].

Openness to change refers to the extent to which academics are flexible in the work environment and adaptive to continuous learning and meaningful experiences. According to van den Heuvel, Demerouti, Bakker and Schaufeli [28], individuals who are open to new experiences and change tend to be more adaptive to work dynamic requirements, allowing them better manage and deal with stress-related matters. Wolhuter, van der Walt, Higgs, and Higs [29] found that academics did not perceive the ever-changing academic environment as an obstacle. Lichy and Pon [30] found that change initiatives in French HEIs enable academic staff to change their work activities as they wish. Furthermore, the continuous internationalisation of higher education in the 21st century creates opportunities for academic staff to enroll for post-doctorate studies abroad, which, in turn, enhances their tenure and scholarly productivity [31].

Career resilience is the extent to which individuals are optimistic about their career opportunities and work, the extent to which they feel that they have control over the destiny of their careers, and feel that they are able to make a marked contribution through their work [23]. According to Martin and Marsh [32], resilience relates to one's ability to effectively deal with setbacks, stress, and pressure in the academic environment. Martin and Marsh [32] further indicated that resilience comprises self-belief (confidence), a sense of control, low anxiety (composure), and persistence (commitment). A study by Cora-Brumble, Zhang, and Castillo-Page [33] showed that career resilience can enhance the productivity of academic staff. DeCastro, Sambuco, Ubel, Stewart, and Jagsi [34] stated that early career academics need to be career resilient in the face of criticism and rejection by senior academics.

Career motivation in the context of dispositional employability refers to the extent to which academics can make specific career plans and strategies, be in control of their own career management, and set career goals [23]. According to Siddique, Aslam, Khan, and Fatima [35], highly qualified and motivated academics can develop students both personally and professionally. However, they added that such talented and competent staff members are not motivated enough by their supervisors, and that dissatisfaction with their job, the organisation, and

management will lead to them leaving. According to Gmelch [36], the higher education system is rich with different interests, goals, priorities, values, needs, and motivational instincts, compared to other organisations. Higher education leaders can therefore use various intrinsic and extrinsic factors to motivate academics to put extra effort into their work.

Work- and career proactivity is a term used to refer to tendencies of individuals to gain information that will potentially affect their jobs and career opportunities, both within and outside of their current place of employment [23]. A study by Said, Rasdi, Samah, Silong, and Sulaiman [37] showed that proactive behaviour has a significant impact on the career success of academic staff when institutional support is available.

Work identity refers to the degree to which individuals can define themselves in terms of their particular organisation, job, profession, or industry [23]. Currently, the work identity of academics is affected by the numerous changes in the higher education environment. The significant decrease in government- and research funding has transformed public universities into 'academic capitalists' who are compelled to generate a third stream of income [38]. This may eventually compromise teaching, research, consultancy skills, or other forms of application of academic knowledge, and lead to a loss of professional autonomy, scholar identity, and psychological ownership [6]. As mentioned by Quigley [39], academic identity lacks precision, because it is influenced by many competing influences. A study by Smit, Crafford, and Schurink [40] found that the activities in which academics engage are of critical importance to their work identity. Nyamupangedengu [41] found that early career academics need to develop a common language to negotiate their space in HEIs.

III. RESEARCH DESIGN

A mixed-method research approach was used in the present study. According to Cresswell [42], mixed-method research is rapidly expanding in social and human sciences globally. Onwuegbuzie, Bustamante, and Nelson [43] defined mixed-method research as a process that combines quantitative and qualitative methods to gain a broader and deeper understanding of research. The present study followed a sequential mixed-method design, where quantitative data were gathered first, followed by collection of qualitative data [44].

A. Research Participants

The respondents were academic staff from 11 public HEIs in South Africa. A total of 294 surveys were distributed to a purposive convenience sample of academics. A response rate of 40% (n = 117) was achieved. A total of 51.3% of the sample consisted of women, while male respondents made up 46.2% of the sample. The ethnicity of the sample was divided into 47.9% white, followed by 37.6% black African, 7.7% Indian, and 3.4% Coloured. The age group with the highest number of respondents was 40–49 years (34%), while, on a cumulative basis, 82% of the respondents were older than 40 years. The largest single group of respondents was those in possession of a Master's degree (49.6%), and, combined, 75.4% of the respondents had either a Master's degree or a doctorate. The largest group of respondents was employed on lecturer level (54.7%), followed by senior lecturer level (33.3%). The majority of respondents had 0–5 years' work experience in academia (53%), and had been employed for 0–5 years in their current job (70.9%).

Follow-up interviews were conducted with 23 early career academics from selected HEIs. Most of the participants in were male (N = 15), employed as lecturer (N = 16), in possession of a Master's degree (N = 13), and representative of the black African ethnic group (N = 14).

B. Measuring Instruments

Two measuring instruments were used in the present study: a Talent Development Scale [13] and the Dispositional Measure of Employability [23]. The Talent Development Scale consists of 15 items and measures three dimensions: Skill utilisation, Participation in career decisions, and Role clarity. Responses are measured on a four-point Likert scale ranging from Never (1) to Always (4). This questionnaire obtained acceptable internal consistencies in the South African context [13].

An adapted version of the Dispositional Measure of Employability, developed by Fugate and Kinicki [23], was used to measure the respondents' orientation towards their work and their employability. The adapted questionnaire consisted of 19 items and measured five dimensions: Openness to change, Career proactivity, Career resilience, Career motivation, and Optimism. Responses were measured on a six-point Likert scale ranging from Strongly disagree (1) to Strongly agree (6). This questionnaire has been validated in the South African context [24].

Permission for the project was first obtained from the Head of Skills Development of Higher Education South Africa. The questionnaires were distributed in hard copy, via the skills development facilitators, to a convenience sample of academics in the identified HEIs. Permission to use the questionnaires was obtained from the relevant developers, and their use was subjected to an ethical clearance process. Questionnaires were treated anonymously, to protect the identity of the respondents.

C. Data Analyses

Data analyses were carried out with the aid of SPSS software [45]. Exploratory factor analysis was performed to determine the factor structure of the measurements. Cronbach alphas were used to determine the reliability of the questionnaires. A cut-off point of 0.7 was used as a guideline for acceptable reliabilities [46]. Descriptive statistics, such as

means, standard deviations, skewness, kurtosis, and cross-tabulations were used, due to the descriptive nature of this study. The quantitative findings of this study were supplemented by verbatim quotes from the participant interviews.

IV. RESULTS AND FINDINGS

The Kaiser-Meyer-Olkin measure of sampling adequacy (MSA) was used. An MSA of 0.780 was obtained for the Talent Development Scale. According to the guidelines, an MSA greater than 0.6 is adequate for factor analysis [47]. Principal components analysis was done of the 15 items of the Talent Development Scale. The initial results showed that three factors could be extracted, based on the eigenvalues. A subsequent principal components analysis was done, using varimax rotation, to specify three factors. Four items were deleted because of problematic loadings. The three factors explained 68.05% of the variance, and were labelled Role clarity (Factor 1), Skill utilisation (Factor 2), and Participation in career decisions (Factor 3).

Principal component analysis was performed on the 19 items of the Dispositional Measure of Employability. The initial results showed that five factors could be extracted, based on the eigenvalues. A subsequent principal components analysis was performed, using varimax rotation, to specify five factors. The five factors explained 67.324% of the variance, and were labelled Optimism (Factor 1), Career proactivity (Factor 2), Openness to change (Factor 3), Career resilience (Factor 4), and Career motivation (Factor 5).
Next, the descriptive statistics and reliabilities of the measurements are reported, in Table 1, below.

TABLE I
DESCRIPTIVE STATISTICS OF MEASUREMENTS

	Mean	SD	Skewness	Kurtosis	α
Talent development					
Skill utilisation	2.9915	.68065	-.415	-.495	.802
Career decisions	2.9715	.65004	-.389	.339	.749
Role clarity	2.7350	.71415	-.153	-.416	.865
Dispositional employability					
Optimism	4.6560	.89342	-1.457	3.423	.783
Career proactivity	4.8085	.72796	-.906	1.129	.798
Openness to change	5.0235	.60528	-.675	1.283	.811
Career resilience	4.9715	.74481	-1.382	4.185	.718
Career motivation	4.4843	.90813	-.414	-.065	.691

The results in Table 1 show acceptable reliabilities for all the measurements according to the guideline of $\alpha \geq 0.70$ (Field, 2009). The above results are further explored in the next section and supplemented by verbatim quotes from the participant interviews.

A. Theme: Talent development

From the results, it is evident that early career academics are able to apply their skills in the workplace. They have influence in decisions relating to their careers, and they have role clarity. The interview participants, in particular, highlighted opportunities for rapid progress in academia:

"Rapid progress is very possible without being favoured by your input. So, if you can come and you start as a junior lecturer, within four years, you can become a senior lecturer, which may not be the case if you joined with someone in the public service" (Participant 1, male, senior lecturer, doctorate, black African).

Another participant highlighted the opportunity to apply skills and be creative:

"I think it's really an environment where one can be creative. I consider myself as a creative person. I like to busy myself with the creation of new concepts, new ways of thinking, and new ways of solving problems" (Participant 11, male, lecturer, Master's degree, white).

Other participants, however, highlighted the need to develop certain academic skills further. One participant noted:

"Allow academics to supervise Masters' students, because the more you supervise, you're going to publish articles, and that works towards your growth as an individual in terms of getting promotion" (Participant 12, male, lecturer, Master's degree, black African).

In support, Participant 3 added:

"In some other universities, they have this thing 'work-integrated learning,' where they give you an internship programme for about six months, that you can graduate. I think, if they could also implement that here, it will also give us an opportunity to be able to, not only teach theory to students, but, if we can actually tell them something practical, that would be perfect for us" (Participant 3, junior lecturer, female, honours degree, black African).

B. Theme: Dispositional employability

Generally speaking, the early career academics displayed high levels of dispositional employability. From the mean scores, it was evident that early career academics are optimistic about their careers, which was mentioned by one of the interview participants:

"I love it. I love my job, and not one day I felt like I don't want to do it. I believe that not everything is perfect, you have frustrations, but my major philosophy in life is that you've got a choice how to handle adversities, and I think I'm very resilient, because I'm positive" (Participant 10, female, senior lecturer, doctorate, white).

Another participant added that he was optimistic about the future of academia, and stated:

"*Yes, in the sense that there will be a future in the academic system when the academics take upon themselves*

the responsibility of improving the school, the purpose, the quality, the visions, and the missions of education" (Participant 7, male, senior lecturer, doctorate, black African).

The academics in this sample also displayed high levels of career proactivity. One of the participants stated:

"I think it also depends on the career opportunities — what you create for yourself, and I think that is something that's possible in the university — to create career opportunities for yourself. Career opportunities are progressing in terms of lecturing, but are also progressing in terms of research" (Participant 8, female, lecturer, Master's degree, white).

Participants further noted:

"*There are a lot of structures and interventions that is available through the university, so I would like to develop as a researcher very strongly. I've got a really clear picture of what it is that I want to do in my research going into the future... You can keep your finger on the pulse, so you can really be up to date with what is happening"* (Participant 11, male, lecturer, Master's degree, white);

And

"Well, what I know is, upon joining the university, I realised that measures had been put in place for me to pursue further studies, and those measures are still available, and it is upon individuals to take up the offer available and work" (Participant 1, male, senior lecturer, doctorate, black African).

The results furthermore showed that the respondents displayed high levels of openness to change relating to career exploration and development. One of the interview participants stated:

"At this stage, I don't want to limit myself in terms of fields. I think I'm still young enough, where I think I still need to explore. We have such diverse research fields that I'm still open to change it" (Participant 8, female, lecturer, Master's degree, white).

Another participant highlighted the need for higher education systems to change:

"*Yes, first and foremost, the entire system of education must be fully revisited, because, at the moment, my point of view is that the system has totally collapsed. It must not just be education for the sake of education ... it must be education that is meant to build"* (Participant 7, male, senior lecturer, doctorate, black African).

The respondents also appeared to display career resilience. One of the interview participants stated:

"Specifically, I want to find myself career advancement, and the one that I'm looking for is in the academics. He has to occupy his specific role in the recession under social economic and political environment, and to help also to motivate and supervise under difficult circumstances" (Participant 7, male, senior lecturer, doctorate, black African).

Another participant added:

"One of the biggest problems they may have is the progression on their further studies, and, if there is a delay in acquiring further qualifications, they tend to get frustrated, as they then stagnate in the positions in which they are. Opportunities are there for them to apply for further qualifications and improving their qualifications, and the university made provision for them to work towards senior posts" (Participant 1, senior lecturer, male, doctorate, black African).

The results also showed that the respondents experienced career motivation. One of the participants stated:

"I think the first point is a position where one can develop oneself, because when you come to an environment where we have doctors and professors, it actually motivates you to keep on — I mean inspired by that, and get to the highest level" (Participant 2, lecturer, male, Master's degree, black African).

Another participant, however, cautioned that career advancement can have a negative impact on career motivation, stating:

"The problem is that most of them will compare themselves to others, to their counterpart, to the contemporaries that would have gone in other areas. There are other areas where you can progress very fast, and that can be very frustrating to them" (Participant 1, senior lecturer, male, doctorate, black African).

V.DISCUSSION

The main objectives of this research were to determine, firstly, early career academics' perceptions of career development opportunities in South African HEIs, and, secondly, the extent to which early career academics take responsibility for their own career development through dispositional employability.

The results of the research show that the early career academics experience role clarity in terms of their career development opportunities [12]. The results also indicated that they can make joint decisions relating to their career development opportunities with supervisors, and apply the skills learned on their jobs [13]; [14]. In this context, the HEIs allow early career academics to be creative in their jobs. In line with previous research, the participants also observed that the availability of career development opportunities enables them to progress rapidly in their careers [7]. However, some participants highlighted the need for more development relating to certain functions of the academic profession, such as student supervision. In line with Garraway [3], these findings highlight the need for HEI management to implement programmes to develop the contemporary academic skills required by HEIs. Participants also highlighted the need for further development in teaching skills and the implementation of programmes such as work-integrated learning to enhance the employability of students.

In line with the findings of Fahnert [1], it is clear that the participants also recognised the need for teaching excellence in higher education.

The results of this research also show that early career academics take responsibility for their own career development and advancement. The early career academics in this sample generally displayed high levels of optimism, career proactivity, openness to change at work, career resilience, and career motivation. As with previous studies, the respondents showed that they were able to deal with frustration and adversity in the work environment [32]. The participants also believed that they should be proactive and take it upon themselves to improve their work environment and the quality and vision of the institution [35]. In a similar vein, other participants felt that they were responsible for creating their own career, and should use the opportunities that the universities present to advance their teaching and research.

The participants also indicated that they are open to change, and want to use the opportunities brought about by change to advance their careers [29]. Other participants indicated that they were motivated by the fact that the university provided them with opportunities to further their qualifications [33]. The participants, however, did highlight that they feared stagnation after obtaining a qualification. In this context, the availability of post-doctorate studies could be beneficial in enhancing their career success [30]. Participants, however, also raised concerns that the education system is collapsing, and that more emphasis should be placed on practising teaching that builds societies.

VI. IMPLICATIONS

From a practical point of view, this research showed that career development opportunities are available for early career academics. However, there must be a balance the between teaching and research skills development of academics. Furthermore, early career academics require proper career development guidance in an ever-changing higher education environment, to ensure that they remain relevant and employable. Higher education managers are also encouraged to develop a talent culture with more in-house, state-of-the-art career development programmes that will contribute to a pipeline of talented novice scholars. Higher education management should further capitalise on the high levels of dispositional employability of early career academics, and use it as a tool to motivate the self-development of academics, while, at the same time, retaining them.

VII. LIMITATIONS AND RECOMMENDATIONS

This research had some limitations. First, a cross-sectional research approach was used, which means that perceptions of career development were measured at one point in time. Given the current changing situation of HEIs, these perceptions are likely to change over the long term. Therefore, longitudinal research should be carried out to detect perceived career development opportunities over the long term. Second, this research only focused on early career academics. As a result, the findings cannot be generalised to other academic job levels.

For future research, it is recommended that the sample size be expanded to include other academic job levels, to enable a comparative analysis regarding career development opportunities. The research should also be expanded to include higher education management and human resource management departments, to obtain a more holistic perspective on academic career development in HEIs. The results of the present study show that the early career academics were positive about their career development opportunities, and that they displayed high levels of dispositional employability. Future research could benefit from including variables (e.g., management support) that can explain academics' perceptions of career development. Furthermore, future research should also focus on the individual and organisational outcomes of career development opportunities for early career academics.

VIII. CONCLUSION

In conclusion, this research highlighted the importance of career development for early academics in South African HEIs. Although the results are positive, there is a critical need to develop more customised talent development processes and programmes for early career academics, to ensure a future pool of talent scholars who can make a valuable contribution to society through excellence in their teaching and research.

REFERENCES

[1] K. Maree, "Barriers to access to and success in higher education: Intervention guidelines: Part 2," *South African Journal of Higher Education*, vol. 29, no. 1, pp. 390-411, 2015

[2] B. Fahnert, "Teaching matters — academic professional development in the early 21st century," FEMS Microbiology Letters, vol. 362, no. 20, pp. 1-6, 2016.

[3] M. D., Mohan, S. Muthaly, and J. Annakis, "Talent culture's role in talent development among academics: Insights from Malaysian government linked universities," *Journal of Contemporary Issues in Business and Government*, vol. 21, no. 1, pp. 46-71, 2015.

[4] J. Garraway, "Academic staff development in foundation provision," *South African Journal of Higher Education*, vol. 29, no. 1, pp. 26-44, 2015.

[5] A. Styger, van G. W. Vuuren, and A. Heyman, "Government funding framework for South African higher education institutions," *South African Journal of Higher Education*, vol. 29, no. 2, pp. 260-278, 2014.

[6] E. M. Bitzer, "The professoriate in South Africa: Potentially risking status inflation," *South African Journal of Higher Education*, vol. 22, pp. 265-281, 2008.

[7] M. Pang, B. Chua, and C. W. L. Chu, "Learning to stay ahead in an uncertain environment," *International Journal of Human Resource Management*, vol. 19, pp. 1383-1394, 2008.

[8] J. Hopkins, "A comparative study examining academic cohorts with transnational migratory intentions towards Canada and Australia," *Higher Education Quarterly*, vol. 70, no. 3, pp. 246-263, 2016.

[9] D. Maslić Seršić, and J. Tomas, "The role of dispositional employability in determining individual differences in career success," *Društvena Istraživanja*, vol. 23, no. 4, pp. 593-613, 2014.

[10] N. D. De Cuyper, B. I. J. M. Van der Heijden, and H. De Witte, "Associations between perceived employability, employee well-being, and its contribution to organizational success: A matter of psychological contracts?" *The International Journal of Human Resource Management*, vol. 22, no. 7, pp. 1486-1503, 2011.

[11] M. Van der Klink, B. van der Heijden, J. Boon, and van S. W. Rooij, "Learning to stay employable," *Career Development International*, vol. 19, no. 5, pp. 508-525, 2014.

[12] N. Bashir, and C. S. Long, "The relationship between training and organisational commitment among academicians in Malaysia," *Journal of Management Development*, vol. 34, no. 10, pp. 1227-1245, 2015.

[13] E. N. Barkhuizen, "*Work wellness of academic staff in South African higher education institutions*" Unpublished doctoral thesis, North-West University, Potchefstroom, South Africa, 2005.

[14] I. Svetlik, and A. Braček Lalić, "The impact of internationalisation of higher education on academic staff development — the case of Slovenian public universities," *Studies in Higher Education*, vol. 41, no. 2, pp. 364-350, 2016.

[15] J. M Frantz, L. Leach, H. Pharaoh, S. H. Bassett, N. V. Roman, et al., "Research capacity development in a South African higher education institution through a north-south collaboration," *South African Journal of Higher Education*, 28, no. 4, pp. 1216-1229, 2014.

[16] L. Ansmann, T. Flickinger, S. Barello, M. Kunneman, S. Mantwill, et al., " Career development for early career academics: Benefits of networking and the role of professional societies," *Patient Education and Counseling*, vol. 97, pp. 132-134, 2014.

[17] A. Stes, and P. van Petegem, "Instructional development for early career academics: An overview of impact," *Educational Research*, vol. 53, no. 4, pp. 459-474, 2011.

[18] M. Weimer, and L. F. Lenze, "Instructional interventions: A review of the literature on efforts to improve instruction" In R. Perry Ed. and J. Smart, *Effective teaching in higher education*, pp. 205-240. New York: Agathon Press, 1998.

[19] A. Brew, "Evaluating academic development in a time of perplexity," *International Journal for Academic Development*, vol. 12, no. 2, pp. 69-72, 2007.

[20] S. Y. Essack, and I. Naidoo, "Teaching and learning indicators in university rankings," *South African Journal of Higher Education*, vol. 27, no. 1, pp. 42-47, 2013.

[21] L. S. Botha, and F. J. Potgieter, "Understanding skills development in South African higher education institutions," *South African Journal of Higher Education*, vol. 23, no. 2, pp. 28-45, 2009.

[22] R. J. Singh, "Current trends and challenges in South African higher education," *South African Journal of Higher Education*, vol. 29, no. 3, pp. 1-7. 2015.

[23] M. Fugate, and A. J. Kinicki, "A dispositional approach to employability: Development of a measure and test of its implications for employee reactions to organizational change," *Journal of Occupational and Organizational Psychology*, vol. 81, pp. 503-527, 2008.

[24] K. Botha, *The relationship between dispositional employability and career success of HR Practitioners in the South Africa*. Unpublished Master's dissertation, Department of Human Resource Management, University of Pretoria, Pretoria, South Africa, 2011.

[25] A. M. Jasmer, *Dispositional employability and the relationship to career success: A meta-analysis*. Unpublished Master's thesis, Faculty of California State University, San Bernardino, 2015

[26] J. Torrent-Sellens, P. Ficapal-Cusi, and J. Boada-Grau, "Dispositional employability and online training purchase. Evidence form employees' behaviour in Spain," *Frontiers in Psychology*, vol. 7, p. 831, 2016.

[27] M. Smith, *The relationship between work stressors, work wellness and intention to quit of managers at a large South African mining house*. Unpublished Master's dissertation, Department of Human Resource Management, University of Pretoria, Pretoria, South Africa, 2013.

[28] M. van den Heuvel, E. Demerouti, A. Bakker, and W. Schaufeli, Adapting to change: The value of change information and meaning-making, Journal of Vocational Behaviour, vol. 83, pp. 11-21, 2013.

[29] C. Wolhuter, H. Van der Walt, L. Higgs, and P. Higgs, "Die akademiese professie in Suid-Afrika se belewing van die huidige rekonstruksie van die samelewing en die hoër onderwys," *Tydskrif vir Geesteswetenskappe*, vol. 47, no.4, pp. 501-515, 2007.

[30] J. Lichy, and K. Pon, For better or for worse: "The changing life of academic staff in French business schools". *Journal of Management Development*, vol. 34, no. 5, pp. 536-552, 2015.

[31] L. Yang, and K. L. Webber, "A decade beyond the doctorate: The influence of a US postdoctoral appointment in faculty career, productivity and salary," *Higher Education: The International Journal of Higher Education Research*, vol. 7, no. 4, pp. 667-687, 2015.

[32] A. J. Martin, and H. W. Marsh, "Academic buoyancy: Towards an understanding of students' everyday academic resilience," *Journal of School Psychology*, vol. 46, pp. 53-83, 2008.

[33] D. Cora-Bramble, K. Zhang, and L. Castillo-Page, "Minority faculty members' resilience and academic productivity: Are they related?" *Academic Medicine*, vol. 85, no. 9, pp. 1492-1498, 2010.

[34] R. DeCastro, D. Sambuco, P. A. Ubel, A. Stewart, and R. Jagsi, "Batting 300 is good: Perspectives of faculty researchers and their mentors on rejection, resilience, and persistence in academic careers," *Academic Medicine*, vol. 88, no. 4, pp. 497-504, 2013.

[35] A. Siddique, H. D. Aslam, M. Khan, and U. Fatima, "Impact of academic leadership on faculty's motivation and organizational effectiveness in higher education system," *International Journal of Business and Social Science*, vol. 2, no. 8, pp. 70-78, 2011.

[36] W. H. Gmelch, *The call for department leaders*, New York: Paper presented at the Annual Meeting of the American Association of Colleges for Teacher Education, 2002.

[37] A. A. Said, R. M. Rasdi, A. A. Samah, A. D. Silong, and S. Sulaiman, "A career success model for academics at Malaysian research universities," *European Journal of Training and Development*, vol. 39, no. 9, pp. 815-835, 2015.

[38] P. Ntshoe, L. G. Higgs, C. C. Higgs, and I. Wolhuter, "The changing academic profession in higher education and new managerialism and corporatism in South Africa," South African Journal of Higher Education, vol. 22, pp. 391-403, 2008.

[39] S. A. Quigley, 2011, "Academic identity: A modern perspective," *Educate*, vol. 11, no. 1, pp. 20-30.

[40] R. A. Smith, A. Crafford, and W. J. Schurink, "Reflections on shifts in the work identity of research team members," *SA Journal of Human Resource Management/SA Tydskrif vir Menslikehulpbronbestuur*, vol. 13, no. 1, pp. 1-12, 2015.

[41] E. Nyamupangedengu, "Finding a voice: Reflections on a long journey from silent student to confident teaching educator," *South African Journal of Higher Education*, vol. 28, no. 6, pp. 2065-2078, 2014.

[42] J. W. Creswell, Steps in conducting a scholarly mixed methods study. DBER Speaker Series. Paper 48. http://digitalcommons.unl.edu/dberspeakers/48, 2013.

[43] A.J. Onwuegbuzie, R.M. Bustamante, and J.A. Nelson, "Mixed method as a tool for developing quantitative instruments," *Journal of Mixed Methods Research*, vol. 4, 1, pp. 56-68, 2010.

[44] F. G. Gonzalez-Castro, J. G. Kellison, S. J. Boyd, and A. Kopak, "A methodology for conducting integrative mixed methods research and data analyses," *Journal of Mixed Methods Research*, vol. 4, no. 4, pp. 342-360, 2010.

[45] SPSS Inc. *SPSS 23 for Windows*. Chicago, IL: Author, 2016.

[46] A. Field, *Discovering statistics using SPSS*. 2nd ed. London: Sage Publications, 2009.

[47] J. F. Hair, W. C. Black, B. J. Babin, and R. E. Anderson, *Multivariate data analysis: A global perspective*. 7th ed. New Jersey: Pearson Education, 2010.

Thermo-Mechanical Behavior of Non Symmetric (Al/Al_2O_3) FGM Sandwich Plates

SAIDI Hayat[a], A. Tounsi[b], EA. Adda Bedia[c]

Abstract— The analytical solution of non-symmetric functionally graded sandwich plates subjected to thermo-mechanical loading has been investigated by the use of a higher order shear deformation theory. This theory accounts for adequate distribution of the transverse shear strains in the thickness of the plate and satisfies the traction free boundary conditions on the top and bottom surface of the plates, thus a shear correction factor is not required.

The governing equations of equilibrium of non symmetric functionally graded sandwich plates can be obtained using virtuel work principle and the closed form solutions are obtained by using Navier technique. The validity of the present theory is demonstrated by comparison with solution available in the literature.

The results are presented for deflections and stresses of simply supported square plates. The influences played by of side to thickness ratio, volume fraction distribution, dimensionless ratio and slenderness ratio.

Keywords—sandwich plates; shear deformation, stress; thermo-mechanical;

I. INTRODUCTION

COPOSITE laminated materials are finding wide application in many engineering fields. Therefore, a number of approximate analytical and numerical methods have been developed in this area. Such composites are made of two or more materials to obtain a good structural performance, which the constituent does not show individually. Recently, advanced composite materials known as functionally graded material have attracted much attention in many engineering applications due to their advantages of being able to resist high temperature gradient while maintaining structural integrity [1]. The functionally graded materials (FGMs) are microscopically inhomogeneous, in which the mechanical properties vary smoothly and continuously from one surface to the other. They are usually made from a mixture of ceramics and metals to attain the significant requirement of material properties. Several studies have been performed to analyze the behavior of functionally graded plates and shells. Reddy [2] analyzed the static behavior of functionally graded rectangular plates based on his third-order shear deformation theory of plates.

There have been a considerable number of studies on the sandwich plates.

Zenkour [3] presented a two-dimensional solution for bending analysis of simply supported functionally graded ceramic–metal sandwich plates. In his study, the sandwich plate faces are made of functionally graded material, the core layer is made of the isotropic ceramic material. Zenkour [4] studied the buckling and free vibration of the simply supported functionally graded sandwich plate. Woodward and Kashtalyan [5] presented the 3D elasticity solution for bending response of sandwich plates with functionally graded core. Zenkour and Alghamdi [6] studied the bending analysis of sandwich plates with functionally graded faces and homogeneous core under the effect of mechanical and thermal loads. Cinefra and Soave [7] presented the closed form solutions for free vibration of simply supported sandwich plate with isotropic faces and functionally graded core.

Saidi [8] studied thermo-mechanical bending response with stretching effect of functionally graded sandwich plates using a novel shear deformation theory.

In the present paper, analysis of non symmetric functionally graded sandwich plates under Thermo-mechanical loading is developed using a higher order shear deformation theory. This theory accounts for adequate distribution of the transverse shear strains in the thickness of the plate and satisfies the traction free boundary conditions on the top and bottom surface of the plates, thus a shear correction factor is not required.

The governing equations of equilibrium of non symmetric functionally graded sandwich plates can be obtained using virtuel work principle and the closed form solutions are obtained by using Navier technique. The validity of the present theory is demonstrated by comparison with solution available in the literature.

The results are presented for deflections and stresses of simply supported square plates. The influences played by of side to thickness ratio, volume fraction distribution, dimensionless ratio and slenderness ratio.

Procedure for Paper Submission

II. PROBLEM FORMULATION

The present plate is composed of three layers, the top and bottom layers of non-symmetric sandwich plate is made of an isotropic homogeneous material ceramic and metal

Hayat Saidi laboratoire des matériaux et hydrologie, Université de Sidi Bel Abbes, département de génie civil, faculté de la technologie, Algérie (phone: 0021391242800; e-mail: hayatsaidi2016@yahoo.fr).

A. Tounsi. laboratoire des matériaux et hydrologie, Université de Sidi Bel Abbes, département de génie civil, faculté de la technologie, Algérie

E.A. Adda.Bedia laboratoire des matériaux et hydrologie, Université de Sidi Bel Abbes, département de génie civil, faculté de la technologie, Algérie.

respectively. The core layer is made of an isotropic material with material properties varying smoothly in the thickness direction only, as shown in Figure1.

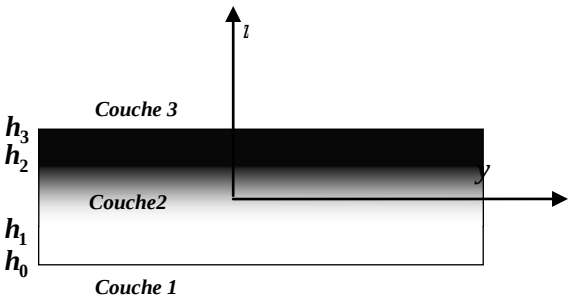

Fig.1 Geometry of the FGM sandwich pate.

The effective material properties for each layer, like Young's modulus and Poisson s ratio, can be expressed as:

$$P^{(n)}(z) = P_m + (P_c - P_m)V^{(n)} \tag{1}$$

Where Pm and Pc denote the property of the bottom and top faces of layer 1, respectively, and vice versa for layer 3 depending on the volume fraction $V^{(n)}$ (n = 1,2,3). Note that Pm and Pc are, respectively, the corresponding properties of the metal and ceramic of the FGM sandwich plate. The volume fraction.

III. GOVERNING EQUATIONS FOR FG SANDWICH PLATE

The displacement field for FG sandwich plates is described in the following equations Saidi [8]:

$$u(x,y,z) = u_0(x,y) - zw_{,x} + f(z)\theta_x \tag{2a}$$
$$v(x,y,z) = v_0(x,y) - zw_{,y} + f(z)\theta_y \tag{2b}$$
$$w(x,y,z) = w_0(x,y) + \hat{f}(z)\theta_z \tag{2c}$$

Where, u, v, w are displacements in the x, y, z directions, u_0, v_0 and w_0 are midplane displacements, θ_x, θ_y and θ_z rotations of the *yz*, *xz*, and *xy* planes due to bending, respectively. $f(z)$ represents shape function determining the distribution of the transverse shear strains and stresses along the thickness and $f'(z) = \partial f(z)/\partial z$.

The linear strain expressions derived from the displacement model are as follows:

$$\begin{Bmatrix} \varepsilon_x \\ \varepsilon_y \\ \gamma_{xy} \end{Bmatrix} = \begin{Bmatrix} \varepsilon_x^0 \\ \varepsilon_y^0 \\ \gamma_{xy}^0 \end{Bmatrix} + z\begin{Bmatrix} k_x \\ k_y \\ k_{xy} \end{Bmatrix} + f(z)\begin{Bmatrix} \eta_x \\ \eta_y \\ \eta_{xy} \end{Bmatrix}$$

$$\begin{Bmatrix} \gamma_{yz} \\ \gamma_{xz} \end{Bmatrix} = f'(z)\begin{Bmatrix} \gamma_{yz}^0 \\ \gamma_{xz}^0 \end{Bmatrix} \tag{3}$$

$$\varepsilon_x^0 = \frac{\partial u_0}{\partial x},\ \varepsilon_y^0 = \frac{\partial v_0}{\partial y},\ \varepsilon_z^0 = \theta_z, \tag{4}$$

$$\gamma_{yz}^0 = \left(\theta_y + \frac{\partial \theta_z}{\partial y}\right),\ \gamma_{xz}^0 = \left(\theta_x + \frac{\partial \theta_z}{\partial x}\right), \tag{5}$$

$$\gamma_{xy}^0 = \frac{\partial u_0}{\partial y} + \frac{\partial v_0}{\partial x},\ k_x = -\frac{\partial^2 w_0}{\partial x^2},\ k_y = -\frac{\partial^2 w_0}{\partial y^2}, \tag{6}$$

$$k_{xy} = -2\frac{\partial^2 w_0}{\partial x \partial y}, \tag{7}$$

$$\eta_x = \frac{\partial \theta_x}{\partial x},\ \eta_y = \frac{\partial \theta_y}{\partial y},\ \eta_{xy} = \frac{\partial \theta_x}{\partial y} + \frac{\partial \theta_y}{\partial x}. \tag{8}$$

The linear constitutive relations are given as:

$$\begin{Bmatrix} \sigma_x \\ \sigma_y \\ \sigma_z \\ \tau_{yz} \\ \tau_{xz} \\ \tau_{xy} \end{Bmatrix} = \begin{bmatrix} Q_{11} & Q_{12} & Q_{13} & 0 & 0 & 0 \\ Q_{12} & Q_{22} & Q_{23} & 0 & 0 & 0 \\ Q_{13} & Q_{23} & Q_{33} & 0 & 0 & 0 \\ 0 & 0 & 0 & Q_{44} & 0 & 0 \\ 0 & 0 & 0 & 0 & Q_{55} & 0 \\ 0 & 0 & 0 & 0 & 0 & Q_{66} \end{bmatrix} \begin{Bmatrix} \varepsilon_x \\ \varepsilon_y \\ \varepsilon_z \\ \gamma_{yz} \\ \gamma_{xz} \\ \gamma_{xy} \end{Bmatrix} \tag{9}$$

where (σ_x, σ_y, σ_z, τ_{yz}, τ_{xz}, τ_{xy}) and (ε_x, ε_y, ε_z, γ_{yz}, γ_{xz}, γ_{xy}) are the stress and strain components, respectively, Q_{ij} are the stiffness coefficients.

The principle of virtual work, the following expressions can be obtained:

$$\int_{-h/2}^{h/2}\int_{\Omega}\left[\sigma_x\delta\varepsilon_x + \sigma_y\delta\varepsilon_y + \sigma_z\delta\varepsilon_z + \tau_{xy}\delta\gamma_{xy} + \tau_{yz}\delta\gamma_{yz} + \tau_{xz}\delta\gamma_{xz}\right]d\Omega\,dz - \int_{\Omega} q\delta w d\Omega = 0 \tag{10}$$

The governing equations of equilibrium can be derived easily from Equation (10).

$$[C]\{\Delta\} = \{F\} \tag{11}$$

Where $\{\Delta\} = \{U,V,W,X,Y,Z\}^t$ and $[C]$ is the stiffness matrix,
$\{F\}$ is the force vector.

IV. RESULTS AND DISCUSSION

Numerous examples are solved to ensure the accuracy of the present theory for the prediction of static analysis under thermo mechanical loading , the closed form solution are obtained using the Navier solution of simply supported FGM sandwich plates.

Table1 contains the dimensionless center deflection $\bar{w}$ for an FG sandwich plate subjected to mechanical and thermal

loads. The deflections are considered for $k = 0,1, 2, 3, 4$ and 5 and different FG plates types:

[(0-1-0), (1-3-1), (2-1-2), (1-2-1), (1-0-1)].

It can be seen from the table1 that the results of the present theory are very close to those of the other shear deformation theories.

It can be observed that the HSDP overestimates the deflections comparatively to RHSDT and this, is due to the thickness stretching effect.

For a sandwich plate, the deflections increase with the power law index k .

TABLE I

DIMENSIONLESS CENTER DEFLECTIONS $\bar{w}$ OF THE DIFFERENT FG SANDWICH SQUARE PLATES.

k	*Theory*	*(0-1-0)*	*(1-3-1)*	*(2-1-2)*	*(1-0-1)*
0	**RHDP**	**0.771340**	**0.891031**	**0.951864**	**0.959500**
	HDPT	0.817556	0.930218	0.983436	0.989882
	SSDPT	0.796783	0.906983	0.958491	0.964718
	TSDPT	0.808168	0.919718	0.972164	0.978509
	FSDPT	0.8957352	1.01729	1.07744	1.08468
1	**RHDP**	**0.939609**	**0.951255**	**0.958373**	**0.959500**
	HDPT	0.989682	0.986027	0.989045	0.989882
	SSDPT	0.964682	0.961091	0.963918	0.964718
	TSDPT	0.978382	0.974764	0.977691	0.978509
	FSDPT	1.08353	1.07988	1.08371	1.08468
2	**RHDP**	**0.974664**	**0.959818**	**0.959418**	**0.959500**
	HDPT	1.02533	0.994145	0.989945	0.989882
	SSDPT	0.999282	0.968891	0.964791	0.964718
	TSDPT	1.01355	0.982736	0.978573	0.978509
	FSDPT	1.12346	1.08928	1.08473	1.08468
3	**RHDP**	**0.991418**	**0.962845**	**0.959755**	**0.959500**
	HYDPT	1.04333	0.997264	0.990245	0.989882
	SSDPT	1.01673	0.971882	0.965082	0.964718
	TSDPT	1.03131	0.985791	0.978873	0.978509
	FSDPT	1.14369	1.09287	1.08505	1.08468
4	**RHDP**	**1.00309**	**0.964518**	**0.959900**	**0.959500**
	HDPT	1.05618	0.999082	0.990382	0.989882
	SSDPT	1.02920	0.973627	0.965209	0.964718
	TSDPT	1.04398	0.987582	0.979000	0.978509
	FSDPT	1.15807	1.09495	1.08519	1.08468
5	**RHDP**	**1.01244**	**0.965664**	**0.959973**	**0.959500**
	HDPT	1.06654	1.00037	0.990445	0.989882
	SSDPT	1.03926	0.974864	0.965282	0.964718
	TSDPT	1.05421	0.988845	0.979073	0.978509
	FSDPT	1.16964	1.09644	1.08526	1.08468

Figures 2 show the variation of the center deflection $\bar{w}$ with side-to-thickness ratio a/h of sandwich plate type (1-2-1) with different volume fraction exponent «k».

The deflections of the FG sandwich and homogeneous plates decrease as a/h increases.

Figures 3 show the variation of the center deflection $\bar{w}$ with the aspect ratio a/b of sandwich plate type (1-3-1).

The deflection of the ceramic plate is found to be of the smallest magnitude and that of the metallic plate, of the largest magnitude. The increase of the aspect ratio a/b leads to a decrease of deflections of the homogeneous and FG sandwich plates.

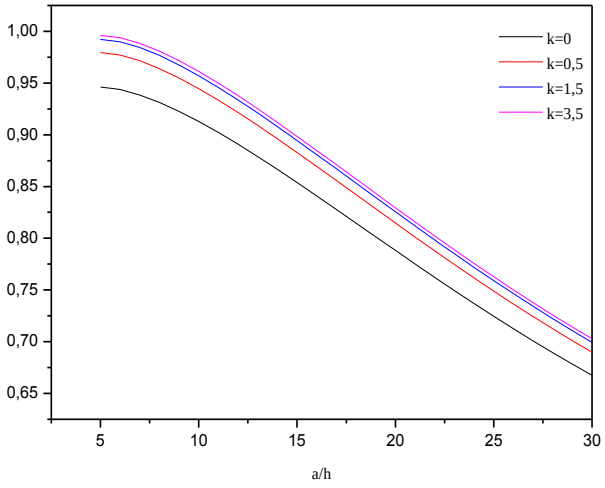

Fig. 2 Dimensionless center deflection $\bar{w}$ as a function of side-to-thickness ratio a/h for sandwich plate type (1-2-1)

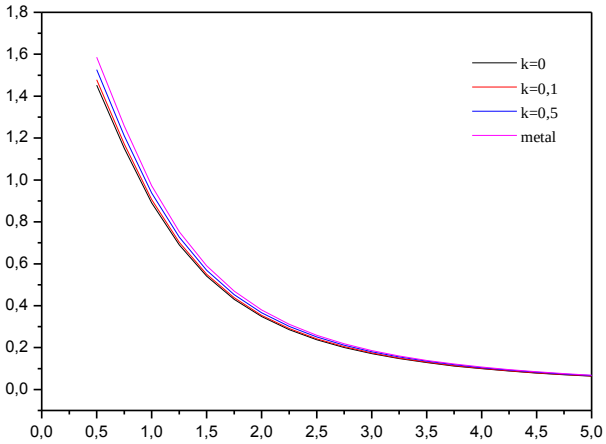

Fig. 3 Effect of the aspect ratio a/b on dimensionless center deflection $\bar{w}$ for sandwich plate type (1-3-1)

V. CONCLUSIONS

The applicability of the higher order shear deformation theory for the analysis of non symmetric functionally graded sandwich plate is assessed using closed form solution. The present theory incorporates the transverse shear stresses and strains and satisfies the conditions of zero transverse shear stresses and strains on the surface of the plate and hence eliminates the need of shear correction factor. The governing equations and boundary conditions are derived by employing the principle of virtual work. These equations are then solved via Navier –type solution. Numerical results are presented for severals types simply supported rectangular sandwich plates

under thermo-mechanical loading. The effect of power- law index, span to thickness ratio and aspect ratio are studied.

It has been confirmed that the deflection of the sandwich plates decreases as the side to thickness and aspect ratios increases. And the deflection increase as the power-law index increases.

The results show also that the including of stretching effect leads to decrease deflections and stresses.

REFERENCES

[1] M. Koizumi "FGM activities in Japan," Composites Part B, vol. 28, 1997, pp. 1–4.

[2] J. N. Reddy, "Analysis of functionally graded plates," Int. J. Num. Meth. Eng, vol. 47, 2000, pp. 663-684.

[3] Zenkour AM. A comprehensive analysis of functionally graded sandwich plates: Part 1—Deflection and stresses. Int J Solids Struct 2005; 42: 5224–42.

[4] Kashtalyan M, Menshykova M. Three-dimensional elasticity solution for sandwich panels with a functionally graded core. Compos Struct 2009; 87:36–43.

[5] Zenkour AM, Alghamdi NA. Bending analysis of functionally graded sandwich plates under the effect of mechanical and thermal loads. Mech Adv Mater Struct 2010; 17: 419–32.

[6] Cinefra M, Soave M. Accurate vibration analysis of multilayered plates made of functionally graded materials. Mech Adv Mater Struct 2011;18: 3–13.

[7] Y. Yorozu, M. Hirano, K. Oka, and Y. Tagawa, "Electron spectroscopy studies on magneto-optical media and plastic substrate interfaces (Translation Journals style)," *IEEE Transl. J. Magn.Jpn.*, vol. 2, Aug. 1987, pp. 740–741 [*Dig. 9th Annu. Conf. Magnetics* Japan, 1982, p. 301].

[8] H. Saidi**,** M. S. A. Houari, A. Tounsi, E.A. ADDABEDEA, "Thermo-mechanical bending response with stretching effect ofunctionally graded sandwich plates using a novel shear deformation theory" , Steel and Composite Structures, Vol. 15, No. 2, PP. 221-245, 2013.

QoS WiMAX and Wi-Fi Performances Analysis based OPNET Modeler

Dr. Adnan Hussein Ali, Dr. Ali Abdulwahhab Abdulrazzaq, Dr. Hassan S. Hamad,
Salman Hussein Omran, Vailet Hikmet Faraj, Rasha Riyadh Ahmed Izzat

***Abstract*—**The fast increasing and wide spreading usage of smart phones and many other wireless devices producing a great growth demand for the network technologies, and leads to the improvements of such technologies. Multimedia applications are earning a user attention with these broadband technologies. VoIP is the most well-known services of WiMAX and is a growing rapidly in telecommunication systems. In this paper, we compare the performance of WiMAX and Wi-Fi networks for voice and (light and heavy) video using OPNET Modeller in terms of throughput and voice packet end to end delay. Quality of service (QoS) support for both technologies provide smooth and steady voice and video transfer. Wi-Fi operates with base line and fiber line subnets and Wi-Fi fiber base can be considered the ideal design for these network. While WiMAX provides a faster and longer distance network to users than Wi-Fi.

***Keywords*—**WiMAX, Wi-Fi, QoS, VoIP, Performance Analysis, OPNET, light and heavy video.

I. INTRODUCTION

The technology of mobile communications advanced quickly as a result of increasing requests for higher data rates as well as with high quality services of mobile communications. Achieving these requests were done by determining a new air interfacing for cellular communications that enhances the performances of global systems and increases the ability of the system[1]. At the present time, the applications of interacting multimedia provide very advanced communication environments which may be used more than a homelike and amusing contexts, but further for professional cooperative business[2].

The significance of mobility produces the utilization of wireless networks become prominent, each day, the utilizing of these networks, such as WLAN, WiMAX, UMTS as well as LTE, are increasing and permits easy and quick infrastructure deployment of networks that might be executed on geographical locations unavailable to wired technologies like xDSL [3]. Indeed, those systems may be classified in two groups, the first presents mobility which has low data rates such as cellular systems and second presents a high data rates with a small as well as large covering area like Broadband WAN [4].

WiMAX is Worldwide Interoperability for Microwave Access specified by standard IEEE 802.16, which is a wireless communication framework provides an access of long-scale coverage broadband in diversity ways from point-to-point connections to mobile cellular access . It makes an IEEE 802.11 WLAN enhancements by expanding a wireless access to Broad Area Networks in addition to Metropolitan Area Networks(MANs). The early form of WiMAX, IEEEs802.16-2004, had been designed for providing connectivity of broadband wireless to fixed users and nomad for the last mile [5]. The limited coverage area to 50 km, with speed up to 40 Mbps letting utilizers to acquire broadband connectivity in non-line of sight (NLOS) conditions[6]. Another form is IEEEs802.16-2005 which considered Mobile WiMAX originates with QoS enhancement by submitting different service modules for both application of real-time and non-real-time traffic and mobility reaching to 120s km/h.

Mobile WiMAX is intended for realizing the gap between WLANs and high mobility WANs[7]. WiMAX Networks considered evolution appearing which proposed supporting services of multiple multimedia like internet browsing, email, voice telephony, video messaging, and so on. Such network services require different QoS (Quality of Service) demands, which involves establishments and managements of a collection of parameters like throughput, transmission delay, average packet delay, Packet Drop Rates, bandwidth, jitter, and minimum throughput requirements [8].

QoS is considered as the network capacity to present an acceptable services comprising high data rates, signal strengths and low distortions. The QoS purposing to be able for treating such parameters agreeing to the applications demands [9].

The technology of WiMAX is known as the last-mile solution for wireless broadband access. WiMAX structures of Media Access Control (MAC) layer is designed to characterize services during traffic groups with various multimedia requirements [10]. WiMAX provides several flexible features which can possibly be exploited to deliver real-time services. Although the WiMAX MAC layer can be

Dr Adnan Hussein Ali is with the Middle Technical University, Technical Instructors Training Institute. Baghdad, Iraq. e-mail: aaddnnaann63@gmail.com

Dr. Ali Abdulwahhab Abdulrazzaq, is with the Middle Technical University, Technical Instructors Training Institute. Baghdad, Iraq. e-mail: aliabdulwahhab@yahool.com).

Dr. Hassan S. Hamad is with the Middle Technical University, Technical Instructors Training Institute. Baghdad, Iraq. (e-mail: hassan1hamad@yahoo.com).

Assist. Prof. Salman Hussein Omran is with the Middle Technical University, Ministry of Higher Education and scientific Research. Baghdad, Iraq. e-mail: asst.prof.salman@yahool.com).

Vailet Hikmet Faraj is with the South Baghdad 2 Gas power station

Rasha Riyadh Ahmed Izzat, South Baghdad 2 Gas power station.

standardized with certain features for exact applications and channels. The transmission of voice over wireless networks is commonly obvious through a huge implementation of mobile system around the world. VoIP can be considered as an example of a quickly developing voice application and be verified from high achievement rates of applications such as Skype [11]. Therefore WiMAX is a very attractive technology for providing integrated voice, video services for VoIP.

VoIP principle is facilitated by digitizing voice data first and then transferring as packets over IP network. On the other hand such packets are decoding and converting back to original analog voice signal, it utilizes Internet Protocol for voice transmitting as packets over IP networks so that it significantly increasing bandwidth efficiency and enables design of new facilities [12].

In this paper, we propose three scenarios for WiMAX, Wi-Fi base line and Wi-Fi fiber line to conduct a comparative performance analysis of WLAN and WiMAX technologies for a small network. We utilize wireless servers for voice and video applications and operate the networks with QoS support.

II. Overview & Comparison between Wi-Fi and WiMAX

A. IEEE 802.11 (Wi-Fi)

Wi-Fi is "wireless fidelity" used commonly as a WLAN synonym . Wi-Fi is a widespread technology that permits many electronic devices to interchange and transmit data by wireless through the network providing increase to high speed internet connections. A device that has Wi-Fi enabled can be connected to internet resources such as personal computers, Smartphones, video game supports, and tablets [13] as shown in fig. 1.

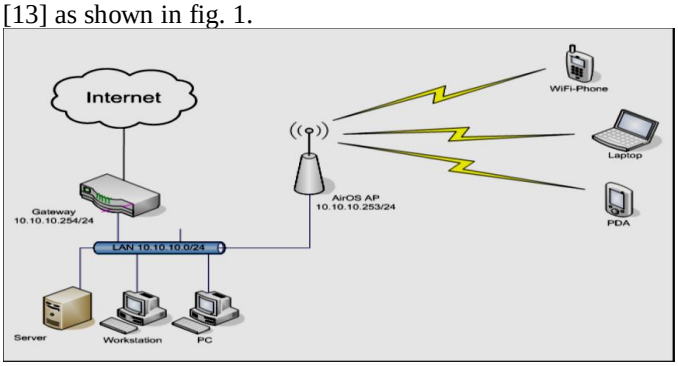

Fig. 1: Wi-Fi network structure

B. IEEE 802.16 (WiMAX)

WiMAX is a standard normally centered on universal interoperability comprising IEEEs802.16d-2004 for fixed, plus 802.16e for mobile high-speed data. It is earning acceptance as a technology that provides carrier-class, and wireless broadband of high speed at low cost whereas large distance covering area than Wi-Fi. It is proposed to process voice, video, and services with high-quality while posing a high QoS [14].

Many applications use these two technologies (WiMAX besides Wi-Fi) and have been increasing while they were originally concentrated on mobiles and PCs and then advanced for many devices and they are increasing continuously with easy for installing and Environmentally friendly.

C. Comparison between Wi-Fi and WiMAX

Wi-Fi offers a connection of Internet/LAN in the range of an access point AP. The purpose of Wi-Fi is to produce a mesh network as well as to offer peer to peer P2P connections among users. On the other hand, WiMAX networks provide higher bandwidth in addition to greater coverage range for providing services to high-speed mobile data and telecommunication like 4G networks. Another WiMAX employment to connect Wi-Fi hotspots.

D. Quality of Service QoS

QoS is the capability to transfer a specific traffic form, in perfect conditions, through many terms. In a mixed networks framework (WiMAX and Wi-Fi), QoS mechanisms employment are very essential, specifically these networks are open access, therefore a management of network access may be dominant.

E. Voice over IP (VoIP)

VoIP can be considered a most collective and low-cost technology for communicating of small and big area distances [15]. Numerous VoIP providers present a free services of charge in spite of distances. A VoIP application principally facilitated as follows. Firstly, the analog signal's voice is sampled, then digitized, and encoded to be as frames. These encoded data will be packetized and then transmitted over IP network by RTP/UDP/IP. At receiver, on the other side, data are de-packetized and progressed to a buffer that smooth out the delay sustained in the network. Then, the data is decoded and reconstructed voice signal is done.

III. WiMAX and Wi-Fi Simulation

A. WiMAX scenario1

The analyzation of the QoS in WiMAX networks need various real time procedure cases to be considered. The WiMAX offers basic IP connection, so that a requirement for mobile devices that are capable of employing WiMAX network to support voice calling over IP.

The WiMAX architecture contains four sections essentially: access services network (ASN), connectivity service network (CSN), mobile stations, and IP backbone as shown in fig. 2. ASN is a transition section with the purpose of connecting mobile stations (or any wireless devices) via a Base Station BS to internet services provider. While CSN Provides controlling and management services for WiMAX subscribers. Finally, the IP network (backbone) is Interconnecting networks and core routers with internet.

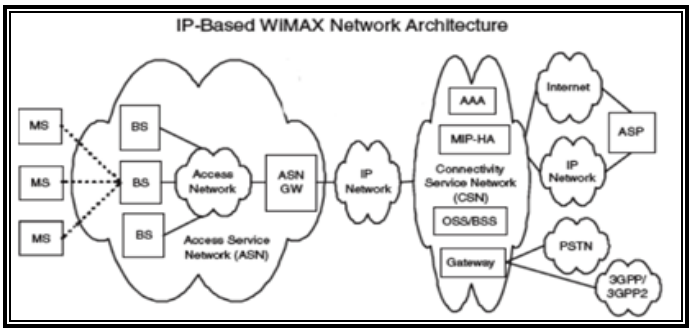

Fig. 2: WiMAX network Architecture

The selected components for implementing WiMAX using OPNET are:

* WiMAX Base Station: represented by WiMAX_BS_ethernet
* Gateway: represented by Ethernet4_Slip8_gtwy for Fixed node.
* Server: represented by Ethernet_server for Fixed node
* IP backbone: represented by Router_slip64_dc
* Workstation: represented by Wlan_skstn_adv for mobile node
* Link Model: represented by 100BaseT

In WiMAX scenario (shown in fig. 3), all configuration links have the same setting to create simple performance analysis comprehensively. In this scenario, the behavior of QoS classes is observed with the traffic is managed on Best Effort basis.

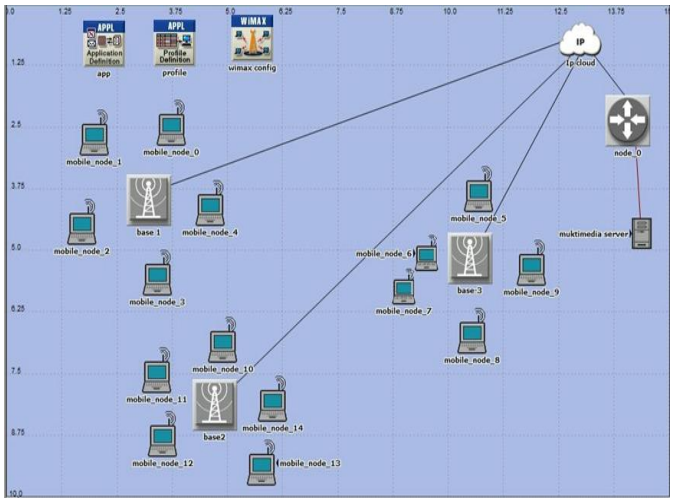

Fig. 3: WiMAX scenario1

WiMAX scenario has many WiMAX–BS-Ethernet that connected to router and WiMAX workstation SS Ethernet. A WiMAX BS is connected with IP cloud by (PPP-link). With this Scenario, the components used for network statistics measurements for both video conferencing and voice with GSM quality.

B. Wi-Fi simulation setup

The Wi-Fi scenarios use parameters shown in Table 1

TABLE I:
WI-FI PARAMETERS

WiFi 802.11g		
	AP (Access Point)	Mobile Node
Tx Power	0.1W	0.1W
Data Rate	11Mbps	11Mbps
Receiver Power Threshold	-95dBm	-95dBm
Buffer Size	1024000 bits	256000 bits
Short Retry Limit	7	7
Long Retry Limit	4	9
Large Packet Processing	Fragment	Fragment
Access Point Functionality	Enabled	Disabled

In Wi-Fi test two scenarios are performed, the first for baseline Wi-Fi and the second for base Fiber Wi-Fi. Also some components are required to simulate Wi-Fi network on OPNET.

A subnet in reign one, BC that has a server, for streaming video and voice, connected to the Internet cloud. There is another subnet in reign two, ON, which receives the video and voice data and distributes the data content from a WiMAX Base Station to various subscriber station (SS) subnets around it. The SS subnets are all WiFi enabled and receive the WiMAX data through their WiMAX and WiFi routers and distribute the data content over WiFi link to different computers.

C. Baseline Wi-Fi Scenario

The Baseline Scenario of WLAN model(802.11g) is produced using different models of the OPNET standard. The behavior of a single infrastructure 802.11g WLAN has been tested within the framework of a deployed WAN to perfect emulate the configuration of an actual network. The backbone Internet is represented by Internet Protocol IP cloud and connected with a Point-to-Point T1 (1.544Mbps) serial link. The group of subnets are located on the various sides of this IP cloud via a IP gateway connected by Point-to-Point Protocol PPP T1 link and two servers connected through a central switch using 100 BaseT, as shown in Fig. 4.

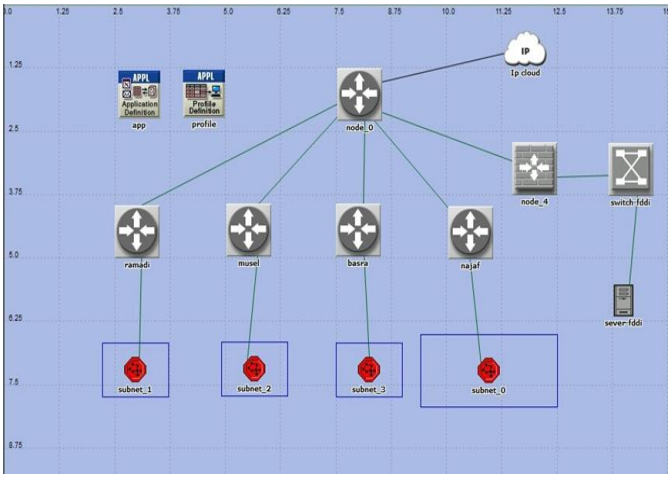

Fig. 4: Simulated Wire Server with four subnets.

The network's traffic server on the one side of this Internet Protocol (IP) cloud is are connected by 100BaseT Ethernet, the server connect to the firewall using 100BaseT Ethernet wiring and are used as the source and destination of all

services: video conferencing, voice applications in the 802.11g WLAN during the simulation. The base line Wi-Fi application configuration was shown Figure 5 where the light, and heavy video, and PCM voice were used in the scenario.

The subnet 1 represents a remote office including an office-LAN having workstations that are connected by a link of 100BaseT. Office-LAN connected through a central switch using 100BaseT Ethernet wiring emulating a real time office environment with a standard Fast Ethernet LAN. An IP gateway connects the LAN to an IP cloud. The gateway connects to the office LAN using 100BaseT Ethernet wiring while the connection between the gateway and the IP cloud is done with a Point-to-Point T1 (1.544Mbps) serial link, as shown in Fig. 5.

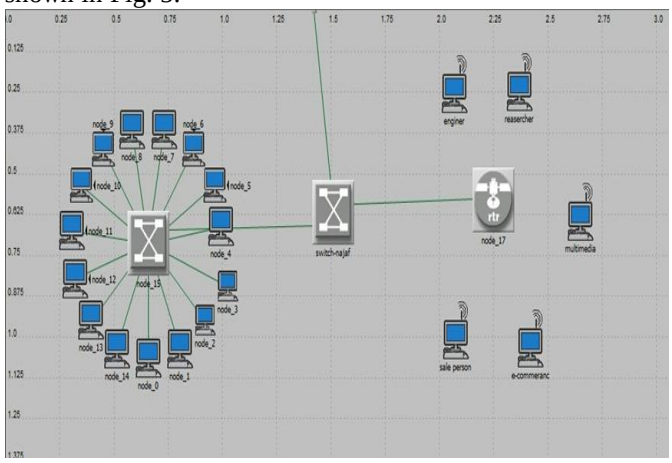

Fig.5: Subnet 1 802.11g LAN

1. Base Fiber Optic Wi-Fi Scenario

In this scenario we replaced all the Ethernet component with fddi, and all the 100baseT link are changed with FDDI link: The FDDI identified for Fiber Distributed Data Interface which requires a 100-Mbps token-passing.

- Ethernet gateway replaced by fddi gateway
- Ethernet firewall replaced by fddi2 firewall
- Ethernet _switch16 replaced by fddi16_switch
- 100baset link replaced by fddi link
- Ethernet server replaced by fddi server

Here, figures 4 & 5 can be shown in figures 6 & 7 for fiber base scenario.

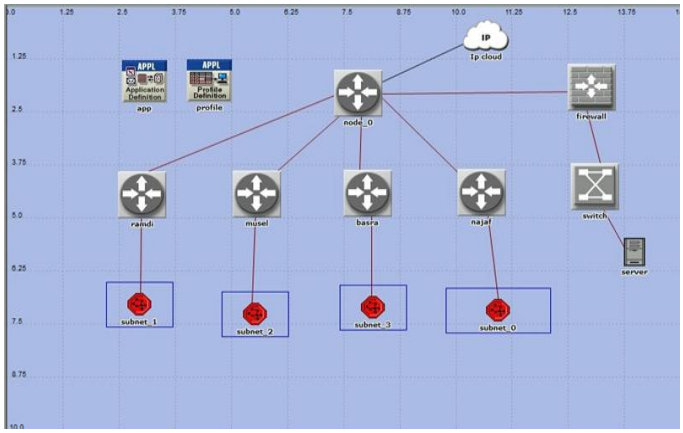

Fig. 6: Simulated fiber Server with four subnets

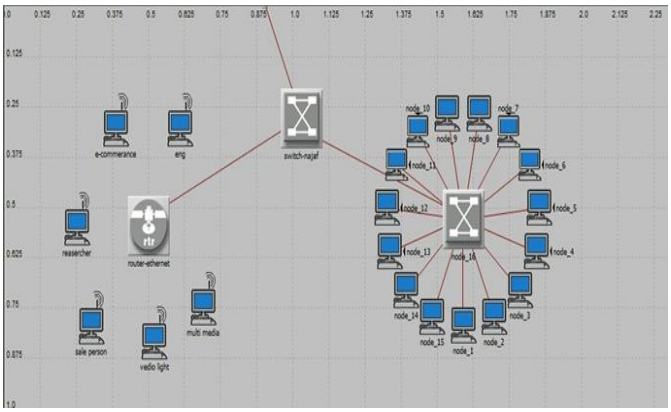

Fig. 7: WiFi base fiber Subnet 2

IV. SIMULATION RESULTS

The results and discussion of the WiMAX , Wi-Fi base line and Wi-Fi base fiber for the voice and video parameters data transmission (voice , light video and heavy video) will be described for time delay and voice-packet end to end delay measurement for both Wi-Fi base line and Wi-Fi base fiber, measurement of voice-packet end to end delay and video packets delay base WiMAX networks with Light and Heavy video, in addition to throughput measurement for WiMAX, Wi-Fi base line and Wi-Fi base fiber.

A. WiMAX QoS

1. **WiMAX voice-packet end to end delay**

The simulation results of the WiMAX voice-packet end to end delay for the PCM voice and light video and heavy video data transmission can be shown in fig 8. It's clear that no connection happened until second 110 where the connection network established, and the communication system reach the steady state at the second 250 and 240 for both types of videos with maximum delay 115 ms and 110 ms, so that the voice with heavy video has a delay less than the delay of voice with light video.

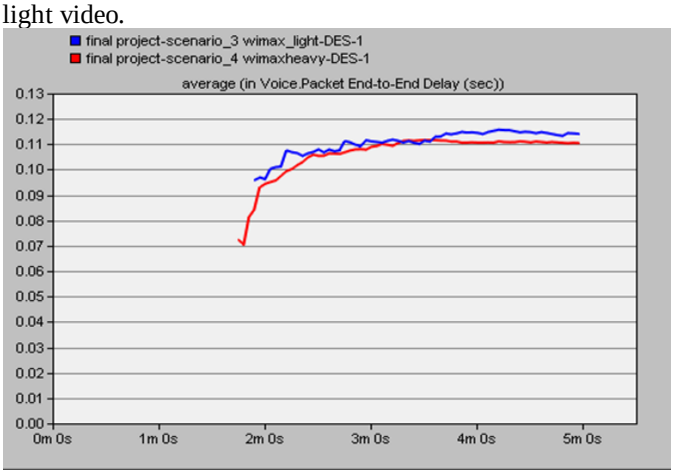

Fig.8: WIMAX scenarios delay of voice light and heavy video.

2. WiMAX Light and Heavy video packets delay

The simulation results for packets delay data transmission of both light and heavy video in WiMAX network is shown in fig. 9, the connection network happened at second 110, and the communication system reach the steady state at the

second 300. From the second 300 in simulation , the light video traffic sent has 6.4 packet/sec and heavy video traffic sent has 37 packet/sec, so the traffic sent of heavy video was larger than light video .

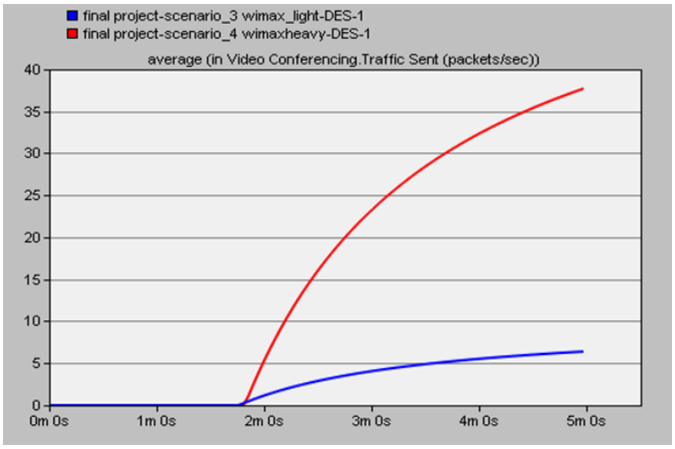

Fig.9 :WiMAX comparing of light and heavy video traffic

3.Throughput

The simulation results of the throughput of WiMAX network can be shown in fig. 10, when comparing between throughput of WiMAX with heavy video data transmission and that with light video data transmission, at the second 300 the light video has 275 packet/sec and the heavy video has 1180 packet/sec so the heavy video has larger throughput than light video as shown in Fig. 10.

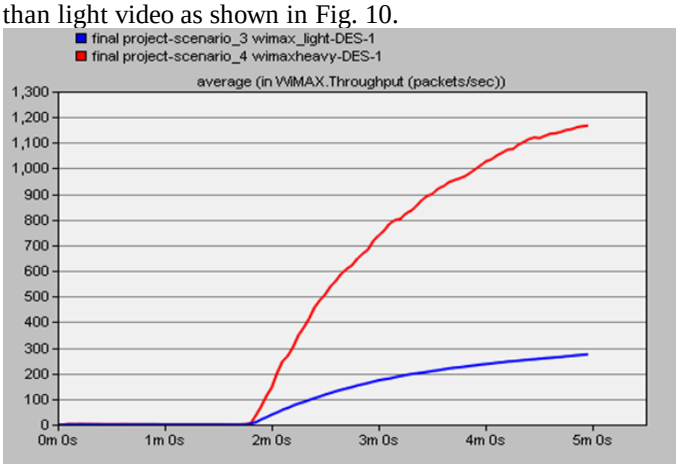

Fig. 10: Throughput of WiMAX light and heavy video

B. Wi-Fi QoS

1. Wi-Fi Delay

An important parameter to determine the successful process of the transmission data and the Required To send/ receive mechanism are overall packet transmission delay and the medium access delay statistics. The end-to-end delay measured in the simulation of the Wi-Fi base line and the Wi-Fi based fiber optic connections shown in Fig.11. From the simulation, no network connection until second 100 and the communication system reach the steady state with maximum delay 0.048 second at the second 200 for base line and delay 0.035 second at the second 200 for Wi-Fi based fiber optic connection. It can be concluded that the base line had delay larger than Wi-Fi base fiber delay.

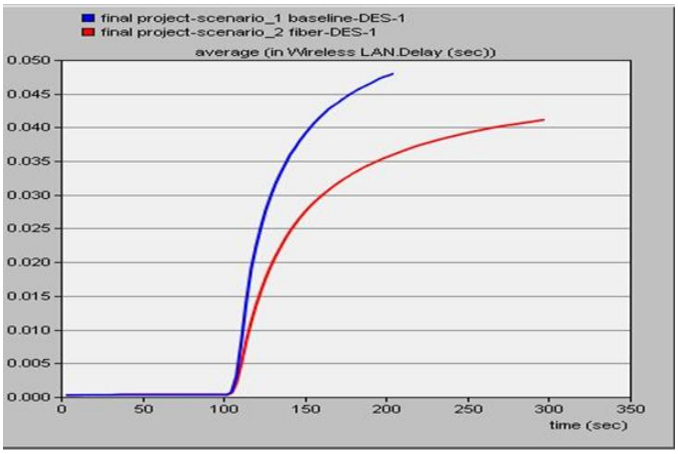

Fig. 11: Delay for Wi-Fi base fiber and Wi-Fi base line

2. Wi-Fi voice-packet end to end delay

The analog signal from the telephone is digitized into pulse code modulation (PCM) signals by the voice coder-decoder (codec). The samples of PCM are then passed to the compression algorithm that compresses the voice into a packet format for transmission across the WAN. From the simulation results of the voice-packet end to end delay Wi-Fi base line and base fiber, a connection network occurred at second 110, and the steady state communication system reach the with maximum delay 1 packet at the second 200 and 10 packet at the second 310 for base line and fiber line Wi-Fi respectively so that the base line Wi-Fi has delay larger than delay Wi-Fi base fiber as shown in Fig.12.

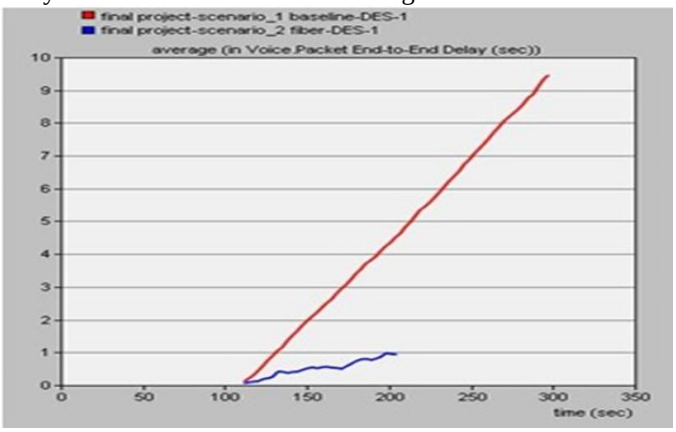

Fig. 12: voice delay for Wi-Fi base fiber and Wi-Fi base line

3. Throughput

In communication networks, the network throughput can be considered as the average rate of successful data message delivery over a communication channel. This data may be delivered over a physical or logical link, or pass through a certain network node. The throughput is typically measured in (bit/s or bps), or in data packets per second or data packets per time slot.

The simulation results of the throughput of Wi-Fi base line scenario at the second 200 the connection was established and arrived a maximum throughput is 7,750,000 bit/sec and the base fiber has 8,750,000 bit/sec so the base fiber has larger throughput than base line shown in Fig.13.

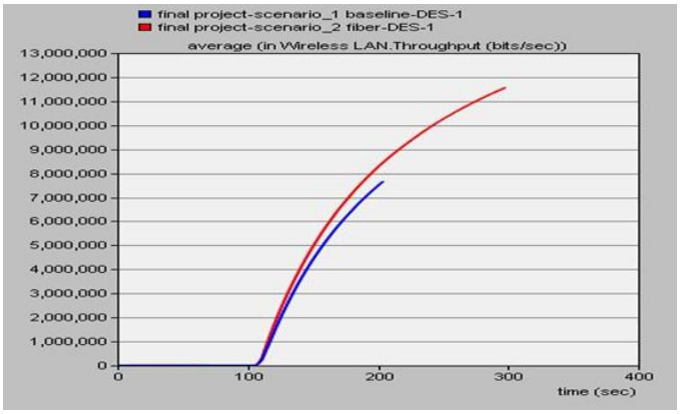

Fig.13: throughput for Wi-Fi based line and fiber optic

V. CONCLUSION

The OPNET Modeller is used to design and characterize the performance parameters of WiMAX. In this paper, a simulation of WiMAX and Wi-Fi scenarios and compared their delay and throughput. It can be concluded from simulation results that WiMAX has an overall better performances compared with Wi-Fi essentially due to the Quality of Service. The QoS purposes are to ensure high data transmission performances like voice-packet end to end delay and throughput can be achieved.

In WiMAX, the voice with heavy video has a delay less than the delay of voice with light video by 5ms and throughput is larger in case of the heavy video than light video. In Wi-Fi scenarios, the base line had voice-packet end to end delay larger than Wi-Fi base fiber delay and base fiber has larger throughput than base line. Wi-Fi fiber base is the perfect design because it provided a flexible, reliable and cost effective approach.

REFERENCES

[1] Nupur R. Malankar, R. Shah, "QoS Analysis over WiMAX Network with Varying Modulation Schemes and Efficiency Modes". International Journal of Computer Applications (0975 – 8887) Volume 162 – No 8, March 2017.

[2] Ali GEZER, Marwa Khaleel, "Performance Comparison of WiMAX and WLAN Technologies using OPNET Modeler" International Conference on Engineering Research & Applications (ICERA), İstanbul (Turkey) May.17-18, 2017.

[3] G. Malik, A. Singh, "Performance Evaluation of Wi-Fi and WiMAX Using Opnet", International Journal of Advanced Research in Computer Science and Software Engineering, Volume 3, Issue 6, 2013.

[4] S. Islam, M. Rashid, and M. Tarique, "Performance Analysis of WiMAX/Wi-Fi System under Different Codecs,‖ International Journal of Computer Applications, vol. 18, no. 6, pp. 13-19, March 2011.

[5] S. Jadhav, H. Zhang, and Zhiyi Huang, "Performance Evaluation of Quality of VoIP in WiMAX and UMTS", in Proceedings of the 12th IEEE International Conference on Parallel and Distributed Computing, Applications and Technologies (PDCAT), 2011, Gwangju, South Korea, 20-22 October 2011, pp. 375 - 380.

[6] K. Kaur, V. Grewal, "QoS Performance Analysis of Video Conferencing Over Wimax using different Modulation Schemes" International Journal of Computer Applications (0975 – 8887) Volume 146 – No.4, July 2016.

[7] N. Jakhar, Ankit, Kuldeep, Suman, "OPNET based Performance Evaluation of WIMAX Network with WIMAX Management using Different QoS", International Journal of Computer Science and Mobile Computing, Vol.3 Issue.6, June- 2014.

[8] Dr. Hussein A. Mohammed, Dr. Adnan H. Ali, Hawraa J. Mohammed, "The Affects of Different Queuing Algorithms within the Router on QoS VoIP application Using OPNET", International Journal of Computer Networks & Communications (IJCNC), Vol.5, No.1, January 2013.

[9] P. Grover, M.Chawla, "Performance Analysis of QoS For WiMAX Using OPNET", IEEE International Conference on Computer, Communication and Control (IC4-2015).

[10] A. Khiat, A. Bahnasse, M. El Khaili, and J. Bakkoury," Wi-Fi and WiMax QoS Performance Analysis on High-Level- Traffic using OPNET Modeler", Pertanika J. Sci. & Technol. 25 (4): 1343 - 1356 (2017).

[11] Ibrahim A. Lawal, Abas Md Said, and Abubakar Aminu , " QoS Performance for Monitoring and Optimization of Data and VoIP traffic in WiMAX Network Mac Layer" Journal of Applied Sciences & Environmental Sustainability (JASES) 1 (3): 21-37, 2013.

[12] Nahla M. Mohammed, and Amin Babikir ," WiMax Vs WiFi: A Comparative Study by Using Opnet Simulator" International Journal of Engineering, Applied and Management Sciences Paradigms, Vol. 23, Issue 01, April 2015.

[13] Adnan H. Ali ,"Performance Evaluation of Wi-Fi Physical Layer Based QoS Systems on Fiber Using OPNET Modeler", International Journal of Soft Computing and Engineering (IJSCE), Volume-5 Issue-3, July 2015.

[14] Azeddien M. Sllame, Hana Soso, Mona Aown, Lamya Abdelmajeed, "A Comparative Study of VoIP over IEEE 802.11(b, g) and WiMax (UGS, ertPS) Wireless Network Technologies", International Journal of Wireless Communications and Networking Technologies Volume 5, No.5, August - September 2016.

[15] Mahdi H. Miraz, Muzafar A. Ganie, Suhail A. Molvi, Maaruf Ali," Simulation and Analysis of Quality of Service (QoS) Parameters of Voice over IP (VoIP) Traffic through Heterogeneous Networks", International Journal of Advanced Computer Science and Applications(IJACSA), Vol. 8, No. 7, 2017.

The Author is **Assist prof.** in the Computer Engineering Department at Institute of Technology, Baghdad, IRAQ. He has been awarded a Doctor of Philosophy in Laser and Opto-Electronics Engineering from University of Technology, Baghdad, in 2007. He has studied Master of Science in Electronics Engineering, Cupper Vapor Laser's Power supply at University of Technology, Baghdad in 2000. He has gained Bachelor in Electrical and Electronic Engineering from University of Technology, Baghdad, in 1987. Currently he is lecturer at Institute of Technology, Baghdad, IRAQ. His research interests are Radio over Fiber, Wireless Network, Laser's Power supply and OPNET.

Ali Abdulwahhab Abdulrazzaq was born in Baghdad, Iraq, 1967. He receive the B.S. degree in Electrical Engineering from Al-Mustansiriya University, Baghdad. Iraq in 1988, M. Sc. Degree in Electrical and Electronics Engineering from University of Technology 2005. The Ph. D from University "Politechnica" of Bucharist . Department of Electrical Power Systems in 2016.

Effect of Polarization on Plasma-Deposited Titanium Nitride W-TiN Layers on Cutting Tools

Djeribaa. Abdeldjalil, Ferkous. Embarek, and Saoula. Nadia

***Abstract*—** Nowadays, materials science has become a very competitive field that takes part in technological development at the service of humanity. In other words, the emergence of new technologies requires the development of new materials that meet the needs of different sectors.

The objective of our work was to deposit hard thin layers of W-TiN under a reactive atmosphere (Ar + N2) by the magnetron sputtering method, using a W / Ti target. The deposition was carried out on different substrates, namely a wafer of a cutting tool K10, 316L stainless steel, glass and silicon. It should be noted that each deposition operation is preceded by a preparation of the substrates. All the experimental steps will be briefly detailed in the following.

***Keywords*—** Coating, Plasma, Tempering, Spray, Wear.

I. Introduction

Nitride thin films such as TiN, W-TIN have been widely used in industry for their chemical stability, hardness, corrosion resistance and decorative appearance. Nevertheless, despite their excellent properties, these binary films show a lack of efficiency for some applications. For example, in the case of high speed machining, generating high temperatures (above 700 ° C), the mechanical properties are degraded by the formation of oxide layers. In addition, the grain structure of the films and TiN in column form, suggests many structural defects, which promote the diffusion of oxygen.

In order to overcome these problems, research has focused on ternary coatings, such as and W-TiN, which make it possible to combine and reinforce the properties of the various compounds. W-TiN, in particular, is one of the most interesting alloys for the protection of cutting tools.

This study therefore aims to develop W-TiN coatings by the magnetron sputtering technique and to optimize this process by applying a negative bias to the substrates. By focusing on substrates in a K10 grade wafer, we are trying to improve their different properties. Procedure for Paper Submission [1] [2]

Djeribaa. Abdeldjalil Déparetement de génie mécanique, université de constantine, constantine, algerie 25000 e-mail: saber_dj25@yahoo.fr

Ferkous. Embarek Département de genie mécanique, université de Constantine, Constantine, Algerie 25000

Saoula. Nadia, Centre de développement des technologies avances CDTA, Baba hassan, Alger Algeria 16000

II. Preparation of Coating and Their Tests

In order to achieve a good deposition, the substrates must have a smooth and well polished surface, which is why it is necessary to carry out polishing and chemical cleaning before each production process. Of course, mechanical polishing is especially for steel substrates. In our case, two types of steel are studied, 316L and K10.

III. Realization of Coating on Cutting Tools

For the deposition of coatings on cutting tools we used the RF sprayer, designed and produced locally at the laboratory of ionized media on the CDTA advanced technology development center, during this study the coatings of W-TIN were developed in the Sprayer enclosure after different preparation of cutting tools.

IV. Deposition and Procedures

After the operations of preparation of the cutting tools and the stripping of the target by a bombardment flux, which lasts a few minutes, the protective screen is actuated and the coating operation is triggered under the favorable conditions and deposition parameters.

TABLE I
DEPOSITION PARAMETERS

Parametres	Detail
Partial pressure of the first gas:	4 .10-5 mbar;
Partial pressure of the second gas:	8.7 .10-4 mbar;
Working pressure Inter-target distance - substrate	30 mtor 3 cm;
Power	200 watt
Intensity applied	0.3 - 0.5 amperes;
Time of deposit.	50 minutes

For the realization of this operation of coating of the cutting tools, which will be subjected thereafter to the various mechanical tests (hardness tests, corrosion tests), and later

one will compare the mechanical characteristics without and with deposit, the Operation of this study involves two steps are:

A. The First Step :

In this step, the guarded control tools were selected as reference samples for the subsequent comparison of the initial mechanical properties.

B. The second step :

In this step the cutting tools on their active part have undergone a layer of coating W-TIN.

V. THE TESTES CARRIED OUT

After completion of the coating operation and obtaining the layers, we proceeded to the determination of certain properties by the submission of these cutting tools to the various tests, which are conditioned beforehand by the properties and the quality of the coatings.

VI. PROPERTIES OF THE COATINGS OBTAINED:

Before subjecting the coated cutting tools to corrosion tests, we present the methods used to characterize the coatings obtained on the cutting tools.

Among the main mechanical characteristics favoring the performance of the cutting tools and their service life, we are interested in the value of the thickness of the deposited layer, its adhesion as well as its hardness and corrosion resistence.

A. Thickness Of The Deposited Layer :

Two methods of measurement can be distinguished:
Direct measurement of thickness: it has two methods:
Mechanical methods use a stylus that moves over the surface of the layer.

Profile meter (with laser emission) (ALTISURF 500) This method requires the creation of a part of the substrate by the deposition or by elimination of the deposit (HNO 3 solution at 10 %). This measurement can be obtained by a mechanical Diamond tip that moves at a constant speed along the line of the workpiece or with a profilometer.

The probe, all remaining permanent contact, whose amplitude is recorded electronically. [4]

B. Adhesion of the deposit:

These tests can be performed using a scratch-test, or a stylus whose diamond tip is applied normally to the surface of the sample while gradually increasing the load and ending with a probe Mechanical (Perthometer-S10 D) mahr, with 5 µm scale and a 5mm stroke will plot the graphs (spectrum) of the surface and the depth of the step. The results can be given as a curve or adhesion diagram. [5]

C. Hardness:

For the case of the measurement of the micro-hardness of the coatings, the most used methods are the Knoop hardness or the Vickers hardness. In this case, the Vickers hardness measurement was carried out on a micro durometer (mechanical laboratory). The TIN coatings were subjected to these tests, under loads ranging from (200 to 1000) gf, it is expressed by the ratio of the maximum load applied to the surface of the contact footprint. [3]

D. Electrochemical Study

In this context, electrochemical measurements have proven to be very useful in predicting the performance of materials and mitigating the risks of their damage. They provide access to information related to surface reactions, thus estimating the resistance and rate of corrosion.

VII. EXPERIMENTAL APPARATUS:

The electrochemical measurements are carried out by means of a cell which uses a conventional three-electrode system, connected to a computer-controlled potentiostat: [8]

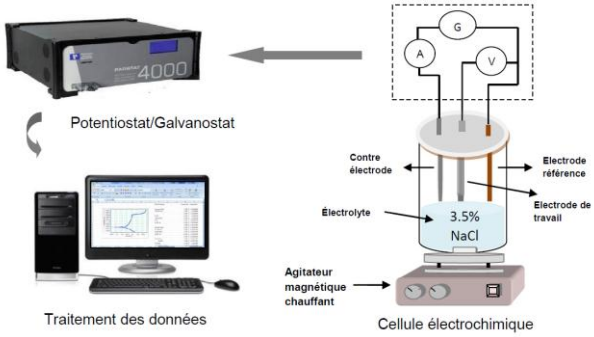

Fig. 1 Corrosion test tools.

VIII. THE RESULTS OF THE VARIOUS TESTS:

A. Thickness Of The Deposited Layer :

In this work we are able to obtain exact results. We measured the thickness of the two methods with an electronic probe (Sth-perthometer-S10), with a scale of 5 µm and a stroke of 5 mm. . we obtained the thickness around 2.50 µm, then to confirm that we use a profilometer with laser, the specter below shows the final thickness value around 2.25 µm.

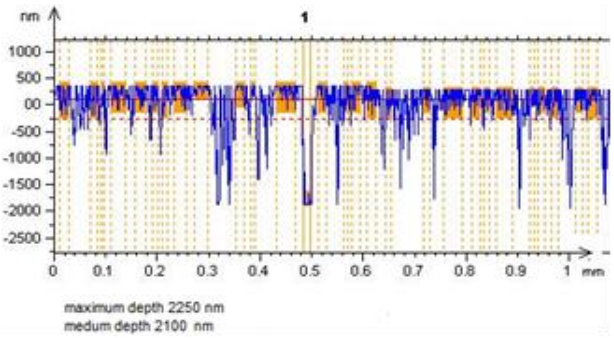

Fig. 2 Thikness of diposited layer.

This figure shows that the value of the thickness of the deposited layer is 2.25 microns.

B. Adhesion of the deposit:

Techniques for determining the adhesion of materials and layers of deposited coatings include the scratch test method and the method of tearing the layer by polishing. [3]
For this study, the second method was carried out on a polisher (KNUTHROTOR.2 strueers). Thus starting from an initial thickness of 2.5 µm, polishing carried out at a speed of 3000 rpm with abrasive paper of 1000, gave a reduction of the thickness of 1.45 µm during a severe exposure of 55 minutes.

This material consumption expressed by the variation of the thickness is represented by the following spectrum Measurement of the depth of the deposited layer after 120 minutes, 0.40 microns.

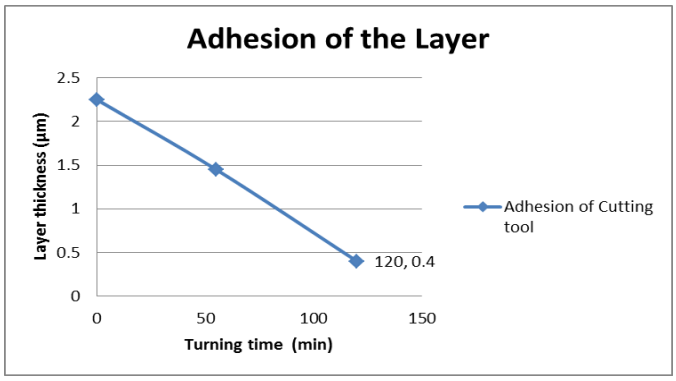

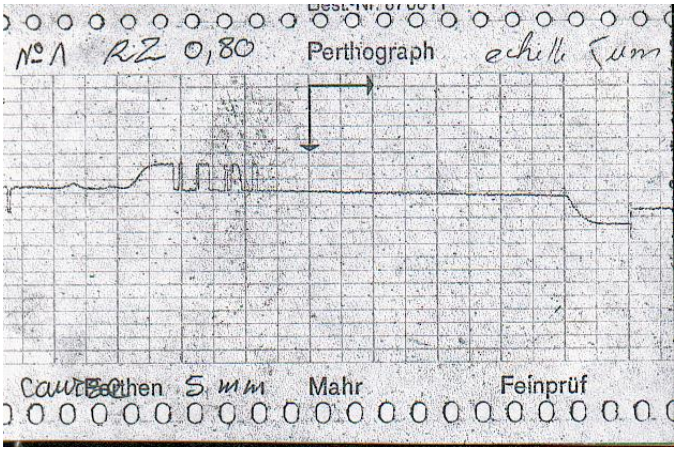

Fig. 3 Measurement of the depth of the layer deposited after 120 Minutes of polishing , 0.40 µm

C. Hardness:

Compared to the hardness value of a non-coated cutting tool, the comparative curves obtained show a clear increase in hardness. The evolution of this hardness is due to the TIN coating layer there is a significant difference in hardness. This hardness gradually improves the initial state of a tool with a traditional surface treatment in the TIN coating state.

The presentation of the variation of the hardness of these high-speed steel cutting tools is expressed on the following graphs:

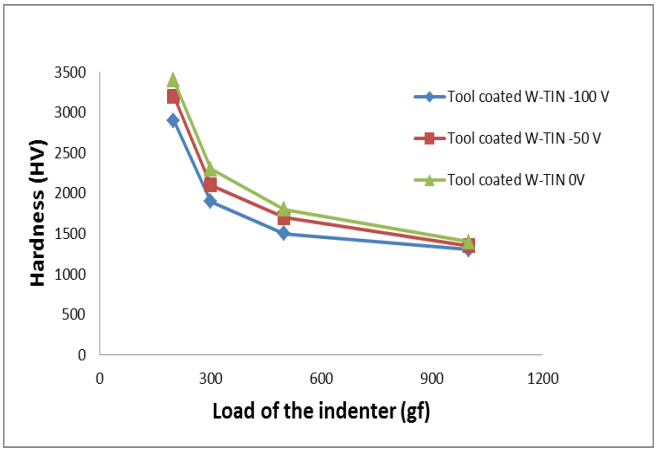

Fig. 4 Hardness curves depends on polarization.

We noticed an improvement over the hardiness compared with uncoated cutting tools, On the other hand, the hardness of the W-TIN layers also corresponds to the polarization, higher polarization gives a high hardness, [3]
0 volt gives a hardness better than -50 volt and -100 volt

In this study, we found that the hardness tends to increase with polarization. This result is directly related to a high dens structure, reduced grain size and a small amount of structural defaults.

D. Electrochemical Study

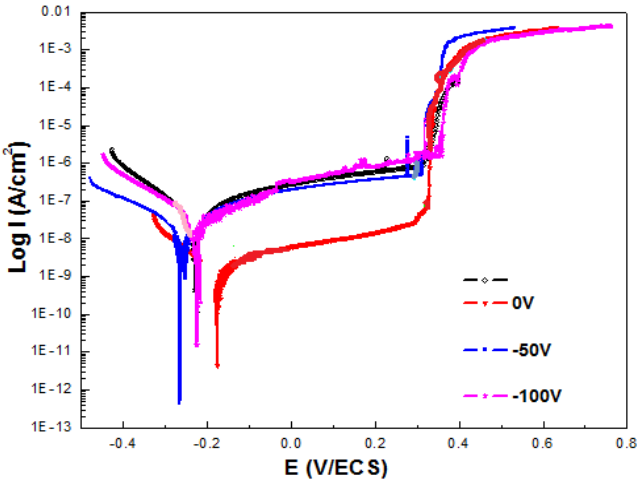

Fig. 5 Measurement Corrosion rate depending on polarization

The Tafel curves shown in Figure 5 show almost the same pace. The anodic domain indicates the presence of a passivation stage; where the intensity varies very little with the potential. It should be noted that the current density is a very important parameter, which makes it possible to evaluate the kinetics of the corrosion reactions.

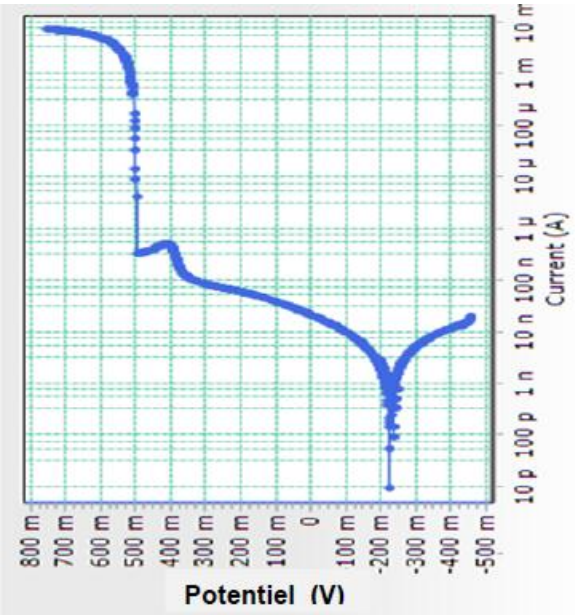

Fig. 6 Measurement Corrosion rate depending on polarization

Therefore, the drop in density means the appearance of passive films, while the abrupt increase of the latter indicates the rupture of this film and the development of pitting corrosion. This is characteristic of the behavior of stainless steel.

The potential Ecorr and the density Icorr are determined by the projection of the intersection of the tangents with the anodic and cathodic curves, on the axes of the abscissae and coordinates. Corrosion parameters including Tafel constants βa, βc, polarization resistance (Rp) and corrosion rate (Cr) are Confirme that the addition of W-TiN coatings can be advantageous, compared to bare stainless which not coated.

IX. CONCLUSION

W-TiN films have been successfully developed by the reactive magnetron sputtering technique. The different properties have been studied by highlighting the influence of the polarization of substrates. The results obtained demonstrated that the application of a polarization led to a decrease in the thickness of the layers on the one hand, and the increase in their roughness of another. This had a direct effect on the mechanical properties, and the electrochemical behavior of the coatings. The W-TiN films have made a considerable improvement in the properties of the steels, in particular on the hardness which has increased by three times the value of the uncoated steel, as well as a better resistance to corrosion.

REFERENCES

[1] W. Herr, B.Mathes, E.Broszeit and S.Kloos. Surface and coating technology 57 (1993)

[2] José Miguel Fernandes Figueiredo. Analysis of the tribological behaviour of W-Ti-N coatings. Mimoire de master. Université de Prague 2013.

[3] V. Severo. Tribological behaviour of W–Ti–N coatings in semi-industrial strip-drawing tests. Journal of Materials Processing Technology 209 (2009) 4662–4667.Page 1

[4] C. Perm. Jindal and Dennis T. quinto. Surface and coating Technology 36 (1988) 683

[5] W. D. Sproul, Thin solid Films, 107 (1983) 141

[6] Elaboration des normes, organisation internationale de normalisation

[7] ISO 3685 (1993), Essais de durée de vie des outils de tournage a partie active

[8] Yu Xi Wang, Sam Zhang, Jyh-Wei Lee, Wen Siang Lew, Bo Li. Surface & Coatings Technology 206 (2012) 5103–5107

[9] Darja Kek Merl, Ingrid Milosev, Peter Panjan, Franc Zupanic. Materials and technology 45 (2011) 6, 593–597

[10] Martin Fenker, Martin Balzer, Herbert Kappl. Surface & Coatings Technology 257 (2014) 182–205

Genetic Algorithm for the Periodic Replenishment Problem of Vending Machines

Yi-Chih Hsieh* and Cheng-Dar Liou

***Abstract*—**This paper studies the periodic replenishment problem of vending machines (PRPVM) in which each vending machine has to be replenished once per day or once per two days by a vehicle. This paper presents a new encoding procedure to convert any infeasible sequence of solution into a feasible one, and then embeds it into a genetic algorithm to solve it. Numerical results of a case in Tainan, Taiwan, were reported and discussed under various capacities of the vehicle. Numerical results show that the adopted genetic algorithm can solve the presented problem effectively.

***Keywords*—**Periodic replenishment problem, Genetic algorithm, Optimization.

Yi-Chih Hsieh is with the Department of Industrial Management, National Formosa University, Huwei, Yunlin 632, Taiwan (corresponding author, phone: +886-5-6315718; fax:+886-5-6311548; e-mail:yhsieh@nfu.edu.tw).

Cheng-Dar Liou is with the Department of Business Administration, National Formosa University, Huwei, Yunlin 632, Taiwan (e-mail: cdliou@ nfu.edu.tw).

Estimating the Willingness to Pay for Renewable Energy in Turkey

Eyup Dogan and Iftikhar Muhammad

***Abstract*—** Turkey is a developing country with rapid economic growth; its energy needs have hugely increased thus putting the development of the sector a top priority. Pursuant to its 2010-2014 action plan framed by the Ministry of Energy and Natural Sources, Turkey has got an ambitious national energy goal of minimizing energy import and maximizing domestic energy and produce 30% of electricity production from renewable energy sources up to 2023. To actualize its ambitious renewable energy targets Willingness to Pay (WTP) plays the central role in directing appropriate policy and therefore based on this discrepancy this study aims to investigate the WTP of the Turkish citizens for green electricity by applying the Tobit model. The study was carried out by conducting face-to-face interviews of 2,500 households in 12 major metropolitan cities of Turkey based on contingent valuation method consisting of a total of 26 questions. The findings indicate that household income, household size, education, environmental conscience and gender are highly related to WTP for green electricity in Turkey. The mean WTP of Turkish citizens is found to be 4.35 Turkish Liras ($1.13). The findings of this study aim to offer useful insights to government agencies as well as utility companies that will help them to carry out the necessary targets.

***Keywords*—** Renewable energy, Contingent valuation, Willingness to pay.

ACKNOWLEDGMENT

This work is supported by the Scientific and Technical Research Council of Turkey (TUBITAK) under Grant No. SOBAG 116K727.

Eyup Dogan is with the Department of Economics, Abdullah Gul University, Turkey (e-mail: eyup.dogan@agu.edu.tr).

Iftikhar Muhammad is with Department of Economics, Erciyes University, Turkey (e-mail: iftikharm895@gmail.com).

Artistic Image in the First Mameluke Era's Epistles

Dr. Nader Masarwah

***Abstract*—** This study discusses the artistic image in the prose of the first Mameluke and it especially focuses on messages and epistles as it represents the most of the production of the era. In addition to this, it personifies the writing styles that dominated that era and other prose styles.

It tries to show and represent the images that spread in the epistles regardless its known types:

Diwaniyah, Ikhwaiyah and Adabiyah taking into consideration the Jihadist one as a remarkable sign of the era depending on the subject. Otherwise, it is included in the previous three types of epistle.

The study sheds the light also on the stereotypes of the artistic images that based on imagery, and metaphor in addition to the dynamic and wealthy images. Then it reveals the sources of these artistic images and its relation to the cultural, educational, natural and social condition of the writer. Not only this, but it also showed the connection between these relations and different types of rhetoric, the usage of Holy Quran, Hadith, Arabic poetry and idioms in the text. Finally, it shows the function of this artistic image and its relation with the aim and the subject of the message.

Dr. Nader Masarwah is Lecturer, Al-Qasemi Academic College, Baqa El-Gharbiam, Israel (e-mail: nadermasarwah@walla.co.il, nadermasarwah@walla.com)

Road Safety in Jordan: Appraisal and Identification of Potential Interventions

Khair. Jadaan[1], Ethar. Braizat[2], Yazan. Albanna[3] and Sandra. Nashquai[4]

***Abstract*—** Road traffic accidents are a considerable concern in both developed and developing countries because of their impact on social, economic and health issues. The level of traffic safety in Jordan, classified as a middle-income country, falls well behind many countries. The speed of economic development and population growth are expected to produce further increase in traffic volume and consequently an increase in traffic accidents. During the last 20 year, traffic accidents increased from 17838 accidents in 1990 to144521 accidents in 2016.The magnitude of the problem, its rates of growth and the associated economical and social impacts are alarming calling the need for a detailed analysis of the present evolution of the problem, its causes, costs and possible effective countermeasures in an attempt to improve road safety. This study provides an overview of accidents trends and characteristics in Jordan. An attitudinal survey is carried out in order to identify the most effective and favorable potential countermeasures, as perceived by road users. The results of the study would help decision makers to take the necessary actions towards encompassing the problem.

***Keywords*—** Road safety; Road traffic fatalities; Traffic safety interventions; Jordan.

I. Introduction

ACCORDING to the World Health Organization (WHO) more than 1.2 million people die each year and more than 50 millions are injured as a result of Road Traffic Accidents (RTA). The majority of these accidents (over 90% of accidents and 80% of fatalities) occur in the low and middle- income developing countries[1].The relationship between RTAs and number of motor vehicles was examined and the ratios of vehicles, population, and fatalities among the High income, Middle income and Low income countries are given in Table 1.

Khair. Jadaan[1] is with the Jordan University, Jordan (corresponding author's phone: +0096796222868, ; e-mail: Kjadaan@gmail,com).

Ethar . Braizat[2], is Dar Al-Handaseh shair and his partners Jordan. (e-mail: Etharbraizat9@gmail.com).

Yazan. Albannah[3] is with the SETS Intel, (e-mail: albanna82jo@hotmail.com).

Sandra. Nashquai[4], is with Middle East University, (e-mail: nsandra@live.com).

TABLE I
THE RATIOS OF VEHICLES, POPULATION, AND FATALITIES AMONG THE HIGH INCOME, MIDDLE INCOME AND LOW INCOME COUNTRIES

	Low Income	Middle Income	High Income
Population	12	72	16
Registered Vehicles	1	52	47
Fatalities	12	80	8
Fatality Rate (/100,000population)	183	201	87

The figures in table 1 and research carried out in various parts of the world reveal that, compared with many western industrialized high income countries, accident rates in developing countries are high and that traffic safety is worsening in many of these countries. The problem continues to be a major socio economic problem for most developing countries due to rapid motorization and other factors with high cost [2,3]

A. Appraisal of Road Safety Situation in Jordan

Current traffic safety conditions are already extremely serious in Jordan and will undoubtedly worsen in the near future, in face of the rapid increase in the use of motorized means, within a travelling and social environments that are not prepared to experience such changes.

A number of studies investigated the magnitude of the problem , its rates of growth and the associated economical and social impacts [4,5,6,7] while other studies focused on the prediction of future number and severity of accidents [8,9,10,11]. A more recent study [12] carried the matter further producing a thorough investigation into the prediction, cost and strategy issues of the problem. In general, the results were alarming showing a low level of traffic safety in Jordan compared to develop and many developing countries and producing large socio-economic losses. The number of accidents has increased more than five-fold between 1995 and 2016 reaching 144521 accidents and 750 fatalities in 2016 with an estimated cost of JOD 323 (US$500) million.[12,13]

i. Vehicle ownership and traffic composition

Two major factors that affect traffic accidents are

population and number of vehicles. Both factors showed consistent increase in Jordan over the years. The population has increased more than 71% between 2007 and 2016 from 5,723,000to 9,798,000. During the same period the number of registered vehicles has increased by about 78% from 841,933vehicles in 2007 to 1,502,420 vehicles in 2016. Many political events that took place in the Middle East region have significantly contributed to the population growth while the rising per capita income added to the reduced customs on imported cars and the inferior public transport service encourage private vehicle ownership.

The growth in population, the number of registered vehicles and the vehicle ownership (vehicles/population) over the 10-year period between 2007 and 2016 are given in table 2, vehicle ownership was about 2390 Veh /10,000 Person.

TABLE 2
GROWTH IN POPULATION, NUMBER OF REGISTERED VEHICLES AND VEHICLE OWNERSHIP

Year	Population	No. of Registered Vehicles	Vehicle Ownership (Veh. / 10,000 persons)
2007	5723000	841933	1471.14
2008	5850000	905592	1548.02
2009	5980000	994753	1663.47
2010	6113000	1075453	1759.29
2011	6249000	1147258	1835.91
2012	6388000	1213882	1900.25
2013	8110000	1263754	2000.78
2014	8800000	1331563	2150.59
2015	9530000	1412817	2255.31
2016	9798000	1502420	2390.78

SOURCE: REFERENCE 13

ii. Accidents and casuality trends and rates

Jordan started to witness a modern development since the seventies which was reflected on the vehicle ownership and consequently on accidents and the resulting causalities during recent years. Annual statistics show that the number of accidents was 11,113 in 1979 with 354 killed. The figures have increased to 43,343 accidents and 612 killed in 1998. The corresponding figures in 2016 have increased to 144521 accidents, 750 fatalities.

Table 3 shows the number of total accidents, injuries, and fatalities in Jordan over the period 2007 -2016. It can be seen that accidents are increasing rapidly at a high rate while traffic injuries and fatalities are both increasing but at a lower rate than accidents. Fatalities have increased with time until they reached their maximum in 2007, and then declined.

TABLE 3
CHANGES IN NUMBER OF ACCIDENTS, INJURIES, AND FATALITIES (2007-2016)

YEAR	Number Of Accidents	Number of Injuries	Number of Fatalities
2007	110630	17969	992
2008	101066	13913	740
2009	122793	15662	676
2010	140014	17403	670
2011	142588	18122	694
2012	112817	17143	816
2013	107864	15954	768
2014	102441	14790	688
2015	111057	16139	608
2016	144521	17435	750

SOURCE: REFERENCE 13

Three parameters, total number of fatalities, fatality rate per population and fatality rate per distance traveled, are considered particularly significant for comparative purposes and economics of projects. The other two parameter, fatality rate per vehicle and fatality index are commonly used to identify the seriousness of the road accident situation in one particular country. However, data availability controls the parameters to be used. For example, data on distances traveled are not available for most of developing countries.

Table 4 shows the changes in injury and fatality rates during the period (2007-2016). During the 10-year period, there has been an increase of almost 63 percent in vehicle ownership accompanied by 50 percent reduction in fatality rate (per 10,000 vehicles) as compared to the growth of population and almost the same fatality rate per 100,000 persons.

TABLE 4
TRENDS OF TRAFFIC ACCIDENTS RELATED STATISTICS DURING THE PERIOD (2007-2016)

	2007	2008	2009	2010	2011	2012	2013	2014	2015	2016
Fatalities/ 1000 accidents	8.9	7.3	5.5	4.8	4.9	7.2	7.1	6.7	5.5	5.2
Injuries/1000 accidents	162.4	137.7	127.5	124.3	127.1	151.9	147.9	144.4	145.3	120.6
Fatality Index *	0.052	0.05	0.041	0.037	0.037	0.045	0.048	0.047	0.038	0.043
Fatality/10,000 vehicles	11.8	8.2	6.8	6.2	6.0	6.7	6.08	5.17	4.3	4.99
Injury /10,000 vehicle	213.4	153.6	157.1	161.8	158.0	141.2	126.2	111.1	114.2	116
Fatality/100,000 populations	17.3	12.6	11.3	11.0	11.1	12.8	11.76	10.31	6.38	7.65
Injury /100,000 populations	314.0	237.8	261.9	284.7	290	268.4	244.3	221.6	169.3	0.13
Severity Rate **	0.17	0.14	0.13	0.13	0.13	0.162	0.16	0.15	0.15	0.13

*Fatality Index = No. of Fatalities/No. of Casualties
** Severity Index = No. of Casualties/No. of Accidents

iii. Contributing Factors

The major factors that contribute to the high rate of accidents may vary between countries. In Low-income developing countries, the factors include lack of safety belt

and helmet use, a large number of old vehicles on roads that often carry more people than their capacity, poor road design and maintenance and the traffic mix on roads[14]. In high-Income rich oil countries human-related factors are the main contributors to high accident and fatality rates including reckless driving, and lack of observance to traffic regulations and traffic control devices. In Kuwait, for example, the level of observance of traffic signs by drivers was found to be very low where only 4% obeyed the Stop sign(stopped fully voluntarily) and over 70% violated the speed limit sign[2,15]

The limited resources of Jordan, classified by the World Bank as a middle-income developing country, may produce the following consequences:

- Many private and commercial vehicles are used beyond their normal life span, with attendant risk of sudden mechanical failure.
- The country is unable to build sufficient good quality roads or have adequate control devices that cope with the continuously growing demand.
- Streets have deteriorated and traffic chaos occurs with different kinds of traffic sharing the same street un-segregated especially in rural areas
- Inadequate Street lighting which, if added to poorly lit vehicles, increases the risk of accidents at night.
- Inadequate pedestrian's facilities, both in quality and quantity.
- There are few refuge islands in the center of wide streets, few markings and very few traffic lights with "walk" sequence, so that pedestrians are usually at risk.
- Moreover, road user behavior is reckless and drivers routinely ignore traffic laws and pedestrians routinely walk in the middle of streets cross without checking for traffic.

Studying the factors contributing to accident occurrence in Jordan showed that road users contributed to 94.74% of total reported accidents, whereas road failures and vehicle defects contributed to 4.46% and 0.80% respectively.

B. Identification of Potential Interventions

The road safety issue has long been the focus of attention in developed countries and their fatality rates are generally improving, while relatively little is done to reduce the magnitude of the problem in developing countries. High-income countries have successfully implemented effective interventions to help reduce the burden of road traffic accidents while low- and middle-income countries have not yet achieved similar results noting that both scientific research and capacity development have proven to be useful for preventing accidents in high-income countries[16].

i. Best Practice Strategy

Jordan suffers from a serious road safety problem that must get more attention from the decision makers. The magnitude of the problem, its rates of growth and the associated economical and social impacts are alarming which requires the researchers and decision makers to provide approaches to reduce the overall number and severity of accidents.

However, the implementation of road safety measures bears a lot on the various stakeholders with multitude of interests leading to the development of what is termed "Best Practice" strategy for road safety [17]

Best Practice" refers to a road safety policy that has proven to be successful meaning brings about a sustainable reduction in the number of road accidents and in particular the number of resulting casualties.

Five pillars were identified as the focus of action to improve road safety. These are:

1. Road safety management;
2. Safer Infrastructure;
3. Safer vehicles;
4. Safer road user behaviour and
5. Improved post-crash care.

ii. Identification criteria of best practices

The best practice candidates are identified and described based on the following criteria [17]:

1. Focus of the measure: a clear definition of the road safety problem to be solved and precise idea of how the measure will affect this problem.
2. Magnitude of the road safety problem
3. Expected effects on safety which addresses the process of implementation.
4. Evaluation of effects on road safety based on accident statistics
5. Costs and benefits analysis
6. Acceptance by public and policy makers
7. Sustainability over time
8. Transferability: using the measure successfully on a larger scale (regional/national level).

iii. Methodology

The process to develop the best practice is carried out by reviewing different approaches that were developed in a various countries. The first phase of the study involved selection of a number of best practice measures that are considered relevant to improve future traffic safety in Jordan. As a starting point, a set of instruments was prepared.

- A list of road safety measures in order to select the best practice measures;
- A decision upon the selection criteria for the best practices which was the acceptance of drivers' population to these practices.
- A questionnaire for data collection in order to provide an insight into these issues with the aim of evaluating how effective road users thought the best practice measures would be in reducing the number of accidents (effectiveness index on a 0-5 scale), and also how much they would be in favor of the measure if actually being introduced (favourability index on a 0-5 scale).

In order to be labeled as Best Practice, a measure should

comply with most of the selection criteria. In particular its effectiveness in terms of expected reduction of road accident, deaths and serious injuries should have been demonstrated in previous scientific work. The acceptance level of drivers' population to these practices is another important factor in the selection process.

iv. The Attitudinal Survey

A predesigned questionnaire was prepared and distributed to collect information on what representative sample of road users with different income and educational level thought about a variety of possible best practice measures

In total, 39 Best Practice nominations were chosen, taking the above selection criteria into account. . The measures were considered to reduce traffic accidents and were devised to gauge how well the public might accept and favor them as countermeasures (CMs), and how effective these measures were as perceived by road users. The public road users were asked to report their attitude towards these measures in terms of "effectiveness " and " favorability " of the CMs .

The effectiveness of the different CMs was obtained using a five point rating scale having a verbal label as follows:1- Negative effectiveness2- Not effective3- Less effective 4- Highly effective 5- Very highly effective. Ratings of how much respondents were in favor of each CM were also obtained using a five point scale as follows:1- Strongly against2- Against3- Neutral4- Support 5-Strongly support

Analysis of the responses involved ranking of the countermeasures according to their perceived effectiveness and favorability using two indices namely "effectiveness index" and "favorability index". Each index represents the arithmetic mean of all the rating responses from 1 to 5 with the higher indices given lower ranking number.

;The effectiveness and favorability indices were combined for each remedial measure, giving equal weight for each index, in order to rank the measures in terms of the merging between effectiveness and favorability. The results shown in table 9which gives a listing of the highest and the lowest ten measures thereby enabling the identification of those interventions with the highest potential for improving road safety in Jordan.

TABLE 5
THE HIGHEST AND LOWEST EFFECTIVE AND FAVOURABLE INTERVENTIONS

Remedial Measure	Effectiveness and Favorability Index	Rank
Control intensification on over speed violations in rural roads	4.085	1
Control intensification on over speed violations in rural roads	4.06	2
Decreasing the maximum speed limits over urban roads	4.015	3
Impose the use of reflecting triangle	4.01	4
Placing of dangerous crossing signs on high accidents places	3.975	5
Increase traffic education in schools	3.96	6
Using automatic jail penalty against drunk drivers causing accidents	3.955	7
Increase the number of play parks to decreasing stopping of cars on the roads	3.88	8
Removing s the obstacles from medians that restricts sight distance like trees.	3.88	9
Provide safe sidewalks for pedestrians free of obstacles.	3.875	10

Increase the penalty value (ticket) for traffic violation	3.67	29
Decreasing max. speed limits during night by 10 Km/h	3.665	30
Impose using of safety belt in the back seats passengers	3.665	31
Decreasing max. speed limits along highways	3.625	32
More concentration of the driving test on written part	3.62	33
Retesting drivers who are over 65 year every five years	3.545	34
Reconsideration of the openings in the median islands for highways and main roads and closing the unjustified among it.	3.54	35
Increase legal age for obtaining driving license	3.53	36
Increase the difficulty level of the driving test	3.475	37
Retesting drivers every five years	3.385	38
Increasing max. speed limits along highways	3.02	39

v. Areas of action for sustainable road safety in Jordan

Road user factors were identified as the most contributors to traffic accidents in Jordan with reckless driving, and lack of observance to traffic regulations are among the main factors. The road network continues to expand in Jordan with improving design and maintenance standards but there is still potential for improving the road safety standards of these networks such as improved street lighting and installing guard rails. Jordan also has high technical standards for newly imported vehicles and for vehicles in use that ensures road worthiness of motor vehicles. However, the level of implementing these standards is not as high as the standards and requires a lot of attention and revision.

Jordan does not have an official national road safety strategy but action plans. Three action plans were prepared 2008-2012, 2010-2013 and the most recent 2013-2017. However the first two plans were not fully implemented as planned. The third plan aims at the followings:

1. Reduce the number, rates and severity of traffic accidents and their social and economical impacts.
2. Provide safe and efficient traffic movement with reduced traffic congestion.
3. Improve the level of traffic and road safety education of the general public.
4. Improve the efficiency of the personnel working in the traffic sector.
5. Treatment of high accident locations as identified by the

studies carried out annually.

In view of the above, some important work which provides future efforts towards improving road safety in Jordan, but not limited to, specific areas of action, are listed below. These actions are based on the application of the five Es (Education, Enforcement, Engineering, Encouragement, and Evaluation) and the two Cs (Coordination and Cooperation).

1. Developing and implementing national road safety strategy focusing on vulnerable road users; pedestrians and young drivers in particular.
2. Developing and updating of highway and traffic manuals, standards, materials and guideline. These include specific documents for design, work zones, Road Safety Audit, and road safety education.
3. Adopting a system for the evaluation of road safety performance
4. Continuous cooperation and coordination between the various stakeholders at all level ; national, regional and international
5. Allocation of sufficient funding and resources
6. Introducing a world –class emergency medical services system.

It should be noted, however, that measures that are very successful in achieving significant major benefits in certain countries may not be that successful in another country, due to the complexity of the inter-relationship that exists among the traffic variables and driver attitudes.

II. CONCLUSION

This work shed some light on the road safety situation in Jordan. The results of the investigation reveal that the magnitude of the problem is alarming and continues to be high compared to developed countries and that the country still suffers from sustainable increase in traffic crashes despite the humble attempts and efforts to reduce their magnitude and severity. However, a review of the progress in road safety initiatives developed or implemented indicate that there is still a considerable room for improvements.

The best practice approach is used and an attitudinal survey is carried out to identify the potential interventions based on the effectiveness and favorability of the various measures as perceived by the road users. Some important work and specific areas of action which provide future efforts towards improving road safety in Jordan, are identified.

REFERENCES

[1] World Health Organization (WHO), Global status report on road safety: supporting a decade of action, Geneva, 2013

[2] K. Jadaan, Traffic safety in Gulf countries with special reference to Kuwait, Transport Reviews, 8(3)(1988) 249-265.

[3] W.Ackaah , M. Salifu, Crash prediction model for two-lane rural highways in the Ashanti region of Ghana, International Association of Traffic and Safety Science (IATSS) Research, 35 (1) (2011) 34–40.

[4] I. Al-Hiyari, The future of traffic safety in Jordan and its impact on national economy,".M.Sc Thesis, Dept. of Civil Eng., University of Jordan, Amman, Jordan, 2011.

[5] W. El-Shajrawi, "A comprehensive in-depth study of the contributory factors in urban accidents," M.Sc. Thesis, Dept. of Civil Eng,. University of Jordan, Amman, Jordan, 1997.

[6] K. Jadaan, I. Al-Hyari, H. Naghawi, R. Ammourah, and Z. Al Nabulsi, Traffic safety in Jordan: magnitude, cost and potential countermeasures", Journal of Traffic and Logistics Engineering, 1(2013) 54- 57.

[7] A. Bener, S. Hussain, S. Al-Malki, M. Shotor, and K. Jadaan, Road traffic fatalities in Qatar, Jordan and the UAE: estimates using regression analysis and the relationship with economic growth,Eastern Mediterranean Health Journal (EMHJ) 15(3) (2010) 318-323.

[8] K. Jadaan, R. Mustafa, and H. Naghawi, "Road Traffic Accidents in Jordan: Prediction and Potential Countermeasures", Traffic Safety Forum, University of Dammam, Saudi Arabia, 2011.

[9] K. Jadaan, M. Al-Fayyad, H. Gammoh, Prediction of road traffic accidents in Jordan using artificial neural network,Journal of Traffic and Logistics Engineering 2 (2014) 92-94.

[10] J. Al-Matawah, K. Jadaan, Applications of prediction techniques to road safety in developing countries, Int. J. Appl. Sci. Eng.(IJASE) 7(2) (2009)169-175.

[11] K. Jadaan, L. Foudeh, M. Al- Marafi, and M. Msallam. Modeling of accidents using safety performance function," in Proc. Int. Conf. on Agricultural, Environment and Biological Sciences. Antalya, Turkey, 2014, pp.104-108.

[12] E. Braizat, H. Gammoh, and S. Al- Rafayah, Classical and innovative road safety issues: prediction, cost , and strategies, Graduation Project, Dept. of Civil Eng., University of Jordan, Amman, Jordan, 2014.

[13] Directorate of Public Security, Jordan Traffic Institute, Statistical Year Book 2013.

[14] Imran M, Nasir JA. Road traffic accidents; prediction in Pakistan. Professional

[15] Med J 22(6) (2015)705-709.

[16] J. Al-Matawah, K. Jadaan, Road user attitudes towards safety initiatives in Kuwait. Int. Journal of Modern Engineering Research (IJMER) 3(3)(2013)1403-1409.

[17] N. Garg , A. A. Hyder, Exploring the relationship between development and road traffic injuries: a case study from India, European Journal of Public Health 16 (5) (2006) 487–491.

[18] K. S. Jadaan, E. Braizat, H. Gammoh, and S. Al-Rafaiah Developing a comprehensive road safety strategy for Jordan, ICTTE conference, Madrid, Spain, 2015.

Warehouse Capacity Determination and Supplier Selection in Industrial Manufacturing

Sadık Çökelez

***Abstract*—** The warehouse capacity determination and supplier selection are important issues in industrial manufacturing. What should be the optimal warehouse capacities that would meet the customer demand at minimum cost? Which suppliers should be chosen? This study will develop a linear programming model capable of determining the optimal warehouse capacities and will also adress the supplier selection issue concurrently. The objective function of the optimization linear program will involve warehouse capacity costs and part of the objective function will involve supplier related inputs. The objective function of the optmization model will be followed by relevant constraints such as warehouse capacity constraints and supplier related constraints. Such an optimization model can be quickly expanded fully and it can easily be solved by a linear programming optimization software such LINDO(Linear Interactive Discrete Optimizer.)

***Keywords*—** warehouse capacity, supplier selection, optimization,linear programming.

Prof. Dr. Sadık Çökelez works at Dept. of Econometrics, I.I.B.F, Süleyman Demirel University, Isparta, Turkey Phone: (90)537-790-7927
E-mail:scokelez2@gmail.com

Quantification of Remeasurable Hard Strata in Pipeline Projects Using SPT before Trenching

Mohammad N. Aladwani

Abstract— During the project life cycle, some quantities are not measureable exactly or reliably beforehand to tender. These quantities are termed as re-measurable quantities, which while execution of the project should measure on the case-by-case basis. Usually these re-measureable items/ quantities will be given with an assumed base-total quantity on tender documents for the bidding purpose. One such quantity is the Hard Strata found under the soil bed at locations where the propose project to be executed.

Here, a successful practical methodology adopted for finding the re-measurable hard strata quantity before trench excavation for the pipeline project for the Kuwait Oil Company's (KOC) Major Project EF1701, a 40" Gas Pipeline from Point 'A' located at North Kuwait to Mina Al Ahmadi Refinery located at South Kuwait, about 142km distance is given.

In this methodology, the site soil stratification, the hard strata, is determined using an in-situ test the Standard Penetration Test (SPT) with the criteria adopted from the KOC Standard for Geotechnical Investigation (Onshore). A generalized computation has been developed based on the SPT blow nos. got for 75mm penetration of the split spoon barrel in the bore-holes done for every 200 meter length along the pipeline centerline route. The required width and depth of the trench are fixed measurements according to the pipeline diameter to be placed with 1 meter soil cover from ground level to the crown of pipe. Only the effective depth of the hard stratum varies at the 200m interval bore-hole SPT conducted values and hence the average effective depth of hard stratum between the two bore-holes SPT conducted is calculated. Thus the total volume of the hard strata along the pipeline can be determined before the excavation of trench for the pipeline. A few assumptions are made in order to generalize the spreadsheet computation.

The data collected from 382Nos. bore-holes with SPTs carried out along the hard-stratum suspected portions along the pipeline right-of-way spanning altogether 78km, during the KOC's Major Project EF1701 is taken as an example to demonstrate in this paper. The same data has been considered for the Fiber Optic Cable (FOC) trench taken along the side of the pipeline trench with 5m distance apart, with less trench width and depth. The distance between the bore-holes can be reduced according to the site and the accuracy of the quantity calculation requirements.

Keywords— SPT, Borehole , Pen Mark, Penetration.

Team Leader Projects Management, Kuwait Oil Company, Kuwait

I. INTRODUCTION

Site investigation and estimation of soil characteristics are essential parts of a geotechnical design process.If your paper is intended for a *conference*, please contact your conference editor concerning acceptable word processor formats for your particular conference.

Geotechnical engineers must determine the average values and variability of soil properties. As stated by Mair and Wood (1987), in –situ testing is becoming increasingly important in geotechnical engineering, as simple laboratory tests may not be reliable while more sophisticated laboratory testing can be time consuming and costly. One of in-situ testing methods is the Standard Penetration Test (SPT). SPT is used to identify soil type and stratigraphy along with being a relative measure of strength.

SPT, developed in the United States , is a well-established method of investigating soil properties such as bearing capacity, liquefaction,…. etc. As many forms of tests are in use worldwide, standardization is essential in order to facilitate the comparison of results from different investigations, even at the same site (Thorburn, 1986). The quality of the test depends on several factors, including the actual energy delivered to the head of the drill rod, the dynamic properties of the drill rod, the properties of the soil, the method of drilling and the stability of the borehole.

According to the unavailability of equipment and also financial and time limitations in a project, in many cases various types of relationships may be needed to estimate the geotechnical parameters from the values extracted from the in-situ tests. One of these important parameters is bearing capacity of the soil which could be estimated from in –situ test such as standard penetration.

The present study area, project pipeline Kuwait, investigated, for the first time, to estimate site characterization of the site that can be used as potential input for designing structures by planner, civil and geotechnical engineers. In the present study, we have analyzed site responses of boreholes at different locations in project pipeline.

II. BACKGROUND

SPT was introduced in the USA in 1902 by the Raymond Pile Company. The earliest reference to an SPT procedure

appears in a paper by Terzaghi in 1947. The test was not standardized in the USA until 1958. It is currently covered by ASTM D1586-99 and by many other standards around the world (Robertson, 2006).

The Standard Penetration Test consists of driving the standard split barrel sampler a distance of 460 mm into the soil at the bottom of the boring, counting the number of blows to drive the sampler the last two 150 mm distances (to obtain the N number) using 63. 5 kg driving hammer falling free from a height of 760 mm (Bowles, 1977) The boring log shows refusal if 50 blows are obtained for a 300 mm increment or 10 successive drops produce no advance. SPT data have been used in correlations for unit weight, relative density, angle of internal friction and unconfined compressive strength (Kuihawy and Mayne, 1990).

Schmertman (1979) provided valuable insight into the mechanics of the Standard Penetration Test. Schmertman (1979) illustrated that the standard Penetration Test is a combination of dynamic end bearing and side resistance must be overcome in order for sampling barrel or split spoon to advance into the ground. By comparison with parallel results from a mechanical friction cone, Schmertman was able to demonstrate the contribution of side resistance and end resistance to the advance of the spoon was a function of soil type.

Zekkos et al. (2004) studied the reliability of shallow foundation design using SPT test. The results of reliability analysis show that the factor of safety approach can provide an impression of degree of conservatism that is often unrealistic. The reliability based approach provide rational design criteria, accounting for all key sources of uncertainty in the foundation of engineering process and thus should be the basis of design.

Lutenegger (2008) showed that the SPT provides three numbers that can be used to evaluate soil properties through an analysis to illustrate how the incremental blow counts may be used to obtain more information from the test.

Hooshmand et al.(2011) used SPT to investigate the strength and deformation characteristics of Tabriz marls and their stress-strain behavior were investigated by a various in-situ and laboratory tests. In order to study deformation behavior of these marls, various experiments were used such as the pressure meter test, Plate Loading Test (PLT) , seismic wave velocity test, uniaxial compression test and Standard Penetration Test (SPT).

Obeifuna and Adamu (2012) presented an assessment of the geological and geotechnical parameters in Wuro Bayare area of northeastern Nigeria. The results indicated that soils are poorly to well-sorted, soils have moderate to high plasticity, slight dry strength and are easily friable. From geotechnical analysis results, recommendations for erosion control were given, such as; construction of drainages, grouting concrete rip-raps and afforestation.

III. CRITERIA

As per the KOC standard for Geotechnical Investigation (Onshore) KOC-C-003 as per attachment (1) , the hard stratum is defined as natural or artificial material including rock, which cannot be penetrated except by the use of chiseling techniques, rotary drilling, blasting or powered breaking tools.

The following conditions apply as per the Clause 3.1.5 of KOC-C-003:

(1) The above definition shall apply during boring using 150 or 200mm diameter boring equipment, provided that the boring rig involved is in good working order and is fully manned.

(2) Under the above stated condition (1), if the boring cannot be able to proceed at a rate greater than 0.5meter per hour through the hard stratum being penetrated.

(3) Under the above stated condition (1), 100mm diameter undisturbed sample tubes cannot be able to drive more than 300mm.

(4) Under the above stated condition (2), a Standard Penetration Test (SPT) shows a resistance in excess of 35 blows per 75mm penetration of the split spoon barrel.

The general and the above conditions draw backs are:

(a) Nobody can able to ascertain hard stratum by its look, texture & color.

(b) No equipment available to scan.

(c) Condition (1) depends upon the person handling, the type of machine and the machine power; which is inconsistent.

(d) Conditions (2) & (3) are still inconsistent, as it depends upon the machine and difficult to ascertain a fixed depth where it started becoming a hard stratum.

Condition (4) is a consistent way, since it gives internationally accepted test method SPT blow-values carried out during borehole tests and the correct depth, which is utilized for the hard stratum datum assessment.

IV. METHODOLOGY

A survey shall be conducted either by the Contractor or KOC approved third party laboratory or agency, from the permanent control points/ bench marks provided, to the pipeline right-of-way (ROW) using either Total Station or GPS instrument. The chainage marker boards shall be place at about 20m distance from the center-line of the pipeline route established. These marker boards shall be established from the starting point to the end-point of the proposed pipeline route and shall kept undisturbed/ protected up to the completion of the project. The suitable coordinates either in UTM Zone 38 WGS84 or UTM Zone 38 International Spheroid can be adopted according to the project requirement.

Then, boreholes with the SPTs shall be conducted along the pipeline center-line route established, by a KOC approved third party laboratory or agency or Contractor, at an intervals of 200meter minimum along the hard-strata suspected areas with location corresponds to the chainage marker boards established. Each borehole is named with an identifying number. The SPT is carried out in each borehole, starting from the depth of 0.5m in order to get clear from the top soil. Then two seating blows applied for the penetration of 75mm depth each by the split spoon/ barrel; consequently another four 7mm penetration blows will be counted separately. In between if at any penetration level 35 or more than 35 No. of blows reached the SPT stop, since the KOC-C-003 criteria being achieved. If not, the SPT continues from 1.0m, 1.5, 2.0 etc. from every further 0.5m depth up to 3m or 3.5m as decided in minimum to the project required trench depth plus about 0.8 to 1m further depth of borehole.

The related Borehole Log and the Pen-mark Penetration Table is prepared (please see the specimens attached for the samples taken in the 'Results and Discussion' section). The activity continues with the other borehole along the pipeline route as decided.

From the depth of the hard-stratum starting, the effective depth is calculated from the fixed project pipeline depth. Since the width of the pipeline trench is fixed and the length in between the boreholes is also known, the volume of the hard strata can be calculated by taking the average depth of hard strata between the two boreholes.

Some assumptions are made in view of practicability, which are:

(a) The No. of blows for the initial two 75mm penetrations (seating blows) will not be taken into account.

(b) If 35 and more No. of blows got at the start of the SPT on the initial level itself, then the effective depth of hard strata will be counted from the ground level (GL).

(c) The effective depth shall be calculated up to the fixed pipeline trench formation level required.

(d) If the hard stratum starting level comes below the fixed pipeline trench formation level, then the effective depth will be taken as zero.

(e) The width of the pipeline trench shall be fixed according to the pipeline project requirement.

V. SITE DESCRIPTION AND MAP

The State of Kuwait situated in northeastern edges of the Arabian Peninsula at the tip of the Persian Gulf. It lies between Latitudes 28O and 31O N; Longitudes 46O and 49O E. In the UTM coordinates, it lies in Zone 38 and extension.

The country is generally low lying, with the highest point being 306m (1,004 ft) above sea level and the flat – sandy desert covers most of the land. The oil fields are located in deserts, where the ground water table is much below the ground level and stratified layers of hard strata soil occurs. The world's second largest Greater Burgan oil field is situated in the southeast of Kuwait; wherein the subject methodology of determining the hard strata quantity carried-out project had taken place.

The project 40" diameter gas pipeline starts from the location named Point 'A' north of Kuwait and ends up in Mina Al Ahmadi Refinery at south of Kuwait with total 142km length of pipeline as per attachment (2) .

VI. RESULTS AND DISCUSSION

In the KOC's Major Project (EF1701) 40" Gas Pipeline from NK to MAA, three series (i.e. at three portions along the pipeline route) of boreholes with SPTs carried out on an average distance of 200m. 1st portion from chainage 10+250.000 to 52+400.000, 42.15km with 211Nos. boreholes; 2nd portion from chainage 53+100.000 to 67+000.000, 13.9km with 71Nos. boreholes and 3rd portion from chainage 111+400.000 to 132+900.000, 21.5km with 100Nos. boreholes.

Results:-

Case-by-case 5 typical samples are taken from the 1st portion of hard strata quantities evaluated in order to discuss the methodology and the results arrived.

For this project pipeline trench cross-section is fixed as: Width = 1.420m & Depth = 2.200m.

Sample case 1: From Borehole A34 (10+250.000) to Borehole A33 (10+450.000) as per attachment (3).

In A34 Borehole Log, it can be seen more than 35Nos. of blows (50Nos.) got at the 4th set of 75mm penetration from initial/ first SPT (i.e. SPT-1), where the required criteria for hard strata has been met. Hence, from the corresponding Pen-mark Penetration Table it can be seen the hard stratum starting depth from ground level (GL) is 0.5 + 0.075 + 0.075 + 0.075 = 0.725m. Since at the 4th set of 75mm penetration reached the required criteria for hard stratum, its penetration starting-point is taken for the start of hard stratum level. Therefore, the effective depth of hard stratum is 2.200 - 0.725 = 1.475m

Similarly, In A33 Borehole Log, it can be seen at 5th set of 75mm penetration from SPT-1 met the required criteria. Hence from corresponding Pen-mark Penetration Table, the hard stratum starting depth from GL is 0.5 + (0.075 x 4) = 0.800m. Therefore, the effective depth of hard stratum is 2.200 – 0.800 = 1.400m

Hence, the average effective depth is (1.475 + 1.400) / 2 = 1.4375m. Since we know the length between the boreholes from the chainage, i.e. A33 – A34 = 10450.000 – 10250.000 = 200.000m; and the width is fixed 1.420m, the volume of hard stratum will be calculated as:

Length x Width x Average Depth = 200 x 1.42 x 1.4375 = 408.25m3

Sample case 2: From Borehole A33 (10+450.000) to Borehole A32 (10+650.000) as per attachment (4).

In A33 borehole, from previous sample case 1, it is already described the effective depth of hard stratum is 1.400m

In A32 Borehole Log & the corresponding Pen-mark Penetration Table, it can be seen that hard stratum criteria has not been reached at any of the penetration levels. Hence, the effective depth of hard stratum is zero (0.000m)

Hence, the average effective depth is (1.400 + 0.000) / 2 = 0.700m. The distance between the boreholes, i.e. A32 – A33 = 10650.000 – 10450.000 = 200.000m. Width = 1.420m. Therefore, hard stratum volume is 200 x 1.42 x 0.70 = 198.800m3

Sample case 3: From Borehole A32 (10+650.000) to Borehole A31 (10+850.000) as per attachment (5).

In A32 borehole, from previous sample case 2, it is already described the effective depth of hard stratum is 0.000m

A31 Borehole Log & the corresponding Pen-mark Penetration Table, it can be seen that the hard stratum criteria has been reached at 4th set of 75mm penetration from SPT-5. Hence, the starting depth of hard stratum from GL is 2.500 + (0.075 x 3) = 2.725m, which is below to the trench formation level fixed i.e. 2.200m. Therefore the effective depth of hard stratum is zero (0.000m) as per the assumption taken.

Hence, the volume of hard stratum for this portion is zero [200 x 1.42 x 0.000 = 0.000m3]

Sample case 4: From Borehole A29 (11+250.000) to Borehole A28 (11+450.000) as per attachment (6).

In A29 Borehole Log & the corresponding Pen-mark Penetration Table it can be seen that the hard stratum criteria has been reached at 3rd set of 75mm penetration from SPT-3. Hence, the starting depth of hard stratum from GL is 1.500 + (0.075 x 4) = 1.800m. Hence, the effective depth of hard stratum is 2.200 – 1.800 = 0.400m.

In A28 Borehole Log & the corresponding Pen-mark Penetration Table, it can be seen that the hard stratum criteria has been reached at the initial level, at the start of the SPT-1 itself and hence, the hard stratum starting level will be counted from the GL as per the assumption taken, i.e. zero level (0.000m). Therefore the effective depth of hard stratum is 2.200 – 0.000 = 2.200m

Hence, the average effective depth is (0.400 + 2.200) / 2 = 1.300m. The distance between the boreholes, i.e. A28 – A29 = 11450.000 – 11250.000 = 200.000m. Width = 1.420m. Therefore, hard stratum volume is 200 x 1.42 x 1.30 = 369.200m3

Sample case 5: From Borehole A21 (12+850.000) to Borehole A20 (13+050.000) as per attachment (7).

In A21 Borehole Log & the corresponding Pen-mark Penetration Table, it can be seen that the hard stratum criteria has been reached at the initial level, at the start of the SPT-1 itself and hence, the hard stratum starting level will be counted from the GL as per the assumption taken, i.e. zero level (0.000m). Therefore the effective depth of hard stratum is 2.200 – 0.000 = 2.200m

Similarly, in A20 Borehole Log & the corresponding Pen-mark Penetration Table, it can be understood the effective depth of hard stratum is 2.200m

Hence, the average effective depth is (2.200 + 2.200) / 2 = 2.200m. The distance between boreholes, i.e. A20 – A21 = 13050.000 – 12850.000 = 200.000m. Width = 1.420m. Therefore, hard stratum volume is 200 x 1.42 x 2.20 = 624.800m3, which is the section full volume.

Spread-sheet computation;

All the data collected is entered into a formulated spread-sheet as shown on attachment (8). The boreholes designations and the initial 'from' & 'to' chainages of the boreholes are entered in their respective columns on the spread-sheet. After that, 'to' chainages of the boreholes should be entered since the 'from' chainages are automatically (formulated cells) populated in the spread-sheet. The hard stratum starting depth from ground level for the 'from' & 'to' boreholes shall be calculated from the respective Laboratory prepared Borehole Log and the Pen-mark Penetration Table and entered into the respective columns of the spread-sheet. The rest of the columns are been formulated to give the results up to the volume of that section. All the section volumes are added up automatically to give the grand total at the end of the spread-sheet.

The portions where there Main Road Crossings using the methods Horizontal Directional Drilling (HDD) and Micro Tunneling (MT) met with hard stratum, were calculated separately and entered into the spread-sheet at their respective chainage position columns.

Further columns can be added for the site verification checks to be carried-out during the actual excavation carry out.

VII. IMPROVISATION

During SPT conducting, there may be chances to have small stand-alone boulders or other artificial blocks to come across the penetration path of the split spoon/ barrel sampler. This can be seen by the sudden big difference on the No. of blows recorded. In order to avoid or improve on these cases, the following assumptions can be included –

(a) If soft stratum found below the hard stratum with a difference of 5 No. of blows or less, then the effective height will be taken from the initial hard stratum found.

(b) If soft stratum found below the hard stratum with the difference of more than 5 No. of blows, then it will be discarded.

Sometimes the hard stratum starting level will come below to the project trench formation level. For example, please see figure (1) & (2) below, let the starting depth of hard stratum at borehole A be 1.00m from the ground level (G.L) and that at borehole B is 2.80m, which is below the pipeline trench formation level of 2.20m. Let the red marked curved line will be the original hard strata profile at site.

In figure (1), by the method adopted, the effective depth of hard stratum at borehole B will be zero. Hence, the cross sectional area (slant lines marked/ shaded) will be more;

wherein the chances of hard stratum occurrence is less.

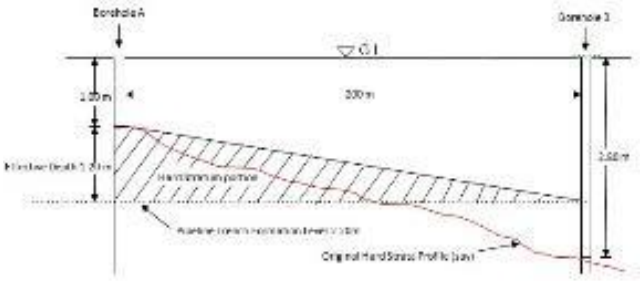

In figure (2), if the actual depth of the start of hard stratum is considered at borehole B, then the cross sectional area (slant lines marked/ shaded) will be comparatively less; wherein the chances of hard stratum occurrence is more.

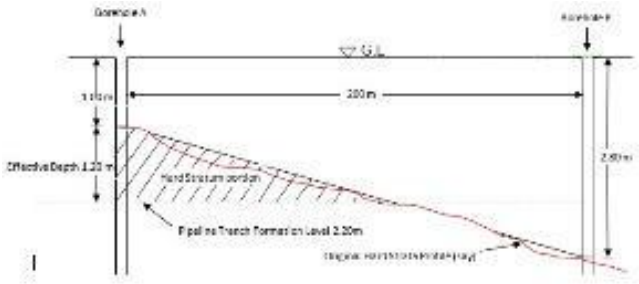

Therefore for this SPTs should be conducted further below the project pipeline trench formation level as decided based on the accuracy required and improvisation can be made by giving conditions for this.

VIII. DISCUSSION

The site verifications were carried-out during the project execution stage with the plus (+) or minus (-) quantities on the suspected portions, agreed between the Contractor and the Company authorized representatives. The variations came below 10% of the estimated total volume and hence the accuracy of the methodology was more than 90%.

IX. CONCLUSION

The methodology adopted in EF1701 project is found practicable with an accuracy of about more than 90% as evident from the site verifications done while executing the trench excavations on the concerned hard starta areas along the pipeline route. Improvisations can be made as described above from the lessons learned from the project. The following merits foresight by adopting this methodology:

(1) A reliable quantity for hard strata is obtained before the actual excavation of the pipeline trench

(2) A baseline quantity or depth will be available to verify at site while the excavation of trench for the pipeline takes place.

(3) Later disputes with Contractor can be avoided.

(4) A well defined procedure can be developed which can put in to the contract documents.

REFERENCES

[1] Bowles, J.E 1997. Foundation Analysis and Design, 5th Edn., Mc Graw Hill, USA

[2] Hooshmand, A., Amonfar M.H Asghari, E. and Ahmadi, H. 2011.

[3] Mechanical and Physical Characterization of Tabriz Marls, Iran. Published Online: 19 Octorber 2011 Springer science + Business Media B.V. Geotech. Geol. Eng. (2012) 30:219-232.

[4] Khulhawy, F.H and Mayne, P.W. 1980. Manual on Estimating Soil Properties for Foundation Design. Electric Power Research Institute. Palo Alto.

[5] KOC standard for Geo Technical Investigation (on shore), DOC.NO.KOC.C-03), Kuwait Oil Company, Kuwait.

[6] Lutnegger, AJ. 2008. The Standard Penetration Test – More Than just one Number Test. Geotechnical and Geophysical site Characterization-Houang and Mayne (Eds) © 2008 Taylor & Francis Group, London, ISBN 978-0415-46936-4.

[7] Mair. R. J and Wood, D.M. 1987. Pressuremeter Testing: Methods and interpretation, CIRIA/Butterworths, London.

[8] Obeifuna, G.I. and Adamu, J.2012. Geological and Geotechnical Assessment of Selected Gully Sites in Wuro Bayare Area, NE Nigeria. Research Journal of Environmental and Earth Sciences, 4(3): 282-302.

[9] Robertso, P.K. 2006. Guide to In-Situ Testing, Inc.

[10] Schmertman, John H. and Palacios, Alejandro. 1979. Energy Dynamics of SPT, Proceedings of the American Society of Civil Engineers, Journal of the Geotechnical Engineering Division, ASCE, 105 (GT8):909-926.

Comparison of Hydraulic and Thermal Performance of Small Capacity Air to Air Cross and Semi-Cross Flow Plate Heat Exchangers Using CFD Analysis

Murat Unverdi[1], Hasan Kucuk[2]

***Abstract*—**In this study, plate heat exchangers (PHE) are designed for use in a heat recovery device to meet the ventilation requirements of small capacities (50-200 m3/h). The thermal and hydraulic performances of two PHEs designed as cross flow (apex angle 90^o) and semi-cross (apex angle 60^o) flow are compared. In the design of the PHEs; the channel heights, the widths of the channels that the air flows into the heat exchangers, the plate widths, the inlet temperatures of the hot and cold air streams and the plate material are the same. The 3-dimensional Computational Fluid Dynamics (CFD) models of the PHEs are designed to evaluate the channel inlet effects of hot and cold air streams. The semi-cross flow PHE according to the investigated criteria, it has performed better than the cross-flow PHE in terms of thermal power recovered on the fresh side, pressure drop, specific fan power, electro-thermal amplification ratio, and thermal effectiveness. The cross flow PHE is more advantageous in terms of average heat flux and specific thermal power.

***Keywords*—** cross and semi-cross flow, heat recovery ventilator, plate heat exchanger, computational fluid dynamics.

I. Introduction

THE adverse effects of harmful emissions from fossil fuels in the immediate vicinity and global scale and the constant rise in energy costs are leading to increased heat recovery applications. The share of energy consumption in buildings and residences has reached 40% in developed countries [1]. The share of heating, cooling and ventilation in this consumption can reach up 60% depending on climate conditions [2].

According to data of 2016, almost all of the natural gas imported in Turkey is used for heating 32% in buildings and 25% in dwellings. Due to climate systems that are becoming widespread in humid climate regions where summer season is hot, electricity consumption is extremely increase in July and August, the hottest days of summer [3,4].

Applications such as window systems and insulated facade systems that reduce energy consumption for heating in buildings also reduce air infiltration. Mechanical ventilation systems have become obligatory for adequate ventilation and protection of indoor air quality [5]. In Turkey, where 80% of the population lives in cities, the use of small and medium capacity ventilation systems and the recovery of heat in these systems is unfortunately not common. Mechanical ventilation, especially for small and medium capacity ventilation requirements, is not as common as it should be in developed countries [1].

In large capacity systems, there is usually not enough ventilation to prevent the increase in energy consumption. Inadequate ventilation due to the reasons mentioned causes problems such as poor indoor air quality, respiratory diseases, and humidity and condensation damages in buildings [6]. Devices with different designs have been developed to recover sensible and latent heat. Energy wheels used to recover the sensible and latent heat in large-capacity ventilation systems, disadvantages such as mixing of fresh air with stale air and the presence of moving parts [2].

With medium and low capacity PHEs, heat can be recovered without mixing fresh air and stale air. Depending on the properties of the plate material, only sensible heat can be recovered or it is possible to recover both sensible and latent heat if materials such as paper and special membranes are used [1,2]. The cross flow arrangement is the simplest arrangement for leak tightness between fresh air and stale air in heat recovery devices where PHEs are used. In addition, cross flow arrangement facilitates maintenance operations such as cleaning and/or replacing the PHE. The PHEs and the heat recovery device are important for symmetrical flow channels, for equalization of fresh air and stale air flow rates, and for balanced ventilation [7].

The Reynolds number in the flow of PHE channels is generally below 2000 in applications, and laminar flow is accepted for obstruction of extreme pressure loss and noise. In the theoretical and numerical study of flow and heat transfer in PHE channels, many assumptions are made to simplifying the solution. The most common assumptions are that uniform velocity distribution at the channel inlets, that the fluid is

Murat Unverdi[1], Faculty of Engineering, Mechanical Eng. Dep., Sakarya University, 54050, Turkey (e-mail: muratunverdi@gmail.com).

Hasan Kucuk[2], Faculty of Engineering, Mechanical Eng. Dep., Sakarya University, 54050, Turkey (corresponding author's phone: +90 264 295 5723; e-mail: kucuk@sakarya.edu.tr).

Newtonian, and that the flow is hydrodynamically fully developed but is thermally developing, and that the thermophysical properties of the fluid and plate material are constant [7].

The local convective heat transfer coefficient in the PHE channel consisting of two parallel plates, asymptotically decreases from a very high maximum value at the inlet to a value at the fully developed flow at the end of the thermal entry length. The value of convective heat transfer coefficient for the fully developed flow depends on the thermal boundary conditions (such as constant heat flux, constant temperature) of the plate surface. The convective heat transfer coefficient in the real flow conditions of the PHE channel is different from the analytical results obtained with respect to the constant heat flux and constant temperature boundary conditions available in many books [8].

The real boundary conditions on the surfaces of plates that constituent the PHE channels convenient to the conjugate boundary condition. Although thermal conductivity of the plate material is not very high, the temperature difference between two surfaces of the plate is very low, as the plates are very thin. The heat released from plate to air on the fresh air side for energy conservation must be locally balanced by the heat from air to plate on the stale air side. Therefore the temperature at each point on the plate is different and is a result of the local interaction between the two air streams. In other words, the local temperatures of two air streams are conjugated. As a natural consequence of this situation, the heat flux at the plate surface is not constant. The temperature difference on plate surfaces and the heat flux depend on the properties of the plate material and on the local conditions of two air streams [7].

Partial differential equations written for conservation of momentum and energy, which continuously develop with changing boundary conditions in the numerical solution of the flow and conjugate heat transfer problem in the PHE channel, are solved by the finite volume method. Numerical solution calculations as a requirement of the conjugate heat transfer must be coupled for fresh air, stale air and plate material. Steady temperature distributions on the surfaces of plate and the air channels are obtained by convergence of the common iterative solution for these three medium [7, 8].

The hydrodynamic and thermal performance of a cross flow PHE with plate dimensions of 185 mm x 185 mm, channel height of 1.8 mm, plate thickness of 100 μm and channel number of 120 was investigated experimentally at flow rates of 50 to 300 m^3/h, corresponding to average channel inlet velocities of 0.2 to 3 m/s. It has been reported that the difference between the experimental results and the numerical solution results is below 15% and that the sensible thermal effectiveness of 80% at 50 m^3/h is reduced to 45% at the highest flow rate of 250 m^3/h [8].

The numerical analysis of experimentally investigated PHE stated that the temperature and heat flux distributions on the plate surfaces are not uniformly distributed and showing a two-dimensional distribution. The Nusselt number (Nu_H=8.23) in the constant heat flux at the channel width / channel height ratio (2b/2a=100) used in the PHE is about 8% higher than the Nusselt number (Nu_T=7.54) at the constant surface temperature. However, it has been shown that the Nu number (Nu_C=8.07) obtained from the numerical solution with the conjugate boundary condition, which is the real boundary condition in PHE, is 2% lower than the result obtained with constant heat flux. Assumption of fully developed laminar flow in the solution of heat transfer between plates requires constant fRe. However, it has been reported that the fRe obtained from the numerical solution are not constant even at very large channel width/height ratios (up to width/height>50). This situation, due to the fact that thermally developing flow along the channel is cannot hydrodynamically fully developed in reality due to the conjugate heat transfer [7, 9, 10].

Cross flow design is the most preferred and simplest flow arrangement for PHEs in terms of design engineering, as it facilitates leak tightness in the heat recovery device channels. However, the thermal effectiveness in the cross flow is lower than the counter flow. Fully counter flow arrangement cannot be applied since a complete leak tightness is not achieved when the air streams are separated at the inlet and outlet of the PHE in the heat recovery unit. For this reason, quasi-counter flow is the best possible choice. To evaluate the experimental/numerical performance of the quasi-counter flow arrangement, a PHE using apex angle 90^o plates is designed. In a quasi-counter flow PHE designed for 150 m^3/h balanced ventilation requirements of an office with 100 m^2 applications, the channel height is 4 mm and the total number of channels is 114. The thermal performance of the PHE was experimentally investigated by keeping the difference between fresh air and stale air inlet temperatures constant at 7 K. It has been reported that the sensible thermal effectiveness of 56% at design point (150 m^3/h) decreases from 80% to 51% in experiments where the flow rate is increased from 50 m^3/h to 200 m^3/h [10].

As in the cross flow case, the uniform velocity distribution at the PHE channel inlet and laminar flow (Re<2300) were assumed in the numerical solution of the quasi-counter flow PHE. Because the flow path is not as straight as in the cross flow due to the channel geometry it has been reported that the two-dimensional velocity field in the cross flow becomes three-dimensional in the quasi-counter flow. It is stated that the importance of hydrodynamic and thermal entry length areas increases, since the flow field is much more complex than the cross flow. It is stated that eddies and turbulence are caused by directional change of the velocity vectors in the PHE channel. It has been reported that as the area of the cross-like flow regions at the PHE inlet and outlet decreases, the counter flow becomes more dominant and the thermal performance increases. However, cross-like flow areas are

required to provide leak tightness and to separate two air streams at the inlet and outlet of the PHE channels [10].

The performance of three PHEs with the co-counter, cross and counter flow with the same membrane area is compared with numerical analysis. It has been reported that the lowest effectiveness is obtained in the co-current arrangement, the highest effectiveness in the counter flow arrangement, performance of quasi-counter flow arrangement is better than cross-flow and the sensible thermal effectiveness is 5% higher. It is stated that the average Nusselt number is greater than the Nusselt number of 7.54, which is the fully developed laminar flow in the parallel plate channel, since most of the channel length remains in the hydrodynamic and thermal entry length region. It has been shown that as the air velocity increases, the thermal entry length region also extends and the channel lengths are shorter than the entrance region in the majority of PHEs [8].

As stated above, the design of PHEs used in air to air heat recovery devices has design limitations that arise from manufacturing difficulties related to leak tightness between the two air streams. Flow and the heat transfer problem in the PHE channels is steady. However, due to short flow paths and conjugated thermal boundary conditions on the plate surfaces, the problem needs to be solved in hydrodynamically and thermally developing conditions.

In this study, a PHE was designed with plates with an apex angle of 60^o so that the flow of air at the inlet and outlet of the PHE can be separated without a leak problem and the flow conditions similar to those of the counter flow where the thermal effectiveness is higher. The thermal and hydrodynamic performance of this new semi-cross-flow PHE design is numerically compared to a plate width and channel heights of the same but full cross-flow (apex angle 90^o).

By reducing the apex angle from 90^o to 60^o, the average velocity in the PHE channels was decreased to extend the duration of air and to increase the thermal effectiveness and to soften the directional change to the PHE channels from the heat recovery device. In order to quantify these effects, channels for the heat recovery device have been added to the domain of numerical solution, at the inlet and outlet of the PHE channels, unlike the studies in the literature. With the solution area being enlarged, it became clear that the velocity distribution at the inlet of the PHE channels, which was made in many numerical studies and was unrealistic, was perpendicular and uniformly distributed to the flow cross section. Sudden cross-section and direction changes include at the entrance of air from the heat recovery device into the PHE channels and at the outlet from the PHE channels to the heat recovery device. In this way, a more realistic model has been created to investigate the effects of PHE on thermal and hydraulic performance.

II. Problem Definition

The performance evaluated PHE is designed to be used in a heat recovery device to meet a ventilation need of small capacities in this study. The dimensions of the PHE were determined taking into account the fresh air flow (50-200 m^3/h) required for a small residence where three to four people inhabitant. The total height, plate width (2W) and channel height (H) of the PHEs were kept constant. Numerical models have extended the fresh air side and the exhaust air side flow areas s=100 mm to take into account the local pressure losses at the inlet and outlet of the PHE. The extended areas were assumed to be adiabatic. The average air velocity in the PHE channels were selected to be flow laminar to prevent excessive noise and pressure loss. The Standard k-ε turbulence model was chosen for numerical solutions to take into account turbulence effects due to the change in flow cross section at the inlet and outlet of the PHE channels [11, 12]. In the numerical model, the exhaust air inlet temperature was 298 K and the fresh air inlet temperature was 283 K. The plate material is paper (k = 0.09 W/m K) and its thickness is 0.2 mm. The thermo-physical properties of air were obtained from reference [13]. Numerical solutions were performed with ANSYS/Fluent which uses finite volume method. Symmetric flow boundary condition was used to reduce the solution time in the 3-D numerical model. The outlet temperatures of the fresh air and the exhaust air and the pressure drops from the channels were obtained from the numerical solutions. Numerical solutions; (a) is steady state conditions, (b) under continuous flow conditions, (c) the velocity is constant at the inlet and is in the horizontal direction, (d) the gravitational effect is neglected, (e) the physical properties of the fluid have not changed, (f) the outflow boundary condition is selected on exit, (g) external forces are neglected, (h) the radiation and vapor diffusion are neglected, (i) system boundaries adiabatic accepted.

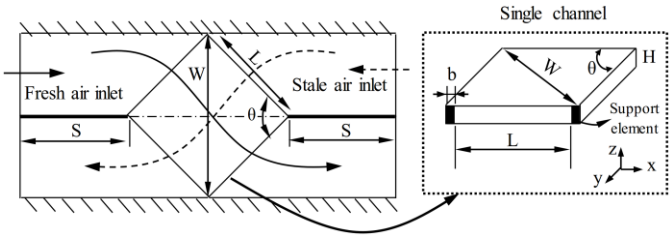

Fig. 1 Numerical solution domain and boundary conditions for heat recovery device and PHE

The schematic presentation, dimensions and boundary conditions of the designed PHE were given in Fig 1. In this study, numerical solutions were performed for two different apex angles (90^o and 60^o), which caused the relative flows of the hot and cold air flows to be evaluated as cross or semi-cross.

Conservation equation of mass for fresh air side and exhaust air side according to the assumptions for numerical solution;

$$\sum_{inlet} \dot{m} = \sum_{outlet} \dot{m} \quad (1)$$

Energy conservation equation between exhaust air and fresh air is as follow;

$$\dot{E}_{inlet} = \dot{E}_{outlet} \quad (2)$$

The geometric specifications of the PHEs designed in Table I were given.

TABLE I
GEOMETRIC SPECIFICATIONS OF PHES

Geometrical specifications	Apex angle-θ, (°)	
	90	60
H-channel height, (mm)	2	2
W-plate width, (mm)	141.42	141.42
L-channel width, (mm)	100	141.42
A-plate area, (cm^2)	100	173.2
b-support element width, (mm)	1	1
N-total numbers of channels for one side	50	50
V-total heat exchanger volume, (m^3)	$1.1x10^{-3}$	$1.91x10^{-3}$

A. Modeling Approach and Assumption

In the presented study, the results were evaluated for 6 different thermal and hydrodynamic performance parameters. According to numerical solution results, (1) the thermal power recovered on the fresh air side, (2) the sensible thermal effectiveness, (3) the average heat flux, (4) the specific thermal power, (5) the fan power, and (6) the Electro-Thermal Amplification ratio (ETA) were calculated.

Recovered thermal power by fresh air (W);

$$\dot{Q}_{fresh\ air} = \dot{m}\, c_p\, (T_{c,o} - T_{c,i}) \quad (3)$$

Where $\dot{Q}$ (W) refers to thermal power, $\dot{m}$ (kg/s) to mass flow rate, c_p (kJ/kg K) to specific heat, T_c (K) to fresh air side temperature, subscripts o and i to outlet and inlet, respectively.

Sensible thermal effectiveness ε (%);

$$\varepsilon = \frac{\dot{Q}_{fresh\ air}}{\dot{Q}_{max.}} \times 100 \quad (4)$$

$$\dot{Q}_{max.} = \dot{m}\, c_p\, (T_{h,i} - T_{c,i}) \quad (5)$$

Where T_h (K) refers to stale side temperature.

Average heat flux (W/m^2);

$$q_{average} = \frac{\dot{Q}_{fresh\ air}}{A_{total}} \quad (6)$$

Where q (W/m^2) refers to heat flux, A (m^2) to total plate area of PHE, respectively.

Specific thermal power (kW/m^3);

$$STP = \frac{\dot{Q}_{fresh\ air}}{V_{total}} \quad (7)$$

Where STP (W/m^3) refers to specific thermal power, V (m^3) to total volume of PHE, respectively.

Fan power (W);

$$\dot{W}_{fan} = 2 \times \left(\frac{\dot{\forall}}{3600} \times \Delta p \right) \quad (8)$$

Specific fan power (W/m^3s^{-1});

$$SFP = \frac{\dot{W}_{fan}}{\dot{\forall}} \quad (9)$$

Where $\dot{W}$ (W) refers to hydrodynamic power required to be given to air in fan, $\dot{\forall}$ (m^3/h) to volumetric flow rate and Δp (Pa) to pressure drop, respectively.

Electro-Thermal Amplification ratio (ETA);

$$ETA = \frac{\dot{Q}_{fresh\ air}}{\dot{W}_{fan}} \quad (10)$$

The Navier-Stokes for steady and incompressible flow and the turbulence model equations were discretized ANSYS/Fluent finite volume using CFD codes [11]. The Second Order Upwind scheme was used for discretization [14]. The Semi-implicit method for pressure-linked equations (SIMPLE) was used for the velocity-pressure coupling [11]. The turbulence intensity at the inlet was kept constant at 7%. The numerical solution used default values for convergence criterions. The criterion for convergence is less than 10^{-3} for all equations (continuity, x velocity, y velocity and z velocity), and less than 10^{-6} for the energy equation. Numerical analyzes were completed in average 250 iterations. Structural mesh was used in the 3-dimensional numerical models of PHE. In the fresh air and exhaust air channels, an increasing mesh was formed towards the surface of the plate. Structural mesh was also used for plastic support elements. The thermal power calculated by models with different mesh densities is nearly constant, obtained from the independence study of mesh number.

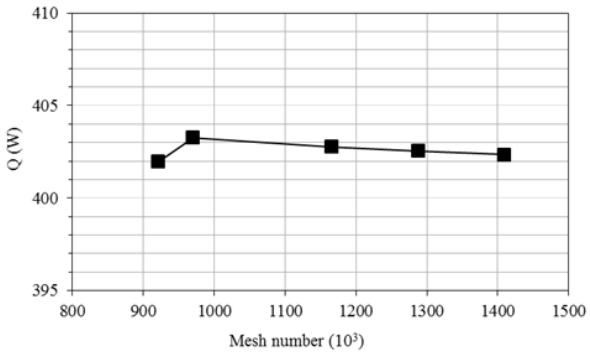

Fig. 2 Independence of mesh numbers for solution domain

As shown in Fig. 2, 5 different mesh densities with 921,200, 970,000, 1,165,200, 1,287,200 and 1,409,200 element numbers were used. In numerical solutions, flow and heat transfer were assumed as three-dimensional. As mentioned earlier, the steady-state was adopted. 1,165,200 for θ=90° and 1,372,500 for θ=60° were used for the models. The average exit temperature and pressure drops for fresh air flow and exhaust air flow were calculated.

III. Results and Discussions

Laminar flow conditions are preferred in PHEs to prevent excessive noise and pressure loss in application. However, the Standard k-ε turbulence model was used in the numerical solutions to account for the turbulence effects caused by the change of the flow cross section at the inlet and outlet of the PHE channels.

Fig. 3 shows temperature contours of the plate surface at 60° and 90° apex angles for 100 m^3/h volumetric flow rate. Although the temperature distributions on the plate surface are qualitatively similar, flow path of the air streams is more extend in the 60° design. For this reason, the duration of air in the PHE is more than 60° design at the same flow rates. The air flow path is increased by average 40% compared to 90°.

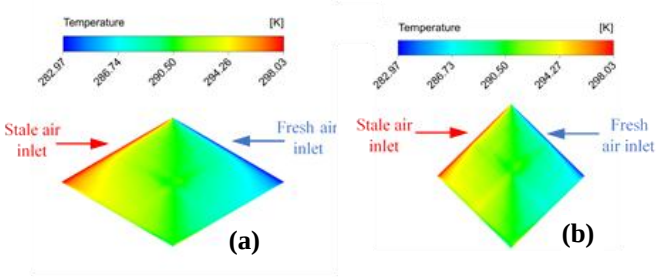

Fig. 3 Temperature contours on the plate for 100 m^3/h (a) 60° (b) 90°

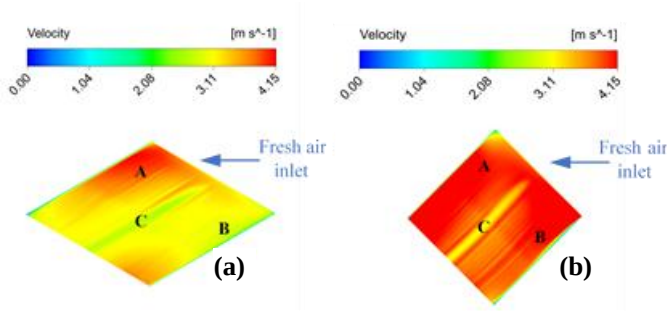

Fig. 4 Velocity contours on the symmetry plane for 100 m^3/h (a) 60° (b) 90°

For the 60° and 90° designs, the velocity distributions at the 100 m^3/h fresh air side symmetry plane are given in Fig.4. In the 60° design, a high velocity region is formed in the flow channel due to flow accumulation in front of the opposite edge (A-area) in the inlet direction. In front of the other side (B-area), a low velocity region is formed due to flow separation. In the middle of these two areas (C-area), a very low velocity and a relatively narrow area were formed. In other words, the velocity distribution in the channel is not uniform in the 60° design. The average velocity are higher and velocity distribution is more uniform in the 90° design. For this reason, higher heat transfer coefficient and heat flux are obtained in 90° design. However, 60° design has more thermal power transferred to fresh air, due to the fact that the air flows through the channel at a lower average velocity and remains longer in the channel. In particular, 60° design requires design changes such as sub-channels and guide vanes to prevent the flow from accumulating in certain regions and direct air streams to low-velocity regions in order to achieve uniform velocity distribution in the channel. Fig. 5 shows changes in the thermal power recovered at the fresh air side and pressure drop in the PHEs according to the volumetric flow rate.

The thermal power recovered on the fresh side increases linearly with volumetric flow rate, while pressure drop increases parabolic. In the 60° design, the thermal power recovered on the fresh side is an average 15% higher than the 90° design. However, the pressure drop in the 90° design is an average of 13% higher than the 60° design. Therefore, 60° design is more advantageous in terms of both heat recovery and pressure drop in the volumetric flow rates being studied.

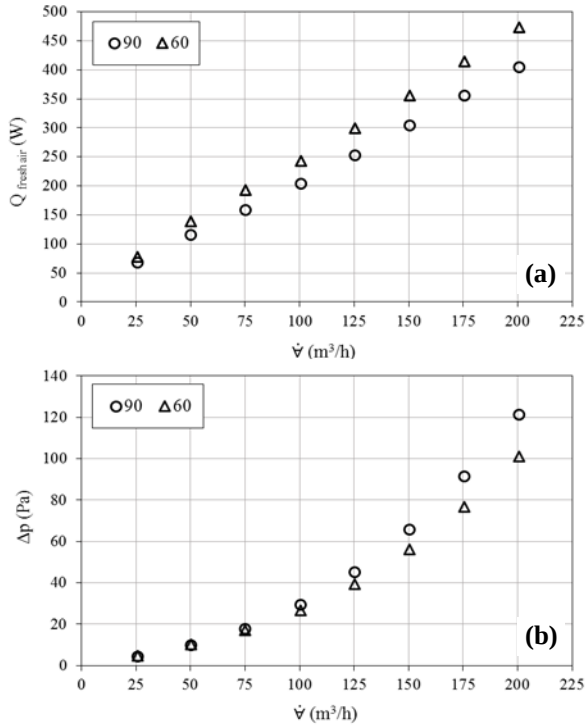

Fig. 5 Volumetric flow rate change of (a) thermal power recovered on fresh side and (b) pressure drop

In Fig. 6, changes of the average heat fluxes and specific thermal powers for PHEs were given with change of volumetric flow rate. 90° design gave an average of 30% higher results than 60° design for both parameters investigated. These results show that 90° design is more advantageous in applications where material cost and heat exchanger volume are important.

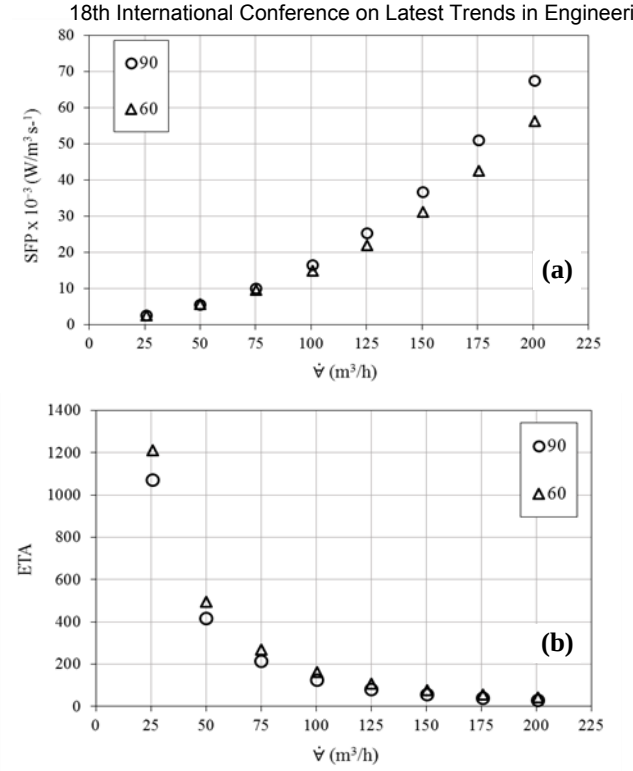

Fig. 6 Volumetric flow rate change of (a) average heat flux and (b) Specific Thermal Power

The specific fan power and the ETA's volumetric rate dependent change for 90° and 60° designs were given in Fig. 7. As the specific fan power increased, the ETA showed a decreasing parabolic change. Due to the higher average velocity in the channel at 90° design, the specific fan power is further increased by volumetric flow rate. The specific fan power is 55% higher at 90° design compare to 60° design.

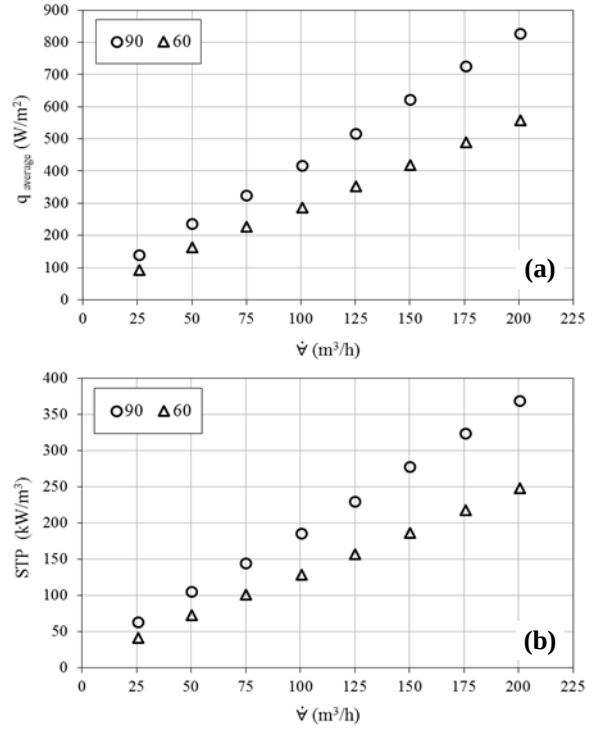

Fig. 7 Volumetric flow rate change of (a) specific fan power and (b) Electro-Thermal Amplification ratio

The reason for ETA ratio being higher in a 60° design compare to 90° design is that the thermal power recovered on the fresh air side is higher and the average velocity in the channel is lower. However, ETA is particularly close to 100 m^3/h in both designs. Therefore, 60° design has a higher ETA ratio and that is advantageous due to the lower specific fan power at volumetric rates below 100 m^3/h.

The change in thermal effectiveness versus volumetric flow rate is given in Fig. 8 for 90° and 60° designs. As the volumetric flow rate increases, the thermal effectiveness decreases in both designs and remains constant over a certain flow rate.

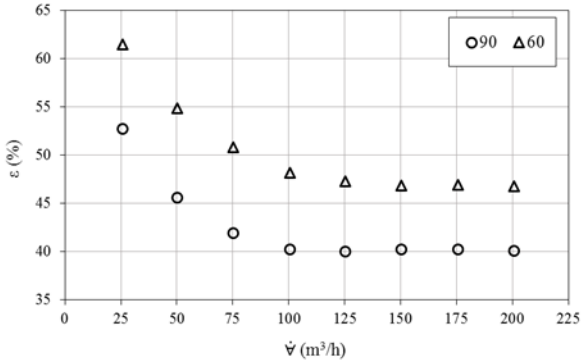

Fig. 8 Volumetric flow rate change of thermal effectiveness for 60° and 90°

The thermal effectiveness of the 60° design is an average 15% higher than the 90° design. The thermal effectiveness remains constant over V≈100 m3/h for both designs. In this case the highest average velocity for a 60° design is 2 m/s while it is 2.85 m/s for 90° design.

Air flow path is longer than the 90° design compare to the 60° design. In addition, the 60° design has a lower average velocity of 100 m^3/h. Therefore, the thermal effectiveness increases, due to duration of the air stay in the heat exchanger increases in the 60° design. But, in order to further increase the thermal effectiveness, design changes are required to reduce the hydraulic diameter of the flow channel etc. The performance results from 90° and 60° designs for 100 m^3/h volumetric flow rate where the thermal effectiveness is fixed at PHEs are summarized in Table II.

TABLE II
THERMAL AND HYDRAULIC PERFORMANCE OF PHES

Performance parameters	Apex angle, (°)	
	90	60
Fresh air side thermal power, (W)	203.7	**243.4 (+20%)**
Average heat flux, (W/m^2)	**415 (+45%)**	286
Specific thermal power, (kW/m^3)	**185 (+45%)**	128
Specific fan power x 10^3, ($W/(m^3s^{-1})$)	16.4	**14.8 (–11%)**
Electro-thermal amplification ratio (ETA)	124	**164 (+24%)**
Thermal effectiveness, (%)	40	**48 (+20%)**
Full domain pressure drop, (Pa)	29.5	**26.7 (–10%)**
PHE channels pressure drop, (Pa)	24.7	**22.4 (–10%)**
PHE inlet contraction pressure drop, (Pa)	8.4	4.1
PHE outlet expansion pressure drop, (Pa)	1.0	0.2

Extension of the numerical solution domain to account for inlet and outlet effects in PHE design allowed calculation of local pressure losses. The pressure drop in the 100 m^3/h volumetric flow rate PHE channels has increased by 18% in the 60^o design and 27% in the 90^o design due to the sudden cross section contraction in the inlet. The effect of sudden cross section expansion on the pressure loss in the PHE channels is 1% for the 60^o design and 4% for the 90^o design.

IV. Conclusion

PHEs are widely used in air conditioning systems where the need for heat recovery and fresh air are important. The PHEs used in air to air heat recovery devices are often designed to be cross-flow due to their ease of manufacture. However, designing PHEs to be both counter and cross-flow conditions increases the recovered thermal power. The thermal and hydrodynamic performance of the two PHEs in the cross and semi-cross flow case, where total height, plate width and channel height are constant, were numerically investigated. ANSYS/Fluent, which is finite volume based software, is used in the numerical solution. In this numerical solution, the Standard k-ε turbulence model was used to take into account the turbulence effects that would be caused by flow cross-section variation at the inlet and exit of PHE channels. In PHE designs with two different apex angles (60^o and 90^o), effect on the thermal power recovered on fresh side, the pressure drop, the average heat flux, the specific heat power, the specific fan power, ETA ratio and the thermal effectiveness parameters are investigated.

The main results obtained are as follows;

1) The apex angle has a significant effect on thermal power recovered on the fresh side, pressure drop, average heat flux, specific thermal power, specific fan power, electro-thermal amplification rate and thermal effectiveness parameters. The recovered thermal power and thermal effectiveness are increasing by reduction of the apex angle.
2) In both designs, with increasing volumetric flow rate, recovered thermal power, pressure drop, average heat flux, specific thermal power and specific fan power increase while ETA and thermal effectiveness decrease.
3) If total height, plate width and channel height of the PHE are the same, average heat flux and specific thermal power are on average 30% higher in 90^o design compare to 60^o design. Therefore, the 90^o design is more advantageous in applications where PHE volume and cost are important.
4) The pressure drops at low volumetric flow rate (<75m^3/h) are nearly similar for both designs. However, as the volumetric flow rate increases, the pressure drop in the 90^o design rises more than the 60^o design.
5) The specific fan power is increased by volumetric flow rate at both apex angles. On the contrary, the ETA ratio decreases with volumetric flow rate.
6) As the volumetric flow rate increases, the thermal effectiveness decrease for both 90^o and 60^o design. In terms of thermal effectiveness, the performance of the PHE with an apex angle of 60^o is higher than that of the 90^o. The thermal effectiveness remains constant above 100 m^3/h in both designs.
7) The fresh air requirement of an indoor in which three or four people live is met with a thermal effectiveness of 40% in a 90^o design while 48% thermal effectiveness in a 60^o design is met. However, in order to further improve thermal effectiveness, design changes must be carried out which will reduce the hydraulic diameter and provide uniformly velocity distribution (sub-channel division and guide vanes etc.) and the effects of these changes on thermal and hydrodynamic performance should be investigated.
8) Using the Standard k-ε turbulence model to take into account turbulence effects at the inlet and outlet of the PHE channels is an appropriate approach at a volume flow rate of 50-200 m^3/h. Especially the pressure drop is high due to the cross-section change at the entry from heat recovery device to the PHE channels. The pressure drop across the PHE channels for 100 m^3/h volumetric flow rate increased by 18% and 1% for the 60^o design and 27% and 4% for the 90^o design, respectively, due to inlet and outlet losses in the channels.

The semi-cross flow arrangement (60^o design) facilitates directional change of the flow in the heat recovery device relative to the cross flow (90^o design), reduces the average velocity as the flow cross section expands and extends the flow path in the PHE, to approximate the stream to counter flow conditions.

References

[1] A. Mardiana-Idayua, S. B. Riffat, "An experimental study on the performance of enthalpy recovery system for building applications", *Energy and Buildings*, vol. 43, pp. 2533–2538, 2011.

[2] C. Zeng, S. Liu, A. Shukla, "A review on the air-to-air heat and mass exchanger technologies for building applications", *Renewable and Sustainable Energy Reviews*, vol. 75, pp. 753–774, 2017.

[3] www.epdk.org.tr/TR/Dokuman/8077, Access date: December, 15th, 2017.

[4] http://www.teias.gov.tr/sites/default/files/2017/12/AylikElektrikIstatistikleri.xlsx, Access date: December, 15th, 2017.

[5] European Commission, Joint Research Centre, 1996, Indoor Air Quality and the Use of Energy in Buildings, (Report No 17), European Commission, Joint Research Centre-Environment Institute, Office for Official Publications of the European Communities, Luxembourg, Access date: December, 15th , 2017.

[6] G. Evola, A. Gagliano, L. Marletta, F. Nocera, "Controlled mechanical ventilation systems in residential buildings: Primary energy balances and financial issues", *Journal of Building Engineering*, vol. 11, pp. 96–107, 2017.

[7] L.Z. Zhang, C.H. Liang, L.X. Pei, "Conjugate heat and mass transfer in membrane-formed channels in all entry regions", *Int. J. Heat Mass Transfer*, vol. 53, no. 5–6, pp. 815–24, 2010.

[8] L.Z. Zhang, *Conjugate Heat and Mass Transfer in Heat Mass Exchanger Ducts*, Academic Press, 2013.

[9] L.Z. Zhang, "Heat and mass transfer in a cross-flow membrane-based enthalpy exchanger under naturally formed boundary conditions", *International Journal of Heat and Mass Transfer*, vol. 50, pp. 151–162, 2007.

[10] L.Z. Zhang, "Heat and mass transfer in a quasi-counter flow membrane-based total heat exchanger", *Int. J. Heat Mass Transfer*, vol. 53, no. 23–24, pp. 5478–5486, 2010.
[11] *ANSYS/Fluent User's Guide*, version 15.0, ANSYS, Inc. 2013.
[12] B.E. Launder, D.B. Spalding, *Lectures in mathematical model of turbulence*, Academic Press, London, 1972.
[13] Y. Çengel, *Introduction to Thermodynamics and Heat Transfer (Second Ed.)*, McGraw-Hill, 2007.
[14] S.V. Patankar, *Numerical heat transfer and fluid flow*, Hemisphere, Washington, DC, 1980.

Influence of Chopped Basalt Fibers on the Shear Strength of RC Beams without Stirrups

Seyit Ziya MAZHARI[1], and Güray ARSLAN[2]

***Abstract*—**This research studied the influence of chopped basalt fibers (BFs) on the shear strength of reinforced concrete (RC) beams without stirrups. The beams including one reference and three basalt fiber reinforced concrete (BFRC) beams were tested under concentrated load at mid-span to determine the shear strength. The test parameters are volume fraction of basalt fibers (V_f) and shear span–to-effective depth ratio (a/d) of beam. The deflection of the beam and the cracking pattern were monitored during the test at certain stages of the monotonic loading until failure. It is observed that the contribution of BFs to the shear strength at the ultimate state decreases as volume fractions of BFs increase from 0% to 1.5%.

***Keywords*—**Reinforced concrete, beam, chopped basalt fibers, shear strength, deflection.

I. Introduction

Nowadays using fiber reinforced concrete (FRC) in structural members has been increasing significantly. It has been well established that the addition of fibers can augment the mechanical behavior of plain concrete such as flexural strength, deformation capacity, impact resistance, compressive and tensile strength, load capacity after cracking, fatigue and abrasion strength, toughness and shrinkage [1-11].

Recently, basalt fibers (BFs) has gained popularity due to some advantages like no additives which makes it cheaper, good insulation characteristic, environmentally friendly manufacturing process, commercial availability, good resistance to chemical attack and temperature, high modulus, sound isolation, low moisture absorption, non-toxic, crack resistance, crack control, vibration resistance, durability and above all excellent interfacial shear strength [11-17] and become a good alternative as a potential competitor in reinforced concrete (RC) applications.

Despite there are considerable studies about FRC, there is limited fundamental research on the effects of chopped BFs on the shear strength of RC beams. Issa et al. [18] observed significant improvements in the shear strength of RC beams with insufficient shear reinforcement strengthened with BF reinforced polimer. Dias and Thaumaturgo [9] investigated the relationship between the mixing value of fiber and fracture toughness of geopolymeric cement reinforced with BFs and they demonstrated that geopolymer cement reinforced with BFs exhibited more displacement and more fracture toughness.

The main objective of this paper is to evaluate the shear strength of basalt fiber reinforced concrete (BFRC) beams without stirrups which were tested under concentrated load at mid-span. The deflections of the beams and their cracking patterns were monitored at the certain stages of the monotonic loading until failure. The test parameters are the volume fraction of basalt fibers (V_f) and shear span-to-effective depth ratio (a/d) of beam.

II. Test specimens

A combination of letters and numbers is used for specimen labels “C” followed by the shear span-to-effective depth ratio to denote all test specimens in this research and “B” followed by the volume fraction of BFs. For example, a beam having a shear span-to-effective depth ratio of 2.5 and with a volume fraction of fibers equal to 1.5% is labeled as C2.5B1.5.The specimen labelled as C2.5R is the reference beam that do not contain any fibers.

The tests were carried out to evaluate the contribution of BFs to the shear strength of RC beams. All beams have the same cross- sectional dimensions 150 mm/240 mm (b/h) with an effective depth of 210 mm, and a constant tensile reinforcement ratio (ρ). Four different volume fractions of basalt fibers as 0%, 0.5%, 1.0% and 1.5% were considered.

Three-point loading tests were conducted to identify the ultimate load capacities of beams using a displacement controlled loading machine and the beams were monitored during the test. The geometrical properties of test specimens are shown in Fig. 1.

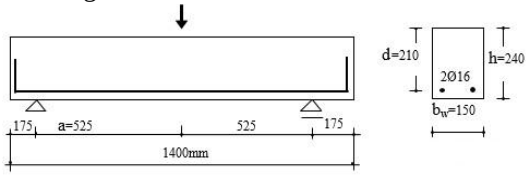

Fig. 1 Geometry and flexural reinforcement of beams

Seyit Ziya MAZHARI[1] is with the Institute of Natural and Applied Sciences, Yildiz Technical University, Istanbul, 34220 TURKEY (corresponding author’s phone: +905372429665; e-mail: ziya_mazhari@yahoo.com).

Guray ARSLAN[2], was with Civil Engineering Department, Yildiz Technical University, Istanbul, 34220 TURKEY (e-mail: aguray@yildiz.edu.tr).

The tensile strength and the elasticity modulus of BFs are 4840 MPa and 90 GPa, respectively. The characteristics of BFs are reported as the application limit temperatures are ± 980ºC, the specific weight is 2.60-2.80 gr/cc, the fiber diameter is 9-23 μm and the length of fibers is 12 mm. This physical and mechanical properties of BFs, provided by the manufacturer.

Reinforcement schemes of the test specimens are shown in Figure 1, the characteristics of beams are shown in Table 1, where f_c is the compressive cylinder strength of concrete and l is the length of beam.

The beams were loaded until either failure or the load dropped below approximately 80% of its maximum value.

TABLE I
PROPERTIES OF BEAMS

Beams	f_c (MPa)	V_f (%)	ρ (%)	a/d	a (mm)	l (mm)
C2.5R	24.85	---	1.28	2.5	525	1400
C2.5B0.5	16.94	0.5	1.28	2.5	525	1400
C2.5B1.0	12.37	1.0	1.28	2.5	525	1400
C2.5B1.5	6.29	1.5	1.28	2.5	525	1400

III. EXPERIMENTAL RESULTS

The failure of all beams occurred in shear. First, vertical flexural cracks was observed around the mid-span of all beams as predicted. With the increase in load, new flexural cracks were formed at a distance of mid-span area. In the last stage, vertical flexural cracks appeared around the mid-span started to proceed towards the loading point. Crack patterns are shown in Fig 2-5.

Test results are given in Table 2 below, P_{co} is the peak load of beam obtained experimentally, P_u is the ultimate load that is assumed to be equal to 80% of P_{co}, $\square_{co}$ and $\square_u$ are the deflection at the peak load and the ultimate deflection of each beam, respectively, and the dissipated energy is the area under the load-deflection curve.

TABLE II
EXPERIMENTAL LOAD AND DEFLECTION VALUES OF BEAMS

Beams	P_{co} (kN)	P_u (kN)	δ_{co} (mm)	δ_u (mm)	δ_u/δ_{co}	Dissipated Energy (kNm)
C2.5R	84.93	67.94	5.12	6.76	1.32	0.3365
C2.5B0.5	84.02	67.21	5.06	5.66	1.12	0.2469
C2.5B1.0	72.43	57.94	3.90	5.18	1.33	0.1528
C2.5B1.5	55.81	44.65	5.16	5.76	1.12	0.1851

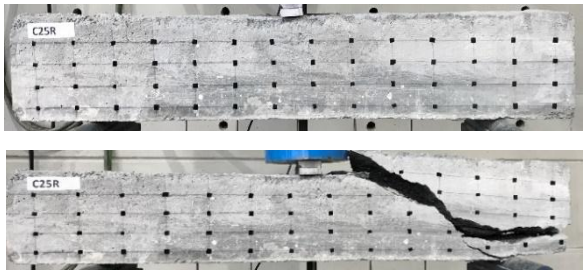

Fig. 2 Crack Pattern of C2.5R

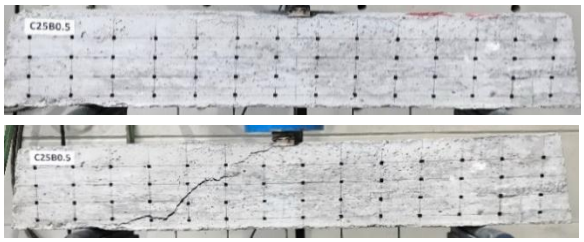

Fig. 3 Crack Pattern of C2.5B0.5

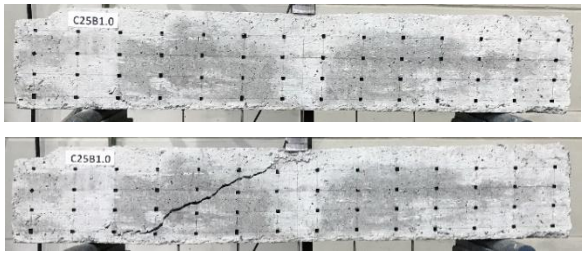

Fig. 4 Crack Pattern of C2.5B1.0

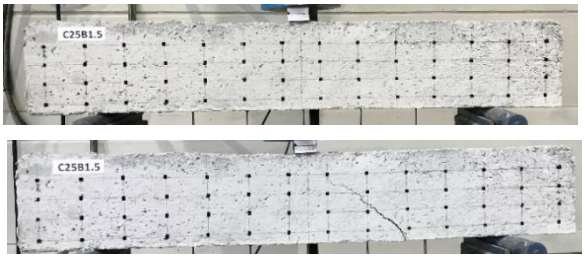

Fig. 5 Crack Pattern of C2.5B1.5

IV. COMPARISON OF LOAD-DEFLECTION RELATIONSHIPS OF BEAMS

The load-deflection curves of beams are shown in Figure 6. It is deduced that:

The beam having BFs in the amount of 0.5% by volume reached a maximum load similar to the load reached by the reference beam, then the load decreased rapidly while a certain amount of deflection of the reference beam was observed beyond the maximum load without a significant loss in the load-carrying capacity.

Introducing BFs in the amount of 1.0% by volume resulted in significant decreases in the load-carrying and deflection capacities. The load-carrying capacity was reduced by approximately 15% and the maximum load was reached at a mid-span deflection approximately %25 less than that of the reference beam.

The addition of BFs in the amount of 1.5% by volume also reduced the load-carrying capacity, 34% compared to the capacity of the reference beam, but the mid-span deflection under the maximum load was similar to that of the reference beam.

By comparing four beams, it is observed that increasing the amount of BFs causes deterioration on both load-carrying capacity of beams and the compressive strength of concrete (f_c).

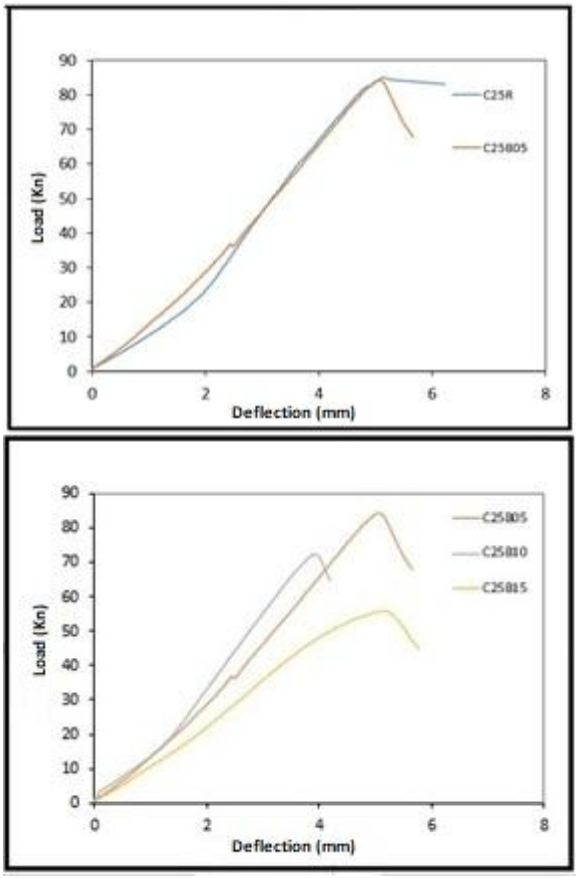

Fig. 6 Load-deflection curves

V. Conclusion

According to the test results in this study, it is observed that the addition of basalt fibers was not able to improve the strength and ductility of RC beam. Contrarily, it resulted in a behavior poorer than the behavior of reference beam. This can be attributed to the inadequate bonding between aggregate and concrete due to the adhering of basalt fibers to aggregate while mixing the fibers with concrete.

References

[1] S.A. Ashour, G. S. Hasanain, F. F. Wafa, "Shear behavior of high-strength fiber reinforced concrete beams," *ACI Struct J*, Vol. 89, no. 2, pp. 176-184, 1992.

[2] K. Noghabai, "Beams of fibrous concrete in shear and bending: experiment and model," *ASCE J of Struct Eng*, Vol. 126, no. 2, pp. 243–251, 2000.

[3] F. Majdzadeh, M. Soleimani, N. Banthia. "Shear strength of reinforced concrete beams with a fiber concrete matrix," *Can J Civ Eng*, Vol. 33,pp. 726-734, 2006.

[4] E. Mondo "Shear capacity of steel fibre reinforced concrete beams without conventional shear reinforcement," *Royal Ins. of Tech*, Vol. 331, pp. 1103- 4297, 2011.

[5] N. Kabay. "Abrasion resistance and fracture energy of concretes with basalt fiber," *Constr Build Mater*, vol. 50, pp. 95-101, 2014.

[6] M.T. Borhan. "Thermal and mechanical properties of basalt fibre reinforced concrete," *World Acad Sci Eng Tech*, Vol. 76, pp.313-316, 2013.

[7] G. Arslan, "Shear strength of steel fiber reinforced concrete (SFRC) slender beams." *KSCE J Civ Eng*, Vol. 18, no. 2, pp. 587-594, 2014.

[8] G. Arslan, R.S.O Keskin, M. Ozturk."Shear behaviour of polypropylene fibre-reinforced-concrete beams without stirrups," *Proc Inst Civ Eng Struct Build*, Vol. 170, no. 3,pp. 190-198, 2017.

[9] P.D. Dias, C. Thaumaturgo. "Fracture toughness of geopolymeric concretes reinforced with basalt fibers." *Cem Conc Comp*, vol. 27, no.1, pp. 49-54, 2005.

[10] R. Narayanan and I. Y. S. Darwish "Use of steel fibers as shear reinforcement," *ACI Struct J*, Vol. 84, No. 3, pp. 216-227. 1987.

[11] J. Branston, D. Sreekante, S. Y. Kenoo, C. Taylor, "Mechanical behavior of basalt fibre reinforced concrete," *Constr Build Mater*, vol. 124, no. 3, pp. 878–886, 2016.

[12] M. Di Ludovico, A. Prota, G. Manfredi, "Structural upgrade using basalt fibers for concrete confinement," *J Compos Constr* Vol. 114, no. 5, pp. 1943-5614, 2010.

[13] V. Fiore, T. Scalici, G. Di Bella, A. Valenza," A review on basalt fibre and its composites," *Comp Part B*, Vol. 74, no. 4, pp. 74-97, 2015.

[14] I. V. Borovskich, V. G. Khozin, N. M. Morozov." Sand bazalt-fiber concrete," *World App Sci*, Vol. 25, no. 5, pp. 832-838. 2013.

[15] C. Jiang, K. Fan, F. Wu, D. Chen, "Experimental study on the mechanical properties and microstructures of chopped basalt fiber reinforced concrete," *Mater Des*, vol. 58, no. 1, pp. 187–193, 2014.

[16] M.E. Arslan, "Investigation on the effects of basalt fibers on the mechanical properties and fracture energy of ordinary concretes," *Pamukkale Univ Civ Eng*, Vol. 23, no. 3, pp. 203-208. 2016.

[17] A. B. Kızılkanat, N. Kabay, V. Akyüncü, G. Erdoğan. "Basalt fibers and mechanical properties of basalt fiber reinforced concrete." *J Eng Nat Sci*, Vol. 32, no. 1, pp. 444-452,2014

[18] M. Issa, T. Ovitigala and M. Ibrahim, "Shear Behavior Basalt Fiber Reinforced Concrete Beams with and without Basalt FRP Stirrups," *J Compos Constr*, vol. 20, no. 4, pp. 249-260, 2016.

Autonomous Quadcopter Design by Using Fuzzy Logic

Zekeriya HACIMUHAMMED and İbrahim SAVRAN

***Abstract*—** The purpose of this paper is to present an Automatic Flight Controller for quadcopters drone by using two-input-single-output (MISO) fuzzy system. The paper supposes that the manual flight control system of the drone is working by default, receives control commands from transmitter and sends speed commands to rotors depending on the computed PID or Fuzzy rules in the flight controller. It working on creating control commands instead of transmit-ter's commands, this will base on the attitude and the drone's velocity to enable the drone to take a route between two GPS point or more. The drone will takeoff and will turn to the right direction then go to the target position. The control system that have to compute along this route is three command (Throttle, Roll, Pitch).

***Keywords*—** Quadcopter; UVA; Flight Controller; Fuzzy system; Route; Drone.

I. Introduction

A quadrotor is a cross-shaped aerial vehicle that is capable of vertical take-off and landing. It has four motors, each mounted per corner equidistant from the centre. The synchronized rotational speed of all the motors is key to the control of the quadrotor [1]. Vertical motion results from the simultaneous increase or decrease of the rotational speeds of all the rotors. The motion along any direction on the lateral axis is obtained by decreasing the rotational speed of the rotors along the desired direction of motion, and increasing the speed of the rotors opposite to the desired direction of motion. Moment produced by rotation of rotors is used to initiate yaw [4]. For instance, clockwise yaw is initiated by simultaneously increasing the rotation speed of the rotors creating a clockwise moment, and decreasing the rotation speed of the rotors creating counterclockwise moment [1][2]. The motion of the quadrotor is described schematically in fig.1

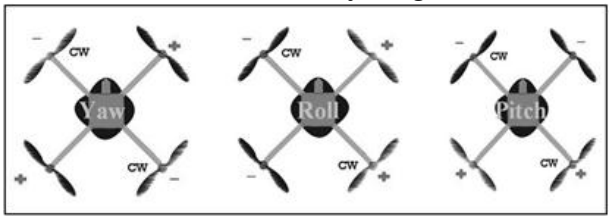

Fig. 1: Yaw Roll Pitch

Department of Computer engineering, Karadeniz Technical University, Trabzon, TURKEY (e-mail:zkriahagmohamad@gmail.com, savran@ktu.edu.tr).

II. Manual Flight Control System

The quadcopter with manual flight control system work by receiving the control commands from RC transmitter as PWM pulse and then will convert from time (1000, 2000us) to suitable value range, in our case Throttle (0, 100), Pitch and Roll (-60, 60) and Yaw (-180,180) [3]. The flight controller compute the rotor's speed command depending on the actual angle of the drone was recived from MPU (Motion Processing Unite) and the desired angle was recived from RC transmitter using fuzzy rules or PID con-troller [2] as we show in fig .2, the Y, P, R values refer to the current quadcopter Yaw, Pitch, Roll angles. The rotors are abbreviated as FR, FL, BR, BL which refer "Front Right", "Front Left", "Back Right" and "Back Left" rotors respec-tively.

Manual flight controller uses stabilized mode for the flight, that means the angle of quadcopter equal to the angle of Sticks that set.

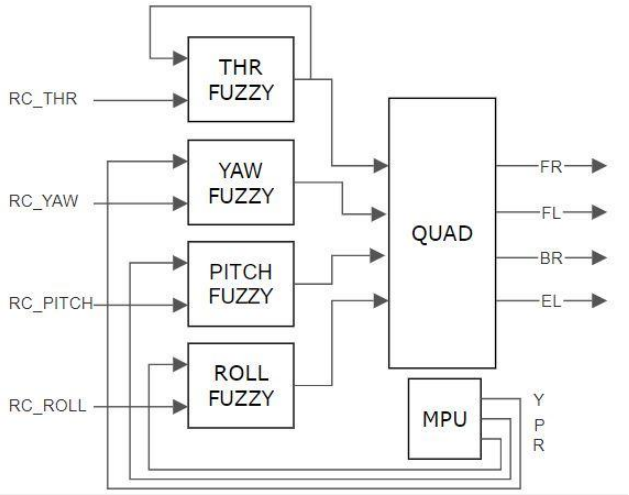

Fig. 2: Manual Flight Controller

III. Automatic Flight Control System

In this paper we assume that the manual flight controller is functioning. The goal is to generate the appropriate signals to enable the drone decide an optimum route automatically.

The quadcopter will takeoff first to achieve target height based on the readings from the Barometer sensor, then will go to a given destination with roll and pitch angles changing continuously based on the readings from GPS, after that the

aircraft will land. In fig .3, T', P',and R'refer to the former values and the NT, NP, NR refer to the current values.

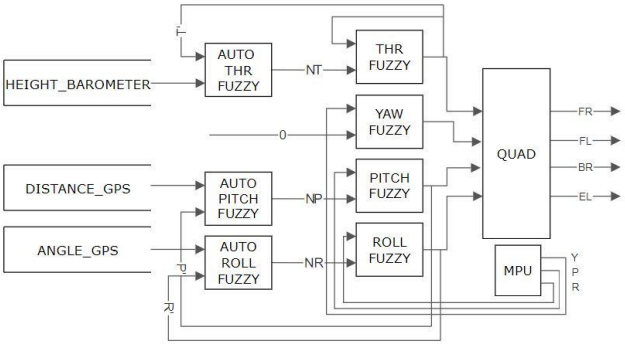

Fig. 3: Automatic Flight Controller

A. Fuzzy Takeoff Control Step

At this stage we define the fuzzy membership functions for the distance and throttle [8], where the throttle has value between 0 and 100 as shown in fig. 4, and the distance is equal to reference height minus the current position. The distance value ranges from negative to large positive as shown below in the fig. 5. The negative value is assigned when the quadcopter crosses the reference height [5].

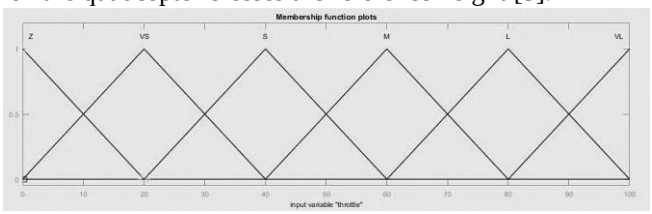

Fig. 4: Throttle

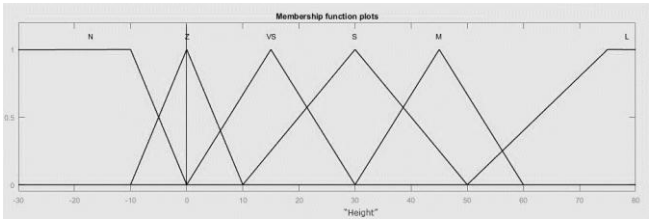

Fig. 5: Distance Membership Function

The output will be as new throttle based on the fuzzy rules that computed from the past throttle and distance.

The rules computed to make the new throttle has value related with every height, keep the current position when the distance become zero. Stay on when the distance is still greater than 0 and decrease when the distance become negative [5] as shown in the Table. 1. Membership functions are encoded as Z (Zero), VS (Very Small), S (Small), M (Medium), L (Large), VL (Very Large), N (Negative).

The plot of Nthrottle surface for the takeoff rules shown in fig. 6.

TABLE I
TAKEOFF RULES TABLE FOR NEW THROTTLE

THR / *DIST*	**Z**	**VS**	**S**	**M**	**L**	**VL**
N	Z	Z	VS	S	M	L
Z	Z	VS	S	M	L	VL
VS	VS	S	M	L	VL	VL
S	VS	S	M	L	VL	VL
M	VS	M	M	VL	VL	VL
L	VS	M	L	VL	VL	VL

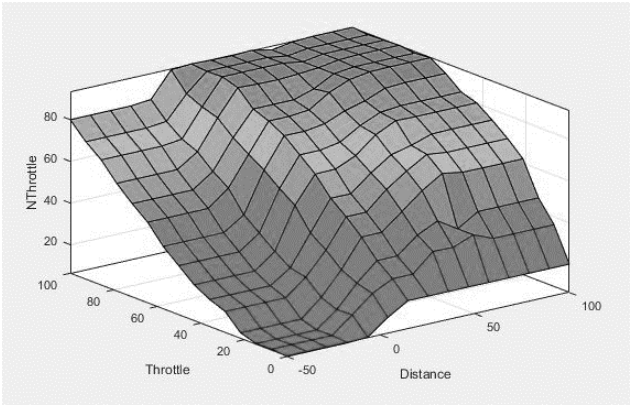

Fig. 6: Plot of Takeoff Rules

B. Fuzzy Landing Control Step

As takeoff phase we define the fuzzy membership functions for the distance and throttle, the throttle has same range and same membership functions but the distance value equals to now height sub the ground reference value and will not be have a negative value because the ground will be at distance value 0 as shown in fig. 7.

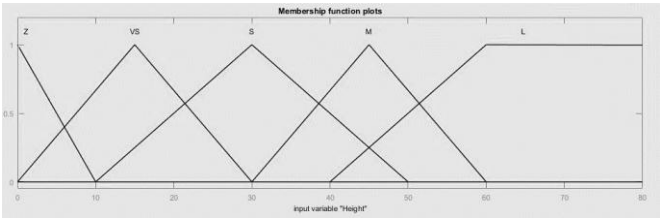

Fig. 7: Distance Membership Functions in Landing Phase

When we look to the table 2, we see that when the quadcopter is not close to the ground and at the same time the throttle is near to zero, the throttle will be increased. Fig. 8 shows the plot of Nthrottle surface for the landing rules.

TABLE II
LANDING RULES TABLE FOR NEW THROTTLE

THR / DIST	**Z**	**VS**	**S**	**M**	**L**	**VL**
Z	Z	Z	Z	Z	VS	VS
VS	VS	Z	VS	VS	VS	S
S	VS	VS	VS	S	M	L
M	S	VS	VS	S	M	M
L	S	VS	VS	S	M	L

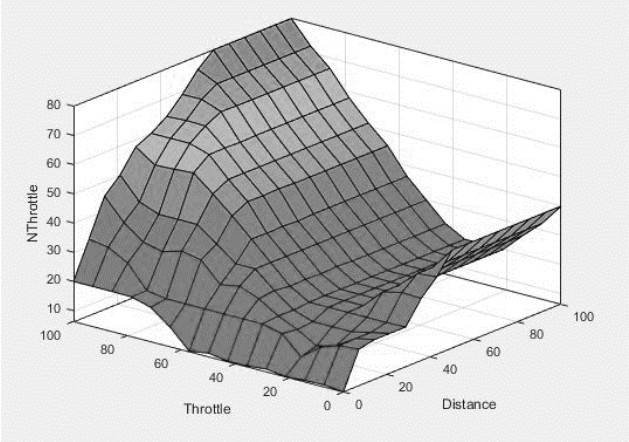

Fig. 8: Plot of landing Rules for current Throttle

C. Route Determination

Deciding a route between two spatial points, human mind intrinsically controls the aircraft as follows:

• To change the velocity, our mind checks the current speed and the distance simultaneously.

• To update the rotation angle our mind compares the angle between the quadcopter direction and the target position.

For that, the work is to make quadcopter a smart drone by adding the control rules based on the necessary parameter (**speed**, **distance**, **angle**, **direction**) [7].

D. Fuzzy Pitch Control

To create a fuzzy membership for pitch control the pitch value will be between -60 and +60. -60 pitch value mean negative very large speed NVL which makes the quadcopter go to backward direction. Zero value mean zero speed and +60 very high forward speed. The membership functions for pitch control is shown in the fig.9.

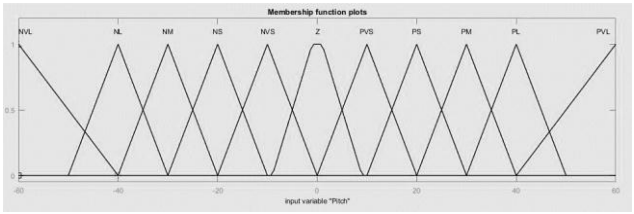

Fig. 9: Pitch membership function

Another parameter must used to compute the new pitch value is the distance between the current position and the target. The distance parameter is in range between negative large to positive large value and the quadcopter can move all directions [6] (please see fig. 10).

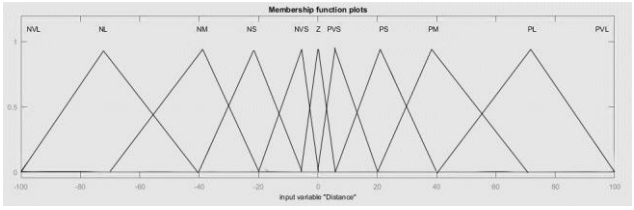

Fig. 10: Distance membership function

Pitch control system determines the distance sign by nearest zero angle to the quadcopter direction as shown in fig. 11. That means when the angle between the quadcopter direction and target position is in the range (0 to 90) or (0 to -90) the direction is forward otherwise backward direction [4].

At this way the quadcopter :

- Will not rotate to back if the target position is behind it, instead of that it will go backward direction.
- When across the target position will go back without turn (as Brakes).

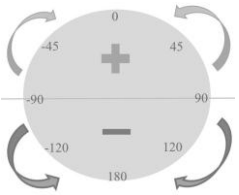

Fig. 11: Wanted dirction

The output will be a new pitch angle as output of the rules based on distance and past pitch angle as:

• The new pitch will increase when the distance is big and decrease when being small as shown in plot surface fig.12.

• Another think show in the rules table. 3 is when the quadcopter is going in a direction and the distance is zero the new pitch be a same speed but in the other way [9].

Where NVL (Negative Very Large), PVL (Positive Very Large).

TABLE III
PITCH RULES TABLE FOR NEW PITCH

PITCH / DIST	NVL	NL	NM	NS	NVS	Z	PVS	PS	PM	PL	PVL
NVL	NVL	NVL	NVL	NVL	NM	NM	NM	NM	NM	NM	NM
NL	NL	NL	NL	NL	NM	NM	NM	NL	NM	NM	NM
NM	NM	NM	NM	NM	NS	NS	NS	NL	NM	NM	NM
NS	NVS	NVS	NS	NS	NS	NS	NM	NM	NM	NL	NL
NVS	Z	NVS	NVS	NVS	NVS	NVS	NS	NM	NM	NL	NL
Z	PVL	PL	PM	PS	PVS	Z	NVS	NS	NM	NL	NVL
PVS	PL	PL	PM	PS	PVS	PVS	PVS	PVS	PVS	PVS	Z
PS	PL	PL	PL	PM	PM	PM	PS	PS	PS	PVS	VS
PM	PM	PM	PL	PL	PS	PS	PS	PM	PM	PM	PM
PL	PM	PM	PM	PL	PM	PM	PM	PL	PL	PL	PL
PVL	PM	PM	PM	PL	PM	PM	PM	PVL	PVL	PVL	PVL

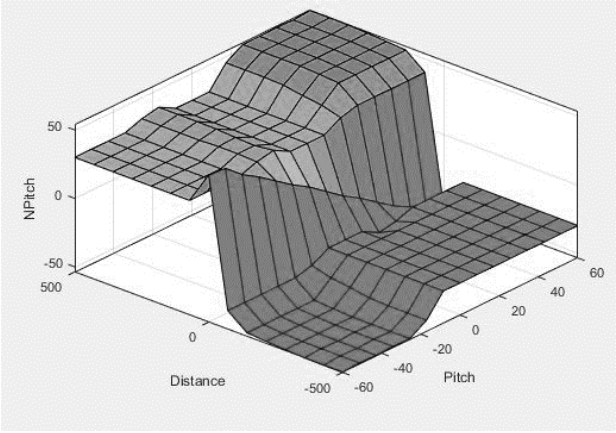

Fig. 12: Pitch plot surface

E. Fuzzy Roll Control Step

As pitch, the roll angle value will define between the -60 and +60 degree like fig. 9 but for roll, the second parameter is the angle between the quadcopter direction and 0 (forward state) and 180 (backward state) we can take another look to fig. 11 and see that the angle must be from -180 to 180 degree and the member function for it shown at fig.13.

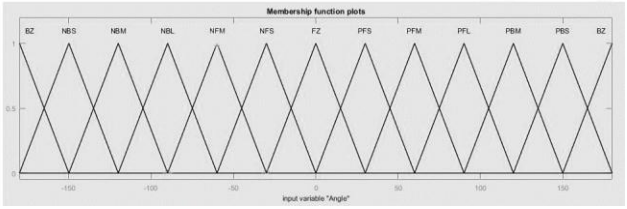

Fig. 13: Angle between quad direction and the target

The rules that applied from past roll and the angle their main goal is to make the angle zero, when the angle large the roll will be large too, the rules shown in the table. 4 below [6] where the negative value of roll means ccw rotate direction [9].

TABLE IV
ROLL RULES TABLE FOR NEW ROLL

ANGLE / ROOL	BZ	NBS	NBM	NBL	NFM	NFS	FZ	PFS	PFM	PFL	PBM	PBS	BZ
NEL	EL	VL	Z	NEL	EL	EL	EL	VL	Z	NEL	EL	EL	EL
NVL	VL	L	VS	NEL	EL	EL	VL	L	VS	NEL	EL	EL	VL
NL	L	M	S	NEL	EL	EL	L	M	S	NEL	EL	EL	L
NM	M	S	M	NEL	EL	VL	M	S	M	NEL	EL	VL	M
NS	S	NVS	M	NEL	VL	L	S	NVS	M	NEL	VL	L	S
NVS	VS	NVS	M	NEL	VL	M	VS	NVS	M	NEL	VL	M	VS
Z	Z	NVS	L	NEL	L	VS	Z	NVS	L	NEL	L	VS	Z
VS	NVS	NM	VL	NEL	M	VS	NVS	NM	VL	NEL	M	VS	NVS
S	NS	NL	VL	NEL	M	VS	NS	NL	VL	NEL	M	VS	NS
M	NM	NVL	EL	NEL	M	NS	NM	NVL	EL	NEL	M	NS	NM
L	NL	NEL	EL	NEL	S	NM	NL	NEL	EL	NEL	S	NM	NL
VL	NVL	NEL	EL	NEL	VS	NL	NVL	NEL	EL	NEL	VS	NL	NVL
EL	NEL	NEL	EL	NEL	Z	NVL	NEL	NEL	EL	NEL	Z	NVL	NEL

CCW

CW

IV. CONCLUSION

When we produce the control commands instead the transmitter we can convert every quadcopter to auto quadcopter (drone) whatever the internal system because we can convert the new (throttle, pitch, roll) values to range between 1000 to 2000 the same range as transmitter's commands, in the other hand as above we can build the complete system. In this paper, the fuzzy control system for quadcopter airplane is proposed by computing rules between the velocity and attitude, it has high performance and reaches to accurate results.

REFERENCES

[1] Duncan Still, "How to build a quadcopter drone" - A complete guide to building a radio controlled quadcopter Kindle Edition
[2] Ian Cinnamon, (2016), "DIY Drones for the Evil Genius" - Design, Build, and Customize Your Own Drones Paperback
[3] David McGriffy, (2014), Make Drones, Teach an Arduino to Fly 1st Edition Illumin – "The Quadrotor's Coming of Age".
[4] Andrew Hobden, (2017), Quadcopters: Yaw. hoverbear.org.
[5] Xu, H.J. and Ioannou, P.A. (2003), "Robust adaptive control for a class of MIMO nonlinear systems with guaranteed error bounds", IEEE Transactions on Automatic Control, Vol. 48 No. 5, pp. 24-34.
[6] Schram, G., Ijff, J.M. and Krijgsman, A.J. (1996), "Fuzzy logic control of aircraft: a straightforward MIMO design", Proceedings of AIAA Guidance, Navigation and Control Conference, San Diego, CA.
[7] Vijaykumar Sureshkumar FNU and Kelly Cohen. (2014) "Intelligent Fuzzy Flight Control of an Autonomous Quadrotor UAV" .
[8] Timothy J. Ross, (2004), "FUZZY LOGIC WITH ENGINEERING APPLICATIONS", University of New Mexico, USA.
[9] Deepak Gautam and Cheolkeun Ha, "Control of a Quadrotor Using a Smart Self-Tuning Fuzzy PID Controller", The School of Mechanical Engineering, University of Ulsan

MVL-MIN: A New Heuristic Minimization Tool For Multiple-valued Logic Functions

Ibrahim Savran

***Abstract*—**In this paper, a new heuristic method to minimize multiple-valued logic (MVL) functions and its implementation results will be introduced. The motivation for this work has been to develop a light weight MVL minimization algorithm which is simpler than existing algorithms so that it can serve as a basis for the future work. MVL-MIN is designed and implemented from scratch and it is compared with MVSIS. MVSIS is a MVL minimization program developed by the Electronic Systems Design group at Berkeley. The advantages of the new algorithm include a new cube calculus based technique for detecting and eliminating the totally redundant prime implicants. A comparison with MVSIS approved that the proposed algorithm is able to solve all test files within a fixed allocation of computer resources. Since conventional testbenches are fairly small, we generated 3 sets of testbench in blif-mv format. Each set includes 8 multiple-valued logic functions. MVL-MIN is able to solve all test-benches about 5 times faster than MVSIS on average.

***Keywords*—**Multiple-valued logic, multiple-valued logic minimization, cube calculus, heuristic minimization.

I. Introduction

THE performance of binary logic is limited due to high number of interconnections, which occupy a large area on an integrated circuit. More than half of the chip area is devoted to wires [1, 2]. As a result, researchers are looking for a way to reduce it. One can achieve a more cost-effective way of utilizing interconnections by using a larger set of signals over the same area in MVL. Using fewer wires to transmit multi discrete values allows denser information content per interconnection and thus results in a circuit with fewer conductors than the binary-valued counterpart [3, 4]. For example, in the case of 4-valued logic, half of the wire space is saved [5].

In modern VLSI technology, the chip size and performance are closely related to the number of wires, pins, etc. In principle, MVL can provide high data processing capability per unit chip area, and decrease the connection between circuit units.

Since 1970s, the Complementary Metal-Oxide Semi-conductor (CMOS) has been the main technology for implementing dense and energy-efficient VLSI circuits. However, the general trend of reducing the size of CMOS (Complementary Metal-Oxide-Semiconductor) technology in nano-scale has confronted many difficulties. The main obstacles include very high leakage currents, high power density, parasitic effects, and restriction of routing and placement processes [6, 7, 8]. Thus, many nano-scale technologies such as Quantum-dot Cellular Automata (QCA) [9], Single Electron Transistor (SET) [10], and CNTFET [11] have been introduced to overcome these challenges. Among them, CNTFET is the most promising candidate to be a successor to the CMOS technology in the near future [12]. Several arithmetic MVL circuits have been proposed [13, 14]. In 2006, IBM demonstrated the first IC built using SWCNTs [15]. Then, a decoder, a sensor interface circuit, stand-alone circuit elements such as half-adder sum generators, D-latches and memory (SRAM) cells have been fabricated [16, 17, 18, 19, 20, 21, 22]. In 2008, Cao et al. [23] announced that they made medium size IC using CNTFETs. Recently, Shulaker et al. [24] fabricated first CNT computer entirely using CNTFETs.

The minimization of logic expressions is an important step in modern circuit design. Unfortunately, since the MVL functions have more literals to deal with, the designing MVL devices is more complicated than those of their binary counterparts [25].

In logic design, the most common optimization metric is the number of terms in the logic expression, which is easily calculated during the minimization phase. The correlation between the number of terms and chip area is very high in the binary case, i.e. it is a good estimate.

Due to the exponential nature of finding the optimal cover, the state-of-the-art optimization algorithms can only handle functions that have a limited number of terms. Therefore, most of the tools rely on heuristic minimization methods such as MVSIS [26]. In the literature, there are several methodologies reported for the synthesis of MVL functions, such as direct-cover-based approaches [27, 28], network learning via local search methods [29, 30], genetic algorithms [31, 32, 33], and artificial intelligence methods [34].

The organization of the paper is as follows: Section 2 covers the background of the study and the terminology. Then, section 3 briefly explains the "Cube Calculus Operators" which are used to find the prime cover. Section 4 describes our MVL heuristic minimization algorithm MVL-MIN, and presents an example. Finally, Section 5 concludes the paper and gives future applications.

II. Background

To be consistent with the literature we want to give definitions and algebraic procedures in this section. For

Ibrahim Savran is with the Karadeniz Technical University, Trabzon, 61080, Turkey (corresponding author's phone: +90 539 302 8329; e-mail: savran@ktu.edu.tr).

simplicity and formality of the explanations in this study the following notation is used.

A. Definitions

- Let S_{on}, S_{off}, S_{dc}, S_{now}, S_{pc} be the set of on-cubes, the set of off-cubes, the set of "don't-care" cubes, uncovered part of S_{on} set, and the prime cover set respectively [35].
- Let X_1, X_2, …, X_n be multiple-valued variables such that each variable X_i can take values from a certain finite discrete set V_i ($V_i = \{0,1,\ldots,r_{i-1}\}$). A literal X_i^{Si} of variable X_i represents a characteristic function of subset S_i of V_i, that is, the literals value is '1' for symbols from this subset. A multiple-valued dont'care is depicted as X_i^{Vi} or X_i^*.
- Let X, be an n-dimensional cube which $X = X_{n-1}X_{n-2}\ldots X_0$ where X_i's are multiple-valued variables.
- Prime cube: cube X is prime if there is no other cube Z such that $Z \supset X$.
- Let f be an n-input 1-output *multiple-valued function*. We can show the MV function as a mapping: $f(X_0, X_1,\ldots, X_{n-1}): \times_{i=0}^{n-1} V_i \rightarrow \{0, 1, *\}$ where V_i is the radix of i_{th} variable. When all radixes are same ($V = V_i$; *for all* i),
  multiple-valued mapping will be simplified, $f: V_i \rightarrow \{0, 1, *\}$.
- Cover: a set of cubes which together cover every element of the set S_{on}.
- Prime Cover: a cover in which all cubes are prime.

The goal of multiple-valued logic minimization is to find an optimal prime cover for a given function

III. Cube Calculus

In this section, we are going to explain the cube operations which are needed for the minimization algorithm [36]. The cube calculus operators in the study of Marek et. al which use positional notation. Thus handling these operators are more complex than what we introduce here.

A. Expansion Operator -$\hat{E}$

This operator is the first operator to find local primes of a given on-set cube. The expansion operator requires two operands: The first parameter is a cube from the set S_{now}, A *2* S_{now}, which is used as the *expander* for the second operand which comes from S_{off} set.

Let $A = A_{n-1}^{\alpha_{n-1}} A_{n-2}^{\alpha_{n-2}} \ldots A_0^{\alpha_0}$ be an n-coordinate expander cube, and let $B = B_{n-1}^{\beta_{n-1}} B_{n-2}^{\beta_{n-2}} \ldots B_0^{\beta_0}$ be the expandee cube where $A \in S_{now}$; $B \in S_{off}$ respectively. The expansion operator produces a new cube $C = C_{n-1}^{\gamma_{n-1}} C_{n-2}^{\gamma_{n-2}} \ldots C_0^{\gamma_0}$, where $C = \hat{E}(A, B)$ as follows:

$$\hat{E}(A,B) = \begin{cases} \text{if } \alpha_i = * \vee \alpha_i = \beta_i \text{ then } \gamma_i = * \\ \text{else if } \alpha_i \neq \beta_i \text{ then } \gamma_i = s \end{cases} \quad (1)$$

The special character s is for coordinates which we need to use in the 'non-disjoint sharp operator.' The byproduct set holds the cubes that are produced by the expansion operators. Here we can express this set as $S_B = \{C | C = \hat{E}(A, B), A \in S_{now}, B \in S_{off}\}$.

B. Elimination Operator –$\hat{X}$

This operator processes the byproduct set S_B which is produced by the expansion operator. Elimination is used to remove the non-maximal cubes from the byproduct set, because these are not necessary for finding primes.

Let A and B be two cubes where A, B ∈ S_B. This operator works based on the following rules:

$$\hat{X}(A,B) = \begin{cases} \text{if } \alpha_i = * \vee \alpha_i = \beta_i, \\ \quad \forall i = 0, 1, \ldots, n-1 \\ \quad \text{then the cube } B \text{ is eliminated} \\ \text{else if } \beta_i = * \vee \alpha_i = \beta_i, \\ \quad \forall i = 0, 1 \ldots, n-1 \\ \quad \text{then the cube } A \text{ is removed} \\ \text{else both of the cubes remain.} \end{cases} \quad (2)$$

The work of this procedure can be expressed as follows. This operator takes two elements –*A, B*- as parameters and does the following:

- If A is non-maximal cube then $\hat{X}(A, B) = \{A\}$,
- If B eliminates A then $\hat{X}(A, B) = \{B\}$,
- If neither A nor B is eliminated then $\hat{X}(A, B) = \{A, B\}$.

C. Non-disjoint Sharp Operator –$\hat{S}$

This MVL operator is introduced in [36] as well. For computing local primes, this process is the final procedure. After eliminating the weak elements by using the X operator, the cubes remained in S_B set are going to be trimmed. The sharp procedure starts with using a full-cube which is a cube where all coordinates are assigned to "don't care", $F = X_{n-1}^* X_{n-2}^* \ldots X_0^*$. A trimmig can be done on any coordinate of the cube F, if that coordinate is not assigned "don't care".

$$\hat{S}(A,B) = A\#B = \begin{cases} \emptyset & \text{when } A \subseteq B \\ A & \text{when } A \cap B = \emptyset \\ A\#_{basic}B & \text{otherwise} \end{cases} \quad (3)$$

Algorithm 1 MVL-MIN Algorithm

$S_{now} = S_{on}$
while $S_{now} \neq \emptyset$ **do**
  $A \in S_{now}$ // Choose a cube from the set
  $S_B = \emptyset$
  for $\forall B \in S_{off}$ **do**
    $S_B = S_B \cup \widehat{E}(A, B)$
  end for
  for $\forall C, D \in S_B$ where $C \neq D$ **do**
    $S_B = S_B - \{C, D\} \cup \widehat{X}(C, D)$
  end for
  $S_P = \{X^*_{n-1} X^*_{n-2} \dots X^*_0\}$
  for $\forall C \in S_B$ **do**
    $S_{Pb} = \emptyset$
    for $\forall D \in S_P$ **do**
      $S_{Pb} = S_{Pb} \cup \widehat{S}(D, C)$
    end for
    $S_P = S_{Pb}$
  end for
end while

IV. MVL-MIN MINIMIZATION ALGORITHM

Due to high complexity of the existing direct-cover minimization methods may be avoided by using the above-mentioned proposition that suggests to expand of cubes *Soff* instead of all possible expanding of the on-set cube, for which it is necessary to obtain the complete sets of prime implicants. This can be done by applying the algorithm 1 for a single output logic function as follows.

V. DATA SETS AND TESTING

A. Blif-MV Format

An MV function can be expressed as a netlist of MV-nodes. An MV-network is a network of nodes; each node represents an MV-relation with a single multiple-valued output. Here we use a subset of the "blif-MV" format that is used to specify MVL functions [37]. *blif-MV* format is a standart by the Verilog to *blif-MV* (vl2mv) tool. After a design specification is read, it is converted into an MV-network, a design representation used within MVL-MIN.

blif-MV is a file format designed for describing hierarchical symbolic sequential MV systems. A system can be composed of interacting sequential subsystems.

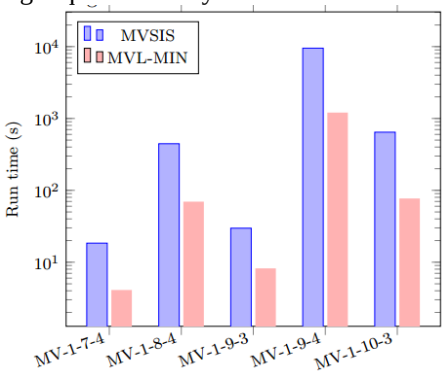

Fig. 1: Run time comparison of MVSIS and MVL-MIN on the first dataset

A multiple-valued logic can be expressed with four basic primitives: multiple-valued variables, tables, wires and latches. A MV-variable takes values from some finite domain. A relation defined over a set of variables is represented by a table. The variables of a table are divided into inputs and outputs. Wires are used connection among tables. A latch is a memory unit saves the value of the input wire, and transfers the values to the output [2].

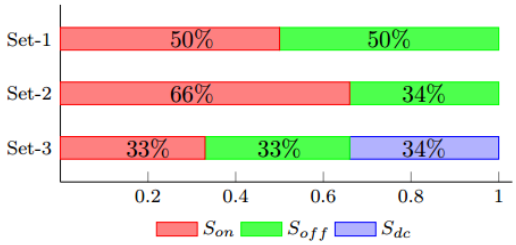

Fig. 2: The Structure of Data Sets

Due to small size of conventional testbenches, we generated 3 sets, each includes 8 multiple-valued logic functions in MV-blif format. The numbers of input variable in Datasets are ranging from 4 to 12. Nomenclature of data file names are based on input variable count and domain of a variable. For example the file names have the form MV-g-v-r, where g is the group number, v is the MV variable count and r is the domain of a variable. MVL functions in the first benchmark group consists of %50 S_{on} cubes and %50 S_{off} cubes. The distribution of the second group test files are %66 S_{on}, %34 S_{off}.

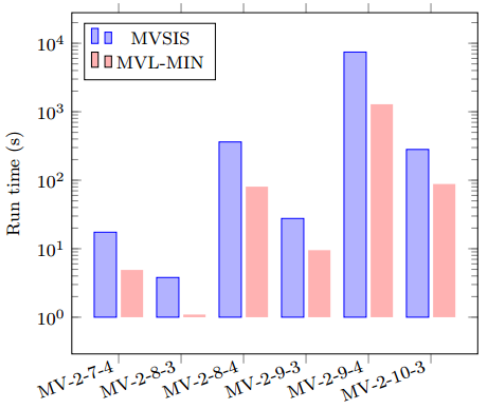

Fig. 3: Run time comparison of MVSIS and MVL-MIN on the second dataset

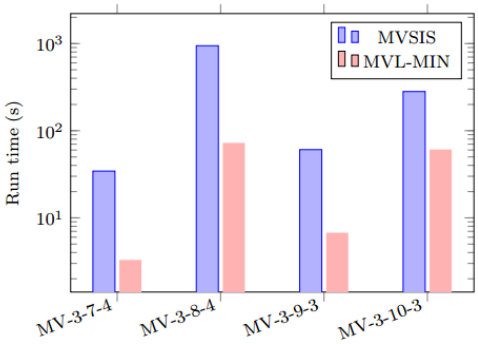

Fig. 4: Run time comparison of MVSIS and MVL-MIN on the third dataset

The third group is constructed evenly su%33 S_{on}, %33 S_{off} and %34 S_{dc}. The fig. 1 depicts the features of the data sets.

MVL-MIN achieved around 5x speedup over MVSIS. A comparison with MVSIS shows that the proposed algorithm is able to solve all test files within a fixed allocation of computer resources.

VI. Results and Future Applications

A heuristic Multiple-valued logic function simplification algorithm has been introduced. This algorithm uses MV cube calculus operations which are "expansion," "elimination," and "Non-Disjoint Sharp."

This can be adapted into the Verification Interacting with Synthesis (VIS), which is a research tool. This application operates on MVL networks as well [38]. Otherwise a new MVL synthesis tool can be compiled by integrating our tool with "vl2mv" and a place and route program, such as ODIN [39].

Marek et. al. accelerated MVL operations on GPUs and on FPGAs [namely cube calculus machine]. We want to compare our algorithm with others but since most of them are using AI, they can only handle limited MVL functions (usually 2-3 MV variable input). The columns labeled as $s(S_{on})$ and $s(S_{off})$ depicts the number of the cubes in S_{on} and S_{off} respectively.

TABLE I
TIMING RESULTS OF MVSIS AND MVL-MIN ON BENCHMARK SET 1

Test Bench	n*	r**	$s(S_{on})$	$s(S_{off})$	Time (s) MVSIS	Time (s) MVL-MIN	Speedup
MV-1-4-3	4	3	40	41	0.030	0.035	0.9
MV-1-4-4	4	4	134	122	0.330	0.192	1.7
MV-1-5-3	5	3	112	131	0.460	0.310	1.5
MV-1-7-3	7	3	1105	1082	3.270	0.704	4.6
MV-1-7-4	7	4	8250	8134	18.410	4.109	4.5
MV-1-7-5	7	5	39152	38973		79.675	
MV-1-8-3	8	3	3362	3199	9.080	0.934	9.7
MV-1-8-4	8	4	32678	32858	445.250	69.054	6.4
MV-1-8-5	8	5	195151	195474		2204.622	
MV-1-9-3	9	3	9732	9951	29.740	8.213	3.6
MV-1-9-4	9	4	131059	131085	9513.500	1207.837	7.9
MV-1-10-3	10	3	29250	29799	644.380	77.657	8.3
MV-1-10-4	10	4	523670	524906		19089.376	
MV-1-11-3	11	3	88391	88756		738.118	
MV-1-12-3	12	4	265355	266086		6714.434	

* # of Input variable
** Radix

TABLE II
TIMING RESULTS OF MVSIS AND MVL-MIN ON BENCHMARK SET 2

Test Bench	n	r	$s(S_{on})$	$s(S_{off})$	Time (s) MVSIS	Time (s) MVL-MIN	Speedup
MV-2-4-3	4	3	57	24	0.100	0.125	0.8
MV-2-4-4	4	4	167	89	0.120	0.087	1.4
MV-2-5-3	5	3	165	78	0.180	0.114	1.5
MV-2-7-3	7	3	1436	751	1.270	0.746	1.7
MV-2-7-4	7	4	10991	5393	17.310	4.918	3.5
MV-2-7-5	7	5	51958	26167		92.744	
MV-2-8-3	8	3	4421	2140	3.870	1.068	3.6
MV-2-8-4	8	4	43781	21755	362.130	80.271	4.5
MV-2-8-5	8	5	260026	130599		2461.869	
MV-2-9-3	9	3	13020	6663	27.660	9.558	2.9
MV-2-9-4	9	4	174746	87398	7436.280	1286.171	5.8
MV-2-10-3	10	3	39391	19658	281.290	88.300	3.1
MV-2-10-4	10	4	699151	349425		22029.749	
MV-2-11-3	11	3	118656	58491		895.367	
MV-2-12-3	12	4	354591	176850		7815.372	

TABLE II
TIMING RESULTS OF MVSIS AND MVL-MIN ON BENCHMARK SET 3

Test Bench	n	r	$s(S_{on})$	$s(S_{off})$	Time (s) MVSIS	Time (s) MVL-MIN	Speedup
MV-3-4-3	4	3	30	33	0.050	0.094	0.5
MV-3-4-4	4	4	105	114	0.090	0.113	0.7
MV-3-5-3	5	3	106	111	0.680	0.461	1.4
MV-3-7-3	7	3	966	977	0.690	0.083	8.3
MV-3-7-4	7	4	6822	6769	34.550	3.209	10.8
MV-3-7-5	7	5	31016	31373		54.173	
MV-3-8-3	8	3	2917	2891	6.720	0.775	8.7
MV-3-8-4	8	4	27245	27361	944.370	72.447	13.0
MV-3-8-5	8	5	155985	156462		1409.629	
MV-3-9-3	9	3	8666	8844	60.850	6.788	8.9
MV-3-9-4	9	4	109345	109129		815.900	
MV-3-10-3	10	3	26339	26217	766.950	60.972	12.6
MV-3-10-4	10	4	436750	437043		13591.574	
MV-3-11-3	11	3	78795	78489		570.188	
MV-3-12-3	12	4	236031	236300		5290.462	

REFERENCES

[1] J.T. Butler, "Multiple-Valued Logic in VLSI," IEEE Computer Society Press Technology Series, Los Alamitos, CA, 1991.

[2] T. Furusho, T. Nishi and M. Konishi, "Distributed Optimization Method for Simultaneous Production Scheduling and Transportation Routing in Semiconductor fabrication bays," Int. J. of Inn. Com., Inf. and Con., vol.4, no.3, pp.559-578, 2008.

[3] S. L. Hurst. "Multiple-valued logic - its Status and Future." IEEE Trans. Comput., vol. 33, pp. 1160-1179, 1984.

[4] E. Ozer, R. Sendag, and D. Gregg, "Multiple-Valued Logic Buses for Reducing Bus Size, Transitions and Power in Deep Submicron Technologies," Adv. Net. and Comm. Hard. Work. (ANCHOR), June 2005.

[5] E. Dubrova, "Multiple-Valued Logic Synthesis and Optimization," Hassoun S. and Sasao T., editors, Logic Synthesis and Verification, Kluwer Acad. Pub., pp. 89-114, 2002.

[6] S. Lin, Y.B. Kim, F. Lombardi, and Y.J. Lee, "A new SRAM cell design using CNTFETs," Proceedings of the International SoC Design Conference, pp. 168-171, Nov. 2008.

[7] E. Ozer, R. Sendag, and D. Gregg, "Multiple-valued logic buses for reducing bus energy in low-power systems," IEE Proceedings of Computers and Digital Techniques, vol. 153, pp. 270-282, Jul. 2006.

[8] D. M. Miller and M. A. Thornton, "Multiple valued logic: Concepts and representations," Synthesis lectures on digital circuits and systems, vol. 2, pp. 1-127, 2007.

[9] C.S. Lent, P.D. Tougaw, W. Porod, and G.H. Bernstein, "Quantum cellular automata," Nanotechnology, vol. 4, pp. 49-57, Jan. 1993.

[10] K. Matsumoto, M. Ishii, K. Segawa, Y. Oka, B.J. Vartanian, and J.S. Harris, "Room temperature operation of a single electron transistor made by the scanning tunneling microscope nanooxidation process for the TiOx/Ti system," App. Phy. Lett., vol. 68, pp.34-36, Jan. 1996.

[11] R. Martel, T. Schmidt, H.R. Shea, T. Hertel, and P. Avouris, "Single- and multi-wall carbon nanotube field-effect transistors," App. Phy. Lett., vol. 73, pp. 2447-2449, Oct. 1998.

[12] R. F. Mirzaee, M.H. Moaiyeri, M. Maleknejad, K. Navi, and O. Hashemipour, "Dramatically low-transistor-count high-speed ternary adders," IEEE 43rd International Symposium on Multiple-Valued Logic, pp. 170-175, May 2013.

[13] S. L. Murotiya, "Low-Power High-Speed and Compact Ternary VLSI Circuit Designs using Carbon Nanotube Field Effect Transistors." PhD Dissertation 2015.

[14] L.S. Phanindra, M N Rajath, V Rakesh, K S V. Patel "A novel design and implementation of multi-valued logic arithmetic full adder circuit using CNTFET," 2016 IEEE Int. Conf. on Rec. Trends in Elect., Inf. & Comm. Tech. (RTEICT). 20-21 May 2016 Bangalore, India.

[15] IBM, "Milestone Advances Effort to Enhance Semiconductors through Nanotechnology." Yorktown Heights, NY, USA, 2006, Mar 24.

[16] S. J. Tans, A. R. M. Verschueren, and C. Dekker, "Room temperature transistor based on a single carbon nanotube," Nature, vol. 393, no. 6680, pp. 49-52, May.1998.

[17] V. Derycke, R. Martel, J. Appenzeller, and P. Avouris, "Carbon Nanotube Inter- and Intramolecular Logic Gates," Nano Lett., vol. 1, no. 9, pp. 453-456, 2001.

[18] A. Bachtold, P. Hadley, T. Nakanishi, and C. Dekker, "Logic Circuits with Carbon Nanotube Transistors," Science, vol. 294, no. 5545, pp. 1317-1320, Nov. 2001.

[19] Z. Chen, J. Appenzeller, Y. M. Lin, J. S. Oakley, A. G. Rinzler, J. Tang, S. J. Wind, P. M. Solomon, P. Avouris, "An integrated logic circuit assembled on a single carbon nanotube," Science, vol. 311, no. 5768, pp. 1735, Mar. 2006.

[20] N. Patil, A. Lin, E. Myers, H. S. P.Wong andS. P. Mitra, "Integrated wafer-scale growth and transfer of directional carbon nanotubes and misaligned-carbonnanotube-immune logic," in Proc. Symp. VLSI Tech., Honolulu, HE, pp. 205 206, 2008.

[21] N. Patil, A.Lin, Z. Jie, W. Hai,K. Anderson, H.-S.P. Wong, S. Mitra, "Scalable carbon nanotube computational and storage circuits immune to metallic and mispositioned carbon nanotubes," IEEE Trans. Nano Tech., vol.10, no. 4, pp. 744 750, July 2011.

[22] M. Shulaker, J. V. Rethy, G. Hills, H. Chen, G. Gielen, H.P. Wong, S. Mitra, "Experimental demonstration of a fully digital capacitive sensor interface built entirely using carbon-nanotube FETs," in Proc. IEEE Int. Solid-State Circ. Conf. Dig. of Tech. papers (ISSCC), Feb. 2013,pp. 112113.

[23] Q. Cao, H.-S. Kim, N. Pimparkar, J. P. Kulkarni, C. Wang, M. Shim, K. Roy, M. A. Alam, J. A. Rogers, "Medium-scale carbon nanotube thin-film integrated circuits on flexible plastic substrates," Nature, vol. 454, no. 7203, pp. 495-500, Jul. 2008.

[24] M. Shulaker, G. Hills, N. Patil, H. Wei, H. Y. Chen, H. S. P. Wong and S. Mitra, "Carbon nanotube computer," Nature, vol. 501, no. 7468, pp. 526-530, Sep. 2013.

[25] A. Srivastava and H.N. Venkata, "Quaternary to Binary Bit Conversion CMOS Integrated Circuit Design Using Multiple Input Foating Gate MOSFETs," Integration VLSI J. vol.36 no.3, pp. 87-101, 2003.

[26] M. Gao, J.H. Jiang, Y. Jiang, Y. Li, S. Sinha and R. Brayton "MVSIS," In the Notes of the International Workshop on Logic Synthesis, Tahoe City, June 2001

[27] G.W. Dueck and D.M. Miller, "A direct cover MVL minimization Using the Truncated Sum," Proc. ofthe 17th IEEE Int. Symp. on Multiple-Valued Logic, pp. 221-226, 1987.

[28] G.W. Dueck, "Direct cover MVL Minimization with CostTables," Proc. of the 22nd IEEE Int. Symp. on MultipleValued Logic, pp.58-65, 1992.

[29] Z. Tang, Q. Cao, and O. Ishizuka, "A Learning Multiplevalued Logic Network: Algorithm and applications," IEEE Trans. on Computers, vol.47, no.2, pp. 247-250, 1998.

[30] Q. Cao, Z. Tang, R. Wang, and W. Wang, "Local Search Based Learning Method for Multiple-valued Logic Networks," IEICE Trans. Fundamentals, vol.E86-A, no.7, pp. 1876-1884, 2003.

[31] W. Wang and C. Moraga, "Design of Multivalued Circuits Using Genetic Algorithms," Proc. of the 26th IEEE Int. Symp. on Multiple-valued Logic, pp. 216-221, 1996.

[32] Y. Hata, K. Hayase, and T. Hozumi, "Multiple-valued Logic Minimization by Genetic Algorithms," Proc. of the 27th IEEE Int. Symp. on Multiple-valued Logic, pp. 97- 102, 1997.

[33] B. Sarif and M. Abd-El-Barr, "Synthesis of MVL functions - part I: The Genetic Algorithm Approach," Int. Conference on Microelectronics, pp. 154-157, 2006.

[34] S. Gao, Z. Tang, C. Vairappan "An Effective Immune Algorithm for Multiple-Valued Logic Minimization Problems," Int. Jour. of Innov. Com., Inf. and Con. 5, 11-A, pp. 3961-3969, 2009.

[35] S. Kahramanli, S. Tosun "A Novel Essential Prime Implicant Identification Method for Exact Direct Cover Logic Minimization," The Int. Con. on Com. Des.,CDES'06, June 26-29,2006, Las Vegas, USA.

[36] M. Perkowski, D. Foote, Q. Chen, A. Al-Rabadi, Jozwiak, L. "Learning Hardware Using Multiple-valued Logic, Part 2: Cube Calculus and Architecture," 2002.

[37] R. K. Brayton, M. Chiodo, R. Hojati, T. Kam, K. Kodandapani, R. P. Kurshan, S. Malik, A. L. SangiovanniVincentelli, E. M. Sentovich, T. Shiple, K. J. Singh, and H.Y. Wang. BLIF-MV: An Interchange Format for Design Verification and Synthesis. Technical Report UCB/ERL M91/97, Electronics Research Lab, Univ. of California, Berkeley, CA 94720, November 1991.

[38] R. Alur and T. Henzinger, "VIS: A system for Verification and Synthesis", The VIS Group, In the Proceedings of the 8th International Conference on Computer Aided Verification, Springer Lecture Notes in Computer Science, 1102, Edited by New Brunswick, NJ, pp. 428-432, July 1996.

[39] P. Jamieson, K.B. Kent, F. Gharibian and L. Shannon,"Odin II - An Open-source Verilog HDL Synthesis tool for CAD Research," Proceedings of the IEEE Symposium on Field-Programmable Custom Computing Machines, pp. 149-156, 2010.

Design and Implementation of GA Filter Algorithm for Baro-inertial Altitude Error Compensation

Jafar Keighobadi[1], Hossein Nourmohammadi[2] and Sadra Rafatnia[3]

***Abstract*—** Providing accurate altitude plays a key role in the long-term performance and reliability of inertial Navigation systems (INSs). In low-cost MEMS-grade INSs, failure to compensate vertical channel instability errors could result in exponentially divergence of computed altitude. Therefore, an integrated baro-inertial altimeter comprising of a damping loop and optimal state estimation mechanizations leads to compensated altitude error in vertical channel of navigation systems. In this paper, considering different environmental conditions in the form of standard and non-standard atmosphere models and using a MEMS altimeter, the barometric altitude is accurately computed. Then, the genetic algorithm (GA) is utilized for integrating the computed barometric altitude with that of the vertical channel of MEMS-grade INS. Vehicular test has been carried out to show the long-term performance of the proposed Baro-inertial integrated system.

***Keywords*—** Integrated Baro-inertial altimeter, Barometric altitude, Vertical channel instability, Genetic algorithm.

I. Introduction

Aided altitude measurement is one of the most important inputs for damping the vertical channel instability of inertial navigation system (INS). In common INS, the barometric pressure is utilized to stabilize and control the divergence of altitude/height and down-ward velocity. Using relatively stable measurements of barometric pressure sensor and suitable atmosphere models, the accurate altitude above sea level can be obtained. According to standard atmosphere models, barometric altitude is simply computed based on the static pressure. Since, the true sea level temperature and pressure are not fixed values, their deviation from the assumed fixed values by the standard atmosphere model results in large altitude errors. Even though the data are established before take-off, climbing or diving, the non-standard atmosphere can result in up to 8% error of the height rate together with corresponding error in the height [1].

Jafar Keighobadi[1] is with the University of Tabriz, Tabriz, CO 5166614766 Iran (corresponding author's; e-mail:Keighobadi@tabrizu.ac.ir).

Hossein Nourmohammadi[2], is with the University of Tabriz, Tabriz, Iran. (e-mail:Hnourmohammadi@tabrizu.ac.ir).

Sadra Rafatnia[3], was with University of Tabriz, Tabriz, Iran. He is now with the Department of Mechanical Engineering, Sahand University of Technology, Tabriz, Iran (e-mail: sa_rafatnia@sut.ac.ir).

In order to avoid the above mentioned drawback, a non-standard atmosphere model is considered in the paper. In this method, the barometric altitude error which arises from non-standard atmosphere conditions is compensated.

Vertical channel damping loop and optimal state estimation algorithms based on Kalman filter (KF) are two main methodologies that have been addressed in literatures concerned to developing integrated baro-inertial altimeters. The vertical channel damping loop is a feedback control system in which a PI feedback of the altitude error between INS and barometer outputs is utilized to compensate the vertical channel errors [2], [3]. Kalman filter as a recursive algorithm to provide optimal estimation of state vector of a linear dynamic system is generalized to its extended type (EKF) dealing with nonlinear systems [4]-[6]. Using stochastic optimal control approach, Widnall and Sinha determined the optimal gains of the baro-inertial vertical channel [7]. Ausman et al. [8] developed a KF algorithm for vertical channel mechanization based on a linear error model including calibration scale factor of altitude. Seo et al. [9] proposed a KF algorithm for estimation and compensation of error dynamics of vertical channel in which GPS output data are used as the measurement vector. Using sigma point hypotheses a new filter design was presented for identification of barometric aiding sensor of the vertical channel damping loop [10]. Different error sources in differential barometry for personal application have been studied in [11]. A stochastic model has been developed in [12] to explore main statistical properties of the barometric altimeter's noises.

In this paper, based on genetic algorithm (GA) as a global optimization method, a new filtering algorithm is designed for the purpose of barometric altitude error compensation in the damping loop of the MEMS INS vertical channel. GA is a stochastic global search method inspired by the process of natural evolution [13], [14]. Compared to the classic KF, the superior estimation of the integrated baro-inertial altimeter is obtained owing to the GA filter attributes as follows.

1) The GA filter is initialized with no knowledge of correct solution and entirely depends on the responses by the environment and the evolution operators (crossover and mutation), and thus reaches to the best solution.

2) By starting at several independent points and searching in parallel, the algorithm avoids local minimal and even converging to suboptimal solutions.
3) The optimal solution of the proposed algorithm is not limited to zero-mean Gaussian noise processes with known covariance matrices. The filter performance is not involved with substantial restriction occurs by using classic KF.

II. VERTICAL CHANNEL MECHANIZATION

This section deals with the formulation of true barometric altitude model in non-standard atmosphere conditions and developing vertical channel damping loop. The barometric altimeter is affected in a large degree by the atmosphere physics. So, it must be calibrated. In the standard atmosphere, the barometric altitude is obtained as follows [1].

$$H_p = \frac{T_0}{L}\left[\left(\frac{P_s}{P_0}\right)^{-\frac{LR}{g}} - 1\right] + H_0 \tag{1}$$

where, the temperature and the pressure at sea level are specified by T_0 and P_0, respectively. In standard atmosphere these variables are assumed to be $288.15\,(°K)$, $101.325\,(kPa)$. L, R, and g are the constant lapse rate, universal gas constant, and gravity constant, respectively. H_0 is taken 0 for sea level data, and P_s stands for the pressure measured by the barometer. For non-standard atmosphere, the constant lapse rate assumption remains valid [15]. However, the temperature and the pressure assumptions cannot be guaranteed as a real atmosphere system. Applying scale factor, s and bias, b as calibration parameters, the barometric altitude compensation is achieved by the following equation of non-standard atmosphere.

$$H \approx H_P + s(H_P - H_0) + b \tag{2}$$

where, H is the calibrated barometric altitude under non-standard atmosphere condition. The scale factor and the bias parameters are defined as follows.

$$s = \frac{\Delta T}{T_0} \tag{3}$$

$$b = \frac{RT_0}{g}\left(\frac{\Delta P}{P_0}\right) \tag{4}$$

In (3) and (4), ΔT and ΔP denote the deviation of true temperature and true pressure at sea level from the corresponding fixed values of standard condition, respectively. To compute the true values of local sea level temperature and pressure around tests region, the following model is used.

$$\begin{aligned} T_t &= T_s + L\,H_P \\ P_t &= P_s + \rho g\,H_p \end{aligned} \tag{5}$$

where, T_t and P_t represent the true temperature and the pressure at sea level, respectively. T_s and P_s are the measured values by sensors.

In many positioning and navigation applications accurate altitude information is required. The main goal of the vertical channel mechanization is to minimize the errors of altitude and down-ward vertical velocity. Through damping loop, the vertical channel data of INS is integrated with aiding barometric system known here as Air-data. The feedback block diagram of damping loop in Fig. 1 shows how the computed data of INS vertical channel are stabilized.

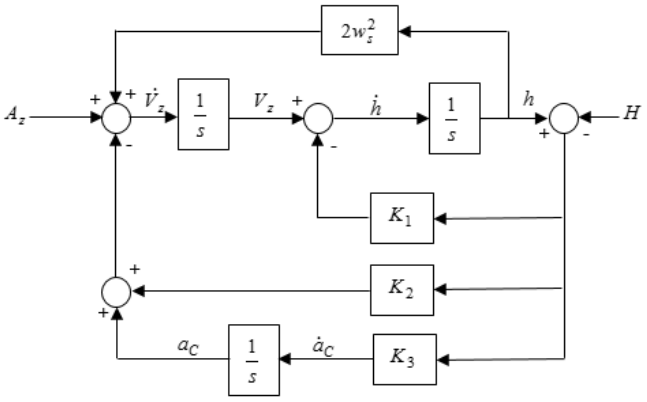

Fig.1 Block diagram of vertical channel damping loop.

The corresponding dynamical equation of the damping loop can be written as follows.

$$\begin{aligned} \dot{h} &= V_Z - K_1(h - H) \\ \dot{V}_Z &= A_Z - a_C + 2w_s^2 h - K_2(h - H) \\ \dot{a}_C &= K_3(h - H) \end{aligned} \tag{6}$$

where, V_Z, h and H stand for vertical velocity, true height and calibrated barometric altitude of non-standard atmosphere condition, respectively. A_Z denotes the measured acceleration along vertical channel. The parameters, a_C and w_s are the outputs of compensator and Schuler frequency, respectively. The feedback gains, K_1, K_2 and K_3 should be determined in such a way that leads to minimized error between the estimated and the reference values of vertical velocity. GA based computation algorithm for optimal values of feedback gains is explained in complete details in the following section.

III. ERROR COMPENSATION BY GA METHOD

In this section, a new binary GA method is proposed. As a matter of fact, GPS and barometer are used as aiding systems of the integrated INS to estimate and compensate its vertical channel errors. The vertical velocity component of GPS system, V_G^{obs} is considered as the reference signal and the value computed by (6), V_Z^a is considered as the estimated value. The mismatch between the N number of reference and

estimated values is designated based on the following cost function.

$$J_O \equiv \sum (V_{Gi}^{obs} - V_{Zi}^{a})^2 \qquad i = 1, 2, ..., N \tag{7}$$

where, the summation extends over the observation grid points by the GPS over a time window of at least one volume scan period. So the problem is formulated as a binary genetic algorithm, and the objective of this problem is minimizing the cost function of (7).

GA operates through a simple but important iteration in four main steps [13]: the creation of population of strings, the evaluation of each string, the selection of the best or fittest strings and finally the genetic manipulation to create the new population of strings. The algorithm starts with initial random sets of individuals called the initial population. The objective function (7) for each individual is evaluated. On the basis of this evaluation, a new set of population is created according to three major genetic operators including selection, crossover and mutation in addition to four control parameters of population size, selection pressure, crossover rate and mutation rate. The procedure is iteratively repeated until a defined terminating condition is reached and satisfied.

- **Selection**

Selection is one of the three major genetic operators that chooses a chromosome from the current generation's population to be included in the population of next generation. Selection operator includes tournament, roulette wheel, top percent and best selection sections. In the tournament step of designed algorithm, a small subset of chromosomes is picked randomly and the chromosome with the lowest cost in this subset becomes a parent.

- **Crossover**

Crossover is an operator that combines two chromosomes to produce a new chromosome [16]. The major idea in crossover is that the child may be better than parents. The crossover operator includes one-point, two-point and uniform operation. Crossover occurs according to definable crossover probability. In the proposed GA filter, the one-point method is used and the crossover probability (P_c) is defined as a fixed value of 0.9.

- **Mutation**

Mutation is a genetic operator that alters one or more gens of a selected chromosome. Mutation points are randomly selected among the $(N_{pop} \times N_{bits})$ bits in the population matrix. If the selected gen in a single point mutation changes from 1 to 0 or conversely, new individuals are created and added to the population. Mutation occurs during evolution according to a certain mutation probability. In the presented algorithm, the relationship between the mutation probability and the generation number is considered as follows [17].

$$p_m = \frac{1}{240} + \frac{0.11375}{2^t} \tag{8}$$

where, p_m denotes the mutation probability and t is the generation number.

Block diagram of Fig. 2 shows the main structure of the proposed GA algorithm of vertical channel filter.

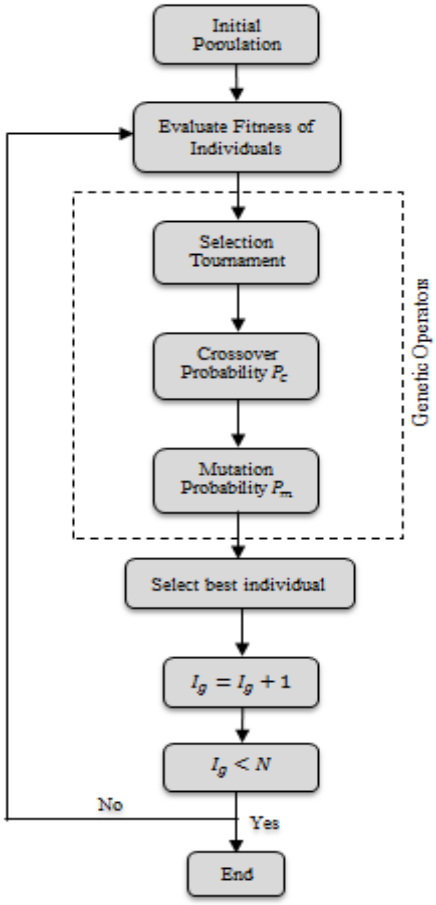

Fig.2 Block diagram of binary GA for vertical channel error compensation.

The proposed GA algorithm of vertical channel filter is summarized in five main steps as follows.

Step 1: The algorithm's parameters comprising of chromosome length, number of initial population, crossover probability (P_c) and number of generation *(N)* are initialized.

Step 2: For the initial population, the gains of vertical damping loop, K_1, K_2 and K_3 are generated.

Step 3: The objective function of (7) is evaluated for each chromosome. In this step, the best individual and also the individuals that have the least parameter distance from the best individual are reserved. The distance between the i^{th} individual and the best individual is calculated as:

$$d^i = \sum_{k=0}^{p_n} (P_k^i - P_k^{\max})^2 \tag{9}$$

where, p_n shows the total number of parameters. P_k^i and $P_k^{\max}$ stand for the k^{th} parameter of individual i, and the k^{th} parameter of the best individual, respectively.

Step 4: The iterative generation, I_g is set. For $I_g < N$, considering the crossover probability condition, crossover operation is done for two selected chromosomes and two children are generated. Furthermore, considering the mutation probability condition, mutation operation is done for the selected pair and another two children are generated. Then, the fitness of the new individuals is calculated and the dominant individuals of the population are updated.

Step 5: I_g is set to $(I_g + 1)$. If $I_g < N$, the algorithm is repeated from step 3. Otherwise, the process is stopped and the best solution is achieved.

Applying the presented algorithm, the feedback gains of vertical channel damping loop are determined and the true height is estimated.

IV. Implementation and Eesults

In this section, the proposed GA filter algorithm for integrated barometric altitude is experimentally verified. Vehicular tests have been performed using "ADIS16407" IMU-barometer sensors and a "Vitans" integrated INS with a "Garmin 35" GPS [18], as shown in Fig. 3. The required temperature and raw pressure data are provided by corresponding sensors of ADIS16407 system. Considering the full scale ranges of the sensors, the pressure data are determined in the interval between 10 *mbar* and 1200 *mbar* and the vertical acceleration data could be measured in the interval -10g to 10g.

Fig.3 Block diagram of vertical channel damping loop.

Vehicular tests have been executed by experienced colleagues in navigation field. Along the mountain road tests, the vehicle's altitude is changed in large range intervals and therefore enriched calibration data are provided.

A. Compensated Barometric Altitude

In this section, the obtained altitude by the proposed compensation method of the barometric altimeter according to nonstandard atmosphere is compared with that of the traditional barometric altitude produced by Vitans system. Both the compensated barometric altitude presented in section II, and the barometric altitude of Vitans system with respect to the GPS altitude data are shown in Fig. 4.

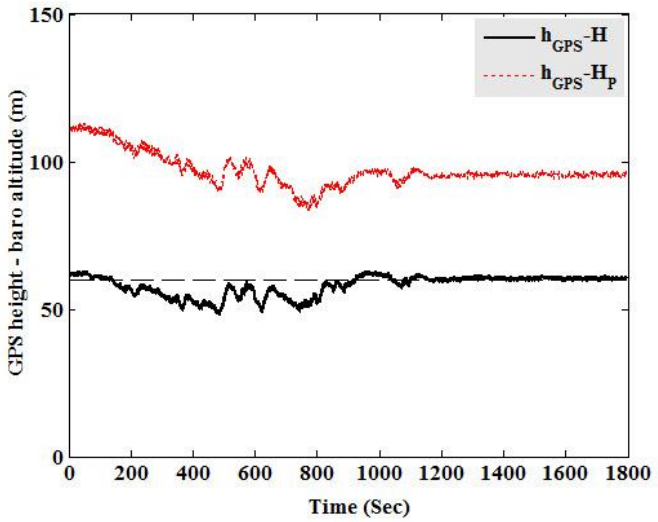

Fig.4 Compensated barometric altitude and vitans' barometric altitude with respect to GPS height.

According to Fig. 4, the error of corrected barometric altitude with respect to that of GPS is approximately 60 m. Using WGS84 data which is the most commonly recognized model of the world geodetic system, the sea level altitude in the test region is 60 m above the mean sea level. Therefore, considering the fact that the GPS gives its altitude with respect to the mean-sea level, the compensated altitude of the non-standard atmosphere is significantly accurate. Consequently, the barometric altitude correction algorithm based on non-standard atmosphere gives near-accurate altitude in comparison to the reference GPS data.

B. Implementation of GA

In this section, the proposed genetic algorithm method presented in section III is experimentally verified using the vehicular test data. In the GA, random initial populations are generated for the gains of vertical damping loop. The optimal gains of the damping loop are obtained through the GA as follows.

$$K_1 = 3.00$$
$$K_2 = 0.6452 \qquad (10)$$
$$K_3 = 0.8710$$

By comparing the estimated height with respect to that of the GPS receiver in Fig. 5, the tracking performance of the GA based damping loop of vertical channel mechanization is assessed. The illustrated result during the vehicular test shows the valuable estimation performance of the proposed algorithm. It can be obviously inferred from Fig. 5 that the proposed GA method in the paper results in a relatively accurate estimation of vertical channel height with respect to the reference GPS height.

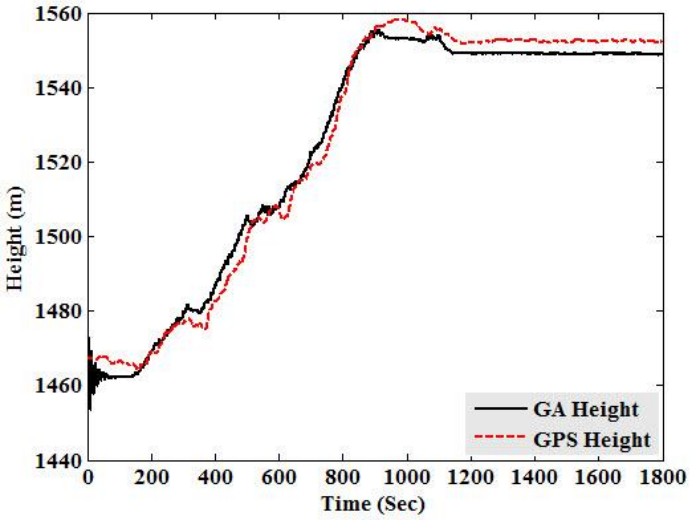

Fig.5 Estimation of vertical channel altitude for vehicular test using GA method.

C. Comparison with Kalman Filter

To legitimize the estimation performance of the proposed GA-based method, the vertical height is also estimated through KF algorithm. Using dynamical equations (6) the following dynamics of the vertical channel error is utilized in the implementation of KF [8].

$$\begin{aligned} \delta\dot{V}_Z &= 2w_s^2\delta h + A_Z + w(t) \\ \delta\dot{h} &= \delta V_Z \end{aligned} \tag{11}$$

where, $w(t)$ represents Gaussian noise signal. Moreover, the bias of the barometer sensor is considered as a first order Gauss-Markov process modeled as [19]:

$$\dot{b}(t) = -\beta b(t) + \sqrt{2\beta\sigma^2}\, w(t) \tag{12}$$

In (12) β and σ are the correlation time and the standard deviation of zero-mean white noise process, $w(t)$, respectively. The dynamical model of (11) and (12) can be rewritten in the following state space model.

$$\dot{\mathbf{x}} = \mathbf{A}\mathbf{x} + \mathbf{B}\mathbf{u} \tag{13}$$

where, the state vector, $\mathbf{x}$ and the input vector, $\mathbf{u}$ are determined as follows.

$$\begin{aligned} \mathbf{x} &= \begin{bmatrix} \delta V_z & \delta h & b \end{bmatrix}^T \\ \mathbf{u} &= \begin{bmatrix} A_z & w(t) \end{bmatrix} \end{aligned} \tag{14}$$

Using (11) and (12), the matrices A and B are obtained as:

$$\mathbf{A} = \begin{bmatrix} 0 & 2w_s^2 & 0 \\ 1 & 0 & 0 \\ 0 & 0 & -\beta \end{bmatrix}, \quad \mathbf{B} = \begin{bmatrix} 1 & 0 \\ 0 & \sqrt{2\beta\sigma^2} \\ 0 & 0 \end{bmatrix} \tag{15}$$

The following measurement equation is used in KF estimation algorithm.

$$h = H + \delta h - b + v_a \tag{16}$$

where, v_a represents measurement noise signal. KF algorithm is imposed on the continuous-time linear dynamic system represented by (13) and the measurement (14). In Fig. 6, the performance of the GA-based vertical channel damping method is compared to the result of KF algorithm.

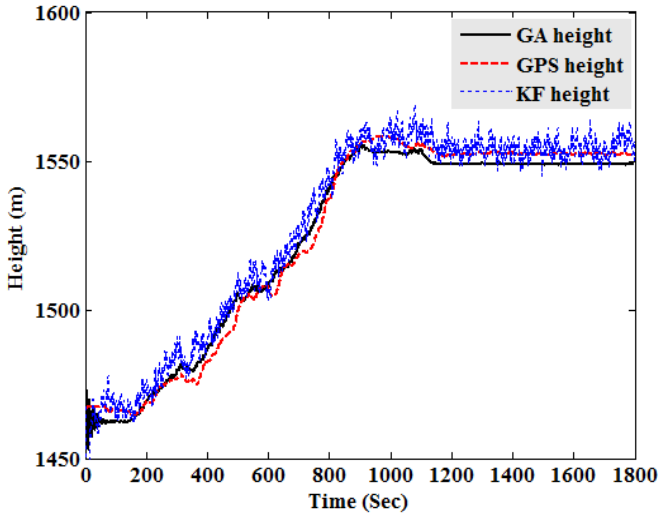

Fig.6 Comparison of GA and KF methods in estimation of vertical channel altitude.

As shown in Fig. 6, the proposed GA method yields a superior tracking compared to KF method. Furthermore, in the estimated height by the GA-based method the oscillation effect of noises has been removed, perfectly. This result becomes more significant by regarding the main advantage of GA method in which no zero-mean Gaussian noise assumption is required.

V. Conclusion

In many navigation applications, accurate altitude information is required. The main goal of vertical channel mechanization is to minimize the errors of vertical height and velocity. In this paper, based on binary genetic algorithm, a new algorithm has been proposed for vertical channel error compensation. vehicular test has been performed and the proposed algorithm for integrated barometric altitude was experimentally verified. The tests are executed in maneuvering conditions of the vehicle in mountain roads. It can be inferred from the results that the algorithm has a good performance for estimating the vertical channel height with an acceptable range of precision. For a fair comparison, the vertical channel height was also estimated through KF algorithm. The test results elucidate the superiority of GA method in tracking of accurate altitude compared to KF algorithm. Using GA method, the oscillation effect of noises on the estimated height has been removed, perfectly. Taking into account the limitation of zero-mean Gaussian noise assumption in KF, the results of GA method becomes more significant.

REFERENCES

[1] R. P. G. Collinson, *Introduction to Avionics Systems*, 2nd Edition, Springer, Boston, 2003.

[2] C. R. Spitzer, *Avionics Development and Implementation*, Taylor and Francis, Virginia, USA, 2007.

[3] S. A. A. Shahidian and H. Soltanizadeh, "Optimal Trajectories for Two UAVs in Localization of Multiple RF Sources," *Trans. Inst. Meas. Control*, vol. 38, 2016. pp. 908–916.

[4] J. Civera, A. J. Davison and J.M. Martinez, *Structure from Motion Using the Extended Kalman Filter*, Springer, Berlin, 2012.

[5] H. Nourmohammadi and J. Keighobadi, "Integration Scheme for SINS/GPS System Based on Vertical Channel Decomposition and In-Motion Alignment," *AUT Journal of Modeling and Simulation*, DOI: 10.22060/miscj.2017.12483.5036, 2017.

[6] P. Zarchan and H. Musoff, *Fundamentals of Kalman Filtering: A Practical Approach*, 3rd Edition, Progressed in Astronautics and Aeronautics, AIAA, Inc., 2009.

[7] W. S. Windall and P.K. Sinha, "Optimizing the Gains of the Baro-Inertial Vertical Channel," *J. Guid. Control Dyn*, vol. 3, 1980, pp. 172–178.

[8] J. S. Ausman, "A Kalman Filter Mechanization for the Baro-Inertial Vertical Channel," *J. Inst. Navigation*, vol. 1, 1991, pp. 153–159.

[9] J. Seo, J. G. Lee and C. G. Park, "Bias Suppression of GPS Measurement in Inertial Navigation System Vertical Channel," *Proc. IEEE/ION Position, Location and Navigation Symposium*, Monterey, CA, USA, April 2004.

[10] I. H. Whang, and W. S. Ra, "Barometer Error Identification Filter Design using Sigma Point Hypothese," in *International Conference on Control, Automation and systems*, Seoul, Korea, October 2007.

[11] J. Parviainen, J. Kantola and J. Collin, "Differential Barometry in Personal Navigation," in *Proc. IEEE/ION Position, Location and Navigation Symposium*, Monterey, CA, USA, May 2008.

[12] A. M. Sabatini and V. Genovese, "A stochastic Approach to Noise Modeling for Barometric Altimeters," *J. Sensors*, vol. 13, 2013, pp. 15692–15707.

[13] M. Moness and A. M. Moustafa, "Tuning a Digital Multivariable Controller for a Lab-Scale Helicopter System Via Simulated Annealing and Evolutionary Algorithms," *Trans. Inst. of Meas. Control*, vol. 37, 2015, pp. 1254–1273.

[14] Z. Jinhua, Z. Jian, D. Haifeng and W. Sun'an, "Self-Organizing Genetic Algorithm Based Tuning of PID Controllers," *J. Inf. Sci*, vol. 179, 2009, pp. 1007–1018.

[15] W. Wuest, Pressure and flow measurement, North Atlantic Treaty Organization, France, 1980.

[16] J. Zhang, H. S. H. Chung and W. L. Lo, "Clustering-Based Adaptive Crossover and Mutation Probabilities for Genetic Algorithms," *IEEE Trans. Evol. Comput*, vol. 11, 2007, pp. 326–335.

[17] T. C. Fogarty, "Varying the probability of mutation in the genetic algorithm," *in Proc. of the 3rd International Conference Genetic Algorithms*, Morgan Kaufmann, December 1989.

[18] H. Nourmohammadi and J. Keighobadi, "Decentralized INS/GPS System with MEMS-grade Inertial Sensors Using QR-factorized CKF," *IEEE Sens. J*, vol. 17, 2017, pp. 3278–3287.

[19] H. Nourmohammadi and J. Keighobadi, "Fuzzy Adaptive Integration Scheme for Low-Cost SINS/GPS Navigation System," *J. Mech. Syst. Sig. Process*, vol. 99, 2018, pp. 434–449.

Jafar Keighobadi received the B.S. degree in Mechanical Engineering from University of Tabriz, Tabriz, Iran, in 1997, M.S. and Ph.D. degrees in Mechanical Engineering and Control Systems from Department of Mechanical Engineering, Amirkabir University of technology (Tehran Polytechnic), Tehran, Iran, in 2000 and 2008, respectively. He joined to the Faculty of Mechanical Engineering, University of Tabriz as an Assistant Professor in 2008. He is currently an Associate Professor of Mechanical Engineering Department, University of Tabriz. His research interests include artificial intelligence, estimation and identification, nonlinear robust control, and GNC.

Hossein Nourmohammadi received the B.S. degree in Mechanical Engineering from Nooshirvani University of Technology, Babol, Iran, in 2010 and the M.S. degree in Mechanical Engineering from Amirkabir University of Technology (Tehran Polytechnic), Tehran, Iran, in 2012. He is currently a Ph.D. candidate in Mechanical Engineering at University of Tabriz, Iran. He has been a Research Assistant with the Navigation, Guidance and Control laboratory at University of Tabriz since 2013. His current research interests include integrated navigation systems, estimation and identification, and nonlinear adaptive control.

Sadra Rafatnia received the B.S. degree in Mechanical Engineering from Guilan University, Rasht, Iran, in 2012 and the M.S. degree in Mechanical Engineering from Tabriz University, Tabriz, Iran, in 2015. He is currently Ph.D. student in Mechanical Engineering at Sahand university of Technology (SUT). He has been a Research Assistant with the Dynamic, Vibration and Control laboratory at SUT since 2016. His current research interests include nonlinear control, estimation and optimization theory.

Investigation of the Effects of Basalt Fibers on the Flexural Strength of RC Beams without Stirrups

Uğur ÖZGEN[1], and Güray ARSLAN[2]

***Abstract*—**This research studied the influence of chopped basalt fibers (BFs) on the shear strength of reinforced concrete (RC) beams without stirrups. The beams including one reference and three basalt fiber reinforced concrete (BFRC) beams were tested under concentrated load at mid-span to determine the shear strength. The test parameters are volume fraction of basalt fibers (V_f) and shear span–to-effective depth ratio (a/d) of beam. The deflection of the beam and the cracking pattern were monitored during the test at certain stages of the monotonic loading until failure. It is observed that the contribution of BFs to the strength at the ultimate state decreases as volume fractions of BFs increase from 0% to 1.5%.

***Keywords*—**Reinforced concrete, beam, chopped basalt fibers, shear strength, deflection.

I. Introduction

In spite of having high compressive strength, proper bonding characteristics and ease of handling, concrete still needs to be used with additional materials for low tensile strength. Technological developments and recent studies have given cause for using new techniques instead of traditional construction materials. Adding fibers into concrete is one of the most promising ways of ensuring high flexural strength without the use of stirrups. Steel and glass fibers have been commonly used in concrete, besides another fiber which has good characteristic properties, is basalt fiber (BF). Among various fiber materials, the use of basalt fiber reinforced concrete (BFRC) has many advantages such as relatively low cost, unlimited reserves, nonflammable, excellent sound and thermal insulator, easy and rapid application, etc [1].

While a substantial amount of researches has focused on the flexural behavior of steel fiber reinforced concrete (SFRC), glass fiber reinforced concrete (GFRC) and polypropylene fiber reinforced concrete (PFRC) beams [2-5], there exists a relatively limited amount of studies concerning the flexural behavior of BFRC beams. Branston et al. [6] tested RC beams to evaluate the potential use of chopped fibers in preventing early age cracking and observed increase in the first cracking strength. Kabay [7] tested the effects of basalt fiber addition in high strength and normal strength concrete with different water-to-cement ratios in terms of physical and mechanical properties. An increase in flexural strength up to 13% is observed. Issa et al. [8] examined the shear strength and behavior of concrete beams reinforced with basalt fiber-reinforced polymer bars with and without stirrups and observed significant improvements in the shear strength of RC beams with insufficient shear reinforcement strengthened with BFRP. High et al. [9] investigated the use of basalt fiber bars as flexural reinforcement for concrete members and the use of chopped basalt fibers as an additive to enhance the mechanical properties of concrete. Jiang et al. [10] studied the effects of the volume fraction and length of BF on the mechanical properties of fiber reinforced concrete and observed significant improvements in the tensile strength and flexural strength in their experiments.

This paper presents four beams without stirrups tested to investigate the influence of BF on the RC beam strength. The beams with a shear span to effective depth (a/d) ratio of 6.0 and fiber contents (V_f) of 0%, 0.5%, 1.0% and 1.5% by volume were tested under a concentrated load at mid-span.

II. Experimental Program – Test Specimens

A combination of letters and numbers is used for specimen labels: "C" followed by the shear span-to-effective depth ratio to indicate all test specimens in this research and "B" followed by the volume fraction of BFs. For example, a beam having a shear span-to effective depth ratio of 6.0 with a volume fraction of fibers equal to 1.0% is labeled as C6.0B1.0. The specimen labeled as C6.0R is the reference beam that does not contain any fibers.

TABLE I
Properties of Beams

Materials	Mix Proportions (kg/m^3)
0-1 mm Natural Sand	350
0-3 mm Crushed Sand	550
5-12 mm Crushed Stone	1000
Cement CEM I 42·5R	300
Water	165
Superplasticiser	3

Uğur ÖZGEN[1] is with the Institute of Natural and Applied Sciences, Yildiz Technical University, Istanbul, 34220 TURKEY (corresponding author's phone: +905363105432; e-mail: ugurozgen@yahoo.com).

Guray ARSLAN[2], was with Civil Engineering Department, Yildiz Technical University, Istanbul, 34220 TURKEY (e-mail: aguray@yildiz.edu.tr).

The concrete mix proportions for all beams are given in Table 1. The properties of test specimens are given in Table 2, where ρ is the tensile reinforcement ratio, V_f is the volume fraction of fibers and f_c is the concrete compressive strength.

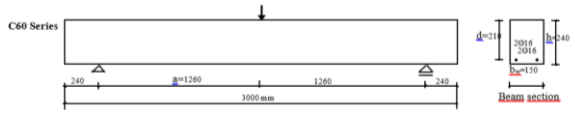

Fig. 1 Geometry and Reinforcement Arrangement of Beams

All beams have the same cross-section of 150 mm by 240 mm with an effective depth of 210 mm and are 3000 mm long. The shear span-to-effective depth ratios (a/d) of all beams are 6.0. Deformed bars with diameters of 16 mm were used as the tensile reinforcement. The geometrical properties and reinforcement arrangement of test specimens are shown in Figure 1.

TABLE II
PROPERTIES OF BEAMS

Beams	f_c (MPa)	V_f (%)	ρ (%)	a/d	a (mm)	l (mm)
C6.0R	23.48	---	1.28	6.0	1260	3000
C6.0B0.5	19.905	0.5	1.28	6.0	1260	3000
C6.0B1.0	14.72	1.0	1.28	6.0	1260	3000
C6.0B1.5	7.38	1.5	1.28	6.0	1260	3000

The chopped BFs with a length and a diameter of 12mm and 9-23μm, respectively, were used throughout the study at varying contents. The density of BFs is 2.8 g/cm^3.

III. TESTING AND INSTRUMENTATION

A displacement-controlled loading machine (Fig. 2) was used to load the beams at mid-span with a static loading rate of 30 μm/s. A computer-aided data acquisition system was used to determine the time intervals for recordings. The applied load and the deflections at various locations were recorded at those predetermined time intervals. The net deflections were recorded by using potentiometric displacement transducers. The beams were loaded until either failure or the load dropped below approximately 80% of its peak value.

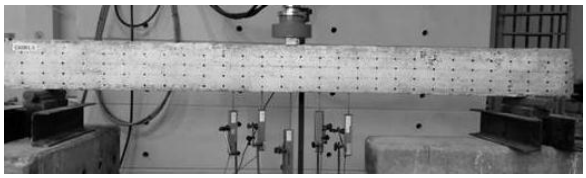

Fig. 2 Test setup

IV. RESULTS AND FINDINGS

The crack patterns of tested beams are shown in Figure 3-6. At the early stages of loading, fine vertical cracks were observed around the mid-span of all beams as expected. As the load was increased, new flexural cracks appeared away from the mid-span area. Some of these cracks were gradually inclined towards the loading point with further increases in the applied loads and the applied load reached its maximum value with the formation of first diagonal crack. The loads carried by the beams decreased rapidly and the C6.0B1.0 and C6.0B1.5 beams failed in shear. While C6.0R and C6.0B0.5 beams exhibited flexural and flexure-shear failures, respectively.

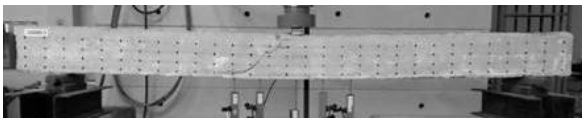

Fig. 3 Crack pattern of C6.0R

Fig. 4 Crack pattern of C6.0B0.5

Experimental results are summarized in Table 3, where P_{co} and δ_{co} are the maximum load and the mid-span deflection at the maximum load, respectively, P_u and δ_u are the ultimate load and mid-span deflection, respectively, and the dissipated energy is the area under the load-deflection curve, which is plotted for each beam in Figure 7 and 8.

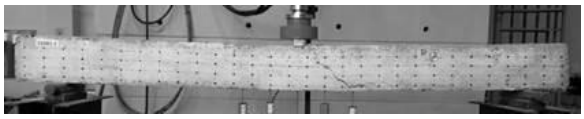

Fig. 5 Crack pattern of C6.0B1.0

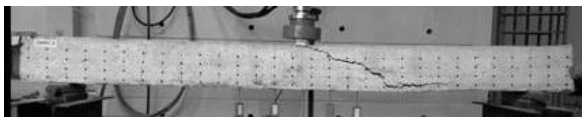

Fig. 6 Crack pattern of C6.0B1.5

The use of BFs in the amount of 0.5% and 1.0% by volume improved the maximum load of RC beams very slightly. Introducing BFs in the amount of 1.5% by volume resulted in a significant decrease in the load-carrying capacity. The deflection capacity of C6.0B1.0, the load-carrying capacity of which dropped immediately after reaching the peak value, was observed to be much less than those of others. It is observed in Figure 7 and Figure 8 that the initial stiffness of all beams are approximately the same except C6.0B1.5.

TABLE III
EXPERIMENTAL LOAD AND DEFLECTION VALUES OF BEAMS

Beams	P_{co} (kN)	P_u (kN)	δ_{co} (mm)	δ_u (mm)	δ_u/δ_{co}	Dissipated Energy (kNm)
C6.0R	55.58	44.46	26.94	51.08	1.89	2.4102
C6.0B0.5	57.54	46.03	15.70	26.22	1.67	1.0562
C6.0B1.0	58.61	46.88	15.42	16.28	1.05	0.5798
C6.0B1.5	34.75	27.80	14.58	22.92	1.57	0.6027

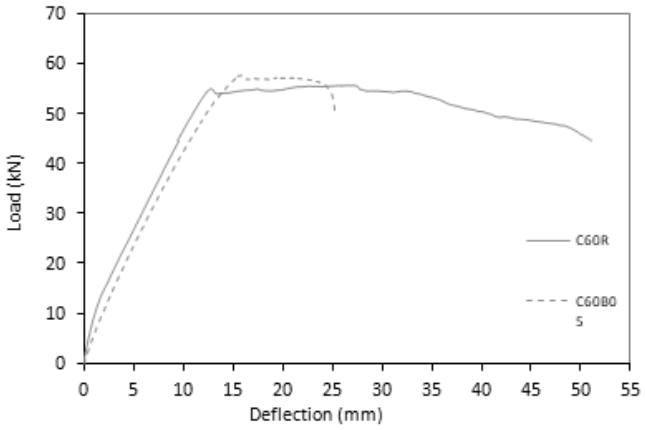

Fig. 7 Load-deflection curves

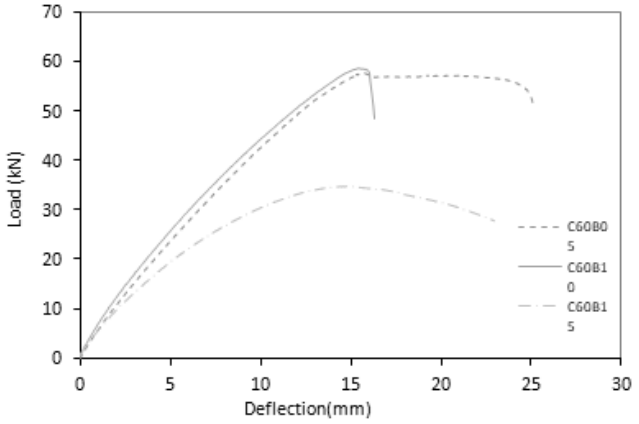

Fig. 8 Load-deflection curves of beams

V. Conclusion

The following conclusions are drawn based on the experiments of BFRC beams.

The beam having basalt fibers in the amount of 0.5% and 1.0% by volume reached a maximum load similar to the load reached by the reference beam, then the load decreased rapidly while a certain amount of deflection of the reference beam was observed beyond the maximum load without a significant loss in the load-carrying capacity. In case of the beam having basalt fibers in the amount of 1.0% by volume, the load decreased immediately after reaching the maximum value.

Introducing basalt fibers in the amount of 1.5% by volume resulted in a significant decrease in the load-carrying capacity. The load-carrying capacity was reduced by 45%.

It is observed that the addition of basalt fibers was not able to improve the strength and ductility of RC beam. Contrarily, it resulted in a behavior poorer than the behavior of reference beam. This can be attributed to the inadequate bonding between aggregate and concrete due to the adhering of basalt fibers to aggregate while mixing the fibers with concrete.

Acknowledgment

This work was supported by Research Fund of Yıldız Technical University under Project No. FYL-2017-3034.

References

[1] K. Singha. "A short review on basalt fiber," *Int J Text*, vol. 1, no. 4, pp. 19–28, 2012.

[2] T. Uygunoglu. "Investigation of microstructure and flexural behavior of steel-fiber reinforced concrete." *Mater Struct*, vol. 41, no. 8, pp. 1441-1449, 2008.

[3] A. Alzate, A. Arteaga, A. de Diego and R Perera. "Shear strengthening of reinforced concrete beams using fibre reinforced polymers (FRP)," Eur J Env Civ Eng, vol. 13, no. 9, pp. 1051–1060, 2009.

[4] H. Aoude, M. Belgidi, W. Cook and J. Mitchell, "Response of stell fiber-reinforced concrete beams with and without stirrups," *ACI Struct J*, vol. 103, no. 3, pp. 350–368, 2012.

[5] G. Arslan, R. S. O. Keskin and Ozturk, M., "Shear behaviour of polypropylene fibre-reinforced-concrete beams without stirrups," *Proc Inst Civ Eng Struct Build*, vol. 170, no. 3, pp. 190–198, 2017.

[6] J. Branston, D. Sreekante, S. Y. Kenno and C. Taylor, "Mechanical Behaviour of basalt fibre reinforced concrete," *Constr Budilg Mater*, Vol. 124, no. 3, pp. 878- 886, 2016.

[7] N. Kabay. "Abrasion resistance and fracture energy of concretes with basalt fiber," *Constr Build Mater*, vol. 50, pp. 95-101, 2014

[8] M. Issa, T. Ovitigala and M. Ibrahim. "Shear Behavior Basalt Fiber Reinforced Concrete Beams with and without Basalt FRP Stirrups." *J Compos Constr.*, 2016, vol. 20, no. 4.

[9] C. High, H. M. Seliem, A. El-Safty and S. H. Rizkalla, "Use of basalt fibers for concrete structures," *Constr Build Mater*, vol. 96, pp. 37–46, 2015.

[10] C. Jiang, K. Fan, F. Wu and D. Chen. "Experimental study on the mechanical properties and microstructures of chopped basalt fiber reinforced concrete," *Mater Des.*, vol. 58, no. 1, pp. 187–193, 2014.

On Analytical Comparative Study Considering Quantified Learning Creativity Analogy versus Ant Colony Intelligence

Hassan Mustafa[1], and Fadhel Ben Tourkia[2]

***Abstract*—** This piece of research introduces an investigational systematic study of an interdisciplinary challenging phenomenon observed in natural world. Interestingly, this study belongs to the two emerging fields of nature-inspired computing (NIC) and computational intelligence (CI) with focusing on the physics- and biology-based approaches and algorithms .Herein, by more details this article concerned with the conceptual analysis and evaluation of quantified learning creativity phenomenon via simulation and modeling of two diverse natural biological systems (human & non-human creatures). More precisely, it is associated to diverse aspects of measurable behavioral learning performance of both biological systems. Therefore, this paper introduces comparative analogy between two diverse biological behavioral systems considering quantification of learning creativity. Referring to, the definition of Swarm intelligence which considered as a relatively new discipline that deals with the study of self-organizing processes both in nature and in artificial systems. Researchers in ethology and animal behavior have proposed many models to explain interesting aspects of social insect behavior such as self-organization and shape-formation. Accordingly, the presented study observed during human interactive tutoring/learning processes with natural environment. Versus ecological behavioral learning of swarm intelligence agents (Ants), while performing foraging process . Systematic investigational study of quantified human learning creativity phenomenon is an interdisciplinary, challenging, and interesting educational issue. At education field practice (classrooms) , while face to face tutoring sessions are performed**,** learning creativity phenomenon is detectable via bidirectional feedback between teacher and pupil. In short, this research work adopts comparative study of simulation and modeling for educational creativity issue considering two disciplinary approaches are namely: swarm intelligence, and neural networks. Both simulated realistically for systematic investigational modeling of creatures' creativity phenomenon observed in nature. Presented creativity models mainly consider observed behavioral learning of ant colony system in addition to in field educational classrooms**.** Conclusively, presented results herein, for both swarm intelligence and neural networks models seemed to be well promising for future more elaborate, systematic, and innovative research in evaluation of human learning creativity phenomenon regarding (NIC) and (CI).

Hassan Mustafa[1] Computer Engineering Department, Al-Baha Private College of Sciences Al-Baha, Kingdom of Saudi Arabia.On leave from Banha University (EGYPT) (corresponding author's phone: 00966-57150965 ; e-mail: prof.dr.hasssanmoustafa@gmail.com**).**
Fadhel Ben Tourkia[2], Computer Engineering Department, Al-Baha Private College of Sciences Al-Baha, Kingdom of Saudi Arabia (e-mail: bintorkih@yahoo.com).

***Keywords*—**Artificial Neural Networks Modeling, Ant Colony Optimization, Noisy Learning Enviornment, Optical Character Recognition, Swarm Intelligence.

I. Introduction

THIS research work deals with an interdisciplinary, interesting, and challenging problem associated with two emerging research fields namely: nature inspired computing (NIC) and computational intelligence (CI), [1]. Furthermore, by referring to [2], it is announced therein: *Natural Computing* is that field of research concerned with investigation of human-designed computing inspired by nature as well as computing taking place in nature by social insects. That is, it investigates models and computational techniques inspired by nature, and also it investigates, in terms of information processing, phenomena taking place in nature. Referring to the instructional methodology of face to face tuition, bidirectional interactive phenomenon observed between teacher and pupil applied in classrooms. Herein, adopted realistic simulation of that tuition methodology is performed by using ANN§ supervised learning modeling (Error correction learning rule). Interestingly, **by** referring to what has been announced by at [3], in the context of attempting to demystify the term Swarm Intelligence (SI). Prof Franks said that although apes could imitate each other, it was a one-way process. According to the accepted definition of teaching in animal behavior, an individual is a teacher if it modifies its behavior in the presence of a naïve observer, at some initial cost to itself, in order that the pupil can learn more quickly. Prof Franks said: "We also believe that true teaching always involves feedback in both directions between the teacher and the pupil. In other words, the teacher provides information or guidance for the pupil at a rate suited to the pupil's abilities, and the pupil signals to the teacher when parts of the 'lesson' have been assimilated". Moreover, Tandem running in the Temnothorax ants met these criteria, he said. Ants laid trails of chemicals, called pheromones, to guide other colony members to food but only they could read the signals. Consequently, the ANNs supervised learning model is well relevant for realistic simulation of adopt an intelligent teaching technique known as tandem running. That approach has been performed by considering ant colony system of Temnothorax albipennis (formerly Leptothorax albipennis).

By other wording, in brief, this paper adopts the analytical and comparative study for the analogy between two distinctly diverse behavioral biological systems. They both characterized by quantified learning creativity versus behavioral swarm intelligence, respectively. That associated to humans (face to face tutoring pupils in classrooms) versus intelligence of social insects (ACS solving TSP optimally),[4][5][6][7]. Furthermore, the paper presents observed effect of noisy environmental nature on performance of learning creativity as well as the behavioral ACS intelligence, [8][9][10][11]. Additionally, the issue of quantified learning creativity has been studied using realistic ANN modeling at some published papers [12][13][14][15][16]. The rest of this paper after the previous introductory first section, is organized in five sections as follows. At the next second section, a revision of conceptual aspects' for instructional process considering modeling of learning paradigms modeling using ANN is introduced. At the third section, the effect of environmental noise on learning performance is presented. Revision for some algorithms to solve TSP using ACS is introduced at the fourth section . Some of obtained interesting simulation results are given at the fifth section. Finally, at the sixth, some of conclusive remarks and suggestions for future work are introduced.

II. LEARNING MODELS' REVISION

This section introduces a revision for the conceptual basis of realistic interactive modeling of teaching/learning process via the three subsections denoted as follows : (*A, B, and C).* At the subsection *A*, relation between an artificial and biological single neuron model is considered along with illustration using basic mathematical formulae. A generalized brief overview of the block diagram describing interactive teaching/learning process that considers (face to face tuition) is given. at subsection *B.* At subsection *C*, the detailed mathematical formulation introduced for both bidirectional communication between any teacher and his learners. That two learning paradigms are namely: guided with a teacher (supervised) and without a teacher equivalently to self-organized (unsupervised). [17][18].

A. Simplified Modeling for a Single Biological Neurone

Realistic modeling of biological neural system, is considered via distributed parallel information processing. However, a single biological neuron is the basic building block of any neural system. In more details, by referring to Fig., inside any single neuron performed information processing transferred among three basic structural components ***(Dendrites, Soma, and Axon)*** **[19].**

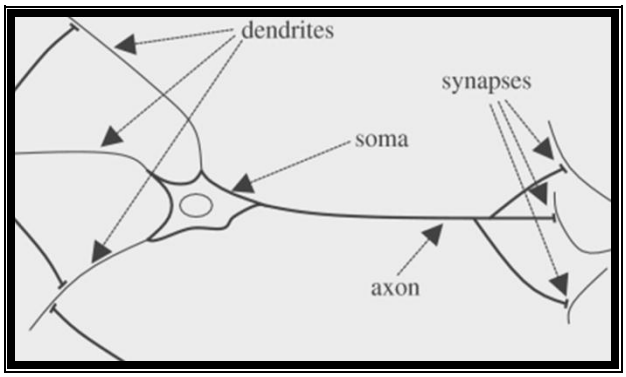

Fig. 1 A simplified schematic structure of a single biological neuron adapted from [19]

Accordingly, realistic neuron model composed of three basic elements of that model given (by referring to the graphical presentation shown at Fig.2. in below) as follows:

- A set of weights, each of which is characterized by a strength of its own. A signal x_i connected to neuron k is multiplied by the weight w_{ki}. The weight of an artificial neuron may lie in a range that includes negative as well as positive values.
- An adder for summing the input signals, weighted by the respective weights of the neuron.
- An activation function for limiting the amplitude of the output of a neuron. It is also referred to as transfer function which squashes the amplitude range of the output signal to some finite value. Two types of the sigmoid transfer (activation)functions are commonly used in ANN applications. First one is the logistic sigmoid and the second other function is the odd sigmoid. There values are given at any arbitrary time instant (n) by equations (3) & (4) respectively.

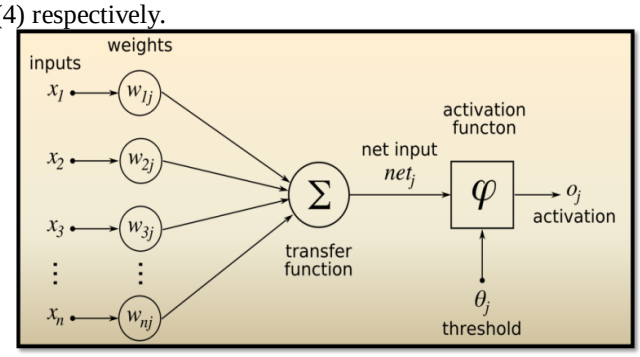

Fig. 2. A single neuron (k) model coupled with synaptic weights from other neurons w_{ki} (i,……,p).

$$V_k = \sum_{i=1}^{p} w_{ki} x_i \quad (1)$$

$$y_k=\varphi(V_k + \theta_k) \quad (2)$$

The odd sigmoid function seemed to be well relevant for realistic simulation of learning brain performance as if this function input stimulus equals zero results in obtaining no output (zero).

$$y_k(n) = \varphi(V_k(n)) = 1 /(1+e^{-\lambda v_k(n)}) \quad (3)$$

$$y_k(n)=\varphi(V_k(n))=(1-e^{-\lambda v_k(n)})/(1+e^{-\lambda v_k(n)}) \quad (4)$$

B. Modeling Of Interactive Learning Processes

Face to face tuition is illustrated as an interactive learning processes presented at Fig. 1. Inputs to the neural network teaching model are provided as a signal provided by environmental stimuli (unsupervised learning). However, correction signal(s) in the case of learning using a teacher's guidance is/are given by output response(s) of the model that evaluated by either the environmental conditions (unsupervised learning) or by supervision of a teacher. Additionally, any tutor plays a role of improvement input data (stimulating learning pattern) by reducing the noise and redundancy of model pattern input. That is motivated by the tutor's experience while performing conventional (classical) learning. Consequently, the tutor provides the learning model with cleared data via maximizing of the signal to noise ratio [20]. Conversely, in the case of unsupervised/self-organized learning, which is based upon Hebbian learning rule [21], it is mathematically formulated by equation (11) presented at the next subsection *(C)*.

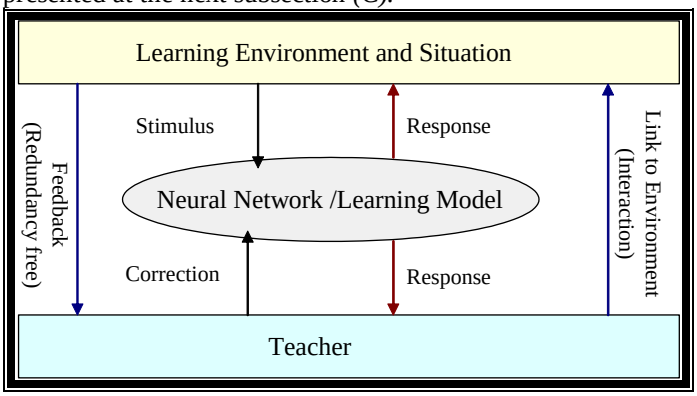

Fig. 3. Simplified view for interactive learning process {Adapted from [22]}.

C. Mathematical Formulation Of Interactive Learning

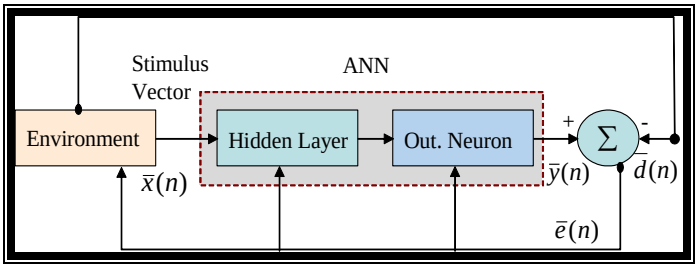

Fig. 4. Generalized ANN block diagram simulating two diverse learning paradigms adapted from [18].

At Figure 4., an interactive learning model through stimulating signals is well qualified in performing realistic simulation for evaluating learner's performance. This Figure illustrates inputs to the neural network learning model which provided by stimuli unsupervised learning environment[18]. The correction signal for the case of learning with a teacher is given by responses outputs of the model will be evaluated by either the environmental conditions (unsupervised learning) [23] or by the instructor. The instructor plays a role in improving the input data (stimulating learning pattern), by reducing noise and redundancy of learning model pattern input .In accordance with instructor's experience, he provides illustrated model with clear data by maximizing learning environmental signal to noise ratio [24].

By more details, referring to above Figure 4; the error vector $\bar{e}(n)$ at any time instant (n) observed during learning processes is given by:

$$\bar{e}(n) = \bar{y}(n) - \bar{d}(n) \tag{5}$$

Where $\bar{e}(n)$ =…..…. is the error correcting signal vector that is controlling adaptively the learning process outcome, $\bar{y}(n)$ …… is the obtained outcome (output) signal developed by ANN model, and $\bar{d}(n)$ …… is the desired vector or numerical value(s). Moreover, the following four equations are deduced:

$$V_k(n) = X_j(n) W_{kj}^T(n) \tag{6}$$

$$Y_k(n) = \varphi(V_k(n)) = (1 - e^{-\lambda V_k(n)}) / (1 + e^{-\lambda V_k(n)}) \tag{7}$$

$$e_k(n) = |d_k(n) - y_k(n)| \tag{8}$$

$$W_{kj}(n+1) = W_{kj}(n) + \Delta W_{kj}(n) \tag{9}$$

Where X is input vector and W is the weight vector. φ is the activation function. Y is the output. e_k is the error value and d_k is the desired output. Note that ΔW_{kj} (n) is the dynamical change of weight vector value. Above four equations are commonly applied for both learning paradigms: supervised (interactive learning with a tutor), and unsupervised (learning though student's self-study). The dynamical changes of weight vector value specifically for supervised phase is given by:

$$\Delta W_{kj}(n) = \eta e_k(n) X_j(n) \tag{10}$$

Where η is the learning rate value during the learning process for both learning paradigms. At this case of supervised learning, instructor shapes child's behavior by positive/ negative reinforcement Also, Teacher presents the information and then students demonstrate that they understand the material. At the end of this learning paradigm, assessment of students' achievement is obtained primarily through testing results. However, for unsupervised paradigm, dynamical change of weight vector value is given by:

$$\Delta W_{kj}(n) = \eta Y_k(n) X_j(n) \tag{11}$$

Noting that e_k(n) equation (10) is substituted by y_k(n) at any arbitrary time instant (n) during the interactive learning process. Referring to Fig.1, the correction signal which provided by a tutor should take into consideration the noisy environmental level inside classrooms (such as noisy crowdedness appears . . In other words, that level is quantitatively measured as signal to noise (S/N) ratio or equivalently the additive noise power (σ) to the ideally sensory clear signal. Consequently, the response time response measured by number of training cycles (n) { as defined at the subsection in the above (*B)* by the two

equations (10) & (11)}. Noting value of (n) should have been increased until reaching learning convergence instant ,when:

$$\Delta W_{kj}(n) = 0 \qquad (12)$$

That above condition given by equation (8), could be fulfilled only if the desired output learning has been obtained after some number of training cycles (response time) in fulfillment of the two equations (10) & (11).

III. Review of Noisy Environmental Concepts [22]

This section presents a comprehensive simulation findings reviewed form the observed concepts of environmental noise levels in nature [11]. It is worth noting that statistical variations(on the average) relating learning rate values versus corresponding learning convergence (response) time. That time is measured by the number of iteration cycles. Referring to Figure 5,obtained output results(of response time) corresponding to the learning rate values (0.1,0.2,0.4,0.6, and 0.8), are given respectively, as (330, 170, 120, 80, and 40) iteration training cycles (At TABLE I.) . Conclusively, convergence time (number of training cycles) is inversely proportional to the corresponding learning rate values. Referring to, Figure 6., an illustration by statistical distribution performance (Similarly, to the bell shape behavioral performance) is presented for the normalized obtained outcomes', considering various values of learning rate:
η (0.05, 0.3, and 0.5)

TABLE I
THE EFFECT OF LEARNING RATE VALUES ON CONVERGENCE LEARNING (RESPONSE)TIME{ADAPTED FROM [22]}

Learning Rate Values (η)	0.1	0.2	0.4	0.6	0.8
Learning Response Time (# cycles)	330	170	120	80	40

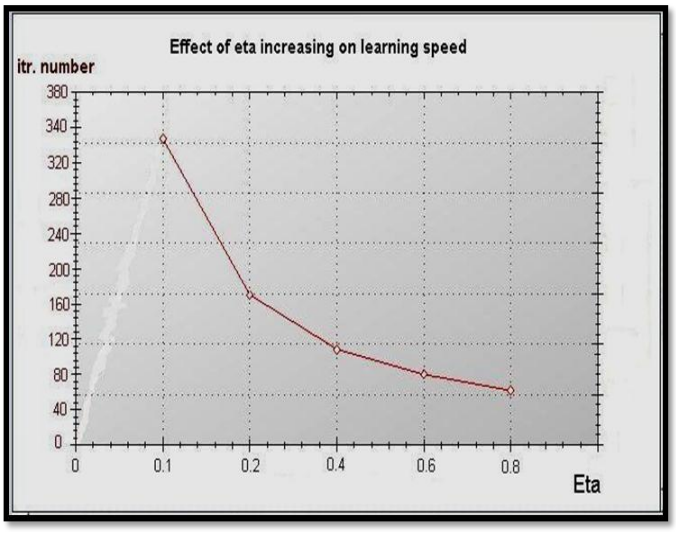

Fig. 5 Illustrates the average (of statistical distribution) for learning response time (number of iteration cycles) for different learning rate values η (eta)

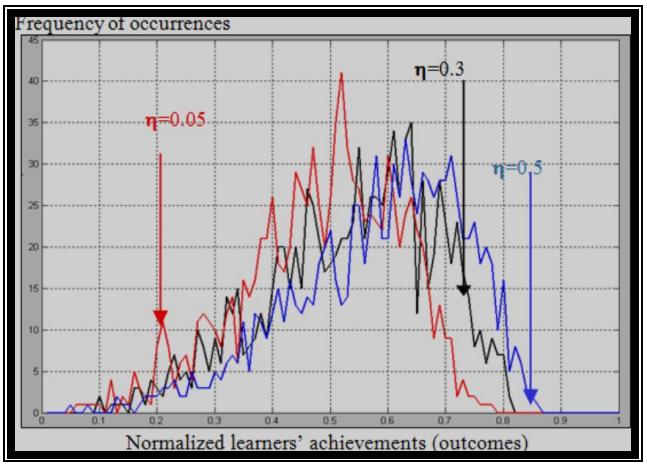

Fig. 6. Illustration of obtained normalized outcomes corresponding to three different learning rate values η (0.05, 0.3, and 0.5).{Adapted from[22]}

B. *Effect Of Noise On OCR Processes* [24]

In nature, optical character recognition OCR as well as pattern recognition processes observed to be carried out under no ideal environmental condition (under effect of noisy data). Interestingly, obtained simulation results for OCR Under different environmental noisy levels are given in a tabulated form at TABLE II. Noting that, noise effect is measured by signal to noise ratio value (S/N) versus the number of training cycles (T) till reaching learning convergence. Conclusively, relation between number of training cycles' values and noisy levels of environmental data (for the case of unsupervised learning paradigm) is illustrated well at Figure 7. Referring to that figure, learning convergence time T in cycles (n), inversely proportional to signal to noise ratio values, (S/N). learning convergence time has been presented at TABLE II. That table derived from, Figure 7. , at [22]. Conclusively, it is observed during interactive learning process that: teaching/learning environment with increasing (S/N) ratio results in decreasing of learning rate parameter value η .That explicitly computed as noise power value (σ) [24].

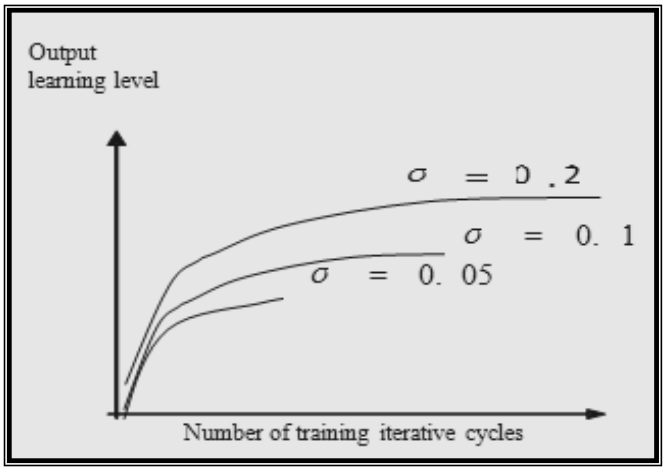

Fig.7. Relation between noise power (σ) that represents non-properly prepared (noisy) learning process convergence, {Adapted from [24]}.

TABLE II
THE EFFECT OF NOISY ENVIRONMENTAL LEARNING ON CONVERGENCE TIME, {ADAPTED FROM [24]}

Signal to Noise (S/N) Power Ratio of Input Data	**5**	**10**	**20**
Noise Power in Learning Environment □□	**0.2**	**0.1**	**0.05**
Convergence Learning Time (# cycles)	**82**	**62**	**47**

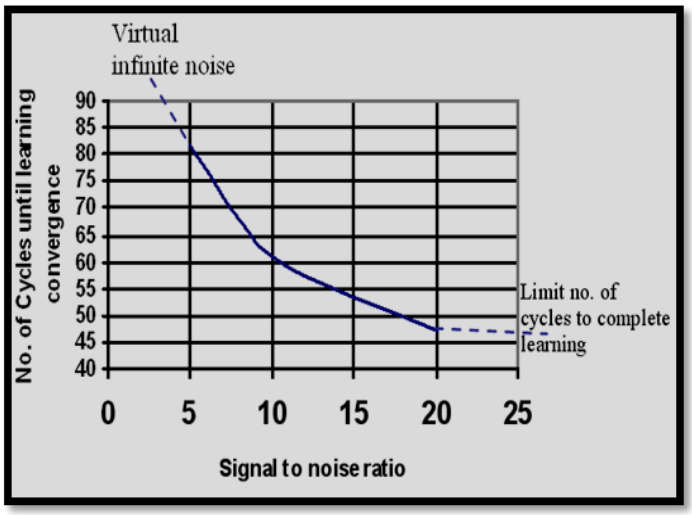

Fig. 8. Graphical presentation for learning performance under noisy conditions with reference to Table 1I.{ adapted from [24]}.

TABLE III
RELATION BETWEEN AVERAGE NO OF CYCLES NEEDED TO REACH OPTIMUM SOLUTION VERSUS SIGNAL TO NOISE RATIO VALUES [25].

Signal to Noise Power Ratio of Input Data	1	10	20
Convergence to Opt. Sol. Time (# cycles)	100	50	30

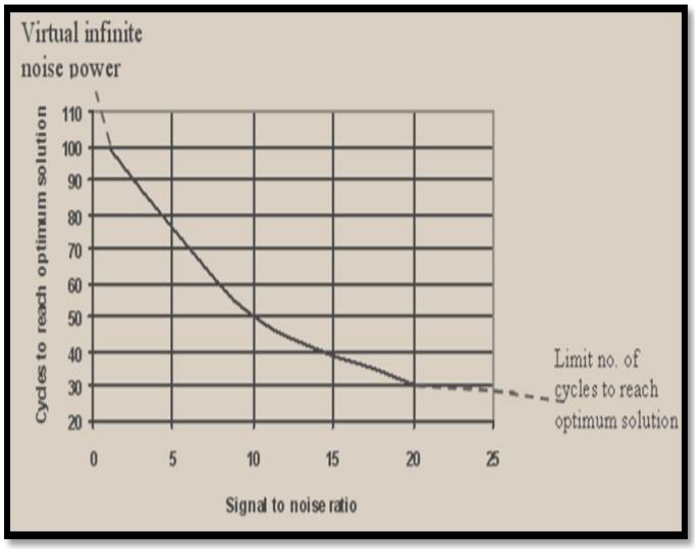

Fig. 9. Graphical presentation for reach optimal solution of TSP under noisy conditions [25]

IV. SOLVING OF TSP USING ACS ALGORITHMS

A. Selection of Minimum Pathway Between Source and Nest [26]

Referring to Figure 10, in the case of bifurcation occurrence due to an existence of an obstacle at some point placed on the pathway between the nest site and that of the source, the transportation process of food (from food source) to food store (nest). is illustrated behavioral ants' responses shown at the simplified sketched figure considering the pheromone trail between nest and food source.

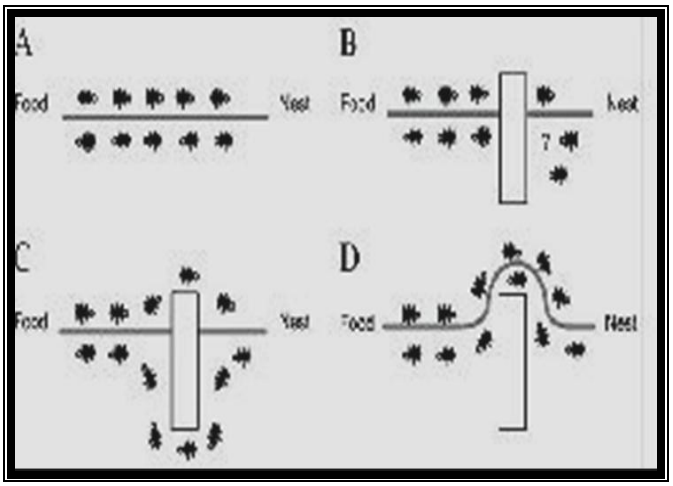

Fig. 10. Ant Behavior A. Ants in a pheromone trail between nest and food; B. An obstacle interrupts the trail; C. Ants find two paths to go around the obstacle; D. A new pheromone trail is formed along the shorter path{Adapted from[26]}.

Interestingly, another type of ACS that is capable to converge to (accomplish) optimal solution of Traveling Salesman Problem (TSP) by adopting an autocatalytic ACS algorithm. That's with dependence upon different intercommunication levels among ACS agents (ants). The reached optimal solutions of TSP obtained by various speeds in accordance with inter-communication levels among ACS agents [27][28][29][30].

B. Analogy between Supervised ANN Model Versus Tandam Learning

Referring to [29], the two Figures (11& 12), present two distinct models for either supervised learning ANN, or the ACS adopting tandem learning strategy, respectively. More precise words, both models has been provided by interactive leaning responses either by guided relationship for teacher/pupil tuition at (Figure 11), or by the environmental learning of leader/follower ants (Tandem running), at (Figure 12). Therefore, in case if the a teacher provides an interactive response, ***information or guidance correction is the stimulating signal for the pupil. Similarly, for ACS the interactive bidirectional response observed between leader and follower.*** Both cases are noticed to be formulated as (supervised learning) or equivalently (learning by a teacher) .That is given by the derived formula according to equation (10) at the above section II.

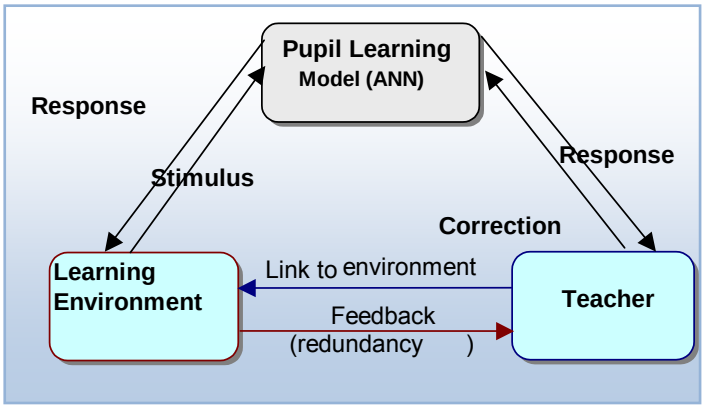

Fig. 11. A Schematic Diagram for (Supervised Learning Interaction Between a Teacher and his Pupil. ANN Based Model)

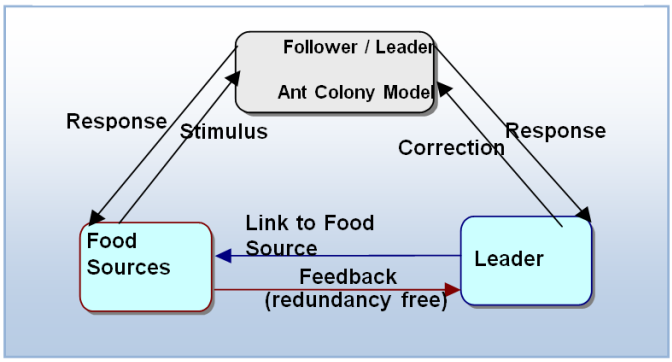

Fig. 12 A Schematic Diagram for Tandem Learning Bidirectional Feedback

C. Tandem Running For A Pair Of Ants [32]

Referring to the Figure 13, in below, it illustrates the interactive tandem learning process in accordance with the bidirectional communication relationship between the pair of two ants (leader and follower).

Fig.13. Illustration of supervised learning process via leader and follower Ants' interaction {Adapted from [31]}

Tandem running technique involves an interactive bidirectional feedback between teacher and pupil corresponding to leader and follower ants respectively. Furthermore, in this figure, depicted block named as (Follower/Leader Ant Colony Model) suggests that tandem follows after learning their lessons so well, that they can become tandem leaders. Tandem leaders have experience of the food source, whilst followers are naïve of its location. The leader proceeds towards the food source (red path) so long as the follower (blue path) maintains regular antennal contact with the leader's legs or abdomen. Progress of the tandem pair is slowed by frequent periods when the leader remains still whilst the follower performs a looped circuit, possibly to memorize landmarks along the path (points 1 and 3) [31][32]

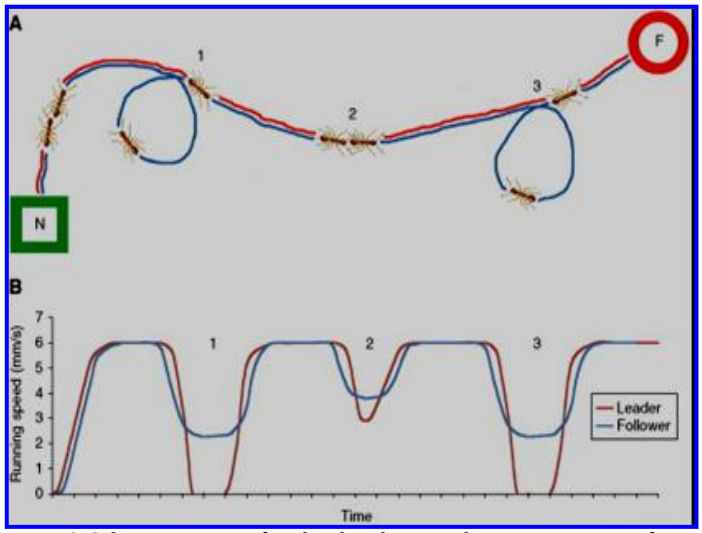

Fig. 14.A Schematic view of path taken by a tandem-running pair of *Temnothorax albipennis* ants from their nest (N) to a food source (F). (B) Running speed of leader (red line) and follower (blue line) during the same tandem-run.

Once this exploratory circuit is completed, and the follower re-establishes antennal contact, the leader continues onwards towards the food. If contact between follower and leader becomes less frequent during a tandem-run, the leader will slow down to allow the follower to catch up (point 2). Interestingly, Tandem leaders pay a cost because they would normally have reached the food around four times faster if not hampered by a follower. But the benefit is that the follower learns where the food is much quicker than it would have done independently. Tandem followers learn their lessons so well that they often become tandem leaders and in this way time-saving information flows through the ant colony. Referring to Figure 14. in below , it illustrates the path taken by tandem running pair of Temnothorax albipennis ants from their nest (Green Square) to food source (Red circle). The leader proceeds towards the food source (red path) so long as the follower (blue path) maintains regular antennal contact with the leader's legs or abdomen [31].

V. Simulation Results

A. Simplified Simulation Program Flowchart

Referring to Figure 15, a simplified macro-level flowchart for simulation program is introduced. It describes briefly the algorithmic steps for a suggested realistic simulation program of adopted Artificial Neural Networks' model taking into account the different number of neurons.(# neurons).

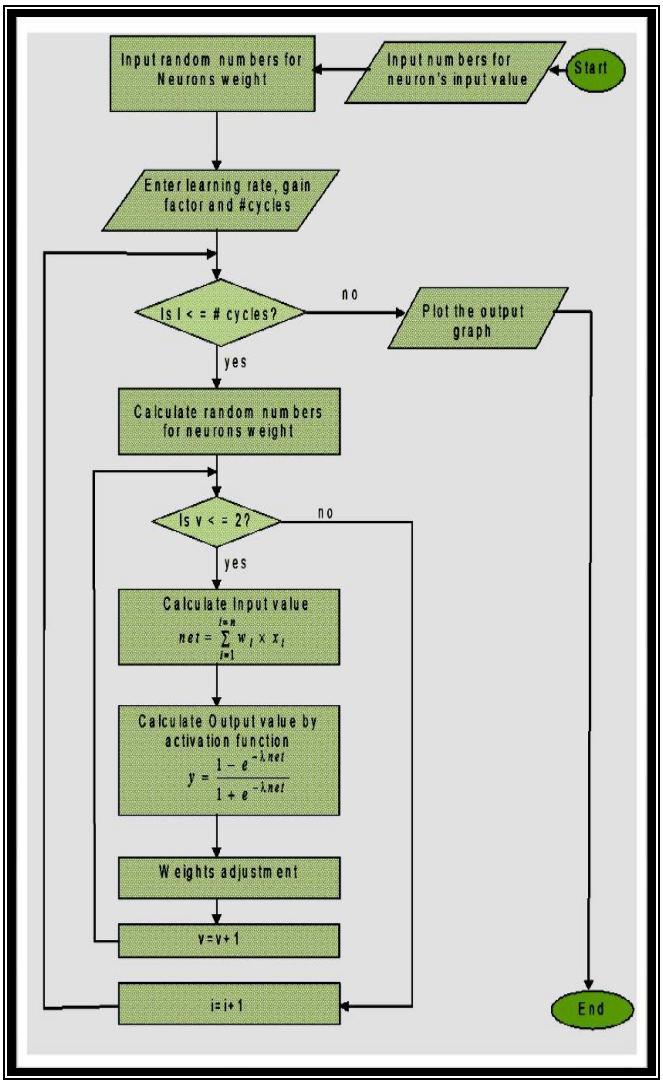

Fig. 15.A simplified macro level flowchart describing algorithmic steps (for various numbers of neurons) using Artificial Neural Networks modeling.

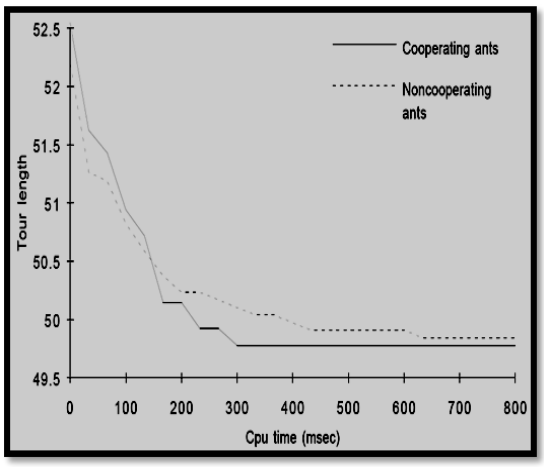

Fig.16. Cooperating ants find better solutions in a shorter time. Average on 25 runs. The number of ants was set to m=4, adapted from [25].

B. Speed Versus Accuracy for Optimal Solution of TSP

The convergence to solve optimally TSP is illustrated at Figure 16. Where it is shown in below, the relation between tour length versus the CPU time is given. It is observed the effect of ant cooperation level on reaching optimum (minimum tour). Obviously, as level of cooperation among ants increases (better communication among ants) the CPU time needed to reach optimum solution is decreased. So, that optimum solution is observed to be reached (with cooperation) after 300 (msec) CPU the while that solution is reached after 600 (msec)

CPU time (without cooperation).

In other words, by different levels of cooperation (communication among ants) the optimum solution is reached after CPU time τ placed somewhere between above two limits 300-650 (msec). Referring to [25],[27], cooperation among processing agents (ants) is a critical factor affecting ACS performance as illustrated at Figure 16. So, the number of ants required to get optimum solution differs in accordance with cooperation levels among ants. This number is analogous to number of trials in OCR process [24]. Moreover, the signal to noise ratio is observed to be directly proportional to leaning rate parameter in self-organized ANN models [18]. That implies the increase of stored experience due to learning by interaction with environment[23]. Additionally, by referring to Figure 17, the relation between various learning rate values and the relative error values is illustrated at[37]. More precisely, that figure presents the relation between relative error values $e_k(n)$ at any number of time cycles(n), versus the speed-accuracy trade-offs [38],considering the error correction learning while solving TSP.

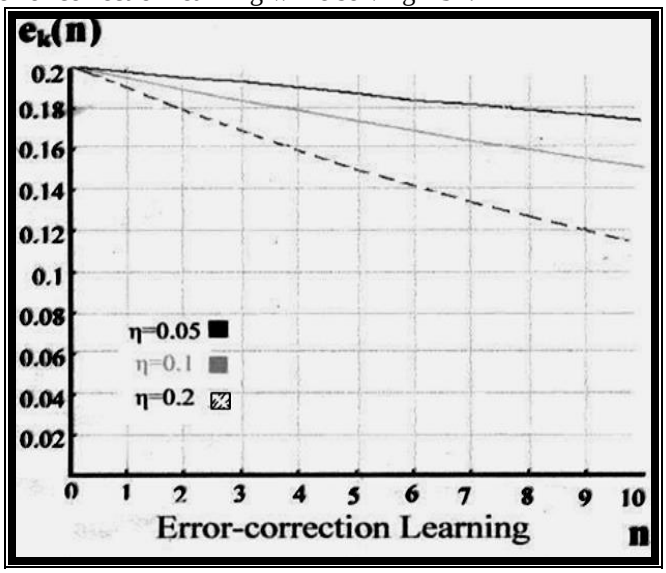

Fig. 17. Adaptability performance concerned with error correction learning algorithm {adapted from [37]}

TABLE IV
ILLUSTRATES THE RELATION BETWEEN INCREASING # NEURONS CONTRIBUTING FOR LEARNIN VESUS RESPONSE TIME AND AVARAGE LEARNING SPEED CONSIDERING ERROR CORRECTION LEARNING RULE.

Number of Neurons Contributing Learning Process	3	5	7	9	11	14
Measured Response Time by (# Cycles)	79.7	61.8	36.9	19.8	14.8	7.3
Average Learning Speed (1/Cycle).	0.013	0.016	0.027	0.051	0.068	0.137

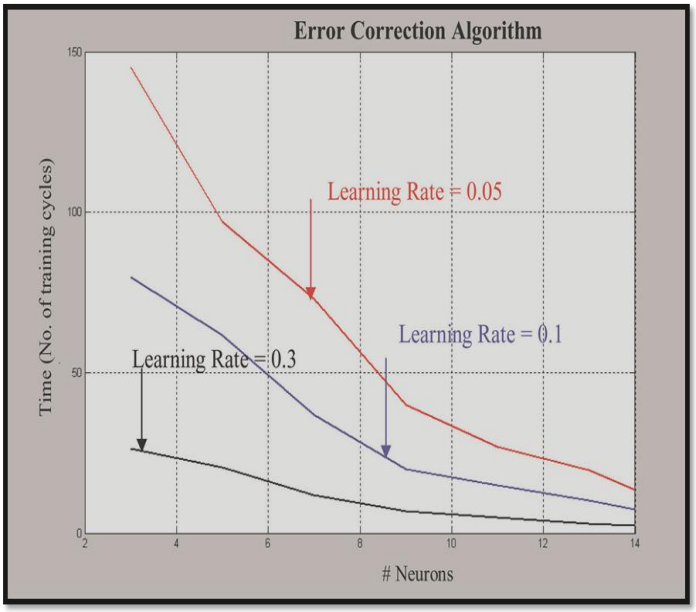

Fig. 18. Illustration of the error correction learning performance considering the tine response (Learning Convergence) for three learning rate value (0.05,0.3, and 0.5)

VI. CONCLUSIONS

This piece of research comes to three interesting conclusive remarks presented as follows:

- The humble ant is not only capable of solving difficult mathematical problems, but is even able to do what few computer algorithms can - adapt the optimal solution to fit a changing problem, deepen our understanding of how even simple animals can overcome complex and dynamic problems in nature, and will help computer scientists develop even better software to solve logistical problems and maximize efficiency in many human industries.
- According to above presented two experimental works associated to the suggested problem of ACS problems based on tandem learning. And, the analysis and evaluation by ANNs modeling, observed to be in well correspondence and analogy with that optimization process performed on the basis of Swarm Intelligence (SI) by ACS. The optimal solution of TSP strategy in ants proved to reach its solution with minimum time rather than the other problem that reaches optimum average speed while solving TSP by referring to the analogous two figures 8&.9. In addition to the analogy between two figures 11, and 12.
- Interestingly, the intercommunication levels among ants shown to be analogous to both learning parameters of ANN (Learning rates and the Gain factor values). Additionally, the number of ants (in ACS) is corresponding to the number of neurons(in ANN). Generally, the introduced approach is very beneficial for more realistic modeling of nonhuman (Social Insects) learning processes versus other realistic artificial neural networks' models , that for more applications in the future.

REFERENCES

[1] Nazmul Siddique , and Hojjat Adeli "Nature Inspired Computing: An Overview and Some Future Directions" Published online on November 30, 2015 doi: 10.1007/s12559-015-9370-8 PMCID: PMC4675795.Available online at: https://www.ncbi.nlm.nih.gov/pmc/articles/PMC4675795/

[2] Grzegorz Rozenberg, Thomas Back, and Joost N. Kok (Eds.) "A Hand Book of Natural Computing " Available online at: http://www.springer.com/978-3-540-92909-3

[3] Roger Highfield "Ants are in a class of their own with tandem teaching Ants are in a class of their own with tandem teaching". Available online on 12 Jan 2006: http://www.telegraph.co.uk/news/uknews/1507587/Ants-are-in-a-class-of-their-own-withtandem-teaching.html

[4] Hassan M. H., et.al. "On Comparative Analogy between Ant Colony Systems and Neural Networks Considering Behavioural Learning Performance" Journal of Computer Sciences and Applications, 2015, Vol. 3, No. 3, 79-89 Available online at http://pubs.sciepub.com/jcsa/3/3/4 © Science and Education Publishing DOI:10.12691/jcsa-3-3-4.

[5] Hassan M. H. "Analytical Comparison of Swarm Intelligence Optimization versus Behavioral Learning Concepts Adopted by Neural Networks (An Overview) American Journal of Educational Research http://pubs.sciepub.com/education/3/7/2/index.html Vol. 3, No. 7, 2015, pp 800-806. doi: 0.12691/education-3-7-2.

[6] Hassan M. H. Mustafa, and Fadhel Ben Tourkia "On Comparative Analysis and Evaluation Of Social Insect Colonies' Behavior During Exploring Food Sources and Their Migration to A New Nest Versus Two of Neural Networks' Learning Paradigms. (Tandem Running Approach)" Published Journal IJATTMAS volume III issue xI nov 2017 Page 33-41

[7] Hassan M. H., et.al "Comparative Performance Analysis and Evaluation for One Selected Behavioral Learning System versus an Ant Colony Optimization System" Published at the Proceedings of the Second International Conference on Electrical, Electronics, Computer Engineering and their Applications (EECEA2015), Manila, Philippines, on Feb. 12-14, 2015.

[8] Maria Klatte,* Kirstin Bergström, and Thomas Lachmann "Does noise affect learning? A short review on noise effects on cognitive performance in children". Available online 2013 Aug 30. doi: 10.3389/fpsyg.2013.00578-at: https://www.ncbi.nlm.nih.gov/pmc/articles/PMC3757288/

[9] Ghoaimy M. A., et al. learning of Neural Networks using Noisy Data, Second International Conference On Artificial Intelligence Application, Cairo, Egypt, 389-399, Jan. 22-24, 1994.

[10] H.M.Hassan, "On Analysis and Evaluation of Non-Properly Prepared Teachers Based on Character Optical Recognition Considering Neural Networks Modeling" Published at Proceedings of the International Conference on Pattern Recognition and Image Processing (ICPRIP'15) that held on March 16-17, 2015 Abu Dhabi (UAE).

[11] H.M.Hassan, and Ayoub Al-Hamadi "An Overview on Classrooms' Academic Performance Considering: Non-properly Prepared Instructors, Noisy Learning Environment, and Overcrowded Classes (Neural Networks' Approach)" has been accepted for oral presentation and publication at the upcoming 2015 6th International Conference on Distance Learning and Education (ICDLE 2015) in Pairs. Furthermore, this paper has been accepted to be published at the International Journal of Learning and Teaching in Vol.2, No.2, 2016 of IJLT.

[12] H.M.Hassan, et al "On Analysis And Evaluation of Multi-Sensory Cognitive Learning Of A Mathematical Topic Using Artificial Neural Networks", Journal of Telecommunications, 1(1), 99-104. (2010).

[13] H.M.Hassan "Quantifying of Learning Creativity Through Simulation and Modeling of Swarm Intelligence and Neural Networks" , published at International Journal of Online Engineering iJOE-Volume 7, Issue 2, May 2011, pp.29-35.

[14] H.M.Hassan "On Quantifying Learning Creativity Using Artificial Neural Networks (A Mathematical Programming Approach) " published at CCCT 2007 conference held on July 12-17,2007-Orlando,Florida,USA.

[15] H.M.Hassan "Analysis and Evaluation of Learning Creativity Phenomenon Using Artificial Neural Networks Modeling (A Quantitative Approach)" , Published at the Sixth Annual Symposium on Learning and Technology ,held on 26-27 April 28, 2008,Jedda Hilton Hotel.

[16] H.M.Hassan, et al "On Comparison Between Swarm Intelligence Optimization and Behavioral Learning Concepts Using Artificial Neural Networks (An over view)", published at the 12th World Multi-Conference on Systemics, Cybernetics and Informatics: WMSCI 2008 June 29th - July 2nd, 2008 – Orlando, Florida, USA.

[17] Kohonen T. "self-organization and Associative Memory": New York, Springer, 1984.

[18] Haykin S., Neural Networks, Englewood Cliffs, NJ: Prentice-Hall, 1999.

[19] J R Soc Interface. 2007 Apr 22; 4(13): 193–206. Published online 2006 Nov.28. doi: 10.1098/rsif.2006.0177

[20] H.M. Hassan" On Simulation of Adaptive Learner Control Considering Students' Cognitive Styles Using Artificial Neural Networks (ANNs)" Published at CIMCA , Austria. 28-30 Nov.2005.

[21] D.O. Hebb, "The organization of behaviour", Wiley, New York (1949).

[22] Hassan. M. Mustafa and Ayoub Al-Hamadi "On Comparative Analogy of Academic Performance Quality Regarding Noisy Learning Environment versus Non-properly Prepared Teachers Using Neural Networks' Modeling" .Published in International Journal of Information and Education Technology, Vol. 6, No. 12, December 2016.

[23] M.Fukaya, et.al "Two level Neural Networks: Learning by Interaction with Environment", 1st ICNN, San Diego, (1988).

[24] Ghonaimy M.A., Al – Bassiouni, A.M. and Hassan, H.M "Leaning of Neural Networks Using Noisy Data". Second International Conference on Artificial Intelligence Applications, Cairo, Egypt, Jan 22-24, 1994.

[25] Alberto C., et al. Distributed optimization by ant colonies. Proceeding of ECAL91, Elsevier Publishing, pp 134-142, 1991.

[26] Yunlong Liu and Hiroki Yokota " Artificial ants deposit pheromone to search for regulatory DNA elements"

[27] .Available online at: https://bmcgenomics.biomedcentral.com/articles/10.1186/1471-2164-7-221.Published: 30 August 2006.The-image-available-online-at:http://media.springernature.com/full/springer-static/image/art:10.1186/1471-2164-7-221/MediaObjects/12864_2006_Article_604_Fig1_HTML.jpg

[28] E. Bonabeau, M. Dorigo, and G. Theraulaz. Swarm Intelligence: From Natural to Artificial Systems. Oxford University Press US,999.

[29] M. Dorigo and T. St□utzle. Ant Colony Optimization. MIT Press,2004.

[30] Hassan M. H. Mustafa, and Fadhel Ben Tourkia "On Comparative Analysis and Evaluation of Social Insect Colonies' Behavior During Exploring Food Sources and Their Migration to A New Nest Versus Two of Neural Networks' Learning Paradigms. (Tandem Running Approach)". Published at IJATTMAS: Nov, 2017, ISSN: 2454-5678 V0LUME-III, ISSUE-XI. Page 33-41.

[31] H. M. Hassan "On Evolutional Study of Comparative Analogy between Swarm Smarts and Neural Network Systems (Part 2)"Published at the 31st International Conference for Statistics, Computer Science and Its Applications, Cairo-Egypt 1-6 April 2006.

[32] EllouiseLeadbeater Nigel E.RaineLarsChittka "Social Learning: Ants and the Meaning of Teaching". Available online: http://www.sciencedirect.com/science/article/pii/S0960982206014114.

[33] N.R. Franks, T. Richardson" Teaching in tandem-running ants" Nature, 439 (2006), p. 153.

[34] Hassan M. H. Mustafa, and Fadhel Ben Tourkia On Analysis and Evaluation of Learning Creativity Quantification via Naturally Neural Networks' Simulation and Realistic Modeling of Swarm Intelligence" . Published at the proceeding of the conference: Eminent Association of Researchers in Engineering & Technology(EARET), held in Kuala Lumpur, Malaysia, on 8-9 January 2018.

[35] Hassan M. H. Mustafa "On performance evaluation of brain based learning processes using neural networks," published at **2012 IEEE** Symposium on Computers and Communications (ISCC), pp. 000672-000679, 2012 IEEE Symposium on Computers and Communications (ISCC), 2012.

[36] Hassan M. H. Mustafa, and Fadhel Ben Tourkia "On Analysis And Evaluation Of Cocktail Party Effect On Applied Educational Practice Theory Using Neural Networks Modeling". Published at International Journal of Advanced Research (IJAR) , on November 2017 : ISSN: 2320-5407 Int. J. Adv. Res. 5(11), 836-849

[37] H. M. Hassan. "Evaluation of Learning / Training Convergence Time Using Neural Network (ANNs)" published at, the Proceeding of 4th International Conference of Electrical Engineering ICEENG Conference, Military Technical College, Cairo, Egypt, pp.542-549, 24-26 Nov. 2004.

[38] H.M. Mustafa, et al. "On Assessment of Brain Function Adaptability in Open Learning Systems Using Neural Network Modeling (Cognitive Styles Approach) , Published at The IEEE International Conference on Communications and Information Technology ICCIT-2011, held on Mar 29, 2011 - Mar 31, 2011, Aqaba, Jordan. pp. 229-237.

[39] James A.R Marshall, Anna Dornhaus, Nigel R Franks, Tim Kovacs Noise, cost and speed-accuracy trade-offs: decision-making in a decentralized-system-published-22-April-2006.doi: 10.1098/rsif.2005.0075. Journal of Royal Society Interface Publishing http://rsif.royalsocietypublishing.org/content/3/7/243

Study of the Rochet Phenomenon under Uniaxial and Multiaxial Loading of 304l Stainless Steel

Messai. Hala, and Meziani.Salim

Abstract**—** This paper is devoted to the study of the 304L stainless steel cyclic behavior in ambient temperature. The effect of the average stress and the amplitude of the stress has been taken into consideration. In first time, we are interested in choosing the behavior model for simulation. Different models based on a linear and nonlinear isotropic hardening, linear and nonlinear kinematic hardening and Chaboche model are tested. The obtained results justify although that Chaboche model more approximate the real behavior. In the second time the identification is done using the Chaboche constitutive model and the investigations have been performed with reference to both uniaxial and biaxial experimental data, (a) strain controlled tests, (b) ratchet tests, (c) ratchet tests after a strain controlled strain tests. Results were reported in graphs representing the type of loading effect on the prediction of material behavior, using the Chaboche model.

Keywords**—** Chaboche model, Uniaxial and biaxial ratchetting, Uniaxial and biaxial experiments

I. INTRODUCTION

AISI 304L stainless steel is widely used in piping systems of chemical and petroleum industries as well as nuclear power generation plants where failure frequently takes place under operating/ accidental loading conditions. In such applications, failure governed by fatigue is predominant and in certain conditions, ratcheting fatigue is the failure mechanism. The metallic structures are often subjected to cyclic loads during their services. In these conditions, we can then attend various phenomena of the macroscopic behavior: softening, adoucissement, hardening, Ratcheting phenomenon..., Ratcheting is a kind of inelastic cyclic accumulation deformation that will be seen in the materials subject to a stress-controlled in the cycle of loading with non-zero mean stress [1],[2]. However the ratcheting behaviour of materials is a very complex phenomenon because it depends on a set number of factors and they are stress, stress amplitude, frequency, loading history and micro-structural features. Over the past few years, a lot of experimental results of uniaxial and multiaxial ratcheting for SS304 and 316 stainless steels are proposed by some researchers [3], [4], [5], [6], [7], [8], [9], [10], [11], [12], [13], [14], ... In this investigation, the evolution of ratcheting strain in AISI 304L stainless steel is examined through stress-controlled uniaxial ratcheting tests, at various combinations of mean stress and stress amplitude. In this work, based on studying the influence of optimized parameters make numerical simulations with different parameters proposed by [15], is used to simulate the ratchet behavior, by comparison of the experimental results realized by [16], [17], with the numerical simulation of stainless steel SS304L at room temperature.

Hala Messai is PhD student with the Laboratory of mechanics, mechanical Engineering Department, Université des Frères Mentouri Constantine 1, Campus ChaabErssas, 25000 Constantine, Algeria (corresponding author's phone: +213 665 410 518 ; e-mail: messai_hala@hotmail.fr).

Salim Meziani is with the Laboratory of mechanics, mechanical Engineering Department, Université des Frères Mentouri Constantine 1, Campus ChaabErssas, 25000 Constantine, Algeria (e-mail: salim.meziani@umc.edu.dz).

II. CONSTITUTIVE EQUATIONS OF CHABOCHE'S MODEL

We briefly presents the main constitutive equations of (time independent) Chaboche's model used in this study. This model use the classical normality flow rule. The evolution of the kinematic hardening variable (X) is described by the sum of four variables following the Armstrong and Frederick model [18]:

$$\underline{X} = \sum_{2}^{4} \underline{X_i} \tag{1}$$

$$\underline{\dot{X}}_i = \frac{2}{3} C_i \underline{\dot{\varepsilon}}^p - D_i \underline{X}_i \dot{P} \tag{2}$$

Where: C_i and D_i are some material parameters

p the accumulated plastic strain which may be deduced from:

$$\dot{P} = \sqrt{\frac{2}{3} \dot{\varepsilon}_{ij}^p \dot{\varepsilon}_{ij}^p} \tag{3}$$

The evolution of the isotropic hardening is governed by:

$$R = b(\dot{Q} - R)\dot{p} \tag{4}$$

Where: Q and b are two materiel parameters; Q is the maximum value of R while b controls the kinetics.

III. MATERIAL AND MODEL

The material used in this study is a 304L stainless steel. The chemical composition is reported in Table 1.

TABLE I
CHEMICAL COMPOSITION OF STUDIED MATERIAL. (IN WEIGHT %)

C	Mn	S	Cu	Si	Cr	Ni	P	N
0.028	1.54	0.026	0.15	0.68	18.83	9.04	0.035	0.085

Chaboche model parameters were identified using the stabilized hysteresis loop in tensile compression of 0.5% imposed strain cyclic tests (Fig. 1).

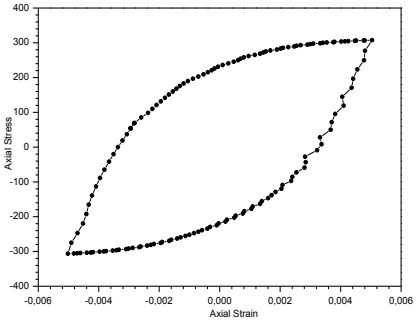

Fig. 1: Stabilized hysteresis loop

TABLE II
IDENTIFIED PARAMETERS

Identified parameters				
Young's modulus E	*yield strength*, σ_y	The constant kinematics C,	The coefficient of saturation b	the parameter of the evolution law of plastic isotropic hardening Q
206000	160	51200	35	45

The Table 3 present the optimized parameters used in this work

TABLE III
OPTIMIZATION PARAMETERS [15]

	Optimization 1	Optimization 2	Optimization4	Optimization 4+5
C1	64665,87089	60000	85000	85425
D1	2838,14652	2500	2287,29918	7000
C2	35039,19153	35000	65000,00001	85000,00001
D2	108,91612	300	850	922,9874
C3	4402,24788	5985,8175	8500	8500
D3	184,59993	600	22	100
C4	706,2892	600	900	893,55291
D4	50,00078	30	20	345,95709
Q	45	81,35013	250	250
b	4	4,08164	5	5
	Optimization 4+6	Optimization 4+7	Optimization 1+2+4+5+67	
C1	84989,02001	95000	95000	
D1	7000	7000	7000	
C2	84994,222	65325	85325	
D2	150	2500	6500	
C3	8499,81907	9500	35000	
D3	219,99223	500	500	
C4	899,98625	9000	9000	
D4	199,99973	500	500	
Q	249,99728	250	150	
b	11,99999	12	12	

Kinematic hardening parameters: C1, C2, C3, C4, D1, D2, D3 and D4. Isotropic hardening parameters: Q and b.

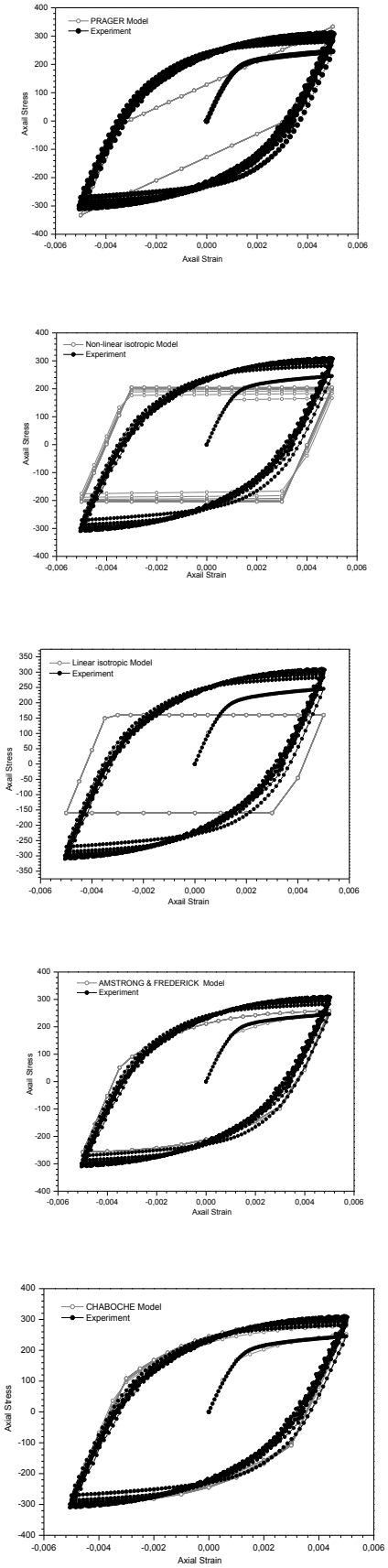

Fig. 2: Superposition of the theoretical and experimental graph for each model of hardening

These are graphs in which the ten cycles are represented between two deformation values 0.005 and -0.005 mm. The curves of Fig. 2 are obtained with imposed deformation for the five models of behavior.

From the results (Fig. 2), we note that non-linear models are closest to the real behaviour of the material, the CHABOCHE model seems to give a better description during cyclic loading.

IV. Numerical Simulation

In this second part, we will be interested in the numerical simulation of the experimental tests realized by [16], [17]. In this work we used Chaboche model optimized by [15]. By using the code ZeBuLon to implement and simulate the following tests and given in the tables (4, 5) by positioning in the same conditions as the experimental tests: that is to say, imposing the same values of the constraints.

A. Uniaxial ratcheting

Ratchet phenomenon was observed in a non-symmetric imposed stress test by tensile-compression cycles between -150 MPa and 250 MPa in 304L steel (Fig. 3). Two types of loading are imposed on steel 304. The loading history are presented in Tables 4 and 5 which shows the uniaxial ratchet depends on the average stress, the strain amplitude and loading history (Figs 5 and 6).

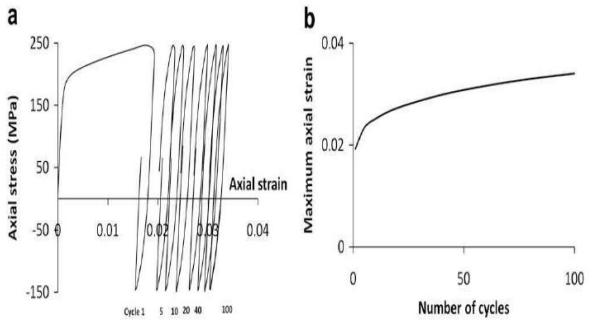

Fig. 3: Uniaxial ratchet on a 304 steel: (a) stress-strain buckles (b) Maximum axial strain according to the number of cycles [17]

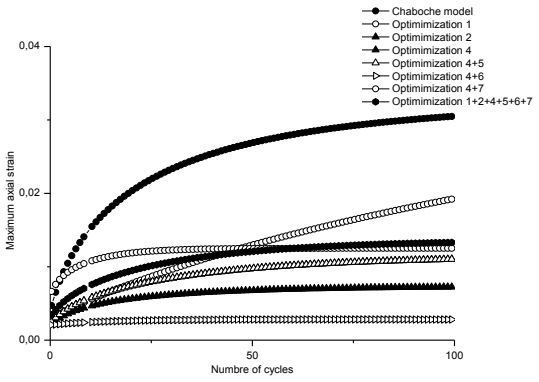

Fig. 4: Superposition of the curves obtained for all the parameters

From the Fig. 4, there is a significant ratchet step for the parameters 1, the progressive deformation continues to increase up to 100 cycles. For other parameters, we notice that the progressive deformation reaches as an asymptotic value and remains constant for certain other parameters after the 25th cycle (parameters 4, parameters 4 + 5, parameters 4 + 6, parameters 4 + 7 and parameters 1 + 2 + 4 + 5 + 6 + 7). The minimum value reached is for parameters 4 + 6, where the maximum deformation achieved does not exceed 1.2%. For the other parameters, such as the experimental value of the maximum axial strain reaches 3.41% after 100 cycles, the ratchet is therefore underestimated. For parameters 1which the maximum value reached does not exceed 1.8%, and by the Chaboche model which gives a good estimate.

TABLE IV
THE LOAD CONDITIONS OF STRESS AMPLITUDE FOR UNIAXIAL CYCLIC TESTS (UNIT: MPA) [16]

Loading history			
Case1 (20c)	Case2 (20c)	Case3 (20c)	Case4 (20c)
52 ± 222	52 ± 248	52 ± 274	52 ± 222

TABLE V
THE LOAD CONDITIONS OF MEAN STRESS FOR UNIAXIAL CYCLIC TESTS (UNIT: MPA) [16]

Loading history				
Case1 (20c)	Case2 (20c)	Case3 (20c)	Case4 (20c)	Case5 (20c)
26 ± 208	78 ± 208	117 ±208	0 ± 208	26 ± 208

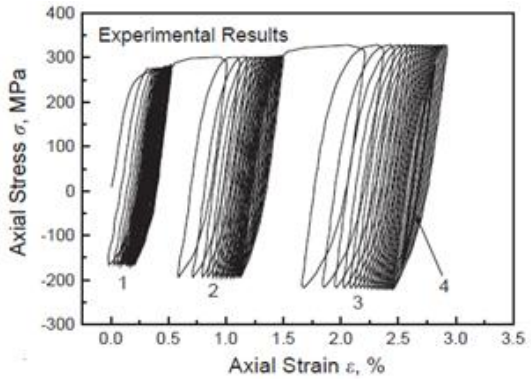

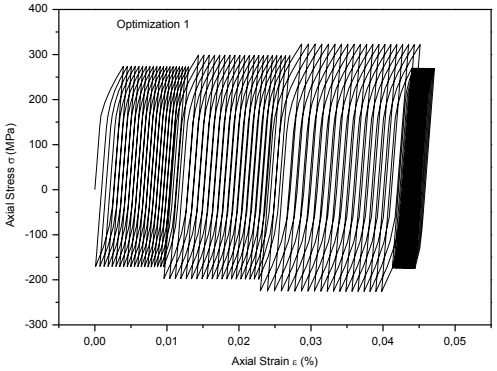

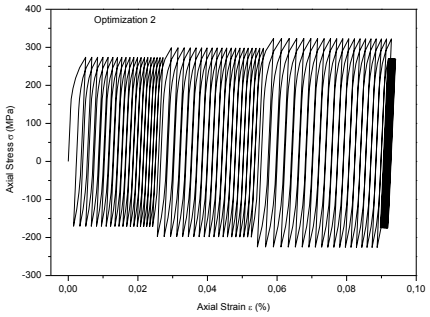

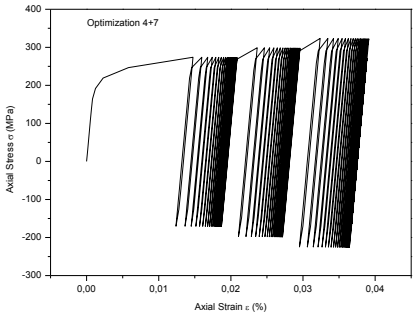

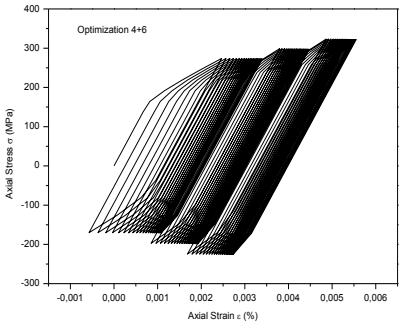

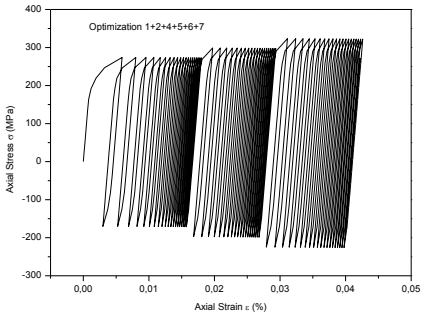

Fig. 5: Diagrams of axial stress σ vs. strain ε under stress cycling with stress amplitude, experimental results and simulated results

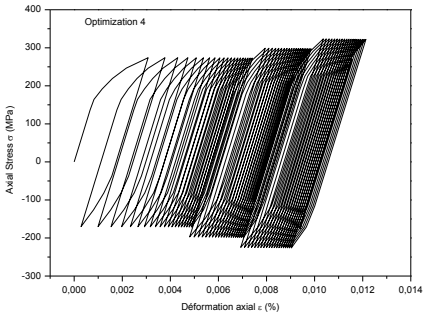

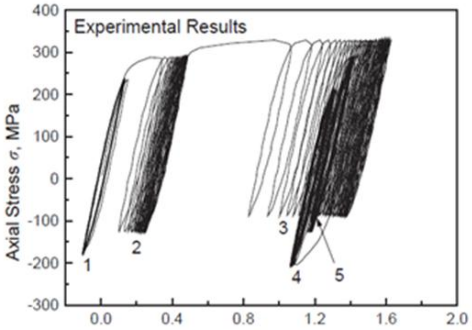

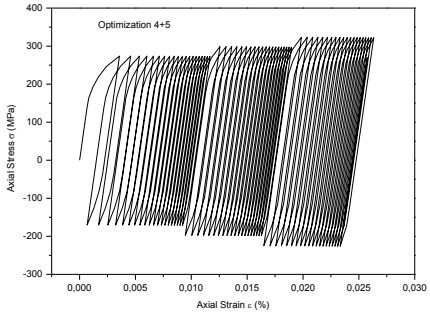

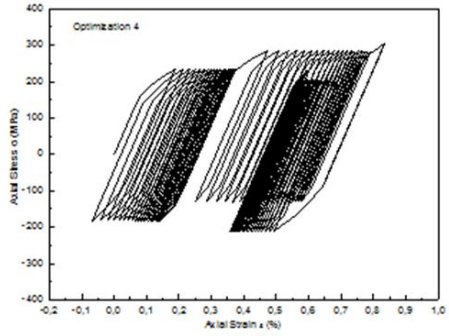

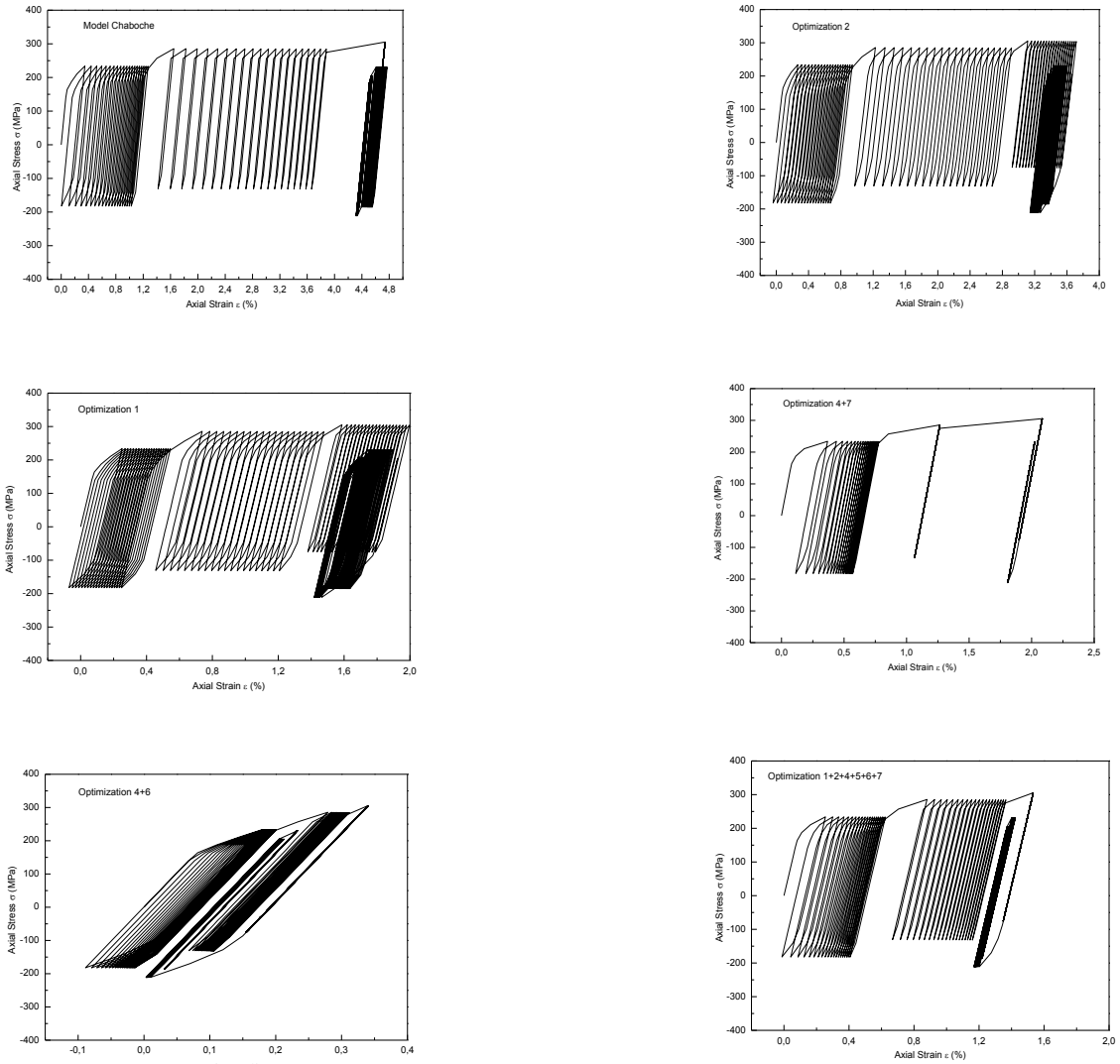

Fig. 6: Diagrams of axial stress σ v. strain ε under stress cycling with mean stress History, experimental results and simulated results

Fig .5 and 6 show the results obtained in the cyclic tension-compression tests with different mean stresses and stress amplitudes, respectively. They give the simulations of the tests performed by [16], under the loading history shown respectively in Table 4 and 5, using the Chaboche model with the seven sets of parameters identified by [15]. In Fig. 5, we can observe that no solution leads to a good prediction of the Rochet test at the amplitude of stress. It is seen that Fig. 6 well present by the parameters (1, 4 + 5, 1 + 2 + 4 + 5 + 6 + 7).

B. Multiaxial ratcheting

Fig. 7 presents the evolutions of the maximum axial deformation as a function of the number of cycles during a multiple cross of the following loading history:

For uni: apply σ_{zz}: 50 MPa → 250 MPa → -150 MPa → 50 MPa … so on;

for Cross we apply σ_{zz} : 50 MPa → 250 MPa → -150 MPa → 50 MPa → $\sqrt{3}\sigma_{\theta z}$ 200 MPa → - 200 MPa → 0 → σ_{zz} : 50 MPa → 250 MPa → -150 MPa → 50 MPa …

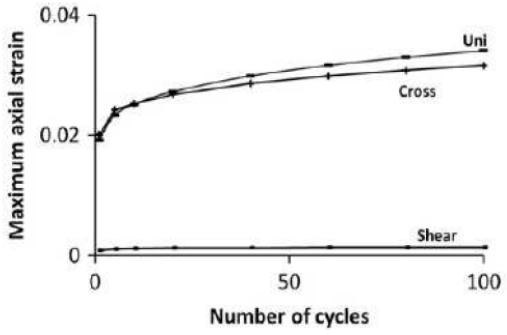

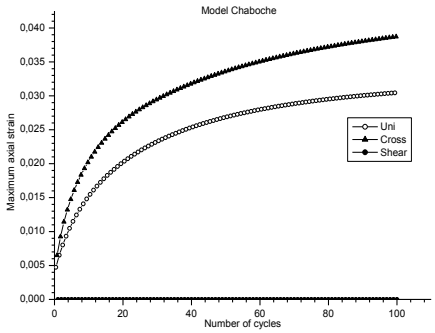

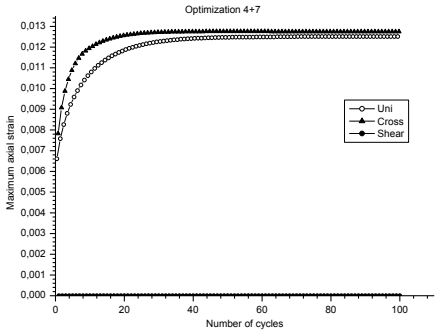

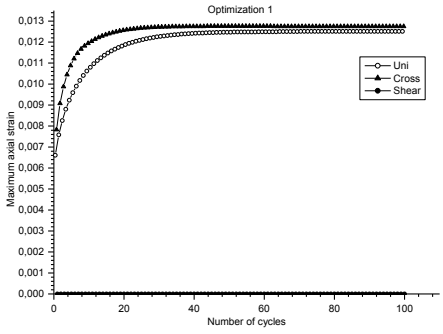

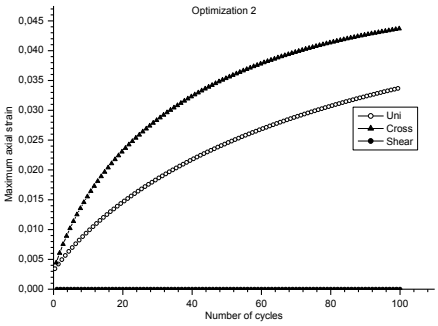

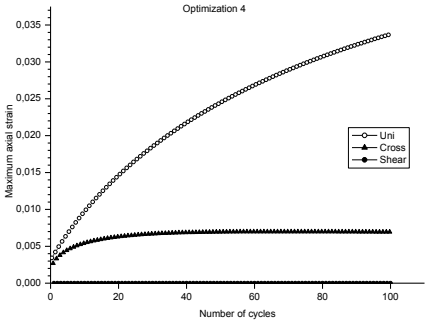

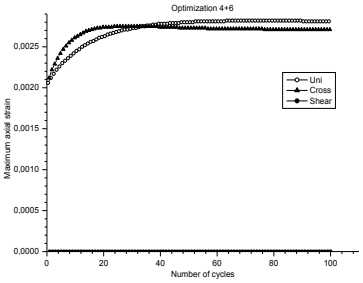

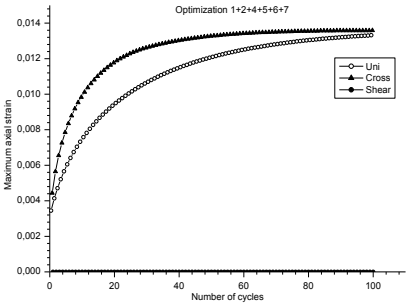

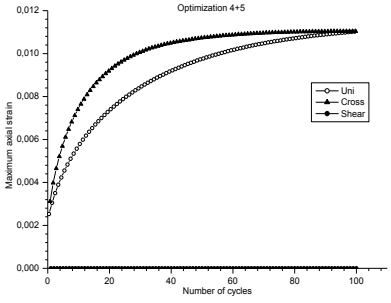

Fig. 7 Evolution of the maximum deformation as a function of the number of cycles

For the simulations represented in Fig. 7, it can be seen at the end of the 100 cycles applied, the value of the ratchet deformation in the axial direction is greater than that of the axial ratchet by the seven parameters. And for experimental the value of the ratchet deformation in the axial direction is less than that of the axial plain ratchet. So No of simulation leads to an acceptable prediction.

V. CONCLUSION

The works presented in this paper are devoted to the study numerical simulation of the cyclic behavior of a stainless steel used in the industry where the density / resistance ratio is required. The numerical simulation of the tests carried out by [16], and. [17], The results found show that these parameters is well presented the ratchet with average stress, on the other hand, a bad prediction of the state of ratchet with amplitude of stress and the ratchet multiaxial. This leads us to reflect on the possibilities of improvement of these parameters of Chaboche so that it can better represent the phenomenas of Rochet So, The study also underlines the importance of the contents of the experimental database used by [15], for the identification of the parameters.

REFERENCES

[1] C.L. Pun, Q. Kan, P.J. Mutton, G. Kang, W. Yan, International Journal of Fatigue 66 (2014) 138–154.

[2] M. Shariati, H. Hatami, H. Yarahmadi, H.R. Eipakchi, Materials and Design 34 (2012) 302–312.

[3] *Ga ng Chen , Xiaochen Zhao (2017) ,Constitutive modelling on the whole-life uniaxial ratcheting behavior of sintered nano-scale silver paste at room and high temperatures, Microelectronics Reliability 80 (2018) 47–54.*

[4] Abdel-Karim M, Ohno N. Kinematic hardening model suitable for ratcheting with steady-state. Int J Plast 2000;16,225-40.

[5] Jiang, Y., Zhang, J., 2008. Benchmark experiments and characteristic cyclic plasticity deformation. Int. J. Plasticity 24, 1481–1515.

[6] Bari S and Hassan T (2000) Anatomy of coupled constitutive models for ratcheting simulation. International Journal of Plasticity 16: 381–409.

[7] Chen X, Jiao R and Kim KS (2005) On the Ohno–Wang kinematic hardening rules for multiaxial ratcheting modeling of medium carbon steel. International Journal of Plasticity 21(1): 161–184.

[8] Chen X and Jiao R (2004) Modified kinematic hardening rule for multiaxial ratcheting prediction. International Journal of Plasticity 20(4–5): 871–898.

[9] Hassan T, Corona E and Kyriakides S (1992) Ratcheting in cyclic plasticity, part II: Multiaxial behaviour. International Journal of Plasticity 8(2): 117–146

[10] Holste C, Kleinert W, Giirth R, et al. (1994) Cyclic stress-strain response and strain localization effects under stress-control conditions. Materials Science Engineering: A 187: 113–123.

[11] Kang GZ, Li YG, Zhang J, et al. (2005) Uniaxial ratcheting and failure behaviours of two steels. Theoretical and Applied Fracture Mechanics 43(2): 199–209.

[12] Kang GZ and Liu YJ (2008) Uniaxial ratcheting and low-cycle fatigue failure of the steel with cyclic stabilizing or softening feature. Materials Science and Engineering A 472(1–2): 258–268.

[13] Kulkarni SC, Desai YM, Kant T, et al. (2003) Uniaxial and biaxial ratchetting study of SA333 Gr.6 steel at room temperature. International Journal of Pressure Vessels and Piping 80: 179–185

[14] Liu Y, Kang G and Gao Q (2008) Stress-based fatigue failure models for uniaxial ratchetting–fatigue interaction. International Journal of Fatigue 30: 1065–1073.

[15] Djimli L., Taleb L., Meziani S., (2010) ,The role of the experimental data base used to identify material parameters in predicting te cyclic plastic response of an austenitic steel International Journal of Pressure Vessels and Piping 87 177-186.

[16] Kang G., Gao Q., Yang X. (2004), Uniaxial and non proportionally multiaxial ratcheting of SS 304 stainless steel at room temperature : experiments and simulations, Int. J. Non-linear Mechanics 39, 843-857.

[17] Lakhdar Taleb, Annie Hauet (2009) Multiscale experimental investigations about the cyclic behavior of the 304L SS . International Journal of Plasticity 25 (2009) 1359–1385

[18] Armstrong PJ, Frederick CO. A mathematical representation of the multiaxial bauschinger effect. CEGB Report No. RD/B/N 731, Berkeley Nuclear Laboratories, 1966; Berkely, UK.

Membrane Ion Transport and Percolation

Samia Bahlouli, Houaria Riane, Fatima Hamdache

***Abstract*—** The plasma membrane plays a fundamental role in the cell, it delimits the intracellular volume and maintains the balance between the cytoplasmic medium and the extracellular medium. The mathematical model offers a simple description of the phenomena studied, it is a way to provide non-reproducible behavior experimentally and expand the understanding of the observed phenomena.

In this work we propose a simple electrical model to study the fractal behavior of the plasma membrane associated to the ion transport using the percolation theory as a mathematical concept. We try to find some important parameters of percolation such as critical exponents and fractal dimensions to verify the efficiency of this theory in the study of different membrane transport.

***Keywords*—** Plasma membrane; Ion channel; Modeling; Percolation; Finite difference method.

Laboratoire de Physique des Plasmas, Matériaux Conducteurs et leurs Applications (LPPMCA), Faculté de Physique, USTO-MB, Oran, Algeria (corresponding author's e-mail: samia_bah@yahoo.com).

New Developments on Thermal and Mechanical Surface Treatments for Fatigue Life of Metallic Materials

Okan Unal

***Abstract*—** Mechanical and thermal surface treatments have been applied to metallic materials to increase fatigue and wear characteristics for several decades. The treatments have been using mechanical (kinetic) and heat energy to achieve desired properties. However, the energy to be applied is aimed to br transformed in an effective way by using plasma, laser and electron beam technology instead of pure heat energy. The application of new thermal treatments could reach the desired mechanical properties with less deteriorative influence of high temperature at longer durations. For instance, conventional nitriding, carburising and boriding applications have been performed in the range of 5500C-11000C for different steel alloys. On the contrary, the plasma activated treatments reduce the temperature to 3750C-6000C intervals. Particularly for biomedical alloy Ti-6Al-4V has been achieved to plasma nitrided at approximately 4000C. Conventional ones are performed at 6500C-9000C intervals.

Mechanical surface treatment such as shot peening, grit blasting and etc. have been oriented through a new way of surface nanocrystallization besides fatigue and wear improvements. Instead of bombarding high velocity shots, ultrasonically vibrated needles and ultrasonically accelerated metal or non-metal shot media is started to use and show higher impact on surface microstructural and mechanical properties by providing deep compressive residual stress, certain nanograined layer and higher endurance limit.

***Keywords*—** Shot peening, plasma nitriding, nanocrystallization, surface treatments.

Karabuk University, Mechanical Engineering Department, Karabuk, Turkey (corresponding author's Tel.: +90 (370) 418 70 50 / 39 37; fax: +90 (370) 418 70 01; e-mail: unalokan78@gmail.com).

Scooter Propulsion System Powered by a Hydrogen Fuel Cell

Yaser Erar, Bashar Dadouch, Jamil Haddad, Abdullah Al-Qassab, Ibrahim Hag-Ali and Mehmet Fatih Orhan

***Abstract*—** The manner is investigated in which a scooter that runs on fuel cells and releases no harmful emissions to the atmosphere is designed and built. In this regard, the overall performance is evaluated and the power output is optimized in order for it to be a viable transportation method in the near future. The studies showed that the range can be extended significantly by implementing a hybrid system with a Lead Acid Cell battery. The fuel cell powers the battery that will in turn drive a motor. To ensure a longer battery life, the fuel cell automatically starts to recharge the battery when its power drops to around 60%. It is also found that a super capacitor implemented into the system improves power and performance for hills and rapid acceleration.

Department of Mechanical Engineering, College of Engineering, American University of Sharjah, PO Box: 26666, Sharjah, United Arab Emirates

Fabrication of Perovskite-Type Photocatalyst and Investigation of its Photocatalytic Activity

Pelin Demircivi*, Esra Bilgin Simsek

***Abstract*—** Titania is one of the most effective photocatalyst and its widely applied for the purification of water systems. The composite forms of semiconductors improve the photocatalytic activity by reducing the recombination of holes and electrons. Perovskites is the one that can be used as photocatalyst. Perovskite-type catalysts are attractive because transition, alkaline or rare-earth metal doping of titania photocatalysts results reduction the band-gap energy and improve charge separation between photogenerated holes and electrons.

In this study, tungsten (W) doped BaTiO3 type perovskite was synthesized by hydrothermal method. Different amounts of W (0-20%) was doped in BaTiO3 structure. 20 mL Ti(IV) n-butoxide was added into BaCl2.2H2O and Na2WO4.2H2O mixture. Hydrothermal treatment was applied in a Teflon-lined stainless steel autoclave at 200 oC. Then, the products were filtrated, washed with distilled water and calcined at 700 oC for 2h. To exhibit the photocatalytic activity of the photocatalyst, 20 mg/L tetracycline solution and 0.2 g/L solid/liquid ratio was used during the experiments. The photodegradation of tetracycline using W doped BaTiO3 catalysts was investigated under UV-A light and visible light irradiation. Tungsten loading ratio decreased the photocatalytic activity. Photodegradation of tetracycline under visible light irradiation was reached at 90% after 180 min. As a result of dark adsorption experiments, adsorption is also a part of photocatalytic degradation and increased the photocatalytic acitivity.

*Yalova University, Chemical and Process Engineering Department, 77100 Yalova, Turkey